Spacelabs Medical

BIOPHYSICAL MEASUREMENT SERIES

ELECTROMYOGRAPHY/ ELECTROENCEPHALOGRAPHY

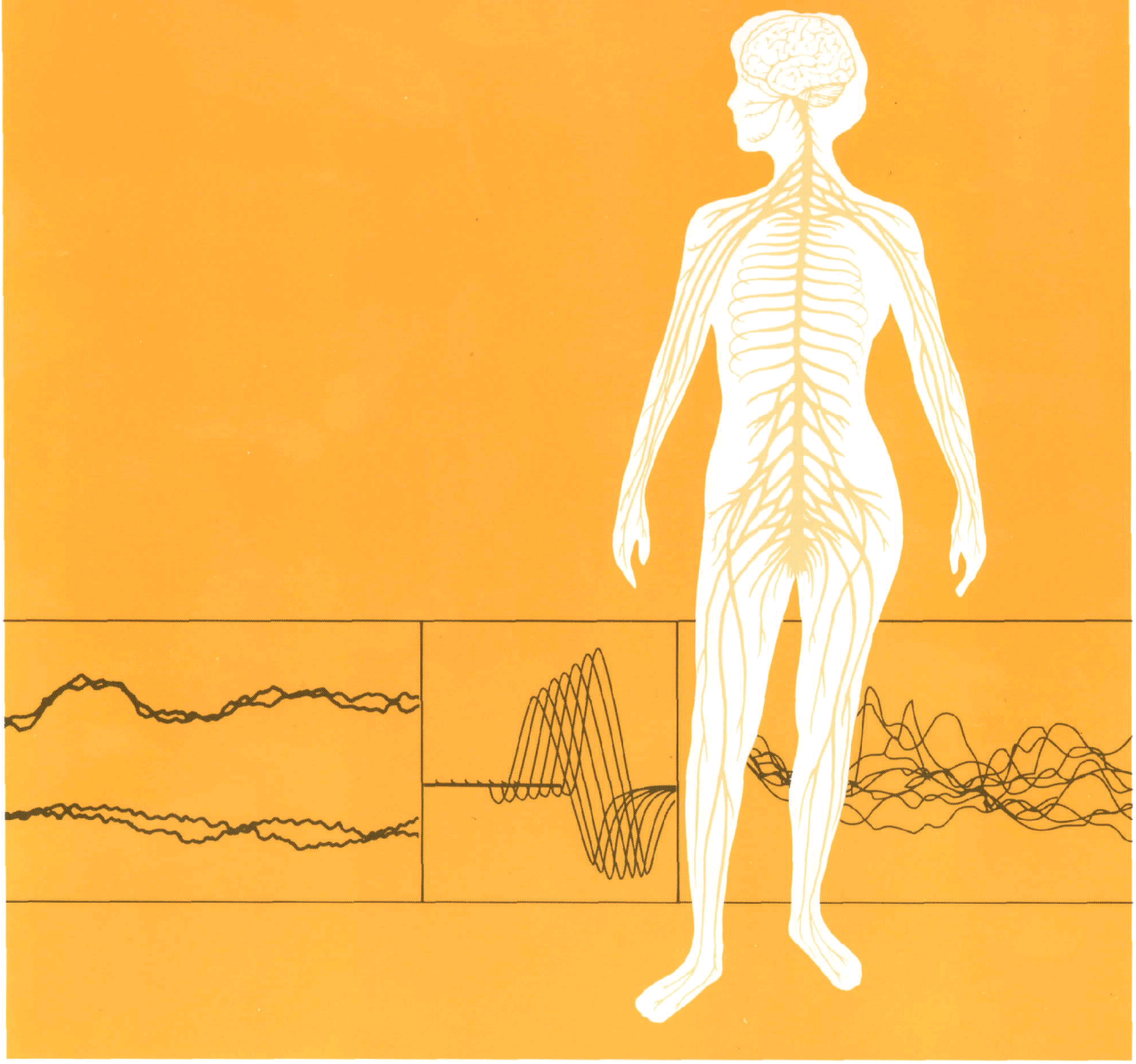

Michael R. Isley, PhD
Gregory L. Krauss, MD
Kerry H. Levin, MD
Brian Litt, MD
Robert W. Shields, Jr., MD
Asa J. Wilbourn, MD

ELECTROMYOGRAPHY/ ELECTROENCEPHALOGRAPHY

Michael R. Isley, PhD
Orlando Regional Healthcare System
Department of Intraoperative Brain Monitoring
Orlando, Florida

Gregory L. Krauss, MD
Johns Hopkins Epilepsy Center
Department of Neurology
Baltimore, Maryland

Kerry H. Levin, MD
Cleveland Clinic Foundation
Department of Neurology
Cleveland, Ohio

Brian Litt, MD
Sinai Hospital of Baltimore
Department of Neurology
Baltimore, Maryland

Robert W. Shields, Jr., MD
Cleveland Clinic Foundation
Department of Neurology
Cleveland, Ohio

Asa J. Wilbourn, MD
Cleveland Clinic Foundation
Department of Neurology
Cleveland, Ohio

This book is part of the SpaceLabs Medical Biophysical Measurement Book Series for biomedical and clinical professionals. The series is an educational service of SpaceLabs Medical, a leading provider of patient monitoring and clinical information systems.

Published by SpaceLabs Medical, Inc.,
Redmond, Washington, U.S.A.

Printed in the United States.

ISBN 0-9627449-7-2

TABLE OF CONTENTS

TABLE OF CONTENTS

INTRODUCTION

This book provides a discussion of the basic concepts and methods of electromyography, electrodiagnosis, electroencephalography, and evoked potentials. Section 1.0 provides a review of the basic and accepted methods of electromyography/electrodiagnosis that are used to evaluate patients with neuromuscular disorders. This section also includes an overview of neurophysiology, electricity and electronics, and the equipment used in diagnostic procedures.

The field of electroencephalography has experienced substantial growth and development during the past 10 years. Clinicians are now working with new technologies that allow them to directly view brain activity with less limitations and distortion. Section 2.0 provides the basic principles behind these new technologies and their role in clinical and research science.

Evoked potentials, the subject of Section 3.0, provide information that compliments electroencephalography. The most common evoked potentials used in clinical test — visual evoked responses, brain stem auditory evoked responses, and somatosensory evoked potentials — are discussed in terms of anatomy, recording methods, recording montage, and clinical applications. Intraoperative monitoring and event-related potentials are also reviewed.

Neurophysiological monitoring during major surgery and anesthesia has become an essential element of the anesthesiologist and surgeon in the operating room and intensive care unit environments. Changes in the electroencephalogram and evoked potentials can be easily displayed and quantified by high-technology, microcomputer-assisted brain monitors for rapid on-line interpretation. Section 4.0 introduces the basic principles and theories of intraoperative brain monitoring, and the interpretation of spontaneous and computer-processed EEG during general anesthesia and major surgery.

Figure 1.1 — Transverse section of the cervical spinal cord and vertebra.

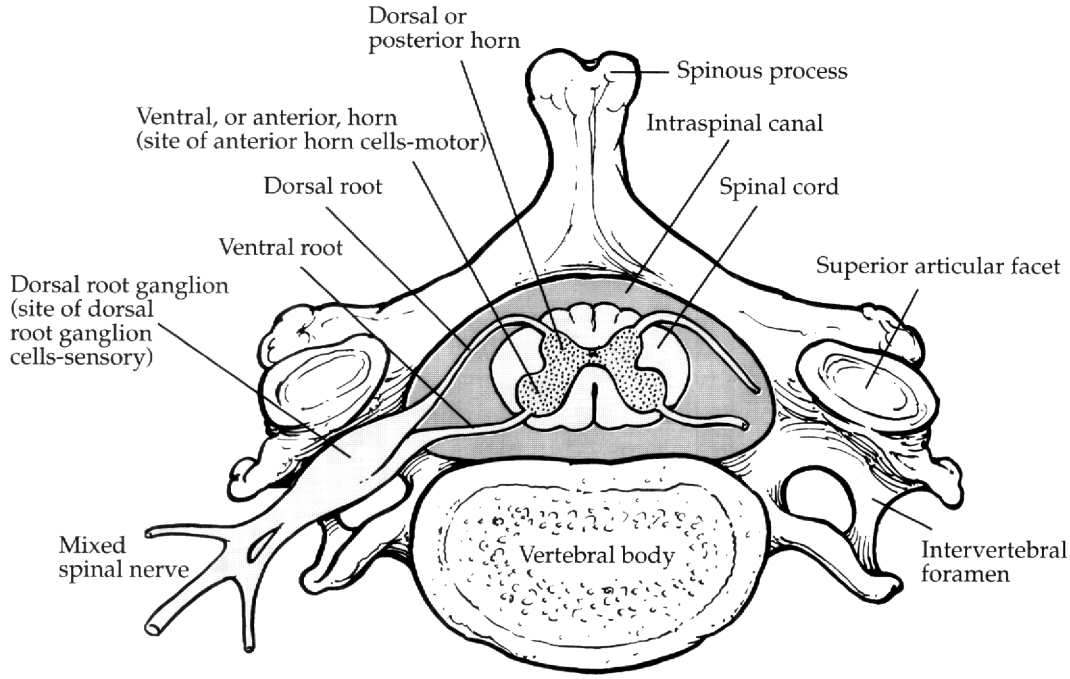

Figure 1.2 — Portions of the peripheral neuromuscular system.

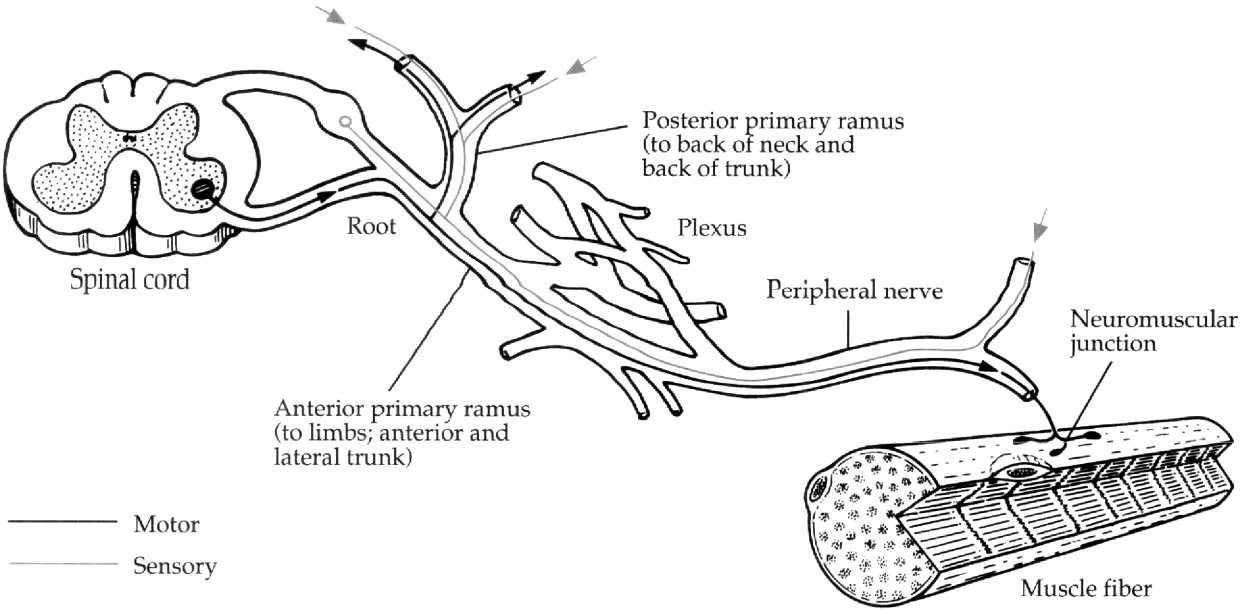

1.0 ELECTROMYOGRAPHY/ELECTRODIAGNOSIS

This section concerns several electrodiagnostic procedures — including nerve conduction studies (NCSs), the needle electrode examination (NEE), F-waves, and H-reflexes — used to assess patients with possible peripheral neuromuscular disorders. These procedures are often grouped under the terms *electrodiagnosis* and *electromyography*, although neither is completely satisfactory. Electrodiagnosis is a very indefinite designation. Even though it has a limited meaning by convention, it justifiably could be used to describe all the various diagnostic tests that measure electrical activity generated in humans and other living creatures, including electroencephalograms, electrocardiograms, and electroretinograms. Electromyography was originally coined to describe just one of the procedures regularly performed in the electromyographic (EMG) laboratory. When used in its expanded sense, it can be both confusing and misleading. Nonetheless, because a more satisfactory term has not been forthcoming, electrodiagnosis and electromyography continue to serve as collective designations for this group of diagnostic procedures.

The electrodiagnostic examination assesses: (1) the peripheral sensory nerves at and distal to their cell bodies of origin in the dorsal root ganglion (DRG) within the bony intraspinal canal but external to the spinal cord, along the more distal portion of the dorsal, or posterior (sensory), root (Figure 1.1); and (2) the motor unit, which is composed of an anterior horn cell (AHC) in the anterior, or ventral, horn of the spinal cord, the motor axon that passes distally from the AHC, all the muscle fibers innervated by its axon's terminal nerve fibers, and the intervening neuromuscular junctions (Figure 1.2). Some of the procedures also assess other nervous system structures. For example, the H-wave test evaluates a portion of the S1 spinal cord segment as well as the sensory fibers connecting the S1 DRG to the spinal cord; the facial motor NCS and the NEE of the facial muscles evaluate the 7th (facial) cranial nerve and its cell bodies originating within the brain stem. The electrodiagnostic examination essentially assesses the peripheral nervous system (PNS), rather than the autonomic nervous system (ANS) or the central nervous system (CNS), which consists of the brain and spinal cord.

Electrodiagnostic examinations are performed on patients for two reasons: (1) to detect an abnormality of the motor unit or the peripheral sensory nerve fibers, or to exclude the presence of a lesion of those same structures; and (2) to characterize known lesions by determining their etiology, underlying pathophysiology, severity, prognosis, and location (with focal lesions).

The electrodiagnostic examination consists of several components. The two basic tests are the NCS and the NEE, which were introduced into clinical use at different times. Historically, the two tests can be performed independently. However, they so often prove complimentary to one another that both usually are performed on every patient.

The NEE is the oldest component of the EMG examination. Its clinical value was first appreciated in the mid-1940s, although it had been used some years earlier on a limited basis for research. The term electromyography initially applied only to the portion of the electrodiagnostic examination. Some physicians continue to view it in that limited sense, although many now employ it as a generic term for the entire electrodiagnostic examination.

During the NEE, a recording needle electrode is inserted into various skeletal muscles. The electrical activity generated in a muscle is then conveyed to the EMG machine where the waveforms and sounds it produces are analyzed.

Figure 1.3 — Three basic nerve conduction studies: (a) motor. (b) sensory. (c) mixed. (S=stimulation sites; R=recording sites; X=shock artifact). Beneath each stimulation site is the response seen at the recording site when stimulation is applied to the nerve at that stimulation site.

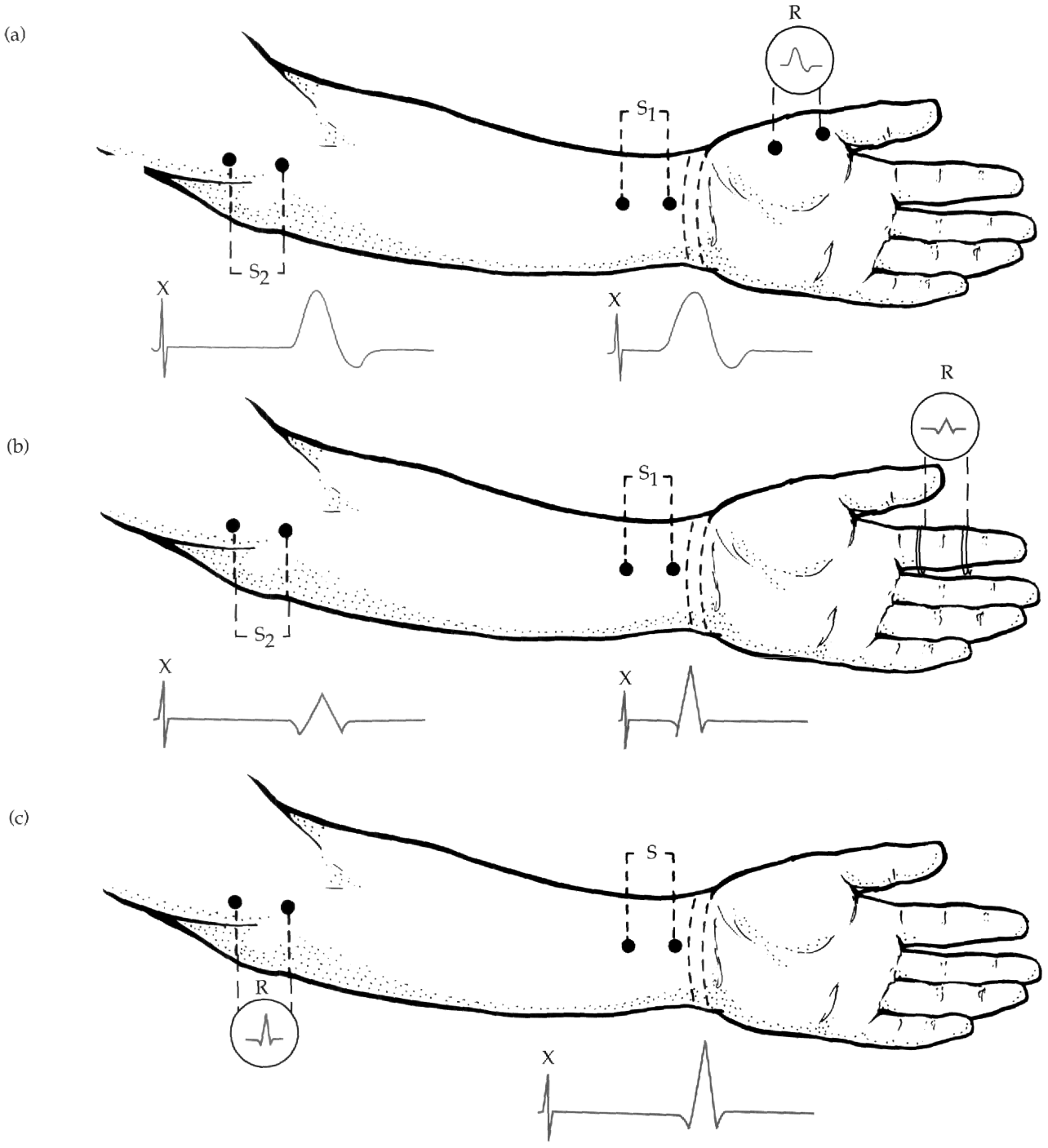

The NCS came into clinical use more than a decade after the NEE, in the late 1950s. During the NCS, brief electrical stimulation is applied to a nerve and the evoked nerve or muscle response is recorded. If motor nerve fibers (i.e., nerve fibers that innervate muscles) are stimulated, the electrical activity, i.e., the compound muscle action potential (CMAP), generated in one of the muscles supplied by that nerve is recorded and the study is referred to as a *motor NCS*. For example, the standard median motor NCS consists of stimulating the nerve at the wrist and elbow while recording over the median-innervated thenar (base of thumb) muscles in the hand (Figure 1.3a). Conversely, if the stimulus is applied to sensory nerve fibers (i.e., nerve fibers that conduct sensation to the spinal cord), the nerve impulses initiated at the site of the stimulus are recorded along the nerve itself at some more proximal or distal point as a sensory nerve action potential (SNAP). The procedure is then referred to as a *sensory NCS*. For example, the median nerve is stimulated at elbow and wrist while recording from the median digital (sensory) nerves supplying the index finger (Figure 1.3b).

Although most of the major limb nerves are actually mixed nerves in that they contain both motor and sensory fibers, for technical reasons their motor and sensory nerve fiber components usually are studied separately. At times, however, mixed NCSs are performed, during which a stimulus is applied to a nerve trunk containing both motor and sensory fibers and the nerve action potentials generated by that stimulus are recorded at a more proximal point. For example, the median nerve is stimulated at the wrist while recording over it at the elbow (Figure 1.3c).

Special electrodiagnostic studies include a number of procedures, such as H-responses, F-waves, blink reflexes, repetitive stimulation studies, and single-fiber electromyography. Except for H-responses and F-waves, these tests have much more limited application than the NCS and NEE. Thus, blink reflexes are performed only when abnormalities of the 5th (trigeminal) and/or the 7th (facial) cranial nerves or their central connections are suspected. Similarly, repetitive stimulation studies are performed only when a defect in neuromuscular transmission is suspected. In contrast, H-responses and F-waves are considered an integral part of the basic electrodiagnostic examination in the majority of EMG laboratories and, therefore, are performed routinely along with the NCS and NEE.

The electrodiagnostic examination has a number of advantages and limitations. A major advantage is that it can provide objective evidence of a peripheral neuromuscular abnormality at a time when the clinical examination is normal or equivocal, or when it is unreliable due to an associated CNS abnormality or from poor patient effort related to hysteria, malingering, or pain on activation. Another benefit is that it often can localize a focal lesion. Moreover, with both focal and generalized nerve lesions, electrodiagnosis can provide important information regarding prognosis by determining the severity of the disorder and the type of pathophysiology present (axon degeneration versus demyelination). Similarly, with both neuromuscular transmission disorders and myopathies, it can determine the severity of the process, help classify it, and aid in determining etiology. Another significant benefit of electrodiagnosis is that it often allows differentiation of disorders that are clinically similar; e.g., some types of anterior horn cell diseases (neurogenic disorders) and some types of muscular dystrophy (myopathic disorders), both of which affect children and adolescents and produce prominent proximal muscle weakness.

A major limitation shared by all components of the EMG examination (including the NCS, NEE, and all the special studies) is that they assess only the large, heavily myelinated nerves. At no time are the unmyelinated or lightly myelinated nerve fibers, such as

Figure 1.4 — An EMG machine.

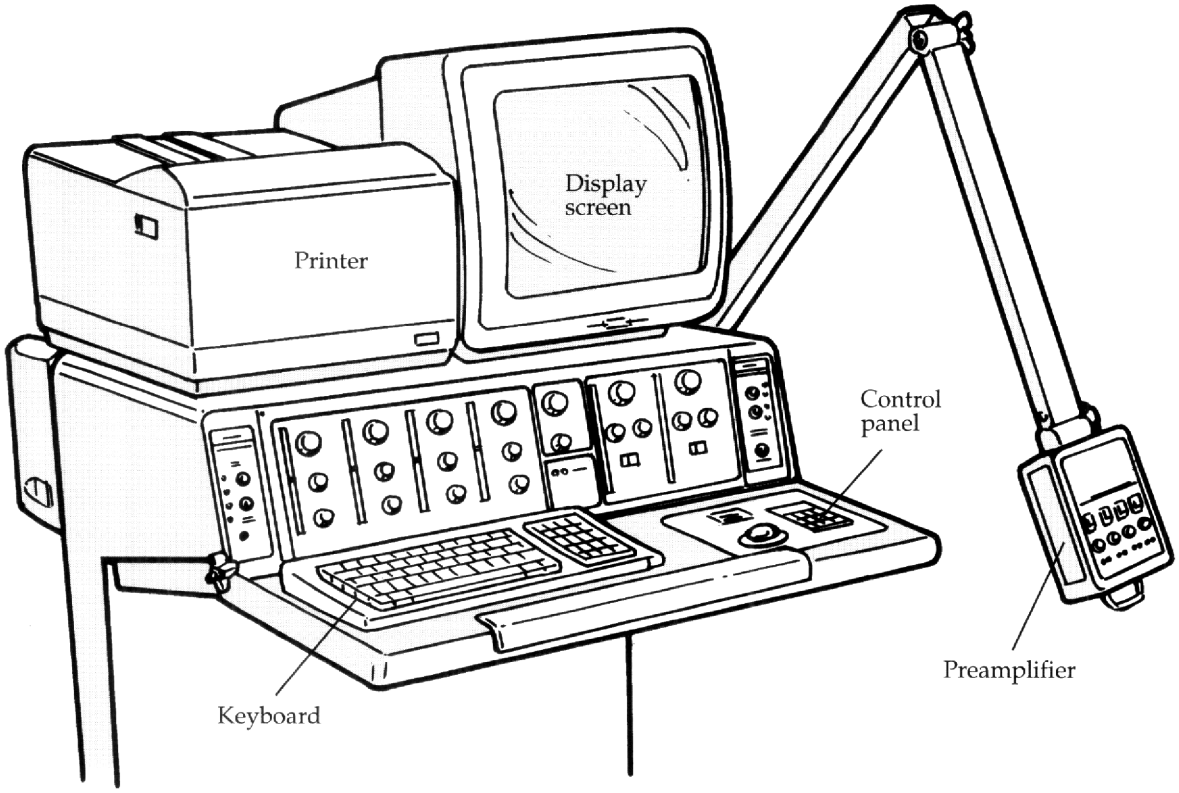

Figure 1.5 — Typical patient, examiner, and machine arrangement.

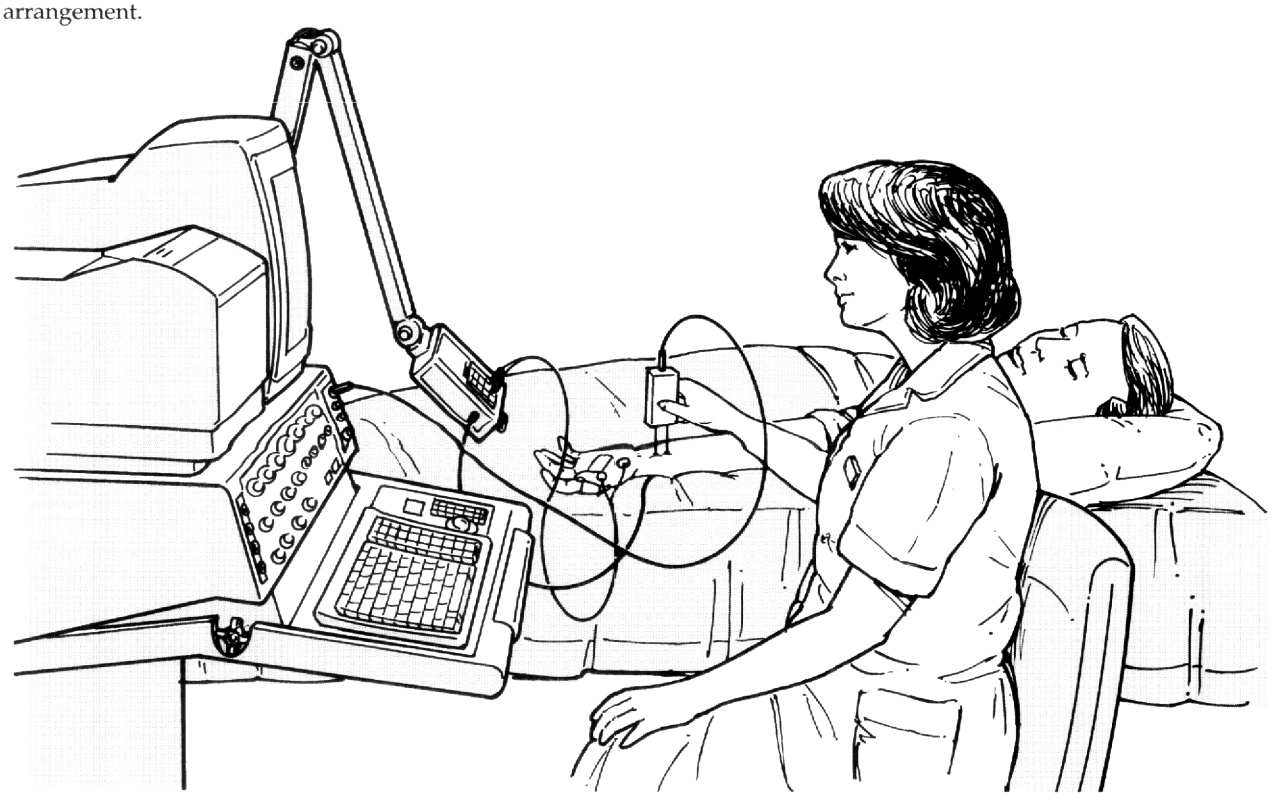

those that carry pain and temperature, evaluated. This limitation often proves more apparent than real because nerve fibers of various sizes are intermixed within peripheral nerves and, consequently, most types of injury do not damage only one type. Moreover, of the relatively few injuries that do so (e.g., compression and stretch), most typically affect only the myelinated fibers because of their greater susceptibility due to their larger size. A second major limitation is that electrodiagnosis has a highly variable sensitivity for different peripheral neuromuscular disorders. This variability extends to members of the same general disease category; e.g., some types of muscle disorders produce striking findings on the electrodiagnostic examination and are readily recognized, while others cause no detectable abnormalities. Thus, false-negative EMG examinations invariably occur and are inherent to the procedure. Finally, a number of factors can severely limit the value of the EMG examination; e.g., it tends to be less helpful in patients at the extremes of age and in patients who had poliomyelitis in their youth.

1.1 *The Electromyographic Examination–Practical Details*

The electrodiagnostic examination typically is performed in a quiet room under somewhat subdued lighting. Usually certain rooms are dedicated to this purpose, although the examination can be performed in other areas, such as the intensive care unit, whenever indicated. The typical EMG examination room contains an examining table covered with a soft pad and made of wood rather than metal to reduce electrical artifact, a chair for the examiner, and the necessary electrodiagnostic equipment. Essentially the same electromyograph machine and associated equipment are used for all portions of the examination, including the NCS and the NEE (Figure 1.4). These consist of various electrodes used to stimulate the nerves, to record responses from the nerves and muscles, and to reduce electrical artifact. Other necessities include connecting cables to transmit the electrical activity between the electrodes and the machine, preamplifiers and amplifiers, various filters, and components which allow the information to be assessed and analyzed by the examiner, such as a cathode ray oscilloscope for visual display and a loudspeaker for aural analysis. A loudspeaker is particularly beneficial during the NEE, because some of the electrical potentials generated can be more easily recognized by their characteristic sounds than by their appearance. Frequently, the electrical activity is not only displayed on the cathode ray oscilloscope screen for instantaneous review, but also captured on videotape, film, or various types of special paper for storage as a permanent record. A nerve stimulation unit is a necessary component of the EMG machine for the NCS and for most of the special studies.

A number of additional items are required whenever electrodiagnostic examinations are performed: adhesive tape to hold the (surface) electrodes in place; electrolytic paste to establish satisfactory contact between the electrodes and the skin; a measuring device such as a tape measure or calipers to establish the set distances between the stimulating and recording electrodes required for some NCS and to determine the distance between the two stimulation points when conduction velocities (see below) are calculated; and, finally, gauze and alcohol to clean the skin before performing the NCS and NEE.

During the typical EMG examination, the patient lies in a comfortable position on the examining table to ensure adequate muscle relaxation. Both the seated electromyographer and the EMG machine face one another beside the examination table (Figure 1.5).

Figure 1.6 — Histologic features of a myelinated motor nerve fiber.

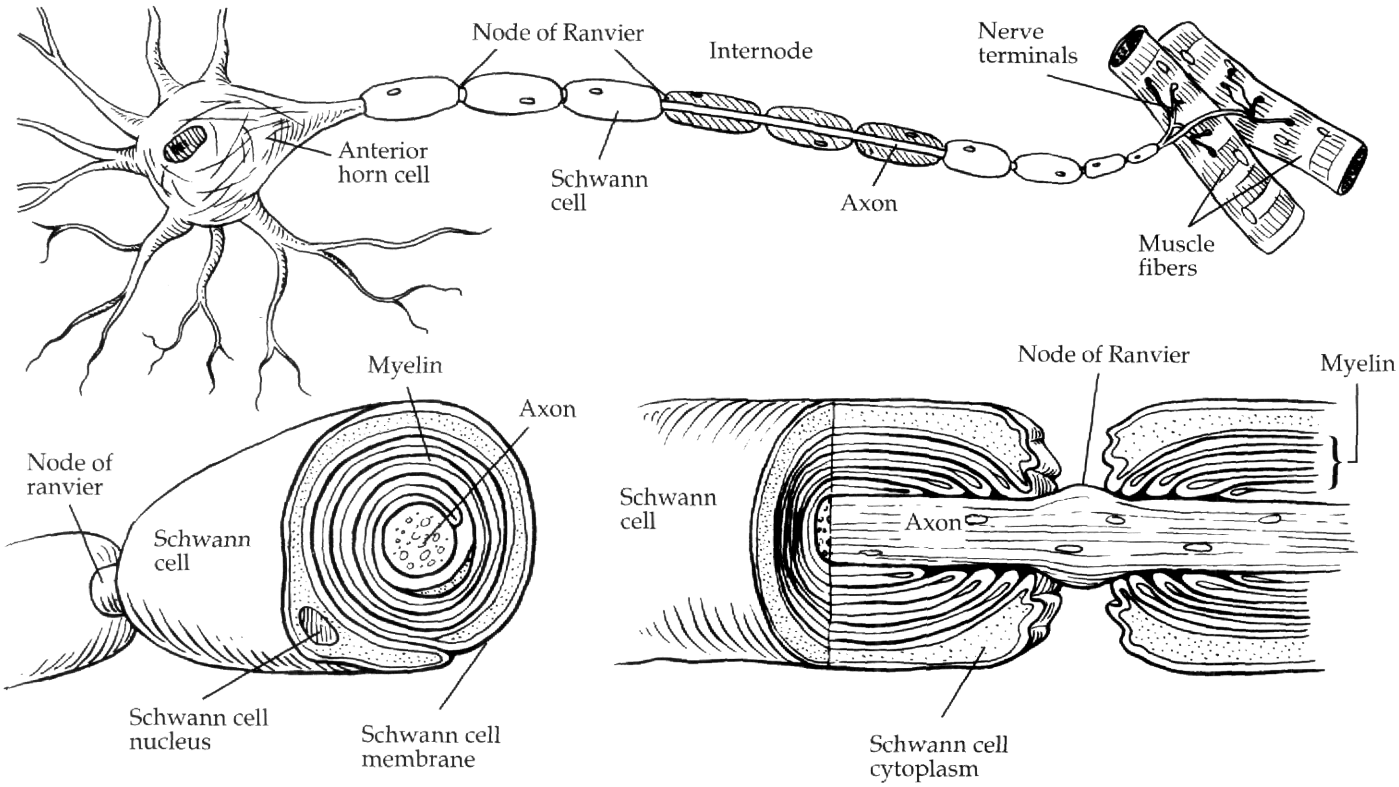

Figure 1.7 — A single motor unit and its component parts.

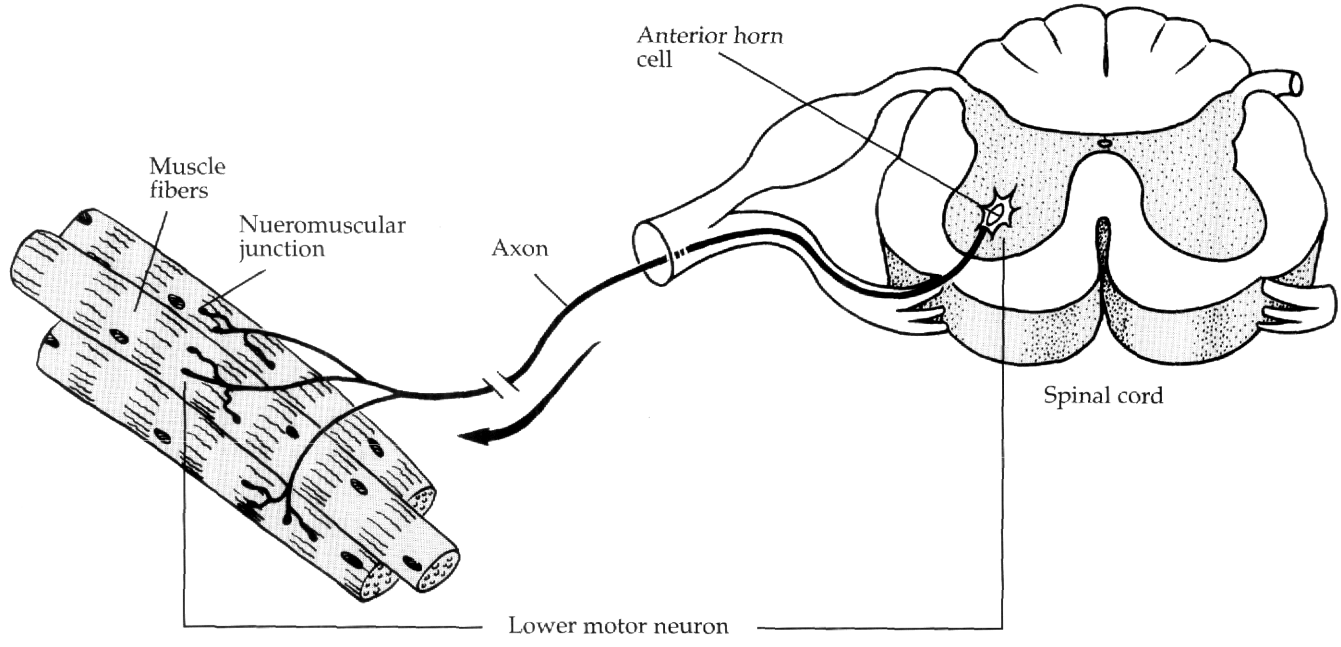

Electromyographers are physicians with special knowledge about both the disorders of the peripheral neuromuscular system and the particular electrodiagnostic changes they produce. In North America, almost all physicians who perform electrodiagnosis are either neurologists or physiatrists (physical medicine physicians). In some high volume EMG laboratories, the NCS portion of the electrodiagnostic assessment is performed by specially trained technicians. This portion of the examination can be delegated as long as the responsible electromyographer determines the particular NCS to be performed, is immediately available at all times for consultation during the NCS, and subsequently interprets it. In contrast, the NEE cannot be delegated to technicians because it is a very fluid procedure which cannot be standardized. Even though most electromyographers routinely assess a certain set of muscles on patients during the NEE (depending upon the particular problem for which the patient was referred), additional muscles frequently must be added as the study unfolds.

Electrodiagnostic examinations are not standardized from one EMG laboratory to another, even for patients with presumably the same disorder. This applies not only to the particular nerves assessed during the NCS and the specific muscles sampled during the NEE, but even to the exact NCS performed on a given nerve. For example, several different techniques have been described to study the various median sensory nerve fibers. The electrodiagnostic examinations in the same EMG laboratory also cannot be standardized from one person to another because the specific studies performed depend on such factors as the reason for referral and what changes, if any, occur as the assessment proceeds. Only when patients studied in the same EMG laboratory are referred for, and have, the same disorder of similar severity are the electrodiagnostic examinations performed likely to be essentially identical. In this respect, even the most basic EMG examination differs considerably from the routine electroencephalographic examination and electroretinographic examination, because far more possibilities exist regarding where and what to assess with it. For example, the electrodiagnostician must decide how many and which limbs to study. For each limb, which of the many available NCSs should be performed and which of the numerous muscles should be sampled on the NEE? What special studies, if any, should be done?

In the following sections, information is presented about fundamental electronics, anatomy, and neurophysiology. The various components of the EMG equipment will be discussed, as will both of the basic portions and procedures of the electrodiagnostic examination (the NCS and NEE). The types of possible altered physiology will be reviewed. Finally, the practical application of the electrodiagnostic examination to clinical disease will be discussed and some of the typical electrodiagnostic findings associated with various disorders of the peripheral neuromuscular system will be presented.

1.2 *Anatomy*

The PNS is divided into a sensory (afferent) system and a motor (efferent) system. Some classifications include the ANS as a third subdivision, although most view it as a separate entity. Major nerve trunks of the extremities almost always carry nerve fibers from all three systems.

All nerve fibers are composed of axons, the tubular structures containing axoplasm and surrounded by the surface membrane or axolemma. The axoplasm contains cytoplasmic material holding filamentous structures and organelles. Microtubules and neurofilaments are elements of the cytoskeleton involved in axonal transport mechanisms and

Figure 1.8 — The neuromuscular junction.

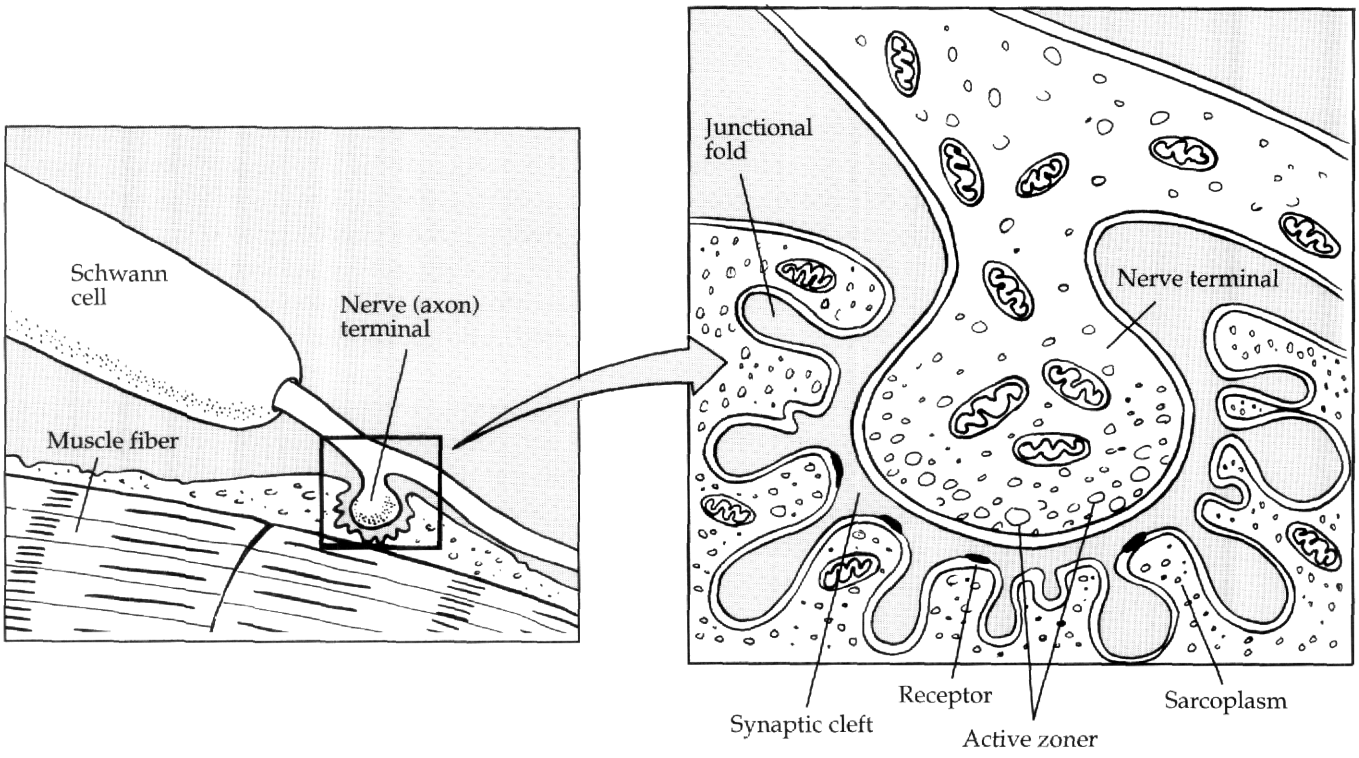

Figure 1.9 — Anatomic relationship between the perpendicularly oriented longitudinal and transverse tubules in a muscle fascicle.

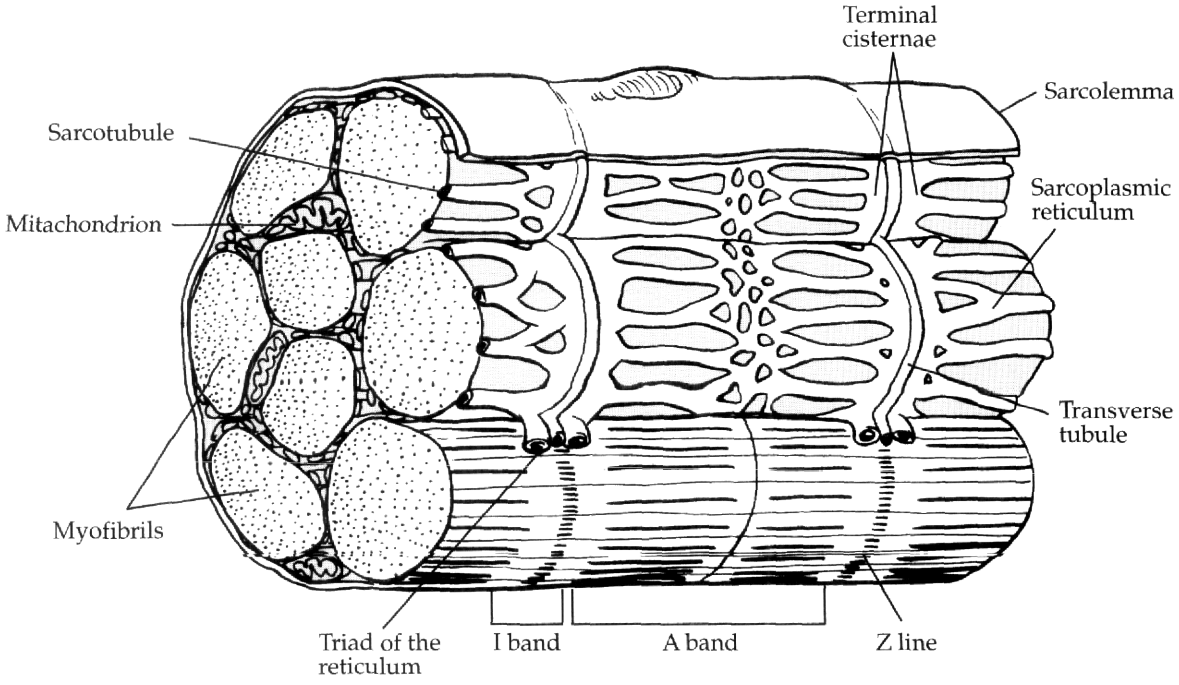

are responsible for moving nutrients and cellular factors to and from the distal regions of the nerve. Axons are surrounded by satellite cells called Schwann cells. The myelin covering of many axons consists of whorls of alternating layers of lipid and protein, produced by the Schwann cells. Myelination is segmental, with tiny spaces at regular intervals left unmyelinated, called nodes of Ranvier, where membrane ion channels are concentrated (Figure 1.6). Myelin serves as an insulation that facilitates electrical impulse generation along the nerve surface membrane. Nerve conduction velocity is increased in myelinated nerves, because the advancing electrical field of depolarization jumps from one node of Ranvier to the next, a property called saltatory conduction.

The size and electrical conductive properties of nerve fibers vary over a large spectrum. The smallest nerve fibers, less than 1 micron in diameter, are unmyelinated and carry autonomic and sensory pain information. The largest fibers, up to 20 microns in diameter, carry either motor or sensory information pertaining to proprioception, vibration, and muscle spindle function. A direct relationship exists between the diameter of the axon and the thickness of its myelin sheath. A direct relationship also exists between the total fiber diameter and the speed of impulse propagation along its surface membrane.

The peripheral motor system is known as the motor unit (Figure 1.7). As noted, it includes the AHC that lies in the anterior aspect of the spinal cord, the axon derived from it, branchings of the motor axon, motor nerve terminals, their adjacent muscle endplates (neuromuscular junctions), and the muscle fibers innervated by all terminal branches arising from the main axon.

The neuromuscular junction is the synapse between the motor nerve terminal and the muscle endplate (Figure 1.8). Vesicles of acetylcholine (Ach) produced locally in the nerve terminal concentrate at active release zones along the terminal's surface membrane. Lying opposite, a highly redundant folding of the surface membrane of the muscle is specifically organized with Ach receptors at the peaks of the membrane folds. Each receptor is part of a large glycoprotein molecule forming the ion channel that opens when Ach occupies its binding site. In the troughs of the folds, acetylcholinesterase lines the membrane, metabolizing Ach to acetate and choline for re-uptake by the nerve terminal.

Groups of individual muscle fibers constitute a muscle fascicle, surrounded by a delicate connective tissue called the endomysium (Figure 1.9). Muscle fascicles, in turn, are grouped together and are surrounded by a coarse perimysium. The whole muscle belly is surrounded by a connective tissue called the epimysium. The smallest contracting unit is the muscle fiber, with a surface membrane (sarcolemma) and internal contents (sarcoplasm). Within the sarcoplasm are many bundles of cylindrical myofibrils which, in turn, are composed of longitudinally-oriented contractile filaments: actin and myosin. During muscle fiber contraction, filaments slide beside each other, thus shortening the muscle fiber and producing muscle contraction.

1.3 *Neurophysiology*

1.3.1 Nerve

One property shared by essentially every cell of the body is the presence of electrical potentials across its surface, or cell, membrane. Some cells (e.g., nerve, muscle) are capable of repeatedly abolishing and then reforming the potential gradient across their cell membranes. By doing so, these cells are able to transmit impulses as information.

At rest, a large nerve fiber has a potential across its cell membrane of approximately 90 millivolts (mV). This means that if a reference, or indifferent, electrode is placed in the interstitial, or extracellular, fluid surrounding the nerve fiber and a very small electrode is then inserted into the nerve fiber itself, an electrical potential of 90 mV is recorded between the two electrodes. By convention, the external electrode serves as the reference, so the interior of the cell is described as negative compared to its exterior (Figure 1.10). For very brief periods during nerve stimulation (approximately 3/10,000 of a second), this transmembrane potential is reversed, passing from -90 mV to +35 mV and then back again to -90 mV. This rapid change is called an *action potential*. The potential change from -90 mV to +35 mV is called *depolarization*, while the second portion, when the potential passes from a peak of +35 mV back to -90 mV and re-establishes the resting potential, is referred to as *repolarization* (Figure 1.11).

Figure 1.10 — A 90 mV transmembrane potential exists between the exterior and the interior of a nerve cell.

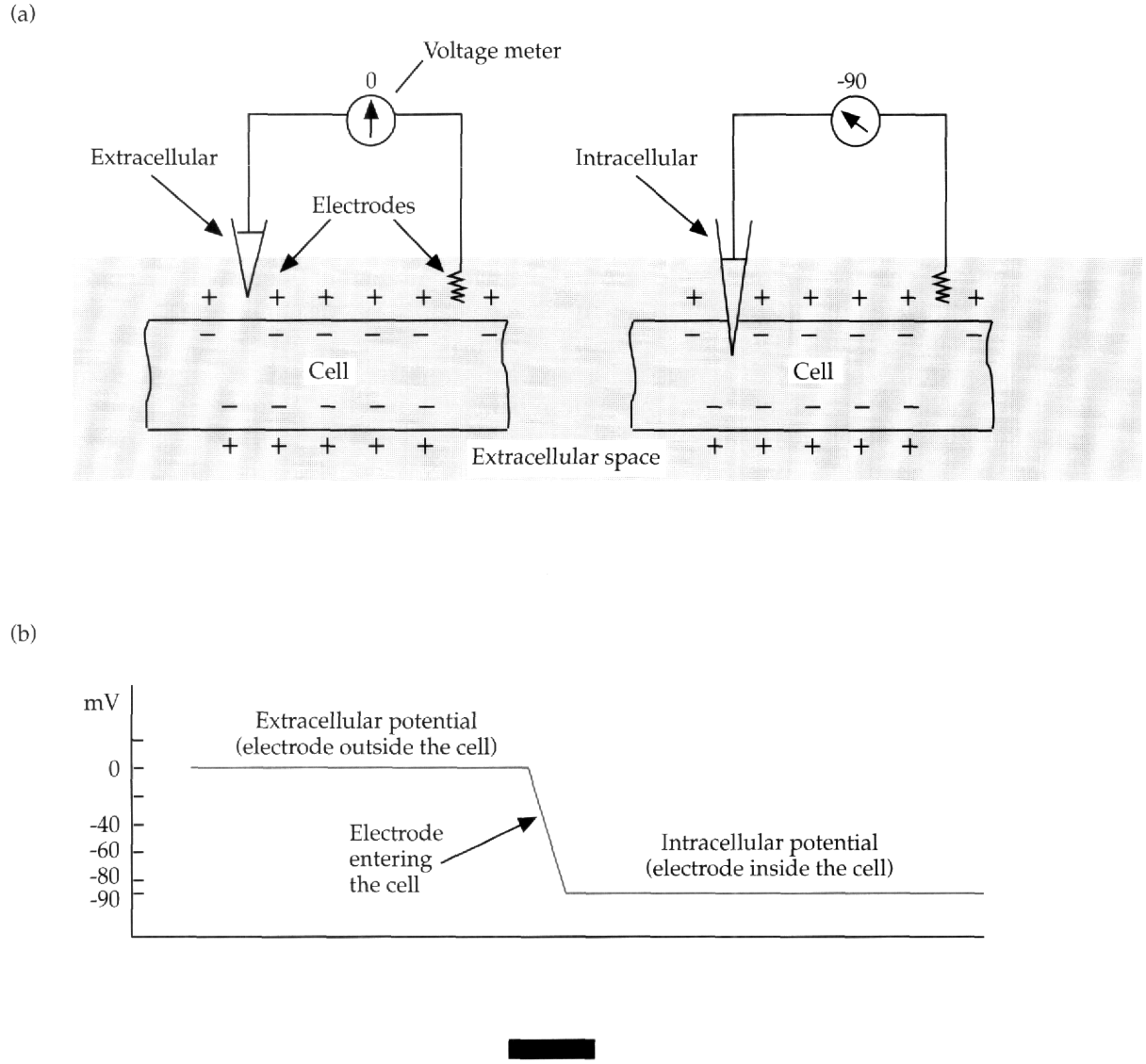

Figure 1.11 — The action potential.

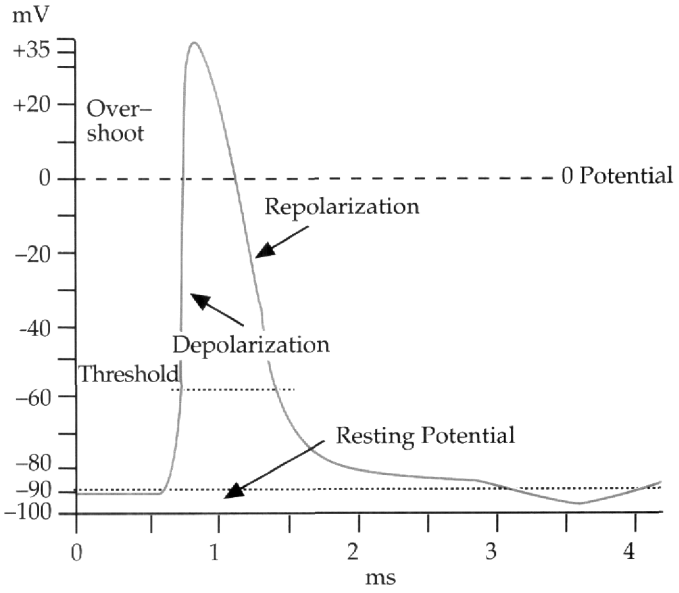

Figure 1.12 — Composition of the intracellular and the extracellular fluids.

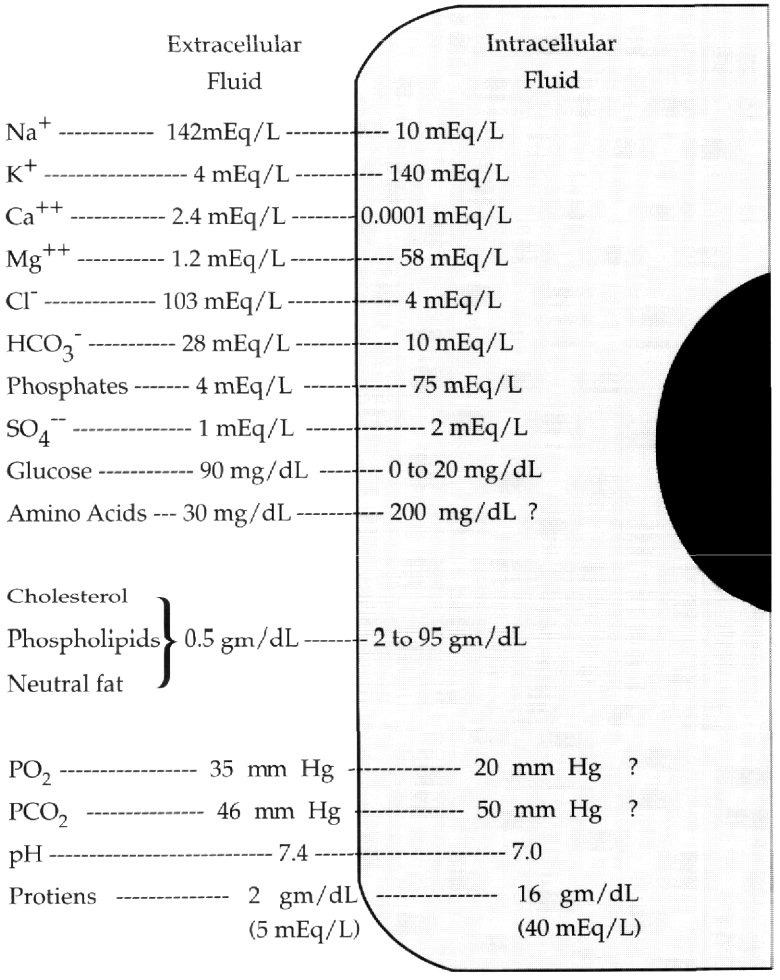

Figure 1.13 — Membrane charge during the resting potential. K^+ = potassium ions; Na^+ = sodium ions; Cl^+ = chloride ions; A^- = fixed intracellular ions (primarily intracellular proteins).

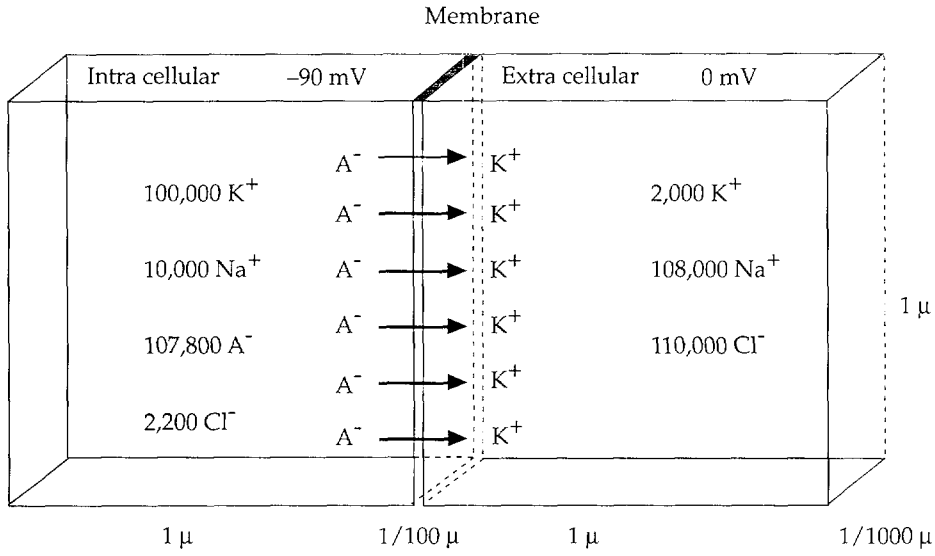

Figure 1.14 — Contributions to the resting membrane potential: (a) passive diffusion of the potassium ions (–86 mV). (b) the sodium–potassium pump (–4 mV).

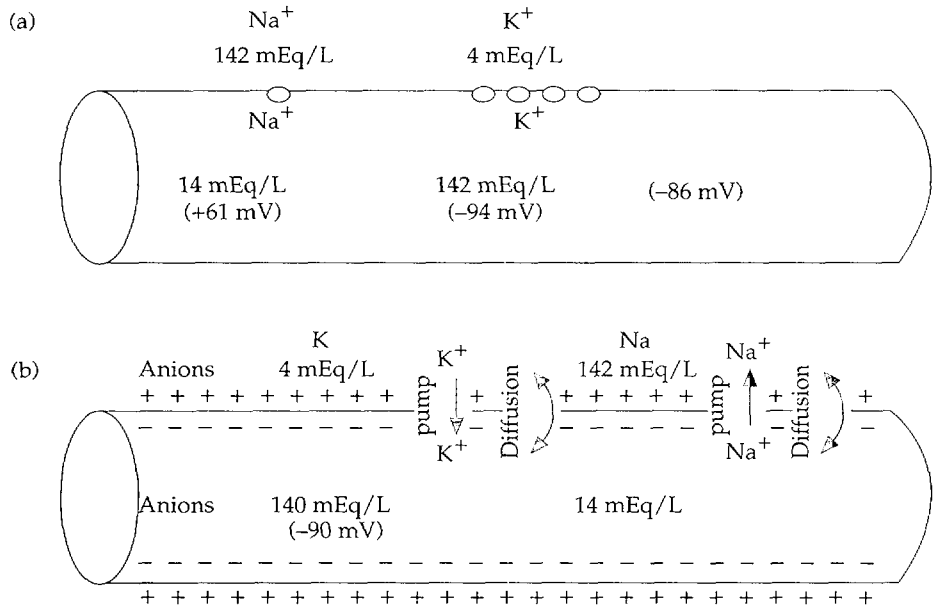

1.3.1.1 The Resting Membrane Potential

The cell membrane of a nerve or muscle fiber is a very thin, complex structure consisting of a bilayer of phospholipid molecules and protein. It has different degrees of permeability for different substances and these can change markedly at times. The membrane is permeable to lipid-soluble substances but rather impermeable to water-soluble substances, such as ions. However, the latter can still move across the membrane. They do so because protein macromolecules are embedded within the membrane that act as channels, or pores, for their passage. Some of these channels are open at all times while others, referred to as voltage-dependent or voltage-gated channels, open or close, depending upon the transmembrane potential. The ion channels can be very selective for the type of ion (sodium, potassium, calcium, etc.) they allow to pass through them in the open state.

To remain in a resting state, a nerve or muscle cell must meet two requirements: (1) equimolarity on the inside with respect to the outside, and (2) electric neutrality.

The first requirement means that the number of particles, organic and inorganic, contributing to the osmolarity of the intracellular and extracellular solution should be equal. This state is accomplished by the extracellular fluid containing mostly inorganic particles, and the intracellular fluid containing a mixture of inorganic and organic particles (Figure 1.12). To achieve the second requirement, electric neutrality, the number of positively-charged ions on both the external and the internal surfaces of the membrane must be equalized by the same number of negatively-charged particles. The negatively-charged intracellular proteins, organic sulfate compounds, and organic phosphate compounds, are restricted to the inside of the cell because the cell membrane is impermeable to them.

Consequently, the major charged ions, or electrolytes, such as sodium, potassium, and chloride, must establish themselves in various concentrations on both sides of the membrane to achieve electric neutrality (Figure 1.13). Whether these ions move into or out of the cell depends upon: (1) their chemical or concentration gradient, and (2) their electrical gradient. These are referred to, collectively, as the *electrochemical potential gradient* for each ion. The degree of importance of each of the major charged ions in determining the transmembrane voltage is proportional to the membrane permeability of each. Whenever the membrane is relatively impermeable to both sodium and chloride, the transmembrane potential is dominated almost solely by the electrochemical potential gradient of the potassium ions. Similarly, the transmembrane potential becomes essentially the product of sodium ion diffusion whenever the membrane becomes selectively permeable to that ion.

The negatively-charged chloride ions are much more prevalent extra-cellularly than intracellularly. Their diffusion gradient, based on their concentration alone, would be towards the inside of the cell. However, the electrical gradient opposes this, because of the negatively-charged ions within the nerve fiber to which the cell membrane is impermeable; e.g., intracellular proteins. Chloride ions pass through the resting membrane in relatively small quantities and the permeability of the chloride channels remains the same during the action potential. For these reasons, chloride ions function rather passively in the establishment of both resting and action potentials.

The potassium ions, in contrast to chloride ions, are positively charged and are much more abundant within, rather than outside the cell. Consequently, their concentration gradient favors outward movement which is prevented by the electrical charge on the membrane. At rest, the membrane is much more permeable to potassium than to sodium ions. Hence, the resting membrane potential is primarily due to the potassium diffusion potential based on the unequal distribution of ions between the inside and the outside of the cell.

Positively-charged sodium ions are in much higher concentration outside the nerve cell than within it, and their charge favors inward movement. Consequently, both the concentration and the electric gradient for sodium are inward. Yet, the sodium ions remain mainly outside the cell during the resting state. This is partly because the membrane during that period is relatively impermeable to sodium by a factor of 1 to 100, compared to potassium. In addition, sodium ions are actively extruded from the interior of the cell during the resting state by an energy-consuming sodium pump. This is actually a sodium-potassium pump in that for every three sodium ions forced to the outside, two potassium ions are carried inside. This 3:2 ratio causes a continuous loss of positive charges from the inside of the membrane, creating an additional small degree of negativity (-4 mV), over that which can be explained by diffusion alone (passive diffusion of the sodium and potassium ions yields a summated resting potential of -86 mV). (See Figure 1.14).

In summary, a number of factors contribute in varying degrees to the establishment and maintenance of the resting membrane potential. However, most of the -86 mV is due to the potassium diffusion potential, while the remaining -4 mV results from sodium-potassium pump activity.

1.3.1.2 The Action Potential

Impulses are transmitted along nerve and muscle membranes by means of action potentials in which the membrane potential undergoes a series of rapid, reversible changes. It converts from a negative resting potential to a positive action potential because of the rapid transfer of positive charges to the interior of the fiber. It then returns to a negative potential again as the positive charges are transported back to the exterior. Whenever the resting membrane potential starts to become less negative, i.e., begins to rise from -90 mV toward 0, some of the sodium channels, impervious to sodium ions during the resting state, begin to open. The inflow of sodium ions causes a continued rise in the membrane potential, opening even more sodium channels. Soon a point is reached, somewhere between -70 mV and -50 mV, when all the remaining closed sodium channels are abruptly opened and the membrane permeability to sodium ions suddenly increases markedly (up to a 5,000-fold increase). The potassium channels also open during depolarization, although slightly after and more slowly than the sodium channels. Because of the influx of sodium ions, the transmembrane potential abruptly shifts from approximately -70 mV to +35 mV. The sodium channels remain open for only a few ten-thousandths of a second and then close. The abrupt decrease in sodium entry into the cell and the simultaneous egress of potassium ions from the cell soon leads to repolarization and the reestablishment of the resting membrane potential (Figure 1.15).

Figure 1.15 — Action potential, with the sodium and potassium ion permeability changes superimposed.

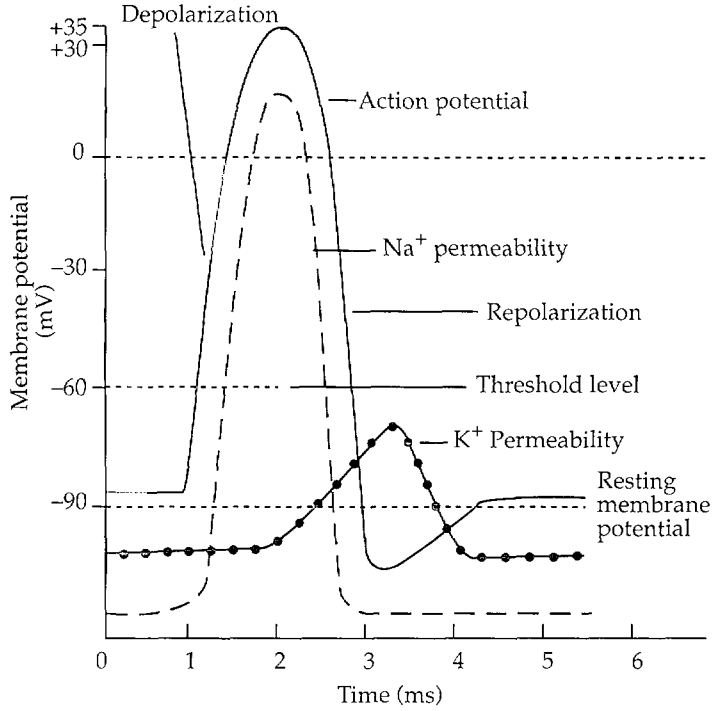

The cell membrane acts as an electrical capacitor in that positive charges, after they are pumped from the inside to the outside of the membrane, line up along the outside surface. The negatively-charged ions, remaining within the cell, line up along the inside surface of the membrane. This means that only a relatively few positive ions must be transported outward to create a negative internal potential, just enough to establish the electrical dipole layer at the membrane. All the remaining ions inside the nerve fiber can have equal numbers of positive and negative charges. Consequently, only a very minute percentage of the total of positively-charged ions — about one five-millionth to one one-hundred-millionth of the ions available — need to be transported from the interior to the exterior of the cell to establish a normal resting membrane potential. Only an equally small number need to move from outside to inside the cell to change the transmembrane potential from -90 mV to +35 mV, which can occur in as brief a time as one ten-thousandth of a second. This incredibly rapid shifting of ions across the nerve and muscle membranes generates the electrical signals recorded in the EMG laboratory.

Nerve action potentials can be produced by electrical stimulation of the nerve because current flows through the tissues between the two prongs — the anode and cathode — of the stimulator. Whenever this current reaches a certain intensity, it enters the nerve fiber and passes longitudinally through a short segment of it, i.e., through the portion situated between the two stimulator prongs, and then exits. Beneath the cathode, negative charges accumulate outside the axon membrane, causing the inside to become relatively more positive. Under the anode, the negative charges tend to leave the cell surface, making the inside of the cell relatively more negative. Thus, under the cathode the transmembrane potential rises toward zero. This causes some sodium channels to open. Threshold voltage is soon reached, the voltage-dependent sodium channels open en masse, and rapid depolarization ensues (Figure 1.16).

Figure 1.16 — A peripheral nerve can be depolarized at many points along its course by percutaneous stimulation.

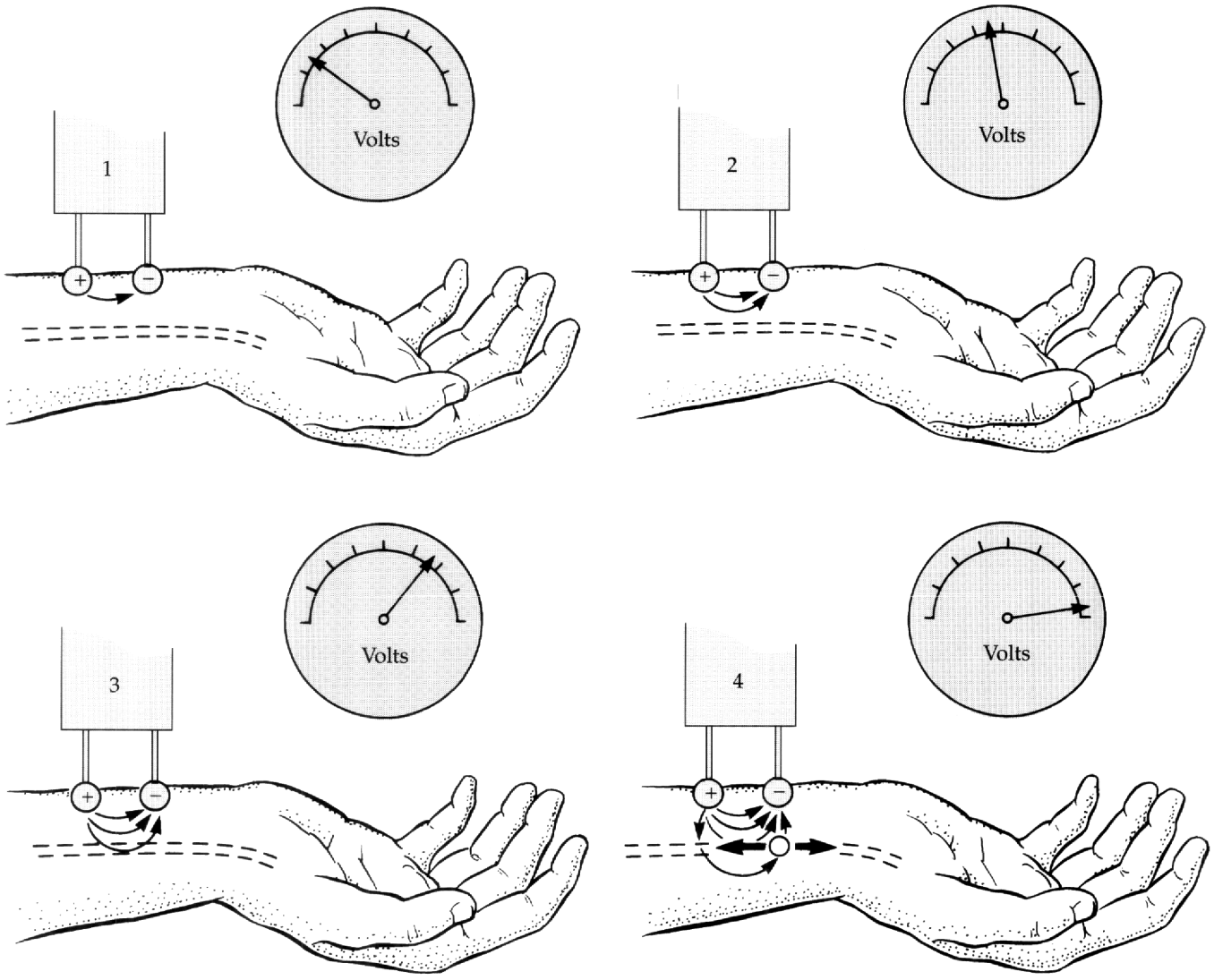

An action potential produced at any single point along an excitable membrane usually depolarizes adjacent portions of the membrane because once the in-rushing positively-charged sodium ions are within the cell, they turn and pass along its core for several millimeters. This increases the transmembrane voltage (by taking it towards zero) in adjacent segments to cause it to rise above threshold voltage. Other action potentials are thereby triggered as the sodium channels in the adjoining areas open. The action potential spreads in both directions from the initially activated site. This is called the *propagation of the action potential*. Under ordinary circumstances, action potentials begin at one end of the nerve fiber (i.e., the AHCs for the motor fibers, and their receptor organs for the sensory fibers) and then travel unidirectionally to the opposite end. However, nerve fibers themselves readily conduct in either direction. Bi-directional nerve impulse transmission results whenever peripheral nerve trunks are stimulated (Figure 1.17).

Figure 1.17 — Once a nerve is depolarized at some point along its course, a wave of depolarization passes in both directions from that point (i.e., both peripherally and centrally), followed by repolarization.

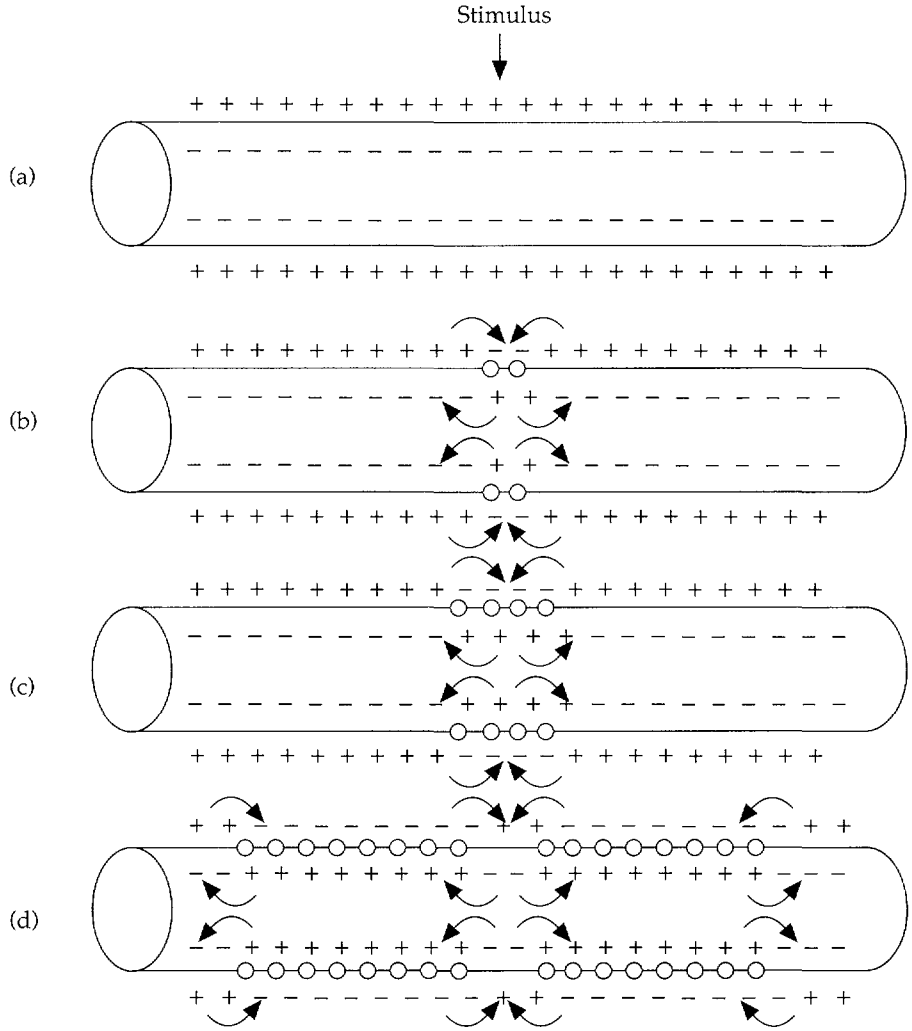

With myelinated nerve fibers, action potentials occur only at the nodes of Ranvier, the regularly repeating points along the axon situated between adjacent myelin segments. At these areas, the axons are essentially uninsulated and ions can readily pass between the intracellular and extracellular fluids. Therefore, only small nerve segments are depolarized (Figure 1.18), unlike the situation with unmyelinated nerves, in which virtually all the nerve membrane is depolarized in a progressive fashion. The node-to-node impulse conduction, or saltatory conduction, along myelinated nerve fibers permits much greater speed of impulse transmission than does the continuous conduction of unmyelinated nerve fibers, because the axon surface area to be depolarized is relatively very small and therefore very rapidly depolarized and because the impulse actually jumps from one node to the next. The large myelinated nerve fibers in humans conduct impulses normally between 40 m/sec to 65 m/sec, or 90 miles per hour to 145 miles per hour.

Figure 1.18 — Saltatory conduction, in which the nerve action potential jumps from one node of Ranvier to the successive one.

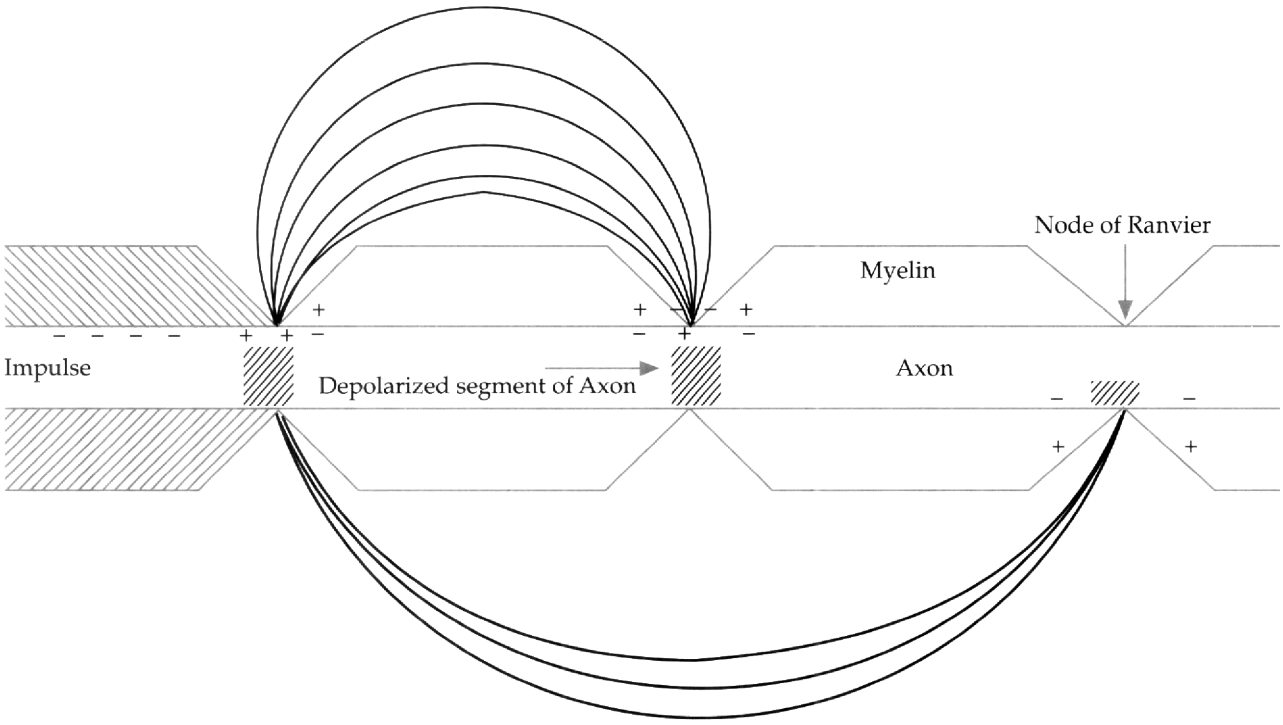

With focal demyelination, the electrical characteristics of the demyelinated nerve segments may be altered by increased internodal capacitance and conductance to the point that adjacent internodes cannot be depolarized, resulting in conduction block. Alternately, the adjacent internode may ultimately be depolarized, but the process may require a longer interval to reach threshold voltage, causing conduction slowing.

1.3.2 The Neuromuscular Junction

Chemical transmission across the neuromuscular junction is mediated by Ach, which is released in vesicles containing 10,000 molecules of this chemical. Release occurs with depolarization of the nerve terminal at active sites of Ach release. These sites can become depleted of Ach vesicles. If release occurs at a steady, slow pace of less than 5 vesicles/sec, the amount of Ach release never falls below that required to produce a threshold depolarization of the postsynaptic muscle membrane, the so-called safety factor.

The postsynaptic portion of the neuromuscular junction is characterized by highly infolded muscle membrane, which holds the Ach receptor molecules. These receptors are integrated structurally with the ion channels responsible for sodium and potassium flux across the muscle membrane. When an Ach molecule reaches the Ach receptor binding

site, a conformational change occurs, opening the ion channel and allowing sodium influx. After leaving the binding site, Ach molecules drift to the troughs of the junctional folds where they are metabolized by acetylcholinesterase into acetate and choline for reuptake by the nerve terminal.

The measurable electrical discharge produced after depolarization of the muscle membrane secondary to release of a single vesicle of Ach is termed a *miniature end-plate potential*. Such electrical discharges are present at rest, since a steady state leakage of Ach vesicles occurs across the neuromuscular junction to maintain structural integrity of the end-plate. Miniature end-plate potentials are insufficient to produce the threshold depolarization of the muscle membrane needed to induce a propagated action potential. Only when many miniature end-plate potentials are summated after massive Ach release can such an action potential be generated.

1.3.3 Muscle

Propagated action potentials proceed from the muscle end-plate, along the muscle fiber membrane. Action potentials reach the sarcoplasmic reticulum of the individual muscle fibers through the transverse tubules. This produces a release of calcium from terminal cisterns of the longitudinal tubules. Released calcium binds to troponin, which shifts the interaction between tropomyosin and actin (Figure 1.19). This frees a myosin molecule to form a new bridge to an actin molecule, pulling actin past myosin as these chemical bridges are formed. The effect is to shorten the sarcomere and develop muscle tension. After the action potential passes, calcium is pumped by ATP-dependent active transport back into the sarcoplasmic reticulum. Tropomyosin loses its position with actin and the bridges between actin and myosin are broken, producing muscle relaxation.

Figure 1.19 — Fine structure of the thin actin filament with actin molecules attached to globular-shaped troponin and rod-shaped tropomyosin in an orderly arrangement.

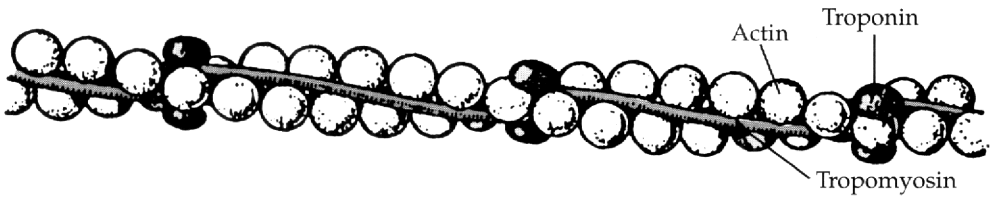

1.4 Electricity and Electronics

Clinical electromyography includes the recording of electrical signals from muscle and nerve. An understanding of the basic concepts of electricity is essential to appreciate the techniques of the nerve conduction studies and the NEE. The following is a brief overview of the basic concepts of electricity and electronics.

Electricity is the phenomenon of flow of electrical charge. Charge (Q) is actually a concept that evolved from empirical observations of electricity in nature and in experiments. Although charge can be either positive or negative, it is the flow of the negative charge of electrons that is responsible for electricity. The primary unit of negative charge is the coulomb, which represents the negative charge of 6.25×10^{18} electrons. Because electricity represents a flow of charge, it must be directional. The direction of charge flow has been arbitrarily defined as flow from positive to negative. Current (I) is the amount of charge flow per unit time. An ampere (A) is the primary unit of current, defined as the flow of one coulomb of charge per second.

Voltage refers to the amount of potential electrical energy between two charged points in space. Voltage, which is often designated by V or by E for electromotive force (EMF), is measured in units called volts. One volt is equal to one joule divided by one coulomb. In other words, one joule of energy is required for one coulomb of charge to move across a potential of one volt.

Resistance (R) is encountered when charge moves in matter. The energy lost from this resistance is dissipated into heat. Conductors refer to matter in which resistance is minimal, while insulators refer to matter in which resistance is very high. The energy lost due to the resistance of charge flow (current) in matter results in a reduction of the voltage between the two points of charge flow. The relationship between resistance, current, and voltage is Ohm's law and may be expressed by the formula:

$$R = V / I \qquad \textbf{Equation 1.1}$$

where

R = resistance
V = voltage
I = current.

It may be expressed in different terms, i.e., $V = R \times I$, or $I = V/R$. The units of resistance are Ohms. One Ohm equals one volt divided by one amp.

Power is the rate of energy flow per unit time and may be expressed as:

$$P = V \times Q / T \qquad \textbf{Equation 1.2}$$

where

P = power
Q = charge
T = time.

This formula may also be expressed as $P = V \times I$, or substituting $I = V/R$, $P = V \times V/R = V^2/R$. The unit of power is the watt, which represents one volt times one amp.

An electrical circuit represents the flow of current along a path. Circuits are often represented according to diagrams as in Figure 1.20. This simple circuit illustrates a battery as a direct constant voltage source, solid lines representing perfect conductors, a switch, and a resistor. In reality, all tissues provide some degree of resistance to flow of charge. In clinical electromyography, sources of resistance include the patient's body, the skin-surface electrode interface, the needle-muscle interface, the electrode wiring and the EMG unit itself.

Using Ohm's law, $V = I \times R$, one can calculate current flow from the positive to the negative terminal of the battery through the resistor (Figure 1.20).

$$V = I \times R \qquad \textbf{Equation 1.3}$$

or

$$I = V/R$$
$$I = 10v/10\Omega$$
$$I = 1\ amp$$

A capacitor is a device in a circuit that can store charge. A capacitor may be conceptualized as two plates separated by a nonconducting insulator (Figure 1.21). In this circuit, current will flow and build up positive charge on one side of the capacitor. This accumulation of positive charge will attract negative charges on the other side of the capacitor. Thus, current flows on both sides of the capacitor without actual current flow across the capacitor's insulator. Current will cease flowing when the source of the voltage driving the accumulation of positive charges on one side of the plate is balanced by the repulsion of the like charges on the plate. The factors that determine the properties of the capacitor include the size and proximity of the plates and the effectiveness of the insulator. The larger and closer the plates, the greater the current flow. The ability of the capacitor to store charge is called capacitance (C). Capacitance equals the charge divided by the voltage and is measured in units of farads.

$$C = Q / V \qquad \textbf{Equation 1.4}$$

One farad equals one coulomb divided by one volt. The current flow equals the capacitance times the change in voltage over time and may be represented by the equation:

$$I = C \times dV / dT \qquad \textbf{Equation 1.5}$$

where dV/dT = change in voltage over time.

When no change in voltage occurs over time, no current flows. The resistance to current flow due to the capacitor is *capacitive reactance* (Xc) and is measured in Ohms. Capacitors block direct current (DC) but pass alternating current (AC). The capacitive reactance to AC current is determined by the capacitance of the capacitor as well as the frequency of the current and may be expressed by the formula:

$$Xc = 1/2\,\pi f C \qquad \textbf{Equation 1.6}$$

where
π = 3.14
f = frequency of AC current
C = capacitance.

The capacitive reactance is not energy lost to heat but to potential energy from the charge on the capacitors. In clinical EMG, capacitance is an integral property of many components of the equipment and the tissues. Capacitance that may alter EMG signals may originate in the skin as well as in the electrodes used to record the EMG signals.

Figure 1.20 — A simple circuit with resistor.

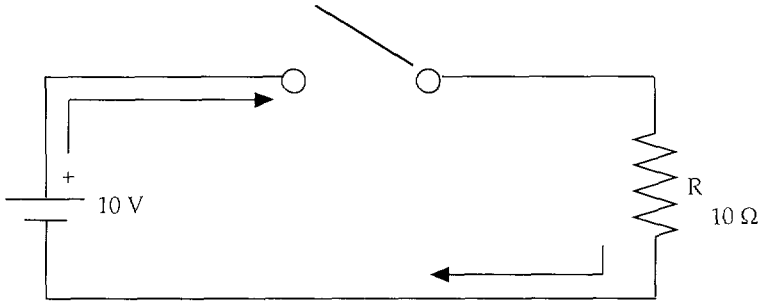

Figure 1.21 — A simple circuit with capacitor.

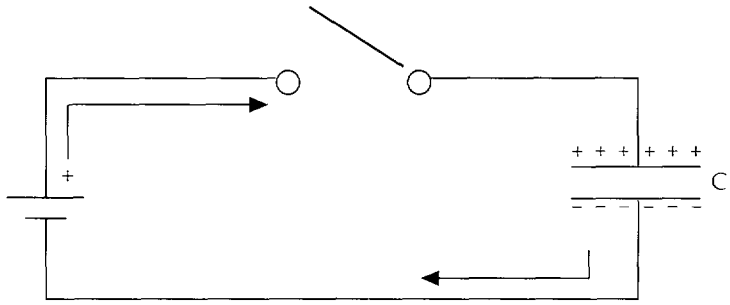

Figure 1.22 — (a) A simple circuit with resistors in series. (b) A simple circuit with resistors in parallel.

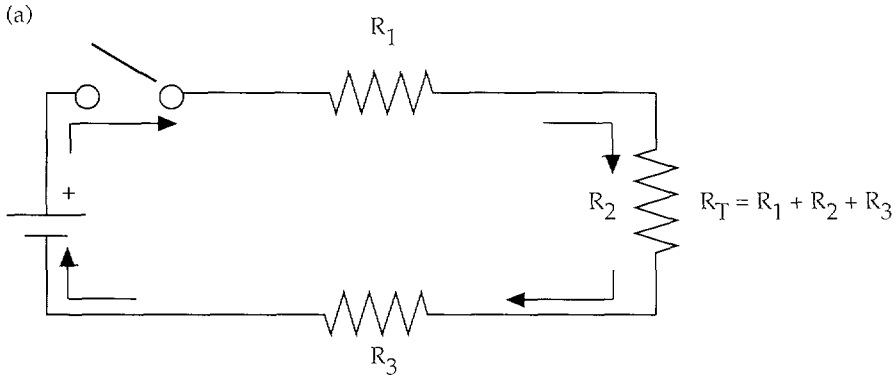

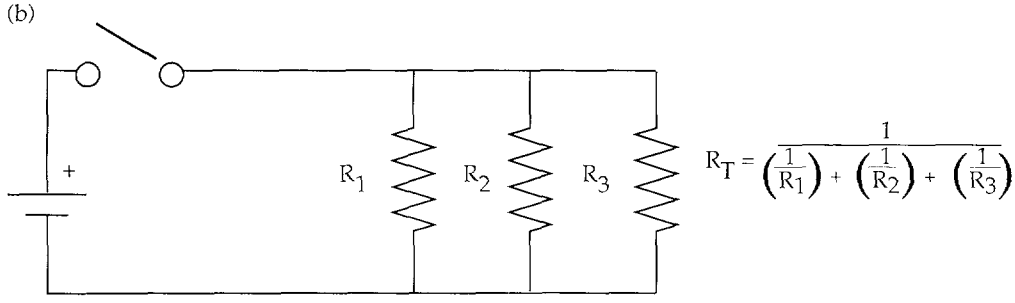

When current flows, a magnetic field is generated perpendicular to the flow. A conductor that may encircle a time-varying magnetic field can generate a voltage. The property of inducing voltage in a conductor is inductance (L) and may be expressed by the formula:

$$V = L \times dI / dT \qquad \textbf{Equation 1.7}$$

The unit of inductance is a Henry (H). One volt is induced by an inductor with an inductance of 1 Henry with a change in current flow of 1 amp per second. The energy lost through inductance is inductive reactance (X_L) and is measured in Ohms. It may be represented by the formula:

$$X_L = 2\pi f L \qquad \textbf{Equation 1.8}$$

where
π = 3.14
f = frequency of AC current
L = inductance.

The energy lost in inductance is not lost in heat but stored in a magnetic field.

Even complex systems composed of multiple voltage sources and resistors can be modeled by a system composed of a single voltage source and one resistor in series. With regard to circuits, Kirchoff's voltage and current laws are very useful. These laws state that all elements in parallel will have the same voltage potential across them and that all elements in series will have the same current passing through them. These laws can be applied to circuits with resistors or capacitors in series or in parallel. In the case of resistors in series, voltage is conserved and current is equal to all elements in series (Figure 1.22a). Thus, the effective overall resistance is equal to the summation of the individual resistors. When resistors are in parallel, voltage is conserved across each of the elements, but a current will be divided among the three resistors (Figure 1.22b). The exact opposite holds true for capacitors in series and in parallel (Figure 1.23 a, b).

In a circuit with a resistor and capacitor in series (Figure 1.24a), the current flowing is a function of the capacitance as well as the change in voltage that occurs with time. Thus, time is an important feature of how the capacitor functions. When the circuit is completed at 1, electrons will flow to the right side of the capacitor plate and begin accumulating negative charge. Initially the voltage across the capacitor is very low, therefore most of the voltage is measured across the resistor. However, as more negative charge builds on the right side of the capacitor plate and positive charge builds on the left side of the capacitor plate, more of the voltage will be observed across the capacitor and less across the resistor, i.e., VC is initially very high and then gradually decays and approaches zero (Figure 1.24b). The charging of the capacitor over time is an exponential function proportional to the capacitor's time constant. The time constant has been defined as the time for voltage across the resistor to fall approximately 37%, or conversely, the time for the capacitor to charge to 63%. These types of circuits are effectively filters because a capacitor resists flow in an inverse relation to the frequency of the current.

AC circuits obey similar laws as DC circuits. AC sources typically refer to sinusoidal waveforms that have both amplitude and frequency. In addition, AC sources exhibit phase, an index of the time shift of the waveform, expressed in degrees in reference to the sine-wave of the current. When a sinusoidal AC current passes through a capacitor, the voltage across the capacitor is delayed in phase by 90°.

Figure 1.23 — (a) A simple circuit with capacitors in series. (b) A simple circuit with capacitors in parallel.

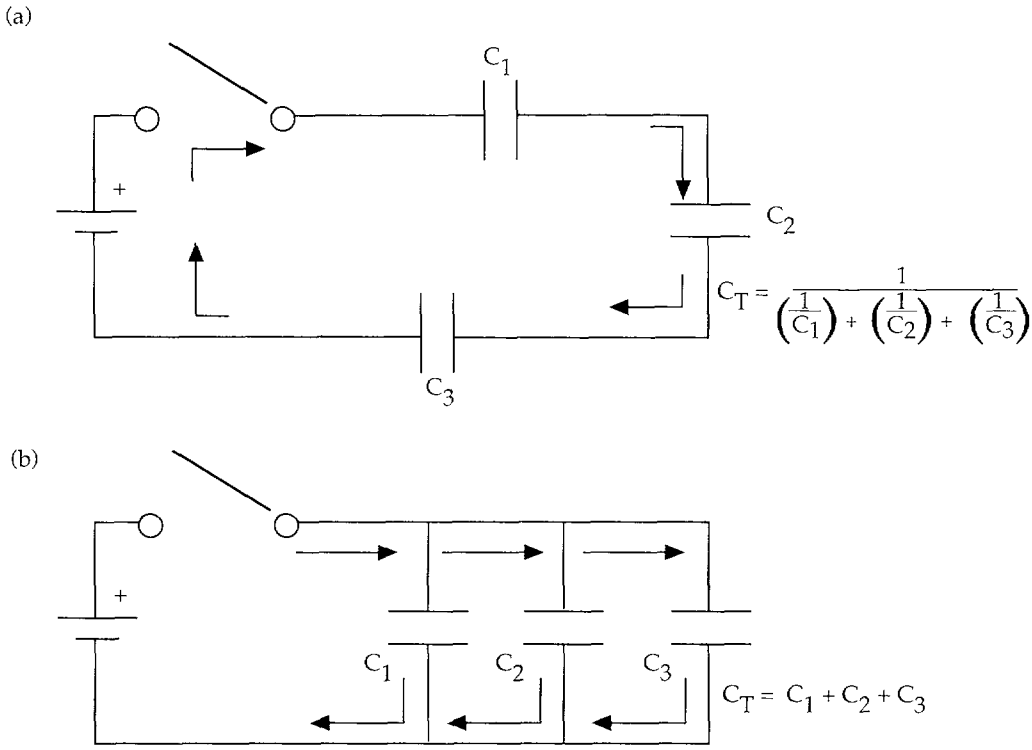

Figure 1.24 — A simple circuit with a resistor and capacitor in series.

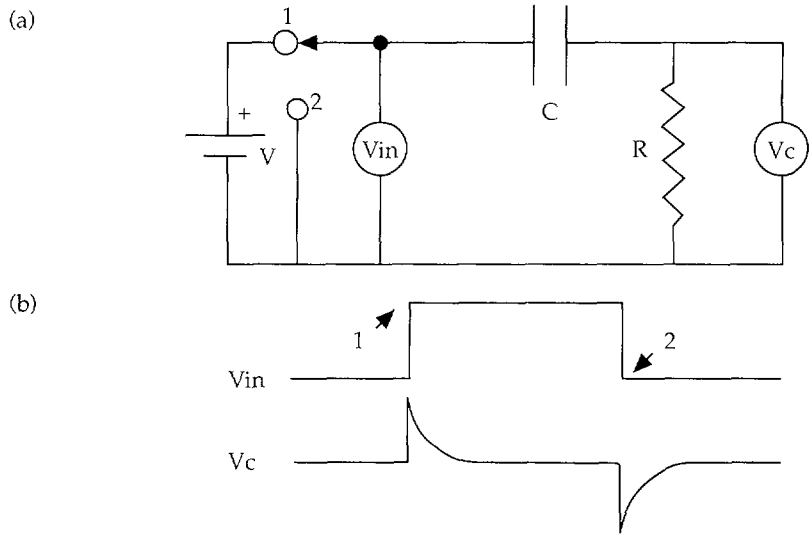

Impedance (Z) represents the combined effects of resistance, capacitive reactance and inductive reactance that occurs in AC circuits. Impedance, which is measured in Ohms, replaces R in the Ohm's law formula for AC circuits.

$$V = I \times Z \qquad \textbf{Equation 1.9}$$

or

$$Z = V / I$$

In clinical EMG, the impedance of the recording electrodes may affect the recorded signal. For nerve conduction studies the impedance of the electrodes are relatively low, however, impedance at the needle electrode is high and can markedly attenuate the voltage recorded. Increasing the input impedance at the amplifier permits more accurate unattenuated recording from the needle electrode tip.

Filtering of electrical signals permits attenuation of frequencies that are not desirable and facilitates recording of those frequencies that are of interest. High pass filters allow high frequencies to move through a circuit unattenuated and low frequencies to be filtered. Low-pass filters permit low frequencies to travel through the circuit unattenuated and higher frequencies to be filtered. Filters may be constructed via a resistor and capacitor in series. The properties of the filter are dependent upon the frequency of the signal and the time constant of the capacitor. For low-frequency filters (high-pass filters), the output is taken across the resistor (Figure 1.24). An index of low frequency filtering is the cut-off frequency:

$$F_C = 1/2\,\pi t \qquad \textbf{Equation 1.10}$$

where t = time constant.

The low-frequency filters will attenuate 30% of the signal amplitude for inputs at the cut-off frequency. Low-frequency filtering results in a positive phase shift of voltage that is also frequency-dependent. At the cut-off frequency, this phase shift is 45° for a single-pole filter.

For high-frequency filtering, the cut-off frequency may be calculated using this same formula. However, the output is across the capacitor instead of the resistor (Figure 1.25a,b). High-frequency filters will attenuate 30% of the signal amplitude for inputs at the cut-off frequency. For high-frequency filtering, there is a negative phase shift of 45° at the cut-off frequency for a single-pole filter. Filters can be combined in a single circuit with low-pass and high-pass cut-off frequencies. These so-called band-pass filters permit frequencies between the two cut-offs to pass with minimal attenuation. The notch filter is simply a narrow band-pass filter designed to pass all frequencies except for a small band. In clinical EMG, notch filters are used to filter 50/60 Hz signals commonly generated from power line interference.

Figure 1.25 — A simple circuit with resistor and capacitor in series.

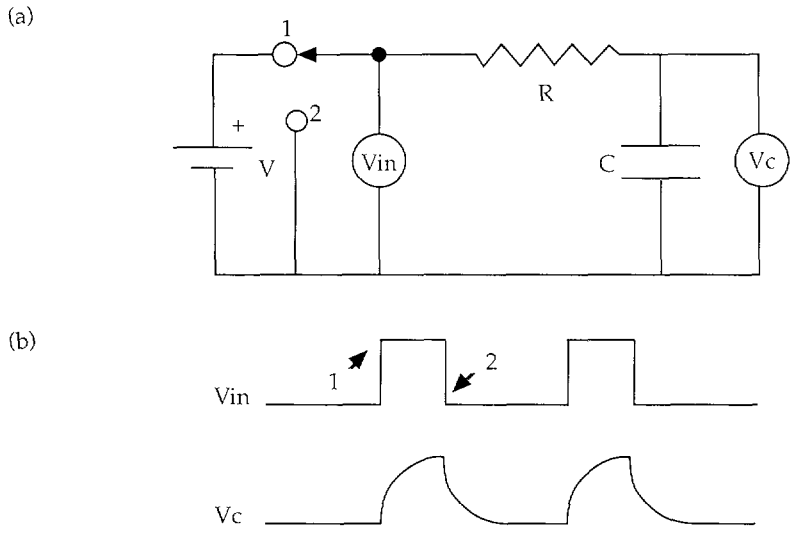

1.5 *Equipment*

The basic components of the EMG unit consist of various recording and stimulating electrodes, preamplifiers, amplifiers, visual display, and audio speakers (Figure 1.26). In addition, many units incorporate specialized components that assist in signal analysis including averagers and delay lines. Most modern EMG units incorporate a computer and analog-to-digital (A–D) converter. An assortment of software programs can be utilized for acquisition and analysis of the EMG signals.

1.5.1 Electrodes

Several types of electrodes are used in clinical EMG. It is important to remember that the electrical and physical properties of the electrode will have a large impact on the shape and size of the biologic signal that is recorded. Surface electrodes are usually small, circular plates of platinum or silver, approximately 1 cm in diameter (Figure 1.27a). These are the most commonly-used electrodes for nerve conduction studies and are occasionally encased permanently in a plastic bar, typically 3 cm apart (Figure 1.27b). These electrodes may be affixed to the overlying skin to record electrical activity from the underlying nerve or muscle. When recording from sensory nerves in the fingers, a metallic ring electrode is often applied around the circumference of the finger (Figure 1.27c). Regardless of which surface electrodes are used, proper preparation of the skin in contact with the electrode is essential to minimize impedance and improve electrical recording. This is often accomplished by cleansing the skin with alcohol and then applying the electrode to the overlying skin with a small amount of electrolyte cream or jelly, such as silver chloride cream.

Figure 1.26 — Schematic diagram of computer based EMG unit.

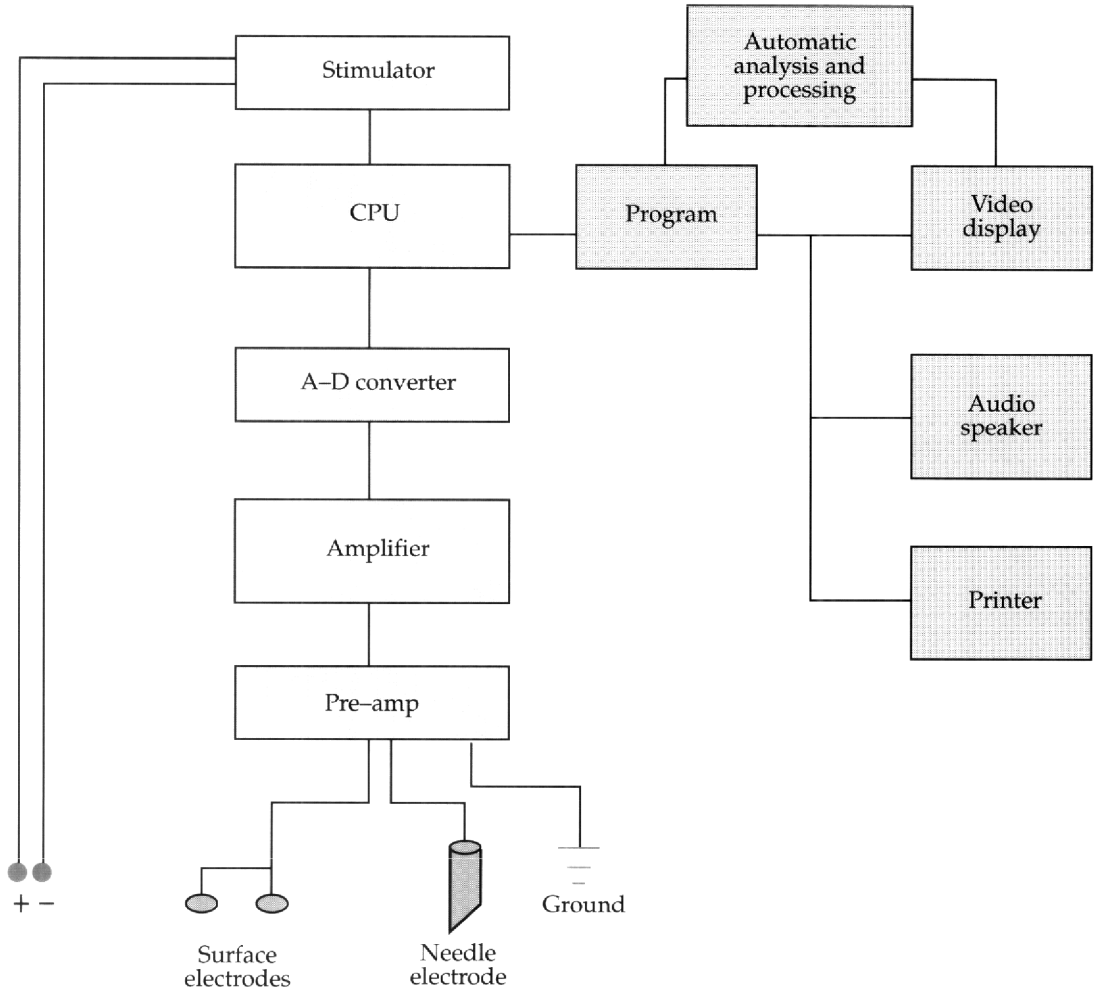

A variety of needle electrodes are used to record the electrical properties of muscle (Figure 1.28). The most common is the concentric needle electrode, which is constructed with a thin, metallic wire approximately 0.1 mm in diameter (Figure 1.28a). The wire is encased in an external canula of approximately 0.3 mm in diameter. The electrode records from the thin wire filament at the tip with the canula of the electrode serving as the reference electrode. With proper application of the surface electrodes, impedance is relatively low. However, impedance can be high with needle electrodes (e.g., impedance is approximately 50 KΩ for the concentric needle electrode).

Figure 1.27 — Commonly used surface and ring electrodes for the nerve conduction studies: (a) surface disc electrodes. (b) bar electrode. (c) ring electrodes.

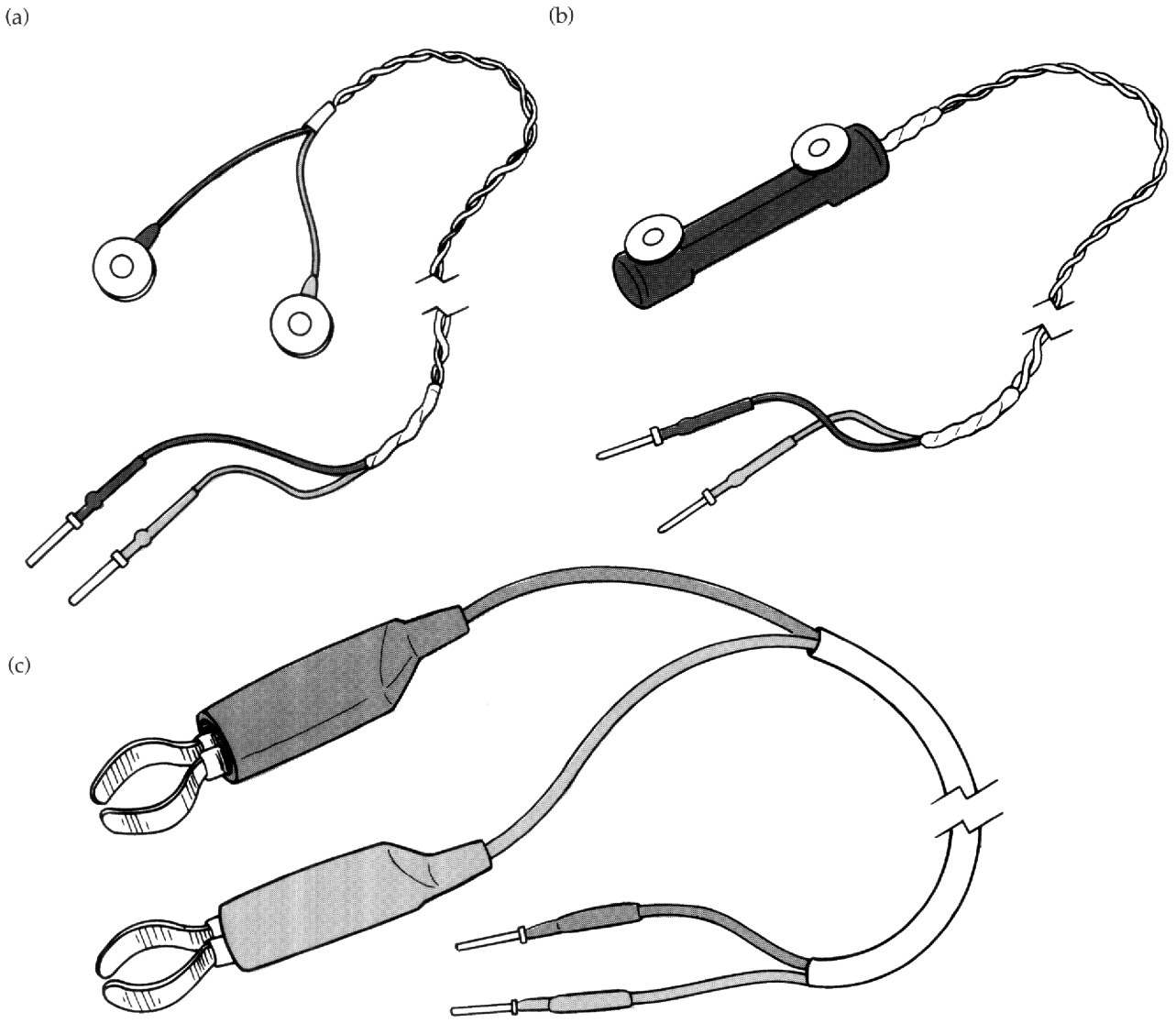

Another commonly used needle electrode is the monopolar electrode, which is composed of a thin metal wire insulated by Teflon except at the recording surface at the very tip, where a distal 0.2 mm to 0.4 mm is exposed (Figure 1.28b). Unlike the concentric needle electrode, the monopolar electrode requires a second monopolar needle or a surface electrode adjacent to the skin as the reference electrode. Monopolar electrode impedance may range between 1.4 MΩ to 6.6 KΩ. Although monopolar electrodes are more comfortable and better tolerated by patients, they produce more electrical interference than the concentric needle electrode. In addition, the recording characteristics of the electrodes are different. Motor unit action potentials (MUAPs) recorded by monopolar elec-

trodes are frequently larger than those recorded by the concentric needle electrode. The needle electrodes must be carefully sterilized after each use. Concerns regarding the effectiveness of standard sterilization procedures for slow virus disorders such as Creutzfeld-Jacob disease have led to the recommendation that needle electrodes be discarded after the examination of patients with dementia. However, the advent of inexpensive disposable monopolar and concentric needle electrodes obviates the concern regarding sterilization. The use of such electrodes is highly recommended and is quickly becoming a standard practice.

During any EMG measurement, whether it be NCSs or needle electromyography, three electrodes are attached to the patient: the recording electrode, the reference electrode, and a ground electrode. The recorded signal represents the voltage difference between the recording and reference electrodes. The ground electrode serves as a low-impedance path to eliminate electrical noise as well as provide a path for current leak. A wide variety of designs and types of ground electrodes are used in clinical electromyography (Figure 1.29). The most popular ground electrodes consist of large, malleable metal plates that can be easily affixed to the limb under study (Figure 1.29b). Smaller ground electrodes can be attached to the face or head and neck with tape (Figure 1.29a). Ground electrodes are typically applied to the skin with electrolyte cream or jelly, but some electrodes are covered in a velcro cloth and immersed in saline solutions before application (Figure 1.29c).

Figure 1.28 — Commonly used needle electrodes: (a) concentric unipolar electrode. (b) monopolar electrode. (c) single-fiber EMG electrode. (d) macro-EMG electrode.

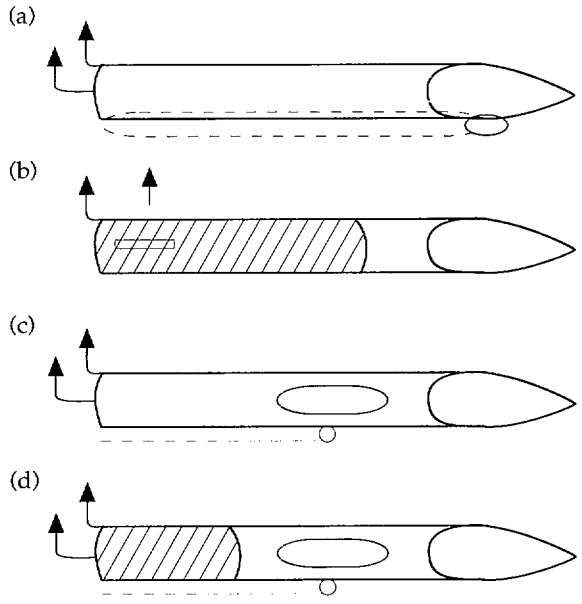

Figure 1.29 — Various types of ground electrodes: (a) circular metal plate ground electrode. (b) malleable metal bar ground electrode. (c) velcro-cloth embedded ground electrode.

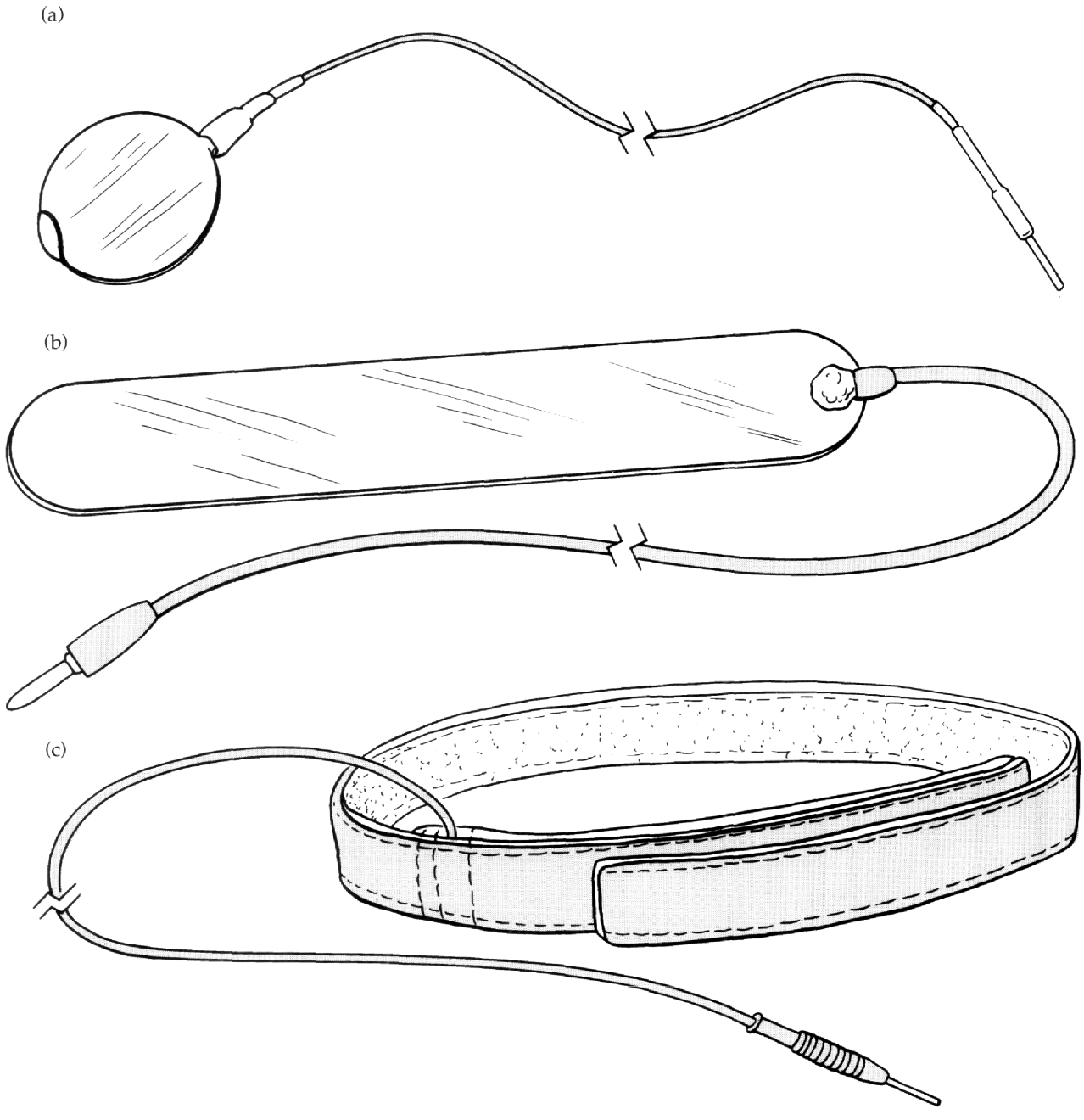

1.5.2 Amplifiers

The potentials recorded from the surface and needle electrodes are very small and require substantial amplification for measurement. In most EMG units, amplification begins at a preamplifier, which must have a large dynamic range to accommodate a wide variety of frequencies without filtering, a low noise level so that additional electrical noise is not introduced into the signal prior to its amplification, and a high input impedance so that electrical signals recorded from electrodes with relatively high impedance are not attenuated.

Electromyographic amplifiers are differential amplifiers, that is, they amplify the voltage difference between the recording and reference electrodes. Inherent in differential amplification is the concept of common mode rejection. Electrical noise or signals from distant sources not of clinical or biologic relevance may be recorded by both the recording and reference electrodes simultaneously, particularly if both electrodes are in close proximity. Because the differential amplifier will only amplify the difference between the recording and reference electrodes, the common mode electrical signals to both electrodes will not be amplified. However, because electrical systems are not perfect, some failure will occur in the amplifier to reject the common voltage at both recording and reference electrodes. The ability of the differential amplifier to reject the common mode may be expressed as the common mode rejection ratio, indicating the efficiency of the amplifier to amplify the difference between two electrodes more than the common voltage at both electrodes. The common mode rejection ratio for EMG equipment should be greater than 100,000. That is, the differential amplifier should amplify the voltage difference between the recording and reference electrodes 100,000 times more than the common voltage at both electrodes.

Another important feature of amplifiers is a high input impedance. For AC sources, voltage is equal to current times impedance. Thus, the input impedance of an amplifier will determine how much current is required to produce a certain voltage response. In the case of a concentric needle electrode recording in muscle, the amount of current flowing to the amplifier will be governed by the total impedance at the electrode and the amplifier input. If the electrode impedance is high, then a considerable amount of voltage will be attenuated at the electrodes and not be available for amplification at the amplifier input. If input impedance at the amplifier is the same as that at the electrode, then 50% of the voltage will be attenuated. On the other hand, if the input impedance at the amplifier is 99 times greater than at the electrode, then 99% of the voltage will be available for amplification at the amplifier inputs. Thus, it is important for amplifiers and preamplifiers to have very high input impedance. The input impedance of many amplifiers in clinical EMG ranges from 10-100 megohms.

1.5.3 Filters

Filters are used with EMG amplifiers to attenuate interference from electrical noise or from biological signals that may interfere with the recording of the biological signals of interest. Standard filters are composed of circuits with a resistor and a capacitor in series. These circuits permit attenuation of frequencies above or below certain values. Filters are often regarded as high-pass (low-frequency filters) or low-pass (high-frequency filters). A high-pass or low-frequency filter permits high frequencies to be amplified without attenuation but filters and attenuates lower frequencies. The low-pass or high-frequency filter does just the opposite. The cut-off frequency of a particular filter indicates the frequency at

which the signal amplitude is attenuated to approximately 70% of its original amplitude. Thus, a high-pass or low-frequency filter with a cut-off frequency of 2 Hz will attenuate signal amplitude of frequencies of 2 Hz and less by 30% or more. A low-pass or high-frequency filter with a cut-off frequency of 1000 Hz will attenuate frequencies of 1000 Hz and above by 30% or more. Commonly used filter settings for clinical EMG are shown in Table 1.1.

Table 1.1 - Typical Filter Settings

	Low Frequency	High Frequency
Sensory NCS	20 Hz	2 KHz
Motor NCS	2 Hz	10 KHz
Needle examination	20 Hz	10 KHz

1.5.4 Output

Once the biological signal is recorded at the electrodes and amplified and filtered by the amplifier and preamplifier, it is then displayed visually and the audio components of the signal play through a loud speaker. Traditionally, EMG units utilize cathode ray oscilloscopes to provide a real-time visual display. Gain settings and sweep speed settings are adjusted to ensure proper display of the signal. Storage scopes are often utilized to freeze an individual sweep, and are particularly useful for NCSs. Analysis of the waveforms can be achieved directly from the oscilloscope screen or a photographic device can produce a hard copy. In recent years, EMG equipment has utilized personal computer operating systems with digitized waveforms and video screen displays. Computer programs have enabled automatic analysis of many nerve conduction measurements including distal or terminal latencies, amplitude and area at the waveforms, and conduction velocity. For the NEE, programs enable storage of MUAPs and automatic analysis of amplitude, phasicity, and duration.

For the NEE, the audio signals often help in interpreting MUAPs and other types of electrical activity. The experienced electromyographer can easily identify the acoustic properties of these potentials.

1.5.5 Stimulators

All EMG units have stimulators to directly stimulate peripheral nerves in the course of NCSs. Generally, stimulators provide square-wave currents ranging in duration from 50 μsec to 1000 μsec and amplitudes up to 500 volts. These stimulators can produce currents of up to 100 mA. Some stimulators provide stimulation via constant voltage. Adjusting the level of voltage results in varying stimulating currents, while constant-current stimulators provide a more consistent stimulus current. Typically, the stimulator output simultaneously triggers the sweep of the visual display, although most units have the ca-

pability of delaying the sweep, thus permitting full visualization of the shock artifact that occurs at the onset of stimulation. The stimulators used in EMG equipment are isolated from the amplifier and recording electrodes to minimize artifact and to provide for more discrete focal stimulation. The stimulating electrode is composed of a cathode and anode. A typical hand-held bipolar prong stimulator comprises two metal shafts with rounded and gently pointed surfaces encased 3 cm apart in a plastic holder (Figure 1.30a). Other types of stimulating electrodes can include needles and surface disk electrodes (Figure 1.30b). Electrical stimulation occurs beneath the cathode.

Figure 1.30 — Various types of stimulating electrodes:
(a) hand-held bipolar prong stimulator. (b) bar stimulator.

(a) (b)

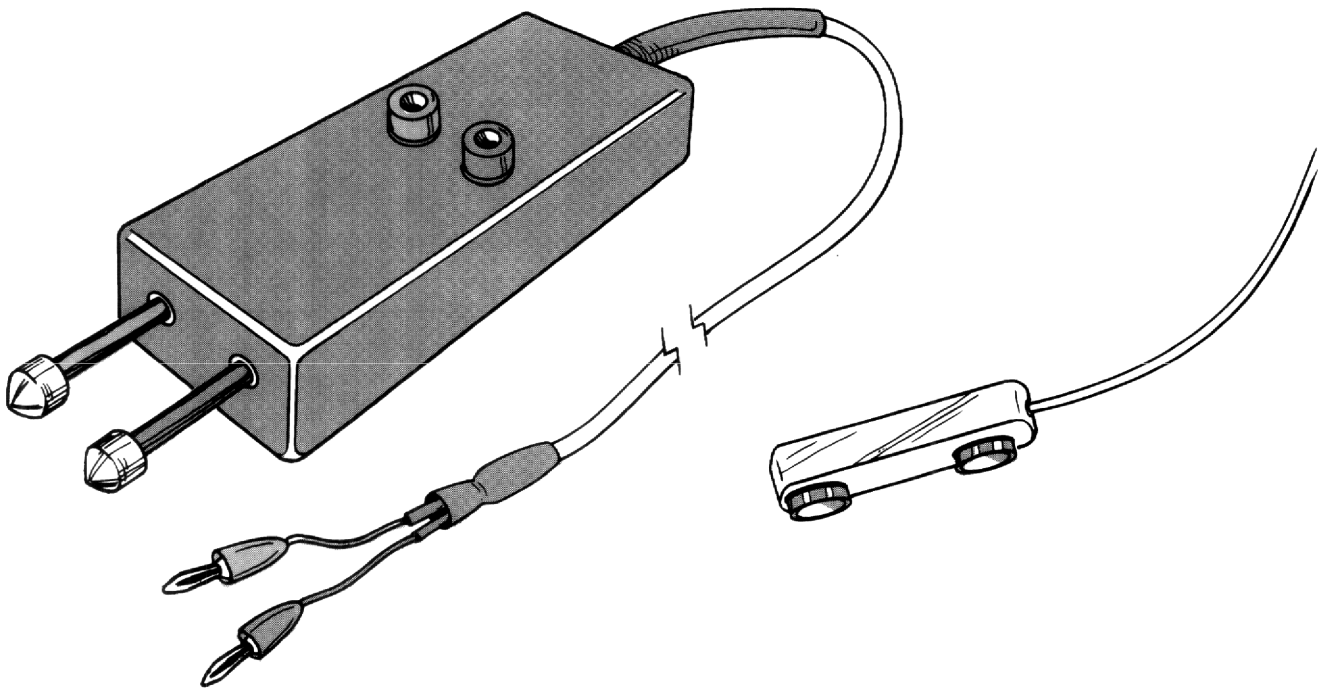

1.5.6 Averaging

When the amplitude of a response recorded in the NCSs is very small, particularly in sensory NCSs, averaging may be utilized to help define the response. Traditional EMG units are often equipped with analog averagers, but later generation computer-based EMG units use special computer programs to average digitized signals. The principle of averaging is to accumulate numerous responses during successive stimulations and recordings. These responses are summated in such a way to reinforce the deflections that occur with each stimulation due to the biological signal and to eliminate the random variable deflections that are caused by the electrical noise and shock artifact.

1.6 *Electrical Safety*

Although standard clinical EMG examinations are performed routinely and safely, electrical injury is possible. Electrical hazard is primarily due to unintended current traveling through the body. Although the threshold for pain from shock in intact skin is approximately 1 mA derived from 120 volts alternating current for 1 second, as little as 50 μA in a patient with a central line or cardiac catheter can cause fatal ventricular fibrillation. The most important sources of electrical hazard are those related to leakage current and loss of ground. Leakage currents can arise from either stray capacitance or stray inductance. Stray capacitance may occur in a power cord during current flow, which induces capacitive currents in the neutral and ground wires. If improper grounding occurs, these capacitive currents may travel through the patient to another source of ground and induce electrical injury. It is unsafe to use extension cords with EMG units because they may increase capacitive currents. Stray inductance is of less magnitude but can also create leakage currents. Current flowing in power cables and in EMG equipment can induce magnetic fields that can produce current flow in other conducting structures, which may be in contact with the patient. Again, if grounding is not adequate, current flow may then find another source of ground through the patient and induce electrical injury. Electromyographic units should be inspected on a regular basis — at least yearly — to assess for leakage current. Maximum leakage currents allowed for patients having casual contact with a medical device is approximately 500 μA, but for EMG equipment where patients have direct contact, leakage should be no more than 100 μA. For high-risk patients, such as neonates or patients who have in-dwelling catheters that could steer lethal leakage currents directly to the heart, recommendations are that leakage be less than 10 μA. Table 1.2 lists the risk current requirements for clinical patient care electrical devices established by the American National Standards Institute/Association for the Advancement of Medical Instrumentation standard (ANSI/AAMI).

Table 1.2 - Risk Current Requirements

	Patient Risk Current		Chassis Source Current			
Category of electromedical apparatus	All Apparatus		Cord-connected Apparatus		Permanently Connected Apparatus	
	Source Current	Sink Current	Ground Open	Ground Intact	Ground Open	Ground Intact
With isolated patient connection	10 μA	10* μA	100 μA	100 μA	5000 μA	100 μA
With nonisolated patient connection	50 μA	NA	100 μA	100 μA	5000 μA	100 μA
Likely to contact patient	NA	NA	100 μA	100 μA	5000 μA	100 μA
No patient contact	NA	NA	500 μA	100 μA	5000 μA	100 μA

*The allowed sink risk current is 20 μA RMS for isolated electromedical apparatus with patient cables when measured at the patient end of the cable (see paragraph 4.4 of the ANSI/AAMI standard). NA=Not applicable.

Electrical hazards may also be the product of improper grounding. With proper grounding, leakage current will be shunted immediately to the ground contact. The EMG unit, like all medical equipment, should only be used with a three-pronged outlet. This will permit leakage current to travel to the earth ground and not through the patient.

In patient care areas it is not uncommon for patients to be connected to or touching many other electrical devices. This creates a problem if the grounds are not identical in all the outlets used. As little as 50 mV difference between grounds could cause hazardous current to flow between grounds and through the patient. Thus, wiring in patient areas should conform to the concept of an equal potential ground bus, such that all the receptacles in the patient rooms have a common ground point. In intensive care units where multiple electrical devices are the norm, isolation jack boxes are typically employed. In the EMG laboratory, the use of a grounding bar to which all power cables may be connected to common ground provides protection against the double-grounding hazard.

1.7 Nerve Conduction Studies

Nerve conduction studies are one of the two basic components of the electrodiagnostic examination, the other being the NEE. The landmark article for modern day NCS generally is considered that written by Hodes, Larrabee, and German, published in 1948. The authors described performing various motor NCS on a number of persons with remote peripheral nerve injuries (presumably sustained during World War II). Although initially used as a research tool, NCS were reported for their clinical value as early as 1956. As time passed, it became increasingly apparent that NCS could be of immense help in assessing patients with both focal and generalized nerve disorders, as well as those with disorders of the neuromuscular junction.

Three basic types of NCS are in use: motor, sensory, and mixed. All three types assess only the large myelinated nerve fibers. During NCS, a peripheral (or cranial) nerve is stimulated by electricity, at one or more points along its course. The resulting volley of nerve action potentials set up in the individual nerve fibers under the cathode of the stimulator is recorded directly at some more proximal or distal point along the nerve (with sensory NCS and mixed NCS), or, indirectly via the near synchronous muscle action potentials they generate (with motor NCS).

Both surface and needle electrodes can be used for stimulating and/or recording. In North America, surface electrodes most often are employed for this purpose. In contrast, needle electrodes usually are preferred in Europe. One of the reasons cited for using needle recording electrodes is that the onset of the responses is sometimes better defined than when surface electrodes are used, permitting the conduction rates to be determined with slightly greater exactitude. Electromyographers who prefer surface recording electrodes counter this argument by pointing out that, with needle recording electrodes, the amplitudes of the responses merely reflect the activity being generated near the needle tips because of the very limited pick-up range of the needle electrodes. In contrast, with surface recording electrodes the amplitudes of the responses are semiquantitative measures of the total number of nerve fibers responding to the stimulus. Often, this is the only important component of NCS. Also, if surface electrodes are used, NCS are a noninvasive procedure and consequently can be performed by non-physicians.

Performing NCS is a deceptively simple task. The particular nerve to be studied is selected and, if it contains both motor and sensory fibers, the type of study to be performed — motor, sensory, or mixed — is determined. The recording surfaces of the recording

Figure 1.31 — The set-up for a median motor NCS.

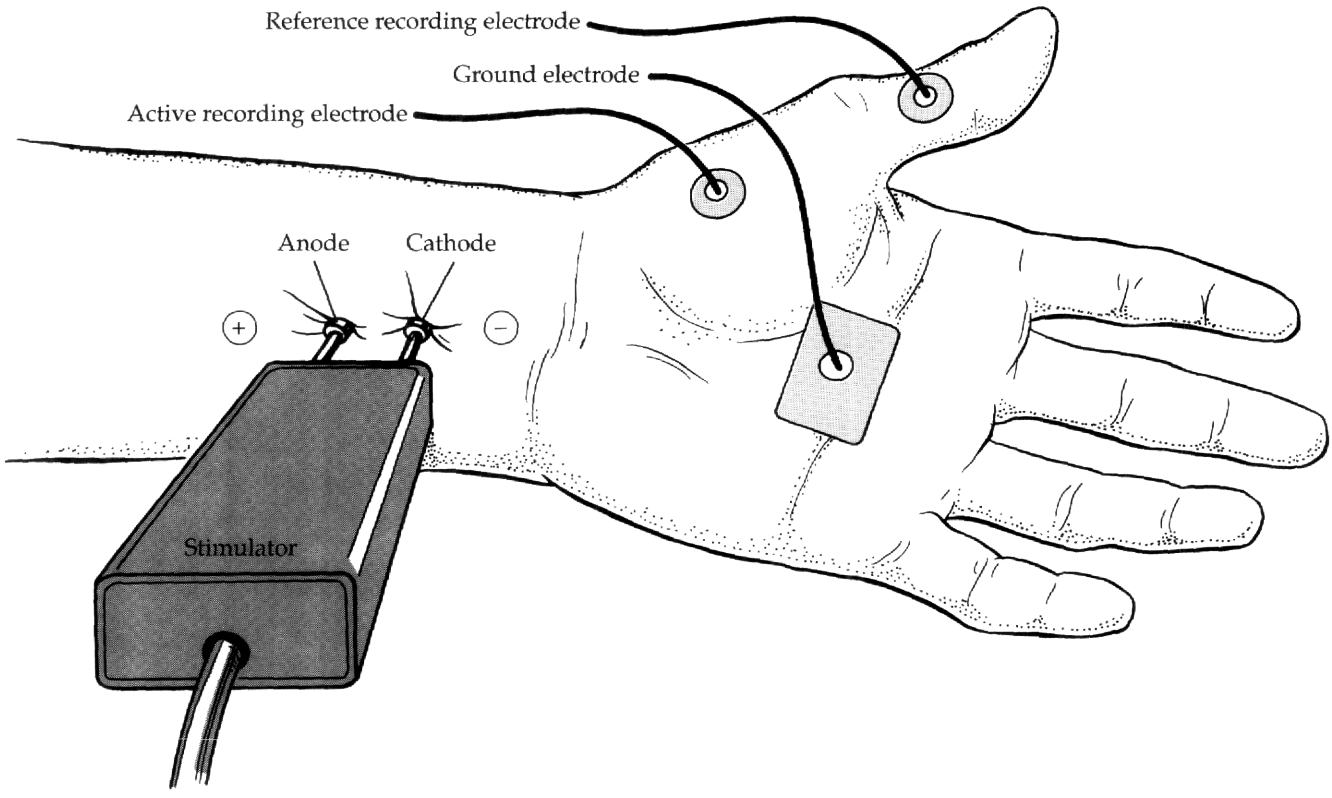

electrodes are coated lightly with electrode paste and then affixed to the skin at the appropriate sites with adhesive tape. For motor NCS, the active recording electrode is situated over the motor point of a muscle innervated by the nerve being assessed, so that the initiation of the muscle action potentials can be recorded (Figure 1.31). The reference recording electrode is secured to the skin at a point distal to the active recording electrode, usually 3 to 4 cm distal, overlying the tendon of the recorded muscle. For sensory and mixed NCS, the recording electrode is secured over the nerve being studied at some site proximal or distal to the point at which it will be stimulated. The reference recording electrode is then placed along the course of the nerve in such a manner that the active recording electrode is interposed between it and the stimulating electrode. Sensory and mixed NCS most often are performed with a fixed, measured distance between the cathode stimulating electrode and the active recording electrode. For many of these studies, the distance between the active and reference recording electrodes is standardized as well. After the recording electrodes have been secured, a ground electrode is affixed to the limb, usually between the stimulating and recording electrodes, to reduce shock artifact (i.e., to prevent the response from being obscured by the electricity produced by the stimulus). The nerve is then stimulated, either by surface-stimulating electrodes affixed to the skin or by a bipolar prong surface stimulating electrode, with the cathode pushed firmly into the skin immediately overlying the nerve to be studied. In either case, the anode is situated either over or away from the nerve, but always behind the cathode (i.e., at a greater distance from the active recording electrode than the cathode). The nerve is then stimulated with a series of single

Figure 1.32 — Development of a compound muscle action potential (in this case, a median motor response) as the stimulus intensity is increased.

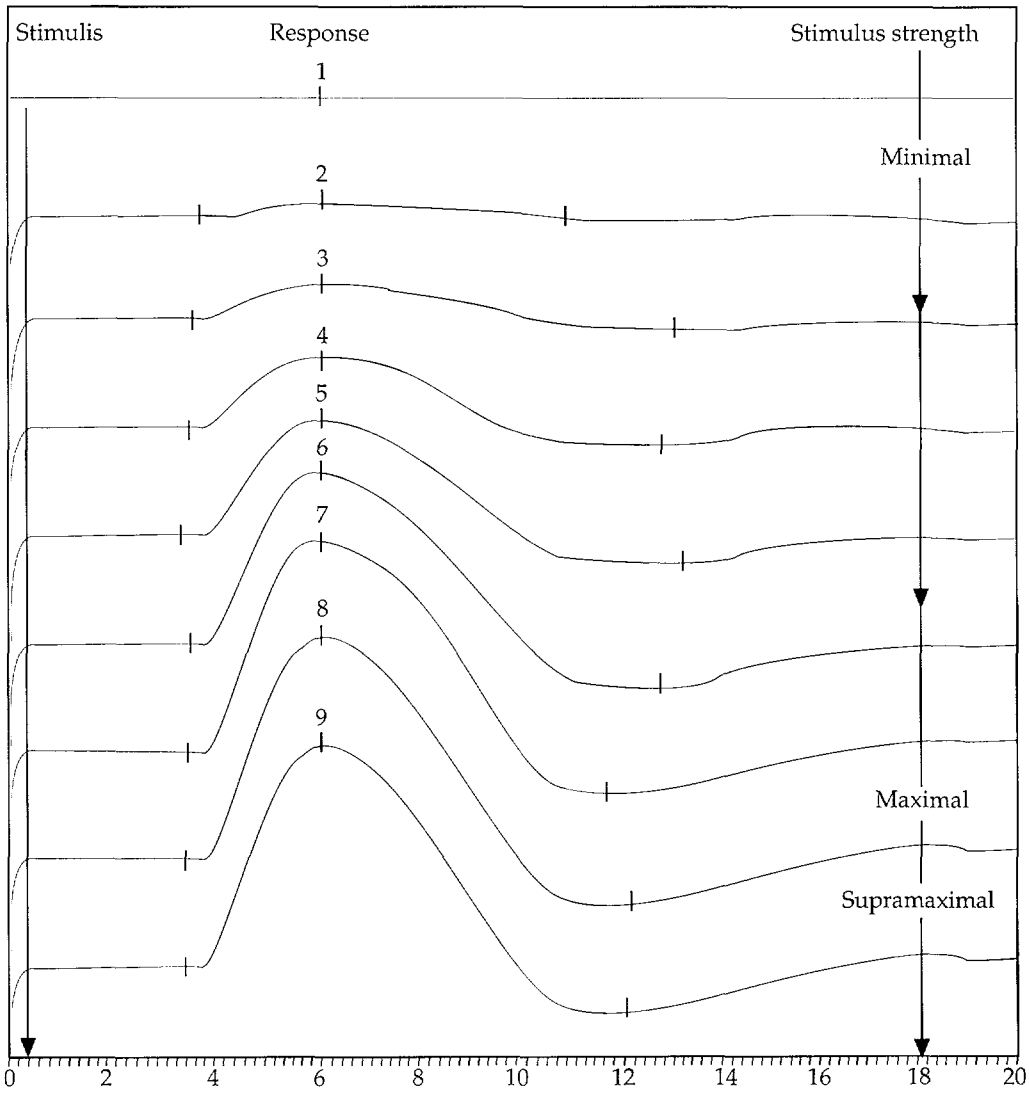

impulses. The stimulus strength is set at a low level initially and then progressively increased between each successive stimulation. Eventually a point is reached at which some of the large myelinated nerve fibers, possessing the lowest thresholds, are activated and a response begins to appear on the cathode ray oscilloscope screen. The response increases in size as the stimulus strength is raised until it remains stable, even though the stimulus power is enlarged further. This is referred to as a supramaximal response, although the term is a misnomer since it is the stimulus, not the response, which is supramaximal; obviously, the response cannot be greater than maximal (Figure 1.32). All the fibers that respond to the nerve stimulation will have now done so. For motor NCS, the recorded response is the CMAP; for sensory NCS, the sensory nerve action potential (SNAP); and for mixed NCS, the mixed nerve action potential (MNAP).

Figure 1.33 — The various components of the motor and sensory nerve conduction response (in this instance, the median motor response, recording thenar muscles, and the median sensory response, recording index finger).

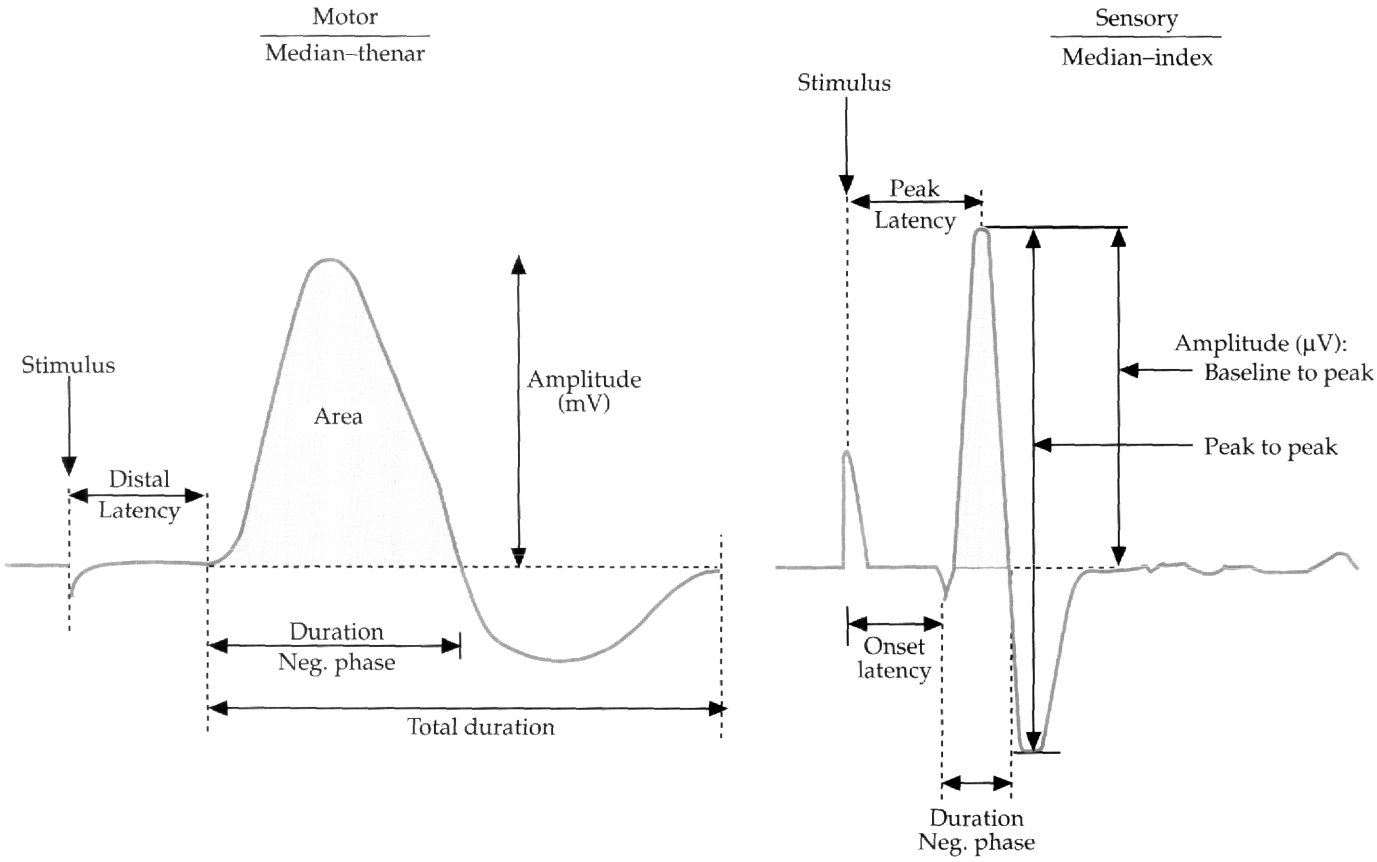

Figure 1.34 — Method used for calculating a conduction velocity along a segment of nerve (in this case, the forearm portion of the median motor nerve).

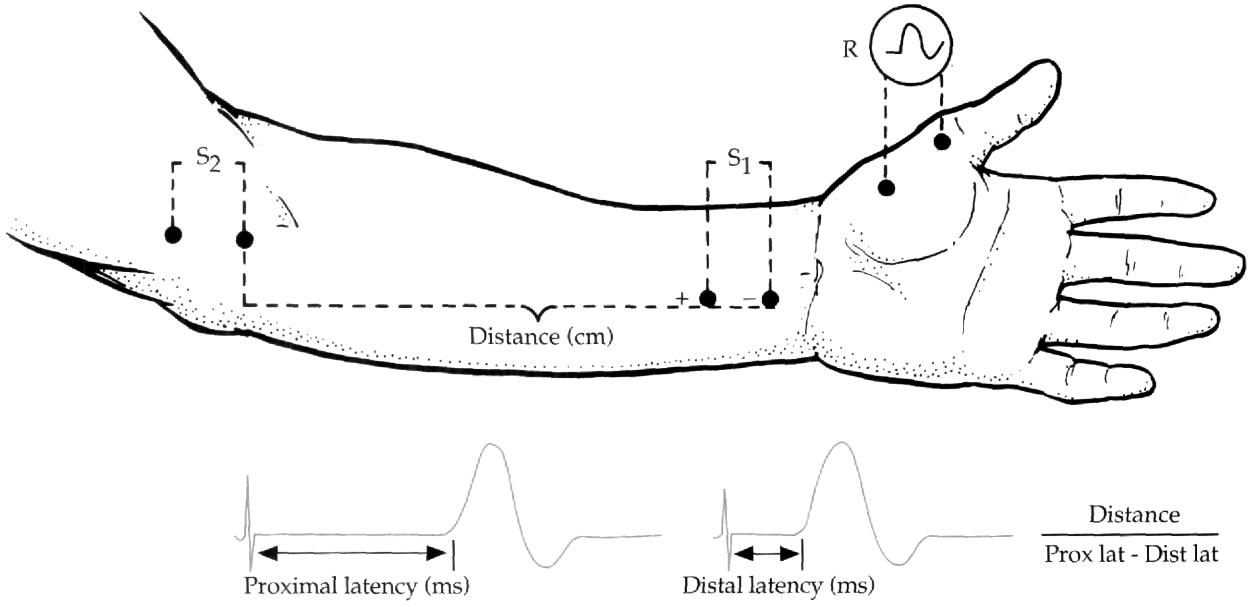

Several components of the evoked response are recorded, but only two, the distal amplitude and the distal/peak latency, are routinely reported. Of the remainder, the proximal latency is used to calculate conduction velocity (CV), which is always reported, while others, such as proximal amplitude and durations of the responses, are mentioned only if abnormal.

The amplitude is the height of the response, measured from the tip of its negative peak to either the baseline or to the tip of its positive nadir. It is expressed in millivolts (mV) for motor NCS and in microvolts (μV) for sensory and mixed NCS. An amplitude is obtained whenever a nerve is stimulated, so if the nerve is stimulated at two points, then both a distal amplitude and a proximal amplitude are recorded (Figure 1.33).

The latency of the response is the elapsed time in milliseconds (ms) between the instant the stimulus was applied, measured from the shock artifact (which interrupts the baseline seen on the cathode ray oscilloscope screen) to either the onset or to the negative peak of the evoked response. For all motor NCS and for many sensory NCS, the rate of conduction along the fastest conducting terminal nerve fibers is determined by measuring the elapsed time between stimulus application at the most distal stimulation site (i.e., the one closest to the recording site) and the onset of the response. This is reported as a distal latency. However, with many sensory NCS the onset of the response is somewhat difficult to determine accurately, and for that reason a peak latency, rather than a distal latency, is determined. In these instances, the elapsed time, in ms, between the stimulus application and the negative peak of the response is determined. Obviously, the conduction rate for the majority of the conducting fibers is being determined here, rather than for the fastest conducting ones (Figure 1.33). If the motor or sensory nerve is stimulated at two points, then a proximal latency is also determined. This is only rarely reported, however. Instead, it is used to calculate a CV by determining the distance in centimeters between the distal and proximal stimulation points, from cathode to cathode (measuring on the surface with a tape measure or calipers), and then by dividing that distance by the difference in ms between the distal and proximal latencies. The resulting CV is reported in meters per second (m/sec) (Figure 1.34).

At first glance, it may seem unnecessarily complicated to report the rate of conduction along the distal segment of the nerve as a distal/peak latency, in ms, while reporting the rate of conduction along some segment of nerve proximal to the distal stimulation point as a CV, in m/sec. However, there are two important reasons for doing so. First, converting the speed of conduction between two anatomical points, e.g., between the elbow and wrist, into a CV allows the conduction rate of one nerve to be directly compared to that of another, regardless of the exact distance over which they are being determined. Thus, the CV along the forearm segment of the median and ulnar nerves of a professional basketball player and a young child can be directly compared with one another, even though they were calculated along forearms of markedly dissimilar length. This would be impossible if only proximal latencies were used, unless a series of normal values, in ms, were obtained for each separate arm length, and for each decade of life, a very tedious task. Second, the distal/peak latencies obtained along the terminal segment of a nerve, when converted to CVs (by dividing the distance between the cathode and the active recording electrode by the distal/peak latency), are always slower than the CVs obtained along the more proximal segments of the same nerve. One reason for this is that distal nerve fibers are narrower and their myelin is thinner; therefore they conduct at a slower rate. Also, for motor nerves, some of the distal latency is consumed by the time required for neuromuscular transmission and for muscle fiber activation.

The duration of the response, in ms, is always assessed, although generally it is not reported unless it is abnormally prolonged, yielding a dispersed response. Also, most of the current EMG machines determine the area of the response as well, which is actually a better indicator of the number of nerve fibers responding to the stimulus than the amplitude alone (Figure 1.33).

In summary, for sensory NCS, the nerve is usually stimulated at only one point — the distal site. Consequently, only a distal amplitude and a distal, or peak, latency are reported. For motor NCS, and occasionally for a sensory NCS, the nerve is stimulated at two (and sometimes more) points along its course, so that both a distal and proximal amplitude and a distal and proximal latency are obtained. Characteristically, the two latency measurements are then used to calculate a CV. For mixed NCS, the nerve is usually stimulated at just one point while recording at a more proximal point (see discussion below).

Of the various components obtained on motor NCS, those most consistently reported are the distal amplitude, the proximal amplitude (if it is significantly different from the distal one), the distal latency, and the CV if it is calculated. The durations of abnormal responses are reported as well.

1.7.1 Motor Nerve Conduction Studies

Motor NCS were the first to be performed, in part because of technical considerations. Unlike sensory and mixed NCS, motor NCS are indirect studies in that the measured endpoint of motor nerve stimulation is a CMAP rather than a nerve action potential. Each nerve fiber controls a variable number of muscle fibers, ranging in the limbs from approximately 350 muscle fibers in the intrinsic muscles of the hand to over 1900 in some of the large leg muscles such as the gastrocnemii. Consequently, the activation of a single nerve fiber results in the near simultaneous activation of many muscle fibers. It is this magnification effect that causes CMAPs to be measured in mV while SNAPs and MNAPs are measured in μV. It also explains why, in the early days of electrodiagnosis, motor NCS were developed and used before sensory NCS — they are much larger responses and therefore require less sophisticated equipment.

To perform motor NCS, one of the muscles the nerve innervates must be accessible, as well as the nerve itself at one point. If a CV is desired, the nerve must be accessible to external stimulation at two or more points along its course. Peripheral nerves generally are more superficial, and therefore more accessible, at the joints. For this reason, the standard upper extremity NCS, the median and ulnar NCS, are performed by recording over intrinsic hand muscles (the lateral thenar eminence muscles and the hypothenar eminence muscles, respectively), while stimulating the appropriate nerve at the elbow to obtain the proximal amplitude and latency, and at the wrist to obtain the distal amplitude and latency. Similarly, the standard lower extremity NCS, the peroneal and posterior tibial NCS, are performed by recording from intrinsic foot muscles (extensor digitorum brevis and abductor hallucis, respectively), while stimulating the appropriate nerve at the ankle and behind the knee, in the popliteal fossa (Figure 1.35).

Figure 1.35 — The peroneal motor NCS, one of the routine lower extremity motor NCS.

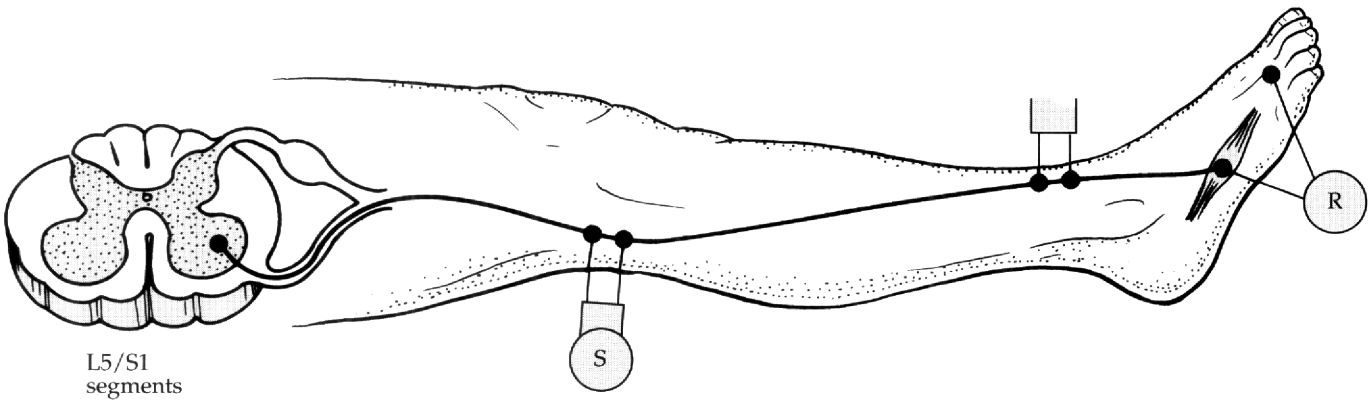

A number of other motor nerves can be studied if necessary. For example, in the upper extremity, ulnar motor NCS can be performed while recording from an ulnar-innervated muscle on the thumb side of the hand (e.g., the first interosseous) or from ulnar-innervated forearm muscles. Also, radial motor NCS can be performed when recording from various extensor forearm muscles. Musculocutaneous and axillary motor NCS can be performed while recording from the biceps and deltoid muscles, respectively, above the elbow. Moreover, for most of these upper extremity motor NCS, the nerves can also be stimulated more proximally, e.g., in the axilla, and above the clavicle. Most ulnar nerve lesions occur at the elbow. Consequently, during ulnar motor NCS, the nerve can also be stimulated immediately below the elbow to better evaluate conduction along the abnormal segment.

For the lower extremity motor NCS, peroneal recordings can also be made from the tibialis anterior muscle, on the anterior surface of the leg, midway between the ankle and knee. Tibial recordings also can be obtained from the gastrocnemius/soleus muscles on the posterior surface of the leg (the latter is routinely recorded as a component of the H-response, one of the late responses to be discussed). In addition, femoral motor NCS can be performed by stimulating the femoral nerve at the inguinal ligament, while recording over the quadricep muscle on the front of the thigh.

1.7.2 Sensory Nerve Conduction Studies

Sensory NCS are direct studies in that their end-point is a SNAP recorded at some more proximal or distal site from the point of generation. Because these responses are only a fraction of the size of a CMAP, the sensory NCS, although first introduced clinically in 1958, did not become standard in many EMG laboratories until the 1970s, after the sensitivity of the EMG equipment had increased significantly.

Sensory NCS are performed: (1) by stimulating and recording from a pure sensory nerve; (2) by stimulating a mixed nerve while recording from a sensory nerve derived from it (antidromic technique); or, (3) by stimulating the distal sensory fibers of a mixed nerve while recording from the fibers more proximally, where they are a component of a mixed nerve (orthodromic technique).

Standard upper extremity sensory NCS are the median and ulnar studies. These two sensory NCS can be performed both orthodromically and antidromically. With orthodromic conduction, the median SNAP is obtained by stimulating the digital nerves of the index finger (or, less often, other median-innervated fingers) with ring electrodes while recording over the (mixed) median nerve at the wrist. The ulnar SNAP is obtained orthodromically by stimulating the digital nerves of the little finger while recording over the (mixed) ulnar nerve at the wrist. Both of these studies often are performed antidromically by reversing the sites for stimulating and recording. Although sensory nerves ordinarily do not conduct nerve impulses centrifugally, the nerve fibers themselves are very similar to electrical cable and conduct freely in either direction. Moreover, there are several technical reasons why antidromic sensory NCS are more helpful than orthodromic ones, including the fact that they are less painful and their responses are of higher amplitude due to less intervening tissue between the nerve fibers and the recording electrodes. A number of other upper extremity sensory NCS can be performed, including a radial sensory NCS, recording the base of the thumb, and various NCS to assess the forearm sensory nerves (lateral, medial, and posterior antebrachial cutaneous NCS).

A standard lower extremity sensory NCS is the sural, which is obtained by recording over the sural nerve as it winds around the lateral malleolus, while stimulating it more proximally, usually at a fixed distance of 14 cm (Figure 1.36). Also, the superficial peroneal sensory nerve and the saphenous nerve, derived from the common peroneal and femoral nerves, respectively, can be assessed.

Figure 1.36 — The sural NCS, the standard lower extremity sensory nerve conduction study.

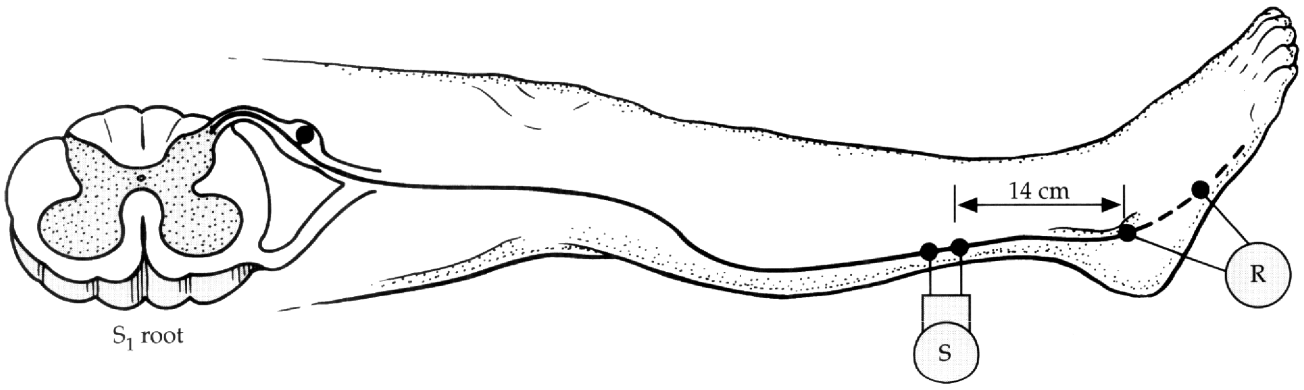

One of the major advantages of sensory NCS is that their responses are more sensitive than the motor NCS responses with many abnormalities of the PNS; i.e., they become abnormal when the degree of nerve fiber injury is such that the motor NCS are still within the normal range.

A major disadvantage of sensory NCS is that, for various reasons, they are far more sensitive to advanced age, minor trauma, and a host of other factors, than motor NCS. Thus, the lower extremity sensory responses often are unelicitable bilaterally in many normal persons over the age of 60 years. Similarly, in patients who have undergone vein

stripping or who are markedly obese, the sensory NCS responses may be unelicitable for technical reasons.

1.7.3 Mixed Nerve Conduction Studies

These studies are performed by stimulating a mixed nerve at one point along its course while recording from it at some other point. The resulting MNAP is due to activation of both the motor and sensory fibers of the nerve. The particular contribution from each type of fiber varies from one nerve to another. To avoid overwhelming electrical artifact from muscle activation, mixed NCS characteristically are performed by stimulating distally while recording more proximally; e.g., stimulating the median nerve at the wrist while recording over it at the elbow. For this reason, mixed NCS often are difficult to perform on large, obese patients because of the amount of intervening tissue between the nerve and the surface recording electrodes at the recording site. Electromyographic laboratories perform relatively few mixed NCS. Those done with some regularity assess the terminal nerve fibers in the feet (plantar NCS) (Figure 1.37).

Figure 1.37 — Plantar nerve conduction studies.

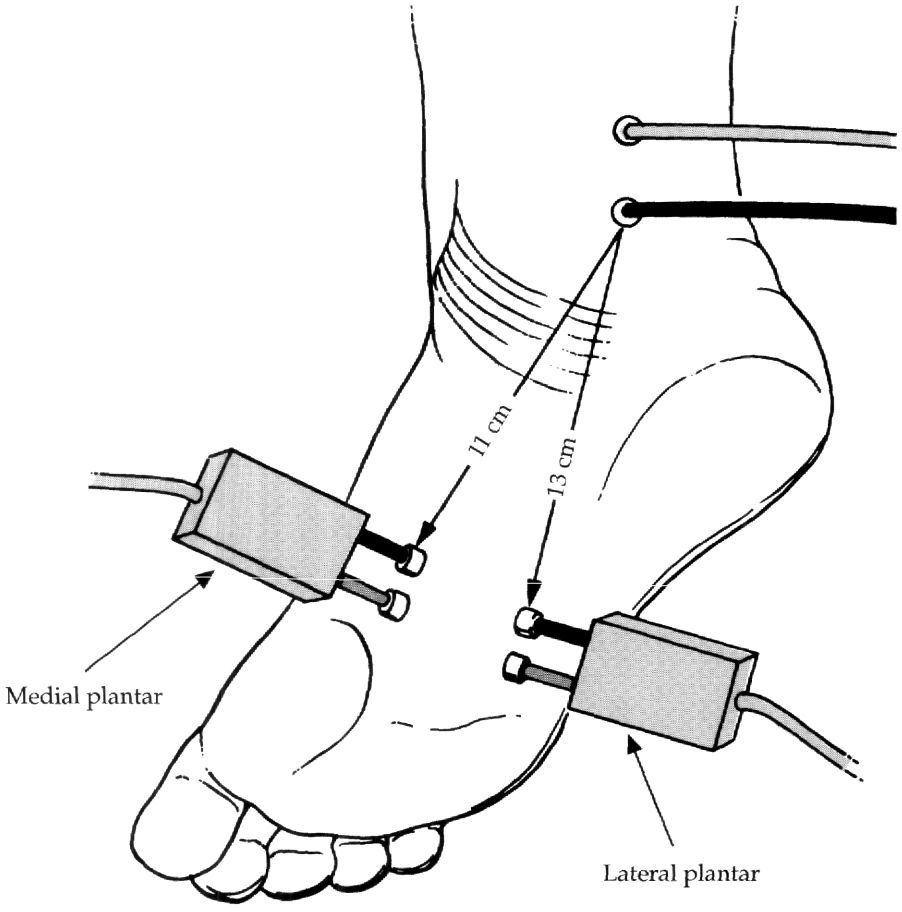

1.7.4 Normal Values

To be meaningful, the results of NCS — motor, sensory, and mixed — must be compared to some normal values. Ideally, each laboratory will obtain its own normal values for each NCS procedure. These must be age-related as well, because conduction rates are quite slow in infants and young children, while amplitudes and conduction rates in adults decrease with age. At the Cleveland Clinic EMG laboratory, for example, a series of normal values for all NCS exist based on each decade of life (Table 1.3). Nonetheless, the most sensitive normal value for a particular NCS usually is obtained by performing the same NCS on the corresponding nerve in the contralateral limb (assuming it is normal). A decrease of more than 50% in amplitude on the affected side is considered abnormal, even if it is within normal limits compared to laboratory values.

Table 1.3 - Nerve Conduction Study Values

	4-9 Years			10-29 Years			30-49 Years		
NERVE	AMP.	P.L./D.L.	C.V.	AMP.	P.L./D.L.	C.V.	AMP.	P.L./D.L.	C.V.
Median (sensory)	>20	< 3.2	>51	>20	< 3.3	>51	>20	< 3.4	>50
Ulnar (sensory)	>18	< 2.9	>51	>18	< 3.0	>51	>12	< 3.1	>50
Radial (sensory)	>18	< 2.6		>18	< 2.7		>18	< 2.7	
Median (APB)	> 6	< 3.6	>51	> 6	< 3.9	>51	> 6	< 4.0	>50
Median-palmer (mx)	>10	< 2.2		>10	< 2.2		>10	< 2.2	
Ulnar-palmer (mx)	> 5	< 2.2		> 5	< 2.2		> 5	< 2.2	
Sural (s)	> 6	< 4.3	>41	> 6	< 4.4	>41	> 5	< 4.5	
Superfic. Pero (s)	> 6	< 4.3		> 6	< 4.4		> 5	< 4.5	
Peroneal (EDB)	> 3	< 5.5	>41	> 3	< 5.5	>41	> 3	< 5.5	>40
Post. Tibial (AH)	> 8	< 5.8	>41	> 8	< 5.8	>41	> 8	< 6.0	>40
H-reflex (M-resp)	> 8	< 7.0		> 8	< 7.0		> 8	< 7.0	
H-reflex (H-ref)	> 1	<35.0		> 1	<35.0		> 1	<35.0	

Amp=μV for sensory and mixed
Amp=mV for motor
DL=motor NCS
PL=sensory NCS

Table 1.3, continued – Nerve Conduction Study Values

NERVE	50-59 Years			60+ Years		
	AMP.	P.L./D.L.	C.V.	AMP.	P.L./D.L.	C.V.
Median (sensory)	>15	< 3.6	>50	>10	< 3.8	>50
Ulnar (sensory)	>10	< 3.1	>50	>5	< 3.2	>50
Radial (sensory)	>14	< 2.7		>10	< 2.8	
Median (APB)	> 6	< 4.0	>50	>5	< 4.0	>50
Median-palmer (mx)	>10	< 2.2		>10	< 2.2	
Ulnar-palmer (mx)	> 5	< 2.2		>5	< 2.2	
Sural (s)	> 4	< 4.6	>40	>3	< 4.6	>40
Superfic. Pero (s)	> 4	< 4.6		>3	< 4.6	
Peroneal (EDB)	>2.5	< 6.0	>40	>2.5	< 6.0	>40
Post. Tibial (AH)	> 4	< 6.0	>40	>4	< 6.0	>40
H-reflex (M-resp)	> 6	< 7.5		>6	< 7.5	
H-reflex (H-ref)	> 1	<35.0		>1	<35.0	

1.7.5 Special Studies

In addition to basic NCS and NEE, a number of other procedures also are performed in the EMG laboratory. These can be grouped under the nonspecific title, Special Studies. Most are variations of NCS, and include the late responses (F-waves and H-responses), repetitive stimulation studies, blink reflexes, and single-fiber EMG studies, among others. Most have relatively limited application compared to the two basic components of the electrodiagnostic examination. Only the late responses and the blink reflex will be discussed in this section.

1.7.6 Late Responses

Late responses consist of two separate procedures, H-responses and F-waves, which are somewhat similar in that nerve impulses travel up to the spinal cord and back before the muscle action potentials they induce are recorded. However, major differences exist between the two.

Figure 1.38 — The set–up for performing an H–response.

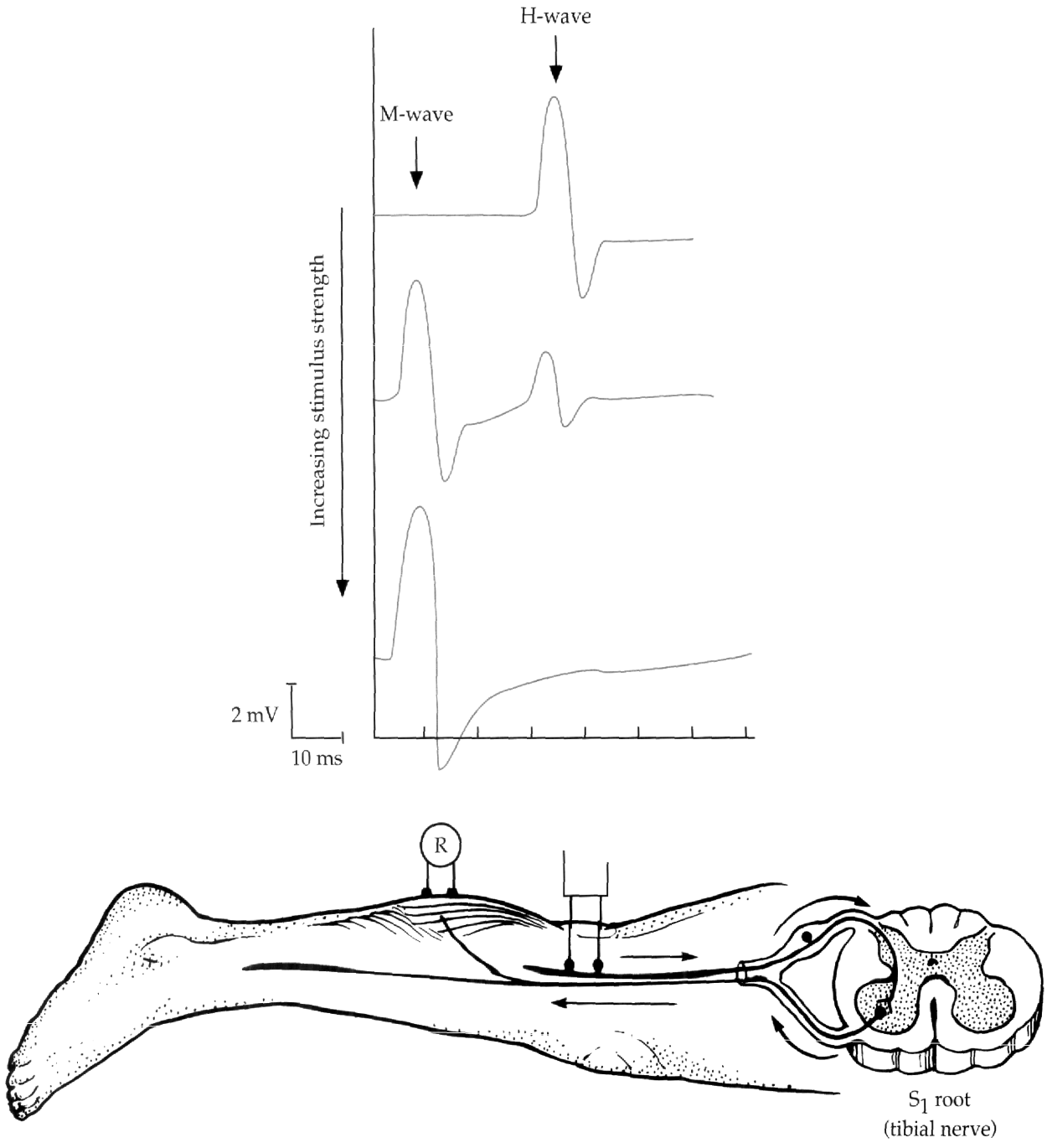

1.7.6.1 H-Responses

H-responses can be consistently elicited in normal adults only by stimulating the tibial nerve in the popliteal fossa while recording from the gastrocnemius/soleus group of muscles (i.e., the calf muscles), which are innervated by the tibial nerve. When the nerve is stimulated in the popliteal fossa with the cathode pointed towards the trunk (rather than the reverse, which is done during standard NCS), nerve impulses are first initiated in the large sensory fibers at the stimulation site because they have the lowest threshold. The sensory nerve impulses that travel distally go undetected, because the NCS set-up is not designed to record them. However, those sensory nerve impulses that travel centripetally along the sensory fibers reach the S1 segment of the spinal cord where they are passed on to S1 motor fibers. The impulses subsequently travel back down the S1/tibial motor fibers to activate a few of the muscle fibers in the gastrocnemius/soleus muscles. This activation is recorded as the initial H-response. As the stimulus is increased, more and more of the sensory fibers are activated and the resulting H-response increases in amplitude. Eventually, however, a point is reached at which the motor nerve fibers at the stimulation site are activated directly by the stimulus. Consequently, two responses begin to appear on the screen: one of short latency (approximately 10 ms) known as the M-response or direct muscle response due to the motor nerve activation, and one of much longer latency (approximately 30 ms) representing the H-response. As the power is increased further, the M-response continues to grow, while the H-response dwindles because those nerve impulses passing orthodromically along the sensory fibers and those traveling antidromically along the motor fibers begin to collide with one another at some proximal point. Since nerve impulses leave an absolute refractory period in their wake, both nerve impulses are stopped at the collision site (Figure 1.38). An H-response is, thus, a submaximally-activated reflex response analogous to the ankle jerk that is elicited by tapping the Achilles tendon with a reflex hammer. For practical purposes, H-responses are of major value only in detecting generalized polyneuropathies and lumbosacral radiculopathies involving the S1 roots.

1.7.6.2 F-Waves

F-waves, in contrast to H-responses, can be elicited from any motor nerve in either the upper or lower extremity. With supramaximal stimulation of a motor nerve, the resulting action potentials travel bidirectionally. Those passing distally along the nerve produce a CMAP, or M-response, a few ms later. Those traveling proximally along the motor nerve fibers sometimes reach the motor nerve cell bodies in the spinal cord when they are in such a state that they backfire, producing another motor action potential, called a recurrent discharge, which then travels centrifugally down to the muscle. The small motor response evoked by the latter, at 20 to 50 ms after stimulation (depending upon the nerve studied and the recording site), is referred to as an F-wave. F-waves are not reflexes because only motor nerve fibers are involved. Moreover, only about 10% of supramaximal stimulations evoke an F-wave, and subsequent F-waves usually are not due to activation of the same fibers. Hence, the F-wave, unlike the H-response, typically consists of a series of small potentials, dispersed somewhat in time.

Theoretically, F-waves should be of real benefit in that they permit NCS assessment of the very proximal segments of the motor nerves. Nonetheless, for a variety of reasons, most electromyographers have found F-waves to be of quite limited value. They are

Figure 1.39 — The set–up for recording blink reflexes.

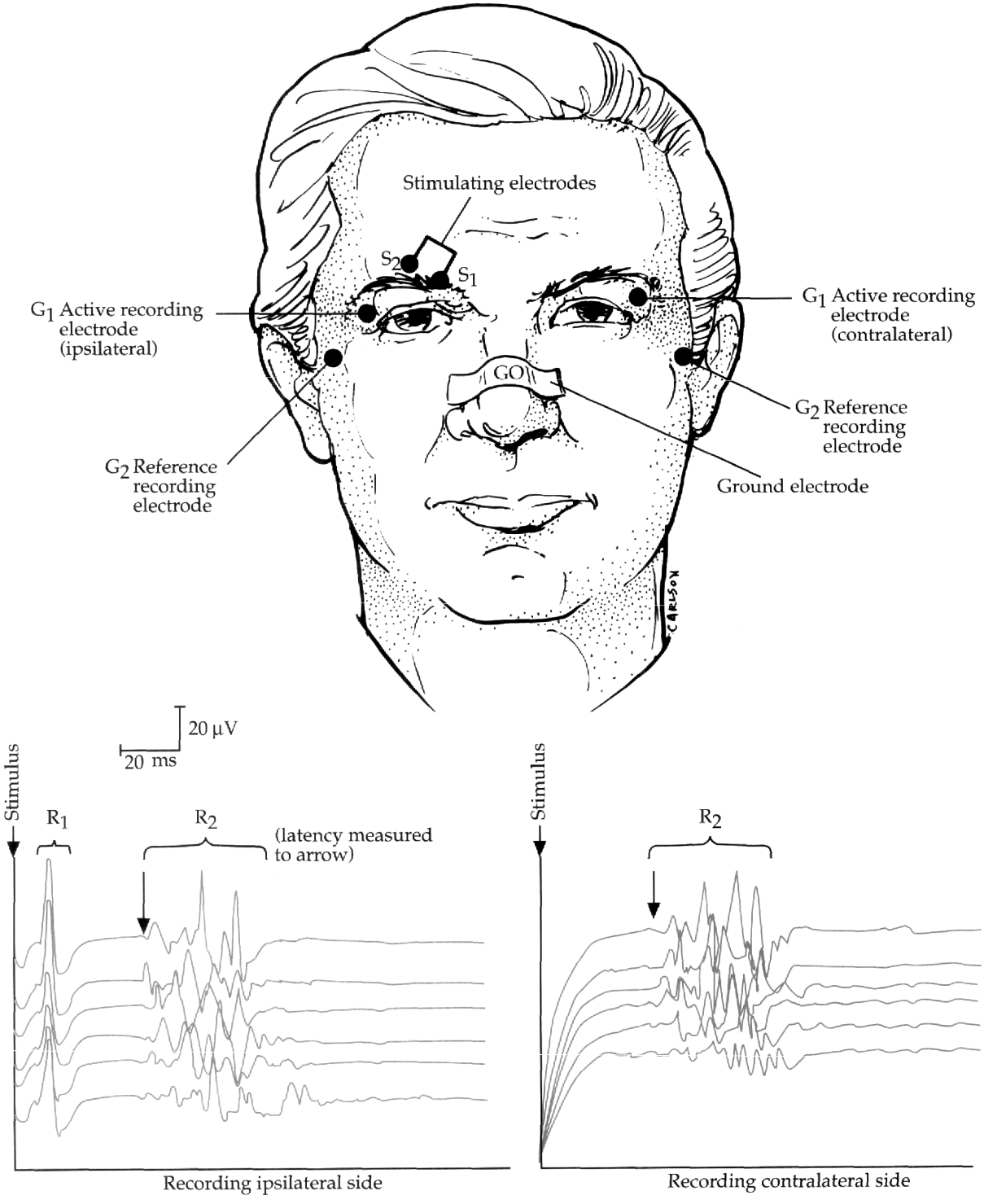

usually normal or redundant, if abnormal, in that some other component of the standard electrodiagnostic examination will have already provided all the information needed.

1.7.7 Blink Responses

Blink responses are action potentials recorded from a small facial muscle, the orbicularis oculi, that surrounds the eye orbit. This muscle is innervated by the facial motor nerve, or the 7th cranial nerve. These facial muscle action potentials result from stimulation of the supraorbital nerve, one of the sensory nerves derived from the trigeminal nerve, or the 5th cranial nerve, that supplies sensation to the skin above the orbit.

After stimulating one supraorbital nerve, the R1/direct response is recorded about 10 ms later on the same side of the face. Subsequently, about 30 ms after the stimulation the R2/indirect responses are recorded simultaneously on both sides of the face (Figure 1.39).

Blink responses are reflex studies. The impulses are transmitted to the brain stem by the trigeminal nerve (from which the supraorbital nerve is derived), make connections within the brain stem, and then pass peripherally in the facial nerve to the orbicularis oculi muscles.

Although blink responses are used somewhat differently by various investigators, they most consistently are performed to assess the 5th and the 7th cranial nerves. They are abnormal, for example, with unilateral facial paralysis, such as Bell's palsy.

1.7.8 Pitfalls in Performance of Nerve Conduction Studies

As noted earlier, performing NCS is deceptively simple. What seems to be an easy task is actually fraught with a myriad of problems and potential errors — anatomical, technical, procedural, and interpretive — that can readily thwart attempts to perform accurate, reproducible and, therefore, reliable NCS. Obviously, only the latter are of clinical value.

Some of the major sources of error are:

- **Nerve anomalies**. An appreciable number of persons have nerve anomalies in both the upper and lower extremities (median to ulnar nerve communications in the forearm; accessory peroneal nerves) that can produce confusing results on NCS if not recognized.
- **Limb temperature variations**. Slight changes in limb temperature can produce substantial alterations in NCS results. The major problem is inadvertent limb cooling, which can cause CMAP and SNAP responses to be increased in amplitude, increased in duration, prolonged in latency, and slow in CV. For this reason, many patients are reported to have focal or generalized nerve lesions when all they actually have are cool limbs.
- **Patient age**. NCS results are very different at the extremes of age than they are in adolescents, young adults, and middle-aged adults. In the young, because the myelin is relatively thin, the nerve conduction values are approximately one-half those seen in adults. These values do not reach the normal adult range until 3 to 4 years of age. Similarly, in the elderly, sensory NCS responses and H-responses are often unelicitable in the lower extremities, while the NCS responses that can be obtained are generally lower in amplitude and slower in conduction rate.

- **Technical-lack of standardization**. To be of any clinical value, NCS must be standardized so that results are reproducible and, therefore, comparable to normal values. Thus, for each NCS performed, the stimulating and recording sites must be consistent from one limb to another, set distances must be measured accurately, etc. Many EMG laboratories lack such standardization.
- **Technical-electrode placement errors**. The recording electrode inadvertently may not be affixed over the motor point of the muscle (for motor NCS) or directly over the nerve (for sensory NCS). The resulting responses may be spuriously low in amplitude and sometimes falsely slow. Moreover, if the recording electrodes are not affixed firmly to the skin, overwhelming artifacts can result. Also, if excessive electrode paste is used, salt bridges can be established between the electrodes, denigrating the recorded responses. Finally, if active and reference electrodes are switched, the response recorded will be a vertical mirror image of the normal response, producing considerable confusion if unrecognized.
- **Technical-stimulation errors**. If the stimulating electrodes are mistakenly placed at some distance from a motor nerve, other nerves in the area may be inadvertently stimulated and the CMAPs that result may, by volume conduction, reach the recording electrodes and be misinterpreted. If too much electrolyte paste is placed on the stimulating electrodes (anode and cathode), salt bridges can form between them, causing a short-circuiting of the current flow, resulting in an inability to stimulate the nerve, even with the use of excessive power. Also, if the cathode and anode are inadvertently switched, the responses will be longer in latency (due to the nerve impulses having to traverse the additional nerve segment between the cathode and anode) and sometimes lower in amplitude (due to a partial anodal block). Submaximal nerve stimulation can result in responses that are both spuriously low in amplitude and sometimes prolonged in latency. Excessively strong stimulation, however, also has undesired consequences: (1) The nerve can actually be stimulated at a distance from the cathode rather than immediately beneath it, which can result in an erroneously short latency being obtained; and (2) The stimulus can spread to other nerves and thereby produce spurious, confusing responses. Inadvertent stimulus spread is particularly likely to occur between the median and the ulnar nerves on stimulations at the elbow and between the tibial and peroneal nerves on stimulations behind the knee.
- **Technical-measurement errors**. As noted, distal/peak latencies are usually determined by using a set distance between the cathode and the active recording electrode, and CVs are calculated by using the distance measured between the two points (cathode) of stimulation. These measurements can be inaccurate for a number of reasons, including inadequate or inaccurate marking of the stimulation points, failing to obtain measurements with the limb in a standardized position, inaccurately reading the distance, etc.
- **Instrumentation errors**. These can occur if the EMG equipment is not properly maintained and calibrated. With older equipment the sweep speed can vary as it traverses the screen. Moreover, with some machines the measurements can be made off the cathode ray screen and parallax usually occurs unless the electromyographer is directly in front of the screen.

- **Other examiner errors.** During CV determinations, some electromyographers change various machine parameters between stimulating at the proximal and distal sites, such as altering the amplification or the sweep speed. Although these are done in an attempt to increase accuracy, they can result in significant errors in latency measurement. In addition, measurements can be made to the wrong portion of an evoked response, artifacts can erroneously be considered responses, and simple arithmetic mistakes can be made when calculating CVs.

1.8 Needle Electrode Examination

The second major component of an EMG study is the NEE. A wire needle, like a hypodermic needle, is inserted into a muscle belly. The needle incorporates both an active recording electrode and a referential electrode and is connected to an oscilloscope and audio system via a differential amplifier. When the muscle is at rest, the NEE relays information about insertional activity and spontaneous activity. When the muscle is in a state of voluntary contraction, the NEE displays discharges on the oscilloscope called MUAPs.

Anatomically, the motor unit includes all the excitable tissues activated by a single AHC in the spinal cord. The final arborization of terminal nerves is arrayed closely within a muscle fascicle. All muscle fibers from a single motor unit are not contiguous, but form a mosaic pattern with other closely overlapping motor units within the same territory.

The MUAP represents an electrical summation of all the individual muscle fiber action potentials activated by the discharge of a single AHC, or motor unit. The normal MUAP is classically a triphasic discharge (Figure 1.40). The unique size and shape of a MUAP is derived from the particular subset of muscle fiber action potentials in that motor unit within the immediate recording territory of the needle electrode at that moment, because the whole motor unit cannot be recorded by a standard needle electrode at one position. A slight movement of the needle electrode will change the number and interrelationship of the muscle fiber action potentials in the immediate recording territory, thus changing MUAP morphology even though the same motor unit is being recorded. A single muscle fascicle contains many individual motor units in a mosaic pattern. Therefore, multiple different motor units will be in the recording territory of a standard concentric needle electrode at any given time.

The MUAP and the M-wave of the CMAP are recorded from muscle fibers. The CMAP, however, is a summation of all the motor units activated after supramaximal stimulation of a nerve trunk. Motor units do not summate together in the volume conductor in a single recorded discharge because each motor unit has a unique activation pattern that separates it in time from other simultaneously activating motor units.

Needle electrodes differ in their recording properties. The surface area of the active recording site determines the recording radius of the needle. Larger surface areas record over larger territories. The standard concentric needle electrode, with an active recording surface of 150 microns x 600 microns, has a recording distance of 10 mm. Eight to 20 muscle fibers belonging to the same motor unit are likely to contribute to the recorded MUAP. On the other hand, a single-fiber EMG (SFEMG) needle electrode has an active recording surface of about 25 microns diameter, with a recording distance of 1 mm. Thus, only 1 to 2 muscle fibers are likely to contribute to a recorded MUAP, allowing detailed comparison of the activation properties of individual muscle fiber action potentials (Figure 1.41).

Figure 1.40 — Example of a normal MUAP with triphasic configuration.

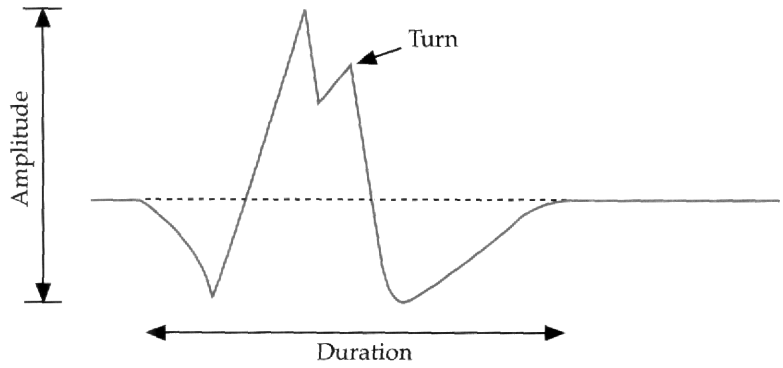

Figure 1.41 — Cross-section of muscle stained for glycogen after stimulating an isolated motor axon showing one motor unit.

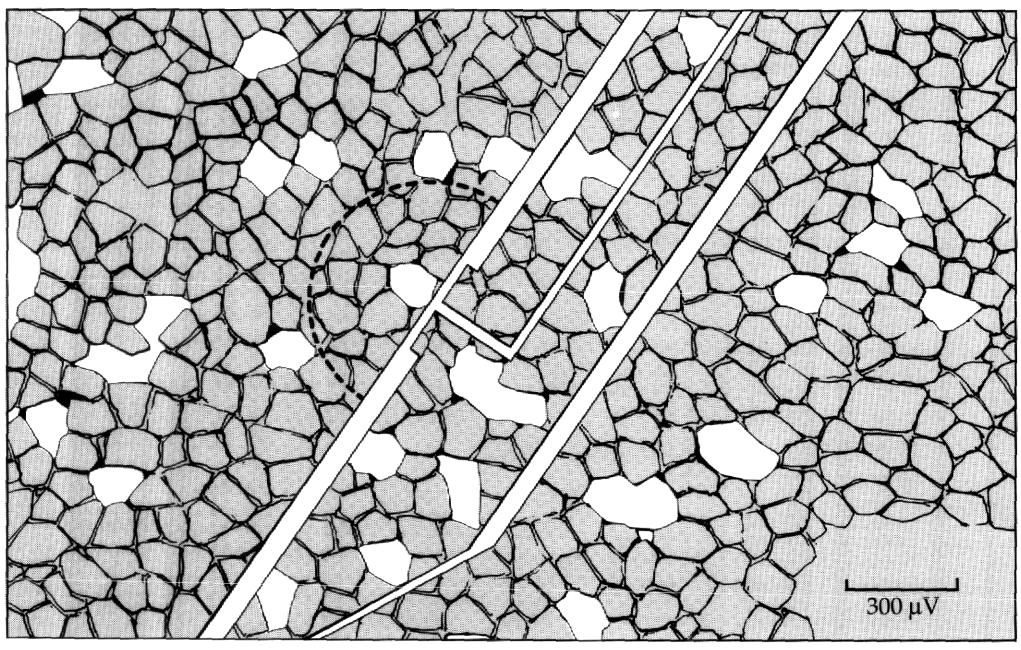

Figure 1.42 — Effect of muscle temperature on MUAP.

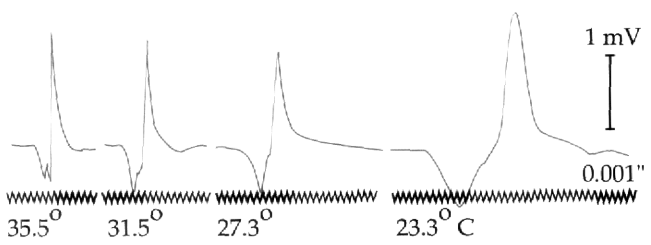

Technical and physiological factors alter the appearance of normal MUAPs, such as the aforementioned size of the active recording surface. Varying the filter settings changes the low-frequency and high-frequency components of waveforms contributing to the discharge morphology. Physiologic tissue is an excellent low-pass filter. Low-frequency components of MUAPs outside the immediate recording area of the needle electrode may contaminate the recorded discharges unless the low-frequency filter setting is at least 30 Hz. Changes in the high-frequency filter alter the MUAP less significantly.

Temperature change has a predictable effect on neurophysiological recordings. Due to the slowing of conduction along peripheral nerve and muscle fiber membranes, the duration of a MUAP increases as temperature decreases (Figure 1.42). While some workers in the field, such as Buchthal, believe the amplitude of the MUAP decreases as temperature decreases, other workers such as Falck and Lang have reported increases in amplitude with decreased temperature. Cooling of excitable tissues slows the inactivation of sodium permeability and the activation of potassium permeability during depolarization of the membrane, which results in prolonged membrane recovery and increased size of the action potential.

The MUAP size varies with age. The MUAPs are smallest in the neonate and largest in the elderly. Factors accounting for this morphologic change include the developmental enlargement of muscle fiber diameters through early life and the subtle reinnervation that occurs secondary to motor unit senescence in later life. In a given individual, normal MUAPs vary in size and configuration in different muscles because innervation ratios (number of muscle fibers per motor unit) vary in different muscles from 25 in platysma to nearly 2000 in gastrocnemius. Secondly, the mean muscle fiber diameter differs, from 20 microns in platysma to 57 microns in tibialis anterior.

Pathologic changes in the motor unit can occur for various reasons. They basically involve damage to the peripheral nerves (axons) or the muscle fibers themselves. In both neurogenic and myopathic changes, the pathophysiologic factors leading to electro-physiologic change in single muscle fiber action potentials and MUAPs are: 1) change in terminal nerve twig length and/or conduction velocity, 2) change in muscle fiber diameter, 3) change in distance between muscle end-plate and recording site of needle electrode, and 4) change in the number of muscle fibers in the motor unit (Figure 1.43).

After acute trauma to a nerve trunk, many motor units may be lost. Muscle end-plates (neuromuscular junctions) of denervated muscle fibers disintegrate and denervated muscle fibers atrophy. The remaining MUAPs may be normal. Reinnervation may proceed either by regeneration of nerve fibers from the site of their trauma, or by collateral sprouting of terminal nerve twigs from surviving axons to innervate neighboring denervated muscle fibers. The process of reinnervation produces morphologic changes in MUAPs (Figure 1.44). Newly regenerated nerve twigs and reinnervated muscle fibers do not have the same properties as they did prior to injury. In most cases, the newly reinnervating nerve twigs are longer and conduct more slowly than the more established twigs. The distance from the neuromuscular junction to the needle recording site is also longer. Finally, the freshly reinnervated muscle fibers are atrophied. All these factors combine to produce newly reinnervated muscle fiber action potentials that arrive late to the recording site and produce satellite potentials that trail after the main component of the MUAP (Figure 1.44). As more muscle fibers are freshly reinnervated, a remodeled MUAP emerges, one that has lost its triphasic appearance and appears polyphasic. When reinnervation is complete, the resulting MUAP is larger than normal because it is the summation of many more muscle fiber action potentials than before collateral sprouting began.

Figure 1.43 — Schematic representation of MUAP generation and recording by concentric needle electrode.

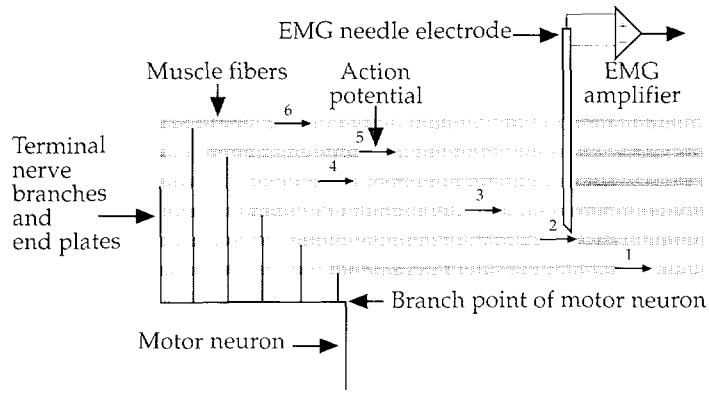

Figure 1.44 — Evolution of changes in a reinnervating MUAP after partial denervation.

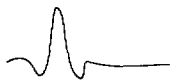

Normal surviving MUAP.

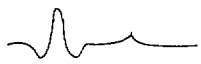

Reinnvervation by collateral sprouting to a single muscle fiber (satellite potential).

Reinnervation of multiple other muscle fibers.

Further reinnervation of denervated muscle fibers from neighboring denervated motor units.

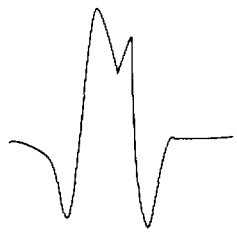

Further reinnervation and maturation of reinnervated terminal twig conduction properties, maturation of neuromuscular junctions and enlargement of muscle fiber diameters.

In primary muscle disease, the same reinnervating process occurs. In addition, permanent muscle fibers drop out occurs. As a result of the disease process, muscle fibers are severely narrowed in diameter, producing small, but highly polyphasic, MUAPs (Figure 1.45).

1.8.1 Recruitment

The NEE also includes an analysis of the firing pattern of MUAPs. Recruitment is the term for the progressive calling up of more motor units to provide more forceful contraction of muscle. In all activities requiring energy, the physiologic system tends to minimize energy expenditure. The motor system does this by choosing specific types of motor units to be activated and by coordinating the timing of recruitment in the contractile process (Figure 1.46). For small but continuous contractile efforts, type I (slow twitch) motor units are activated because of their aerobic and relatively low-energy-requiring metabolism. When more contraction is required, a choice is made between more frequent activation of motor units already firing and the recruitment of new motor units. At a certain point for each firing motor unit, the energy requirement for more frequent activation will exceed the energy requirement to recruit a new motor unit. As more contraction is needed, type II (fast twitch) motor units are recruited because of their faster twitch and greater twitch tension characteristics.

Individual MUAPs often begin firing at a frequency of 5 to 10 per second (5 Hz to 10 Hz). By the time a single MUAP is firing 15 Hz, at least one other MUAP has been recruited. This process continues until a maximal contraction is delivered and the EMG tracing shows a confluence of individual MUAPs too numerous to count (interference pattern).

In a neurogenic process, where motor units drop out (i.e., by death of AHCs or transection of a nerve trunk), the normal recruitment pattern is disturbed. The old orderly activation of motor units with increased contraction no longer occurs because insufficient motor units are connected to muscle fibers to provide that. As a result, existing MUAPs fire at a faster rate to provide the needed contractile force. Thus, the EMG tracing will show a reduced recruitment pattern of too few MUAPs present, each firing at faster frequencies than normal.

In a myopathic disorder, the reverse occurs. At any given contractile force of muscle, more MUAPs are firing than would be expected, while the firing frequency of each MUAP remains normal. This early recruitment occurs because muscle fibers have dropped out of motor units, giving each motor unit less power when activated. Therefore, to produce an equivalent amount of contraction, more MUAPs need to be recruited.

1.8.2 Insertional and Spontaneous Activity

Normal muscle at rest is electrically silent. With needle movement, normal insertional activity is produced by mechanically inducing muscle fiber action potentials. Such activity lasts only as long as the needle movement.

Abnormal neuromuscular states can produce increased insertional activity. A denervated muscle fiber undergoes disintegration of its motor end-plate. Changes occur in the ion channel sensitivities such that automatic, regular depolarizations of the membrane occur, producing propagated action potentials. In the early phases (1 to 3 weeks) after axon loss, these discharges are initiated by needle movement and have waveform characteristics of positive waves or sharp spikes that die out eventually once the needle

Figure 1.45 — Evolution of morphologic changes in the MUAP in a progressive necrotizing myopathy (polymyositis).

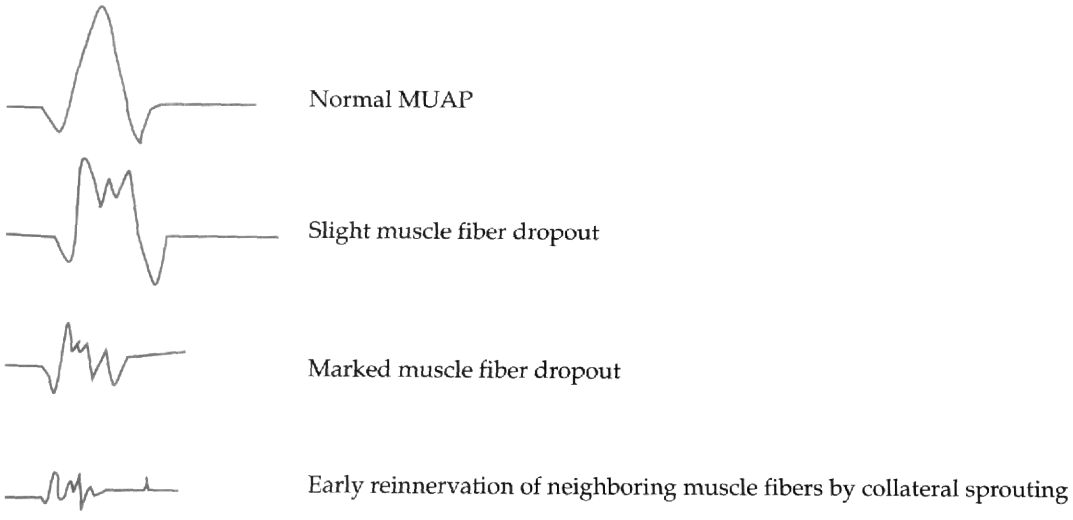

Figure 1.46 — A three–dimensional diagram that summarizes physiologic and histochemical data obtained from motor units of the cat medial gastrocnemius muscle.

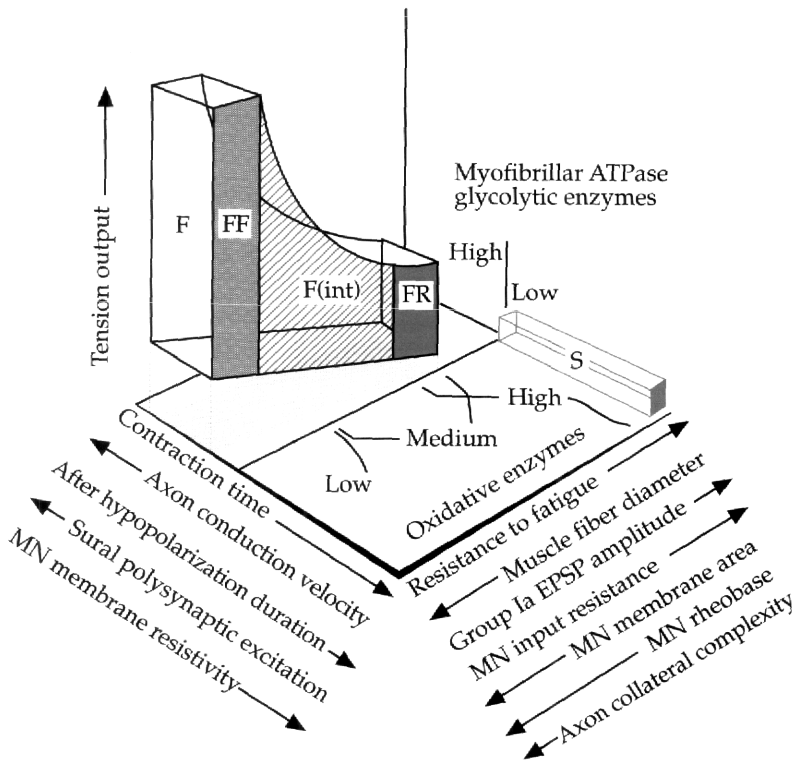

stops moving. In EMG terminology, these discharges are called positive waves. This may be the earliest sign of an axon loss neurogenic process. Another example of abnormal insertional activity is myotonic discharges, which can be seen in hereditary myopathies, as well as chronic acquired neuropathic and myopathic disorders. Abnormally reduced insertional activity can be seen in muscle replaced by fatty tissue or fibrosis and in metabolic states that make the muscle electrically unexcitable (McArdle's disease, paramyotonia congenita, and periodic paralysis).

Spontaneous activity consists of electrical discharges in a muscle at rest, without needle movement. It is always abnormal. Fibrillation potentials are thought to be the continuous, spontaneous form of positive-wave discharges seen in denervated muscle (Figure 1.47). They are the classic EMG feature of recent denervation. Other examples of abnormal spontaneous activity include fasciculation potentials (seen in neuropathies and motor neuron disorders), myokymic discharges (seen in chronic compressive neuropathies and as a result of radiation change to peripheral nerves), and complex repetitive discharges (seen in any chronic neuropathic or myopathic process). Findings of abnormal spontaneous activity help the electromyographer support the diagnosis of disease of the motor unit and can often help in localization of nerve damage and definitive diagnosis.

Figure 1.47 — Fibrillation potentials (top) spike form (bottom).

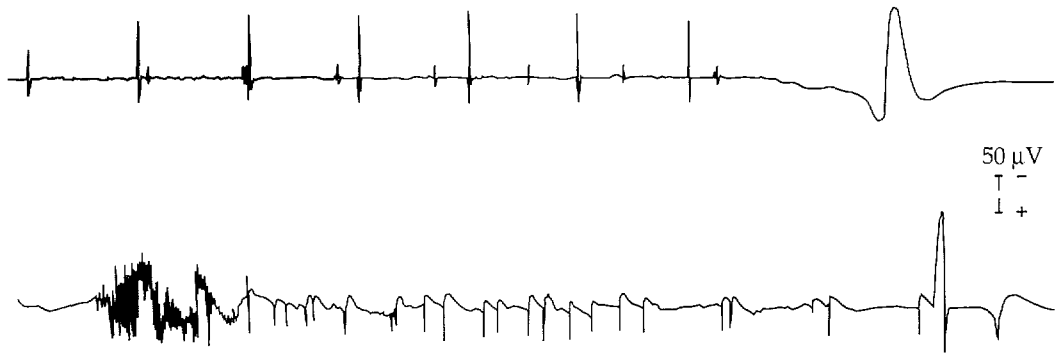

1.9 *Pathophysiology*

1.9.1 Nerve

Peripheral nerve fibers and their cells of origin can be traumatized in a great variety of ways. Nonetheless, their pathological responses to injury are quite limited, and their pathophysiological responses are even more restricted. In general, large myelinated fibers can sustain relatively mild damage that causes focal alterations in their myelin without killing them, or they can undergo more severe injury that causes them to degenerate (demyelination and axon loss, respectively). When axon loss or axon degeneration occurs, the nerve degenerates from the point of injury distally to its furthest extent. For example, motor fibers degenerate down to where they terminate, as the motor end-plate, in the neuromuscular junction. This nerve-degenerating process is referred to as *Wallerian degeneration,*

Figure 1.48 — Characteristic changes produced in a motor-evoked response (obtained by distal stimulation) with various types of pathophysiology (Nl = normal).

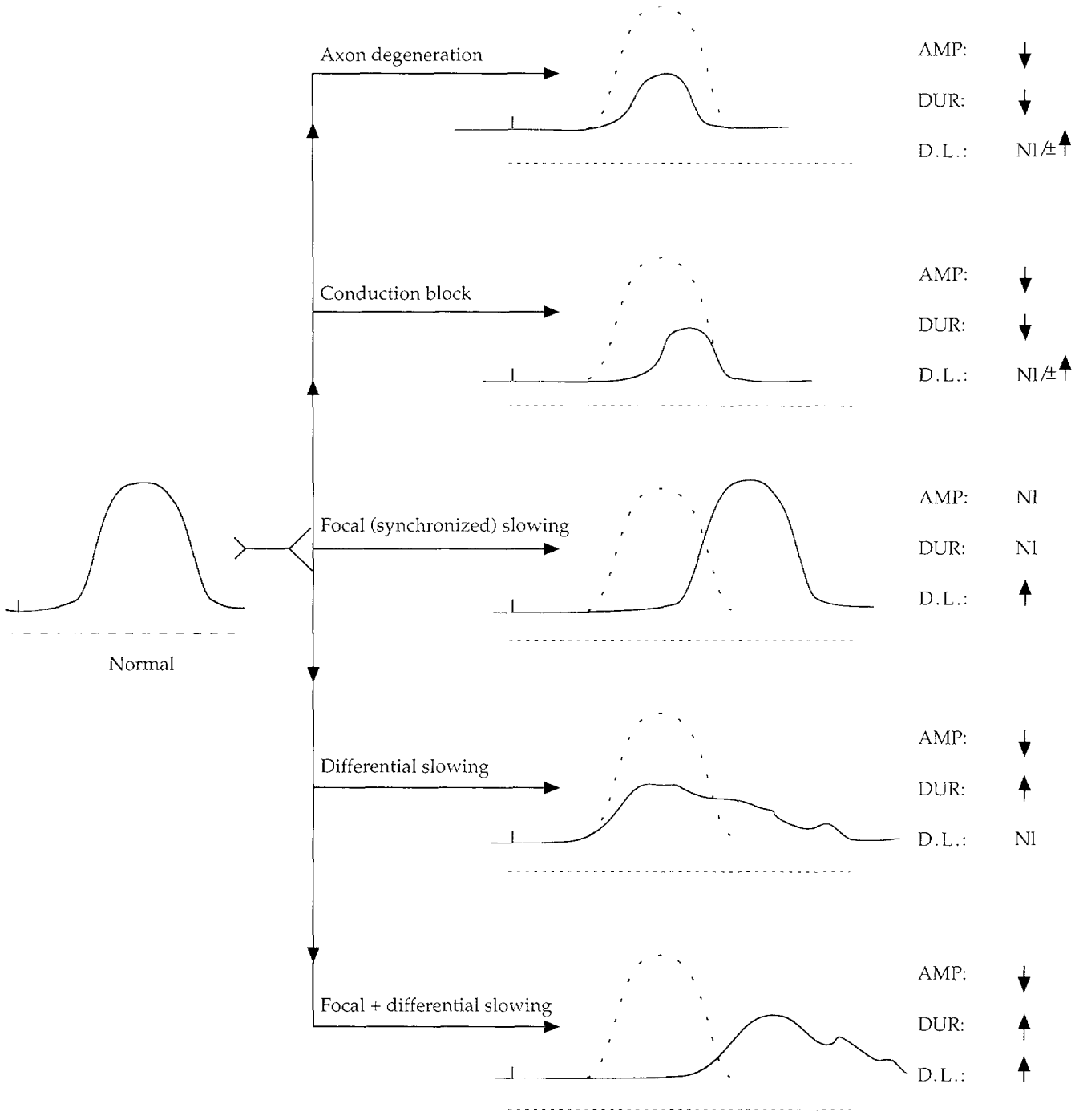

since it was first described by Waller in the 1830s. On the NCS in these situations, the distal stump can conduct nerve impulses for 7 to 11 days, but then, as Wallerian degeneration progresses, conduction failure supervenes. Thus, an axon loss lesion is never focal in regard to its effect; even though the lesion that caused it may have directly impacted on only a very small segment of nerve, the entire nerve segment distal to that point soon degenerates and can no longer conduct impulses.

For individual myelinated nerve fibers, focal demyelination causes one of two conduction changes: conduction slowing or conduction block. With conduction slowing, nerve impulses traverse the injury site, but at a slower rate than normal because, due to myelin damage, a greater amount of the axon at the node has to be depolarized; this consumes time. With demyelinating conduction block, the demyelination is more severe at the lesion site, so that the nerve impulses cannot traverse it, although the segment of nerve distal to that point remains intact and capable of conducting impulses (as can be demonstrated on NCS). The key point about all focal demyelinating lesions is they truly remain focal. Unlike axon loss lesions, they have no appreciable effects on the nerve segments distal (or proximal) to them. Thus, focal demyelinating nerve lesions generally will not be detected by NCS unless the stimulation is applied proximal to them while recording distal to them; i.e., the impulses have to travel through the injured nerve segments for the lesions to be appreciated.

The components of the NCS are affected differently by the various types of nerve pathophysiology, to the point that the specific type of pathology present often can be presumed, based on the NCS changes.

The amplitudes of the NCS responses — the CMAPs, SNAPs, and MNAPs — are semiquantitative measures of the number of nerve fibers capable of conducting impulses between the stimulating and recording sites. They are, therefore, affected by axon-loss lesions located at any point distally from the AHCs (for motor fibers) and the DRGs (for sensory fibers). With incomplete axon-loss lesions, the SNAPs are more severely involved than the CMAPs, i.e., lower in amplitude. Consequently, diminution of SNAP amplitudes is the most sensitive NCS indicator of axon-loss lesions. NCS amplitudes are also affected by demyelinating conduction block lesions when stimulating proximal to the lesions. They remain normal when stimulating (and recording) distal to them. The amplitudes are not affected by focal slowing if conduction along all the large myelinated fibers is altered to the same degree. However, if conduction along only some of the nerve fibers is slow, or if it is slow along all of them but to different degrees, then the evoked responses are dispersed in time, and, as the durations increase, the amplitudes begin to decrease. Finally, the motor amplitudes can be reduced by abnormalities of neuromuscular transmission, and of the muscle itself (Figure 1.48). Generally, NCS amplitudes are considered abnormally low whenever they are below the lowest limits of normal laboratory values, as determined by studying a number of normal persons from each decade of life, and when they are 50% lower than the amplitude obtained by studying the corresponding nerve in the contralateral limb. A conduction block is considered present whenever the response on proximal stimulation is *appreciably* lower in amplitude than that on distal stimulation. *"Appreciably"* is defined differently in different EMG laboratories; e.g., in the Cleveland Clinic EMG laboratory a drop in amplitude of 50% is required.

Figure 1.49 — Analogy of traffic moving along a normal road to impulses passing along a normal nerve.

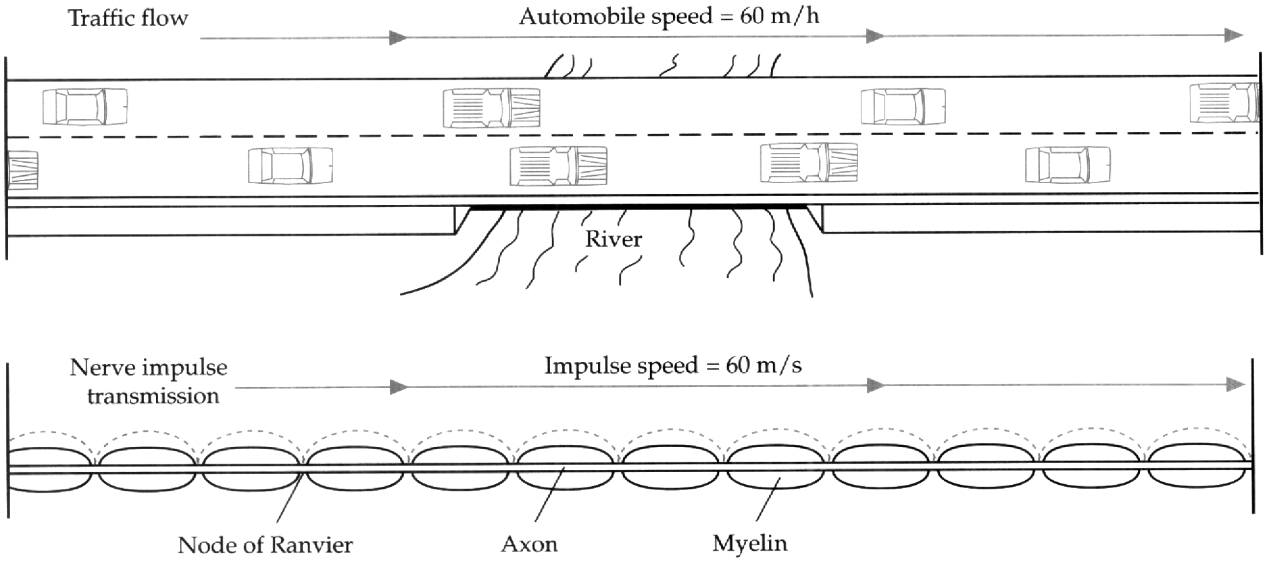

Figure 1.50 — Analogy of a problem along a short segment of highway causing slowing of traffic to focal slowing.

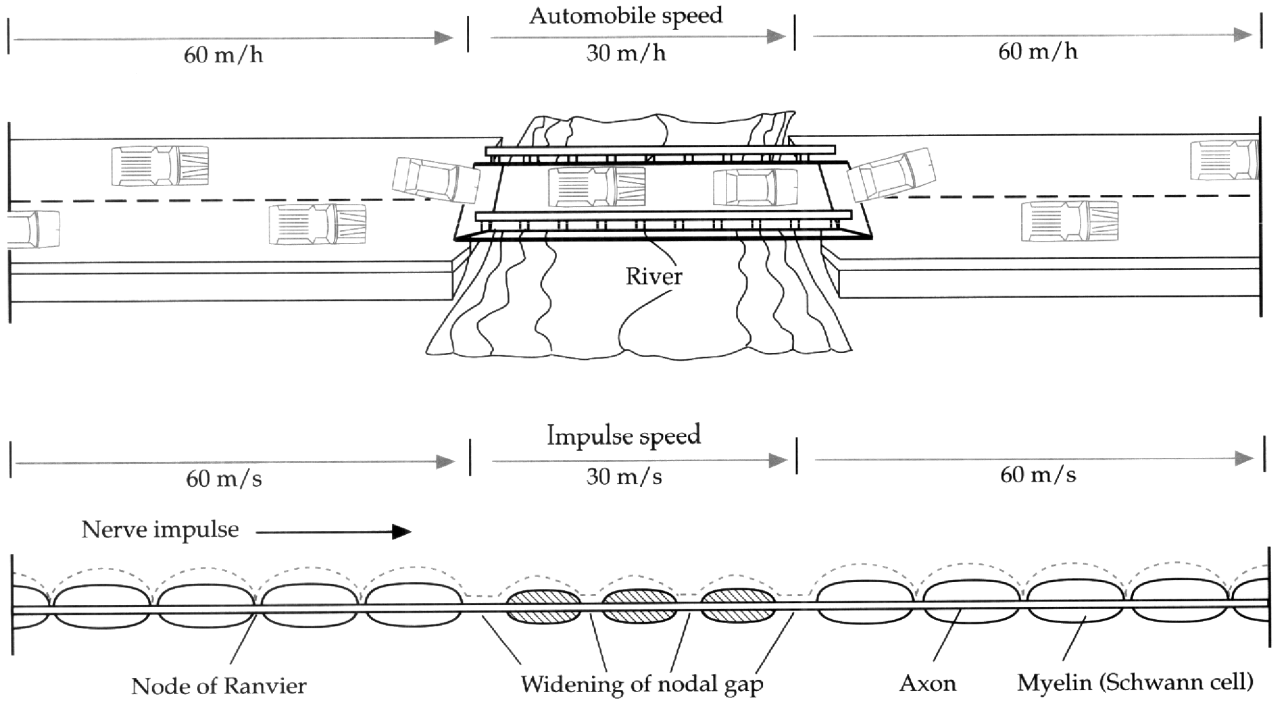

Both distal/peak latencies and CVs are measurements of conduction rate and, consequently, affected by the same types of pathophysiological processes. The most important one, from the electromyographer's viewpoint, is demyelinating focal slowing (Figure 1.48). They generally are not altered by incomplete axon-loss lesions because they are being determined along the surviving fibers, which are usually conducting at their normal rates. Obviously, with complete/nearly complete axon loss lesions, no responses will be obtained and, therefore, neither distal/peak latencies nor CVs can be determined. In contrast, very remote, severe axon loss lesions in which some nerve regeneration has occurred also can produce significant slowing because the conduction rate is being determined along fibers that have regenerated; i.e., fibers that are narrower than the original axons have a thinner coating of myelin and, therefore, conduct at an appreciably slower speed. The latencies and CVs usually are normal with demyelinating conduction block lesions, but sometimes they are spuriously slow because the onset of the proximal and distal responses are for two different sets of nerve fibers. The distal latency is determined by the fastest conducting fibers. The proximal latency is determined by the unblocked, slower conducting ones (i.e., the faster conducting fibers have their conduction blocked and are, therefore, not contributing to the response). The distal peak latencies and CVs are judged as normal or abnormal by comparing them to laboratory normal values, determined by studying normal persons in each decade of life.

In summary, axon loss lesions and demyelinating conduction block lesions affect primarily the amplitudes of the responses, while focal slowing affects the latencies and the CVs.

With lesions causing demyelinating conduction block and particularly with those causing axon loss, sometimes all or nearly all the nerve fibers are involved. In such cases, no evoked responses can be obtained (i.e., the amplitudes of the responses are zero) and, consequently, no conduction rate measurements (distal/peak latencies, CVs) can be determined.

In regard to the NEE, focal slowing has no appreciable effect. In contrast, pure demyelinating conduction block affects only the number of MUAPs firing on maximal effort; with rather severe lesions, they fire in decreased numbers at a rapid rate. With axon loss lesions, minute rhythmical spontaneous action potentials of individual muscle fibers, called fibrillation potentials, appear approximately 21 days after nerve injury. These are extremely sensitive, objective indicators of prior motor axon loss which can neither be produced nor suppressed volitionally. With minor degrees of motor axon loss there may be no significant changes in the MUAPs. However, with more severe axon loss the MUAPs fire in decreased numbers at a rapid rate, identical to that seen with demyelinating conduction block lesions. As time passes, the muscle fibers that were orphaned by the loss of their motor axons, and subsequently were fibrillating, are often adopted by neighboring, surviving axons. As this happens, they cease to fibrillate. The motor units that adopted them now control more than their normal complement of muscle fibers. When they generate action potentials, or MUAPs, the latter are often of increased duration and are often higher in amplitude. This phenomenon is called the *chronic neurogenic MUAP change.*

Some parallels can be drawn between the pathophysiology seen with various nerve lesions and the problems encountered during automobile travel (Figure 1.49). At times, road repair over a limited stretch of highway forces traffic to be reduced to one lane. The automobiles must travel at a slower rate of speed while traversing this segment, but all ultimately get beyond it and then regain their normal speed. This scenario is very similar to focal nerve conduction slowing in that the conduction rate is slowed along the injured segment, but normal along the segments proximal and distal to the injury (Figure 1.50).

Figure 1.51 — Analogy of a problem along a short segment of highway halting traffic to conduction block along a nerve.

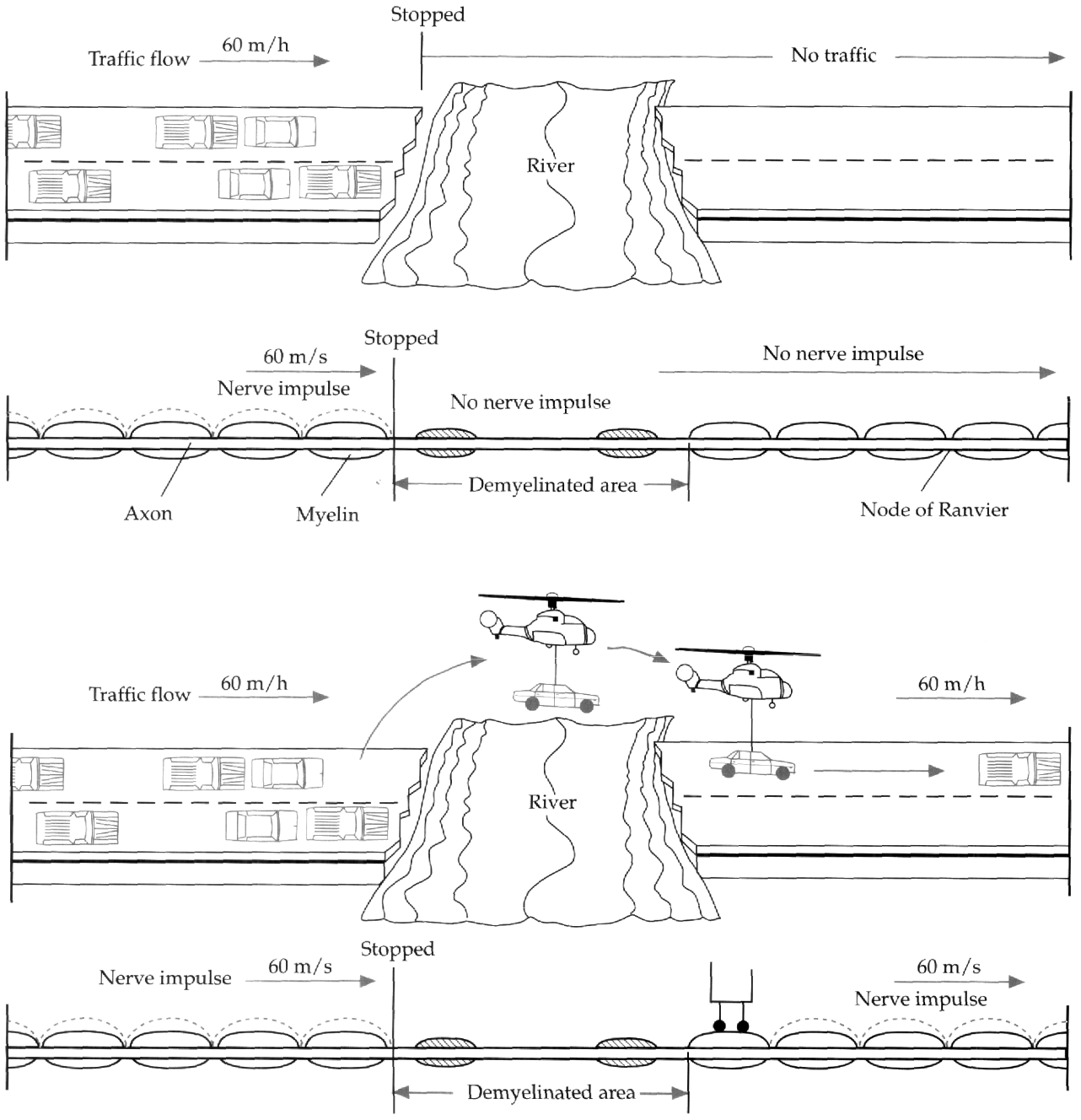

Of note is that, with conduction slowing, all the impulses ultimately traverse the damaged site. For this reason, if the slowing is uniform along all the large fibers, the responses elicited on NCS are normal in their configuration — only if their conduction rate is determined can it be appreciated that a lesion is present. Moreover, the NEE is unaltered. Also for this reason, focal slowing, per se, causes almost no clinical manifestations; slowing along motor fibers, regardless of severity, does not cause muscle weakness, while slowing along sensory fibers usually does not produce a sensory abnormality. Only when varying degrees of slowing are present along those sensory fibers that carry synchronized volleys centrifugally are any clinical deficits noted. For example, when conduction along the large myelinated sensory fibers that transmit vibratory sensation is slowed to different degrees the patient will be unable to detect the vibration of a tuning fork.

Returning to the analogy of road travel, in some instances a segment of highway may be rendered impassable, e.g., by flooding or rock slides. In these situations, all road traffic is stopped at the edge of the site and none progresses beyond that point, although on the far side the road is completely intact. This can be circumvented by transporting an automobile with a helicopter from the near side of the bad stretch of road to the intact highway on the far side so that it can then continue its journey at normal speed. This situation is analogous to demyelinating conduction block. The nerve impulses cannot get beyond the lesion site, but the nerve fibers distal to the damaged segment remain intact. This occurrence can be demonstrated by NCS. When stimulating proximal to the lesion, while recording distal to it, the responses are low in amplitude or unelicitable. However, when stimulating and recording along the segment distal to the lesion site, the evoked responses are of normal amplitude (Figure 1.51).

The road situation analogy usually does not apply to axon loss lesions because the highway must be destroyed, or at least rendered impassable, from a particular point all the way distally to where it terminates. This could occur, for example, if a road were disrupted by extensive flooding. In this situation, a helicopter could not lift an automobile from the edge of the undisturbed section of highway and deposit it beyond the impassable segment because the latter extends as far as the road does (or did). This is the situation with axon loss lesions in which the segment of nerve separated from its cell body dies; i.e., the distal nerve stump undergoes Wallerian degeneration from the point of injury all the way to the periphery. Thus, the degenerated nerve fibers cannot conduct impulses, so stimulating them produces no evoked response. Stimulating the still-viable nerve segment proximal to the lesion site also yields no evoked response because the impulses produced cannot traverse the degenerated segment to reach the recording site (Figure 1.52).

In contrast to demyelinating focal slowing lesions, both demyelinating conduction block lesions and axon loss lesions produce clinical deficits, with their severity directly linked to the number of fibers affected. If only a small percentage of the fibers in a mixed nerve have undergone axon loss or conduction block, no clinical deficits may be apparent. However, with more severe injury to motor and sensory fibers, clinical weakness of the appropriate muscles and loss of position and vibratory sensations is apparent, respectively. Total paralysis and complete loss of position and vibratory sense results from complete demyelination conduction block and/or axon loss lesions (with axon loss lesions, other types of sensations are also lost — e.g., pain, temperature, light touch — but this cannot be detected by the electrodiagnostic examination because the nerve fibers that subserve these sensations are not being studied).

Figure 1.52 — Analogy of a problem along an extended segment of highway to axon loss affecting a nerve.

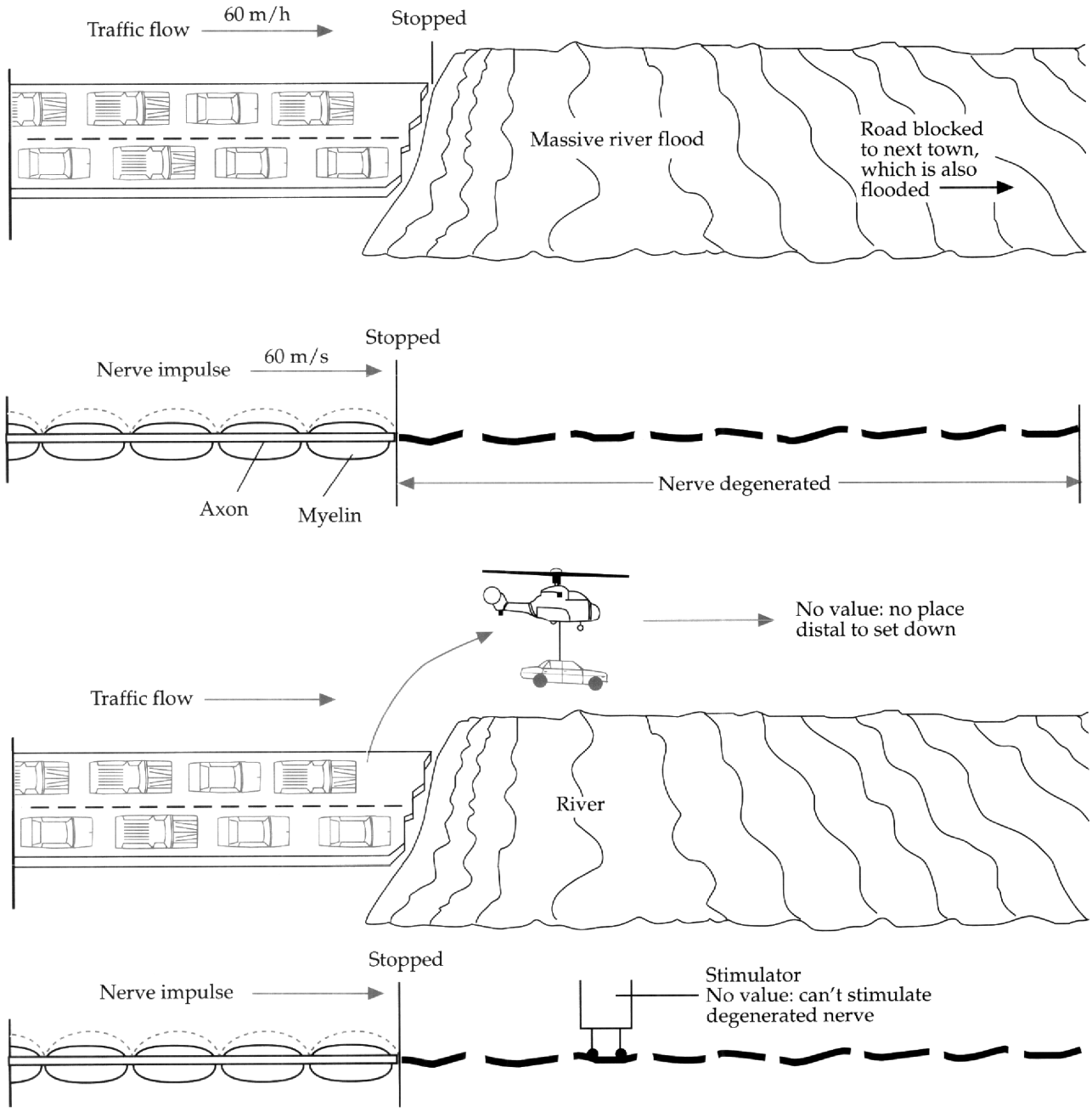

1.9.2 Neuromuscular Junction

The classic example of a postsynaptic defect of neuromuscular junction transmission is myasthenia gravis. The hallmark of this auto-immune disorder is production of antibody against the Ach receptor, resulting in depletion of Ach receptors on the postsynaptic surface, scarring, and simplification of the postsynaptic junctional folds. The cleft between presynaptic and postsynaptic surfaces thus widens and the two cannot communicate.

Acetylcholine receptor antibodies are a heterogeneous group of IgG molecules with specificity for various subsegments of the Ach receptor molecule. Relatively few antibodies are specific for the active binding site of Ach. Among patients with clearly generalized disease, more than 90% will have detectable antibody by radio-immunoassay.

With reduction of the number of acetylcholine receptors at the postsynaptic site, the safety factor is lost. As the amount of Ach released naturally declines in a series of stimuli to the nerve terminal, a point will be reached when too few ion channels are opened to produce a threshold end-plate potential and propagated action potential. When this occurs, the muscle fiber will not fire and the classic decremental response with repetitive stimulation is identified (see below). This corresponds to the clinical observation of fatigue in exercised muscles.

About 75% of patients with myasthenia gravis have some abnormality of the thymus gland. In the majority, the pathology indicates hyperplasia of the germinal centers of the medulla of the gland. In about 10% of patients with thymic abnormality, a locally-invasive malignancy known as thymoma is detected. What role the thymus plays in the induction and perpetuation of the disease is unclear. Removal of a diseased thymus may produce disease remission in some patients and reduction of symptoms in others.

1.9.3 Muscle

Many types of muscle disorders exist, each with its own specific pathophysiology, although the common final pathway is failure of the contractile system. One of the most clearly recognizable disorders is polymyositis (it is thought that this disease is due to auto-immune deregulation, but the specific antigenic trigger and antibody response have not been identified). An inflammatory reaction occurs amid muscle fibers with associated perivascular accumulation of lymphocytes and macrophages. Necrosis of muscle fibers occurs and they become disconnected from their end-plates. Subsequently, these muscle fibers atrophy in the absence of innervation. If the inflammation is treated and repair is allowed to take place, muscle fibers reinnervate and electrophysiologic features develop that are identical to those seen in newly reinnervated muscle fibers after nerve disease (see below).

In the hereditary disorders known as the myotonia, an inborn abnormality of the muscle fiber membrane occurs. In myotonic dystrophy, an abnormality of sodium ion channel function is responsible, while in myotonia congenita reduced chloride conductance across the membrane causes the disease. The hallmark of these conditions is a repeating, rhythmic electrical discharge of muscle (myotonic discharges) induced by mechanical stimulation or spontaneous muscle contraction.

Table 1.4a - Arm Muscles
Mean Action Potential Duration (in ms) in Various Muscles at Different Ages (concentric electrodes)

Age	Deltoid	Biceps brachii	Triceps brachii	Extensor digitorum communis	Opponens first dorsal; interosseus	Abductor digiti quinti
0	9.0	7.3	8.3	6.8	8.1	9.5
3	9.0	7.3	8.3	6.8	8.1	9.5
5	9.2	7.5	8.5	6.9	8.3	9.7
8	9.4	7.7	8.6	7.1	8.5	9.9
10	9.6	7.8	8.7	7.2	8.6	10.0
13	9.9	8.0	9.0	7.4	8.9	10.3
15	10.1	8.2	9.2	7.5	9.1	10.5
18	10.4	8.5	9.6	7.8	9.4	10.9
20	10.7	8.7	9.9	8.1	9.7	11.2
25	11.4	9.2	10.4	8.5	10.2	11.9
30	12.2	9.9	11.2	9.2	11.0	12.8
35	13.0	10.6	12.0	9.8	11.7	13.6
40	13.4	10.9	12.4	10.1	12.1	14.1
45	13.8	11.2	12.7	10.3	12.5	14.5
50	14.3	11.6	13.2	10.7	12.9	15.0
55	14.8	12.0	13.6	11.1	13.3	15.5
60	15.1	12.3	13.9	11.3	13.6	15.8
65	15.3	12.5	14.1	11.5	13.9	16.1
70	15.5	12.6	14.3	11.6	14.0	16.3
75	15.7	12.8	14.4	11.8	14.2	16.5

Table 1.4b - Leg and Facial Muscles
Mean Action Potential Duration (in ms) in Various Muscles at Different Ages (concentric electrodes)

Age	Biceps femoris; quadriceps	Gastrocnemius	Tibialis anterior	Peroneus longus	Extensor digitorum brevis	Orbicularis oris superior; transgularis; frontalis
0	8.0	7.1	8.9	6.5	7.0	4.2
3	8.2	7.3	9.2	6.7	7.2	4.3
5	8.4	7.5	9.4	6.8	7.4	4.4
8	8.6	7.7	9.6	6.9	7.6	4.5
10	8.7	7.8	9.7	7.0	7.7	4.6
13	9.0	8.0	10.0	7.2	7.9	4.7
15	9.2	8.2	10.2	7.4	8.1	4.8
18	9.5	8.5	10.5	7.6	8.4	5.0
20	9.8	8.7	10.8	7.8	8.6	5.1
25	10.3	9.2	11.5	8.3	9.1	5.4
30	11.1	9.9	12.3	8.9	9.8	5.8
35	11.8	10.6	13.2	9.5	10.5	6.2
40	12.2	10.9	13.6	9.8	10.8	6.4
45	12.5	11.2	13.9	10.1	11.1	6.6
50	13.0	11.6	14.4	10.5	11.5	6.8
55	13.4	12.0	14.9	10.8	11.9	7.0
60	13.7	12.3	15.2	11.0	12.2	7.1
65	14.0	12.5	15.5	11.2	12.4	7.3
70	14.1	12.6	15.7	11.4	12.5	7.4
75	14.3	12.8	15.9	11.5	12.7	7.5

1.10 *Special Methods*

Various specialized and quantitative techniques have been developed to supplement the information derived from the standard NEE. Generally, these methods are relatively time-consuming and typically limited in their scope of sampling, usually to one or two muscles in a single examination. Thus, they are reserved for special clinical situations or are used in the course of clinical research.

Quantitative EMG traditionally refers to the methods described by Buchthal. This method employs a standard NEE of a single muscle, recording 20 individual MUAPs. A MUAP may be quite variable in its morphology depending upon positioning of the needle electrode. By definition, the MUAP is recorded when the amplitude is maximum and the peak rise time is <500 ms. The MUAPs may be analyzed for various parameters including duration, amplitude, area, and number of phases (Figure 1.53). Normal values vary from muscle to muscle and change with age (Table 1.4a, b). MUAP duration has been the most clinically-relevant parameter for quantitative EMG. This particular method has demonstrated to be a valuable technique for the study of diseases of nerve and muscle.

Figure 1.53 — A schematic MUAP with characteristics that can be quantitated.

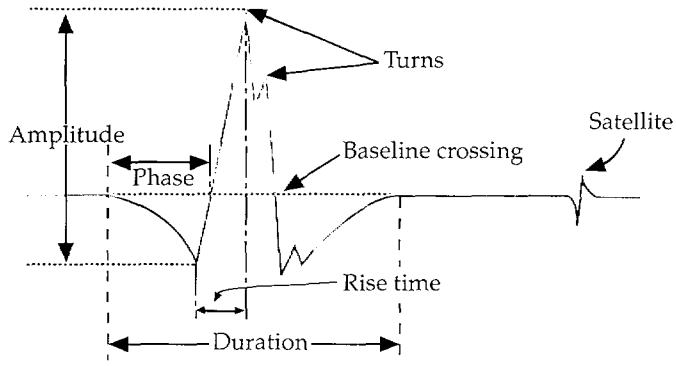

Single-fiber EMG is a technique that enables measurement of the muscle action potentials from individual muscle fibers belonging to the same motor unit. SFEMG can be performed on most EMG units, but special accessories are needed, including a delay line, a counter, and a photographic unit or its equivalent. SFEMG examinations are more efficiently performed on computerized EMG equipment that utilize special programs for acquisition and analysis. They require a specialized needle electrode with a 25 μm-diameter recording surface embedded on the shaft of a needle electrode that serves as the reference electrode (Figure 1.28c and 1.41). Special filtering is also required. The high-pass filter is optimal at 500 Hz, whereas the low-pass filter is typically set at 10 KHz. Single-muscle fiber action potentials are typically biphasic in configuration and have rise times from positive to negative peak of less than 300 μs and a peak-to-peak amplitude >200 μV. Single-muscle fiber action potential waveforms should be stable with successive discharges. SFEMG provides two measurements, fiber density and jitter. The fiber density represents the average number of single muscle fiber potentials recorded from the same motor unit during 20 separate insertions and recordings in a single muscle (Figure 1.54).

Figure 1.54 — Single-fiber EMG recordings in normal and reinnervated muscle.

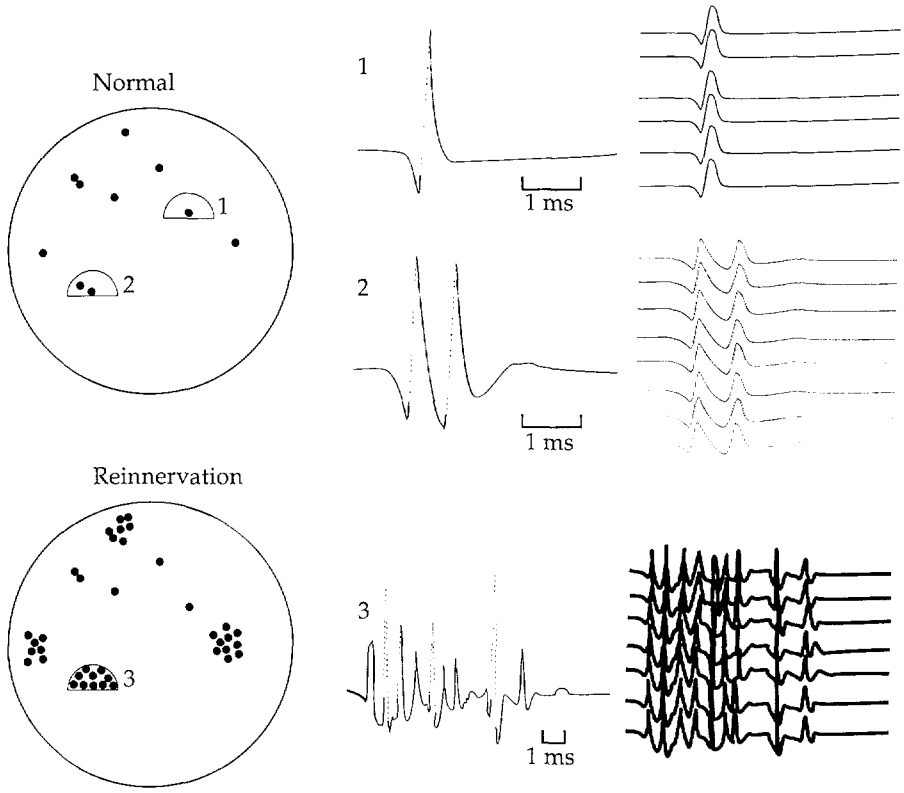

This often entails four or five insertions at different locations in the muscle. Fiber density is an index of the number of muscle fibers belonging to the motor unit. In neurogenic disorders with axon loss and reinnervation, fiber density is typically elevated. Whereas in myopathies, fiber density is usually normal or slightly elevated, particularly in those myopathies associated with muscle fiber degeneration. Normal values for fiber density depend on the muscle examined and the age of the patient, as fiber density tends to increase with advancing age (Table 1.5).

Jitter is a SFEMG measurement that is performed when two or more muscle fibers belonging to the same motor unit are recorded simultaneously. It refers to the variability of the interpotential interval between two single-fiber muscle action potentials during successive discharges (Figure 1.55). Although many factors contribute to the jitter, the important factor is neuromuscular transmission at the muscle endplate. Jitter analysis requires jitter measurements from 20 individual potential pairs. Normal mean jitter values vary from muscle to muscle and tend to increase with age (Table 1.6). Increased jitter in pathological states may be associated with blocking of the impulse. This most often occurs in disorders of the neuromuscular junction such as myasthenia gravis or the myasthenic syndrome of Lambert and Eaton. However, increased jitter and blocking may occur in neuropathies as a consequence of motor axon degeneration with reinnervation, and in muscle diseases that cause myonecrosis, such as polymyositis. Thus, SFEMG measurements are nonspecific and need to be interpreted in the context of findings on the routine NCS and NEE.

Figure 1.55—(a) Schematic explanation of the recording conditions for jitter measurements in a voluntarily-activated muscle. (b) Action potential pair firing at low degree of voluntary effort. (c) Two potentials at a higher sweep speed with a sweep triggered by the first potential and moving down after each discharge. (d) Several discharges superimposed to demonstrate changes in the interpotential intervals (the neuromuscular jitter).

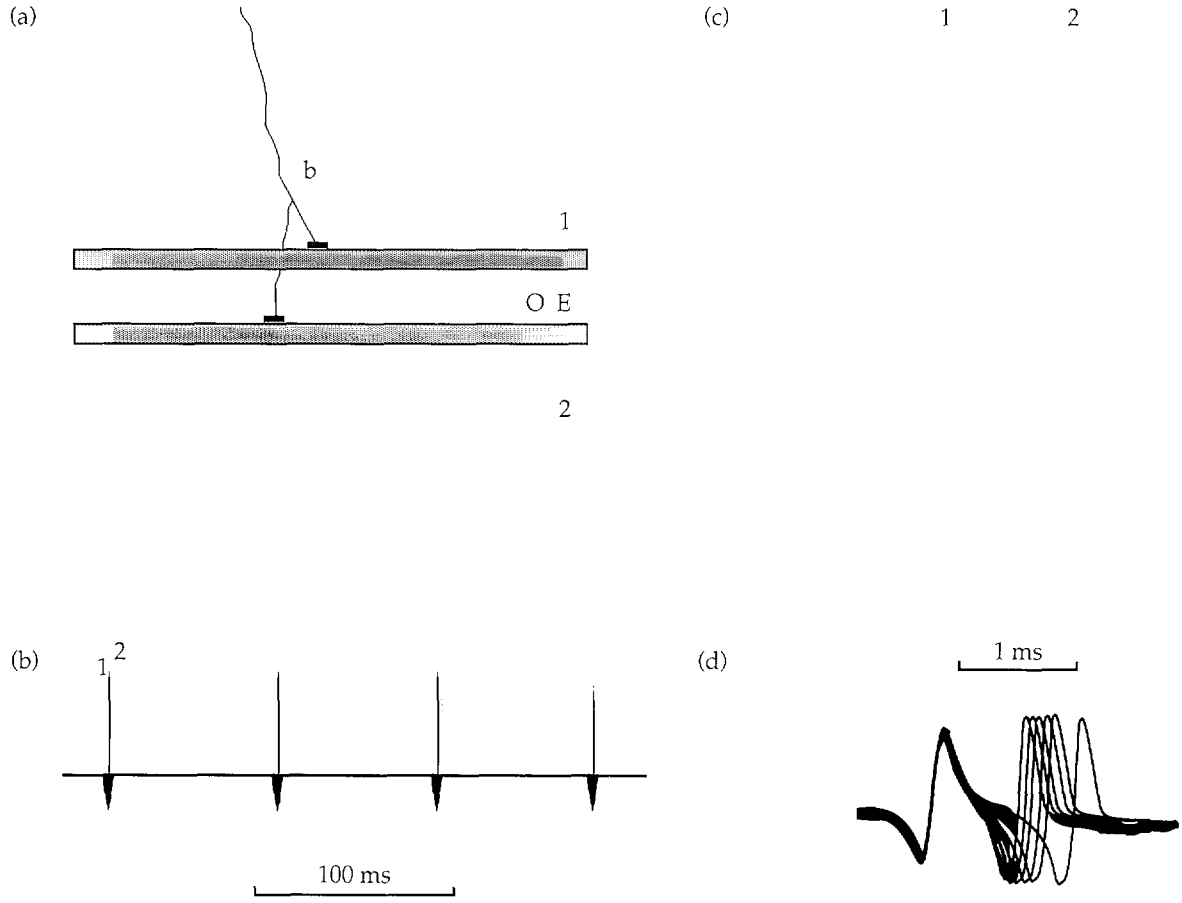

Table 1.5 - Normal Fiber Density Values

MUSCLES	10-25 years			26-50 years			51-75 years			> 75 years		
	m	SD	n	m	SD	n	m	SD	n	m	SD	n
Frontalis	1.61	0.21	(11)	1.72	0.21	(15)						
Deltoid	1.36	0.16	(20)	1.40	0.11	(10)						
Biceps	1.25	0.09	(20)	1.33	0.07	(17)						
Extensor digitorum communis	1.47	0.16	(61)	1.49	0.16	(98)	1.57	0.17	(59)	2.31	0.41	(21)
1st Dorsal interosseus	1.33	0.13	(14)	1.45	0.12	(6)						
Rectus femoris	1.43	0.18	(11)	1.57	0.23	(14)						
Tibialis anterior	1.57	0.22	(18)	1.56	0.22	(21)	1.77	0.12	(4)	3.8		(1)
Extensor digitorum brevis	2.07	0.42	(16)	2.62	0.30	(11)						

m=mean, SD=standard deviation, n=number of subjects.

Macro-EMG is a single-fiber EMG technique that utilizes a specialized SFEMG electrode. The electrode consists of a typical single-fiber EMG recording surface, but the canula is bare over the distal 15 mm (Figure 1.28d). Macro-EMG requires two-channel recording. One channel records the single-fiber EMG potentials and the second channel records the macro-potential (Figure 1.56). The macro-potential is time-locked and triggered from the single-fiber recording but is recorded from the 15 mm bare canula (recording electrode) with a distant surface electrode as the reference electrode. In such an arrangement, the single-fiber macro-canula may record from all the muscle fibers within the motor unit. A typical single-fiber macro-examination encompasses 20 different MUAPs. These are analyzed according to various morphologic features including amplitude and rectified area. Emphasis has been placed on amplitude as the most important parameter of the single-fiber macro-MUAP. Macro-MUAP amplitudes vary from muscle to muscle and tend to increase with age (Table 1.7). Macro-MUAPs are increased in amplitude in diseases of motor fibers that result in motor fiber loss with reinnervation and tend to be normal or reduced in amplitude in muscle diseases (Figures 1.57 and 1.58).

Table 1.6 - Normal Mean Jitter Values

Muscles	Number of potential pairs	MCD - pooled data mean, SD	SD of MCD values from individual subjects mean, SD	Upper normal limit close to mean +3SD
Frontalis (range of means for individual subjects)	258	20.4, 8.8 (15.7 - 29.2)	6.2, 2.3 (5.5 - 8.7)	45
Biceps	125	15.6, 5.9		35
EDC (range of means for individual subjects)	759	24.6, 10.6 (16.5 - 32.0)	8.3, 3.2 (2.3 - 12.4)	55
Rectus femoris	73	31.0, 12.6		60 (65)*
Tibialis anterior	153	32.1, 15.0		60 (75)*
EDB	29	85.3, 68.6		none

*Due to some extreme high values, the data are not Gaussian distributed. A more appropriate upper normal limit is 60 μsec.

Figure 1.56 — Principle for macro-EMG recording.

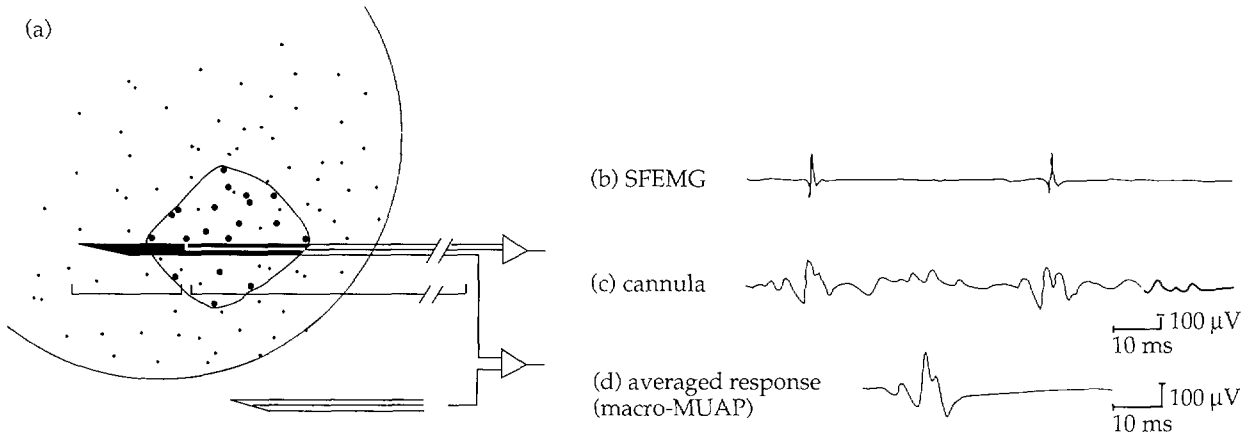

Figure 1.57 — Examples of macro-MUAPs: (a) limb girdle dystrophy. (b) normal muscle. (c) ALS.

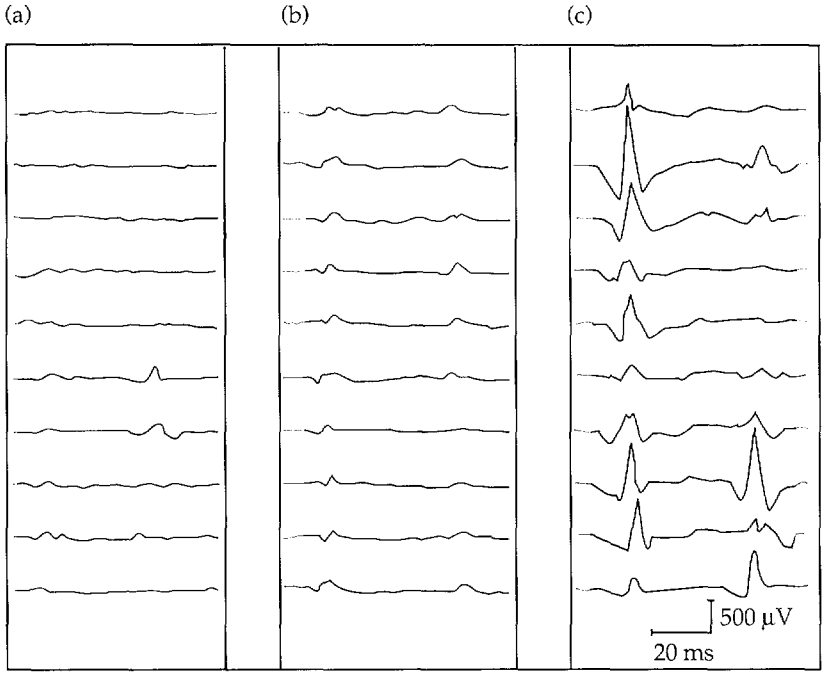

Figure 1.58 — Macro-EMG findings in the case of polymyositis and motor neuron disease from biceps brachii muscle compared to normal.

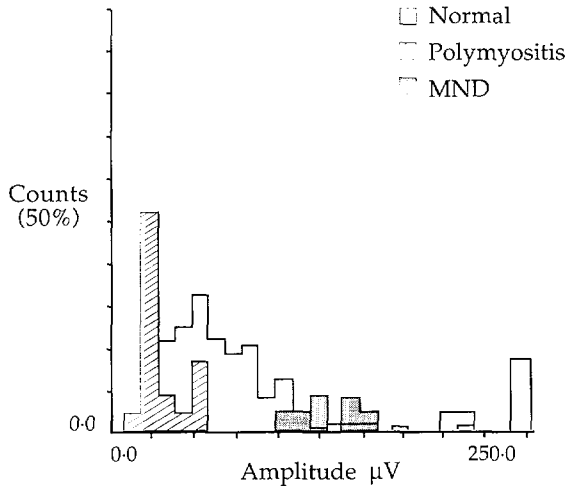

Table 1.7 - Normal Macro-MUAPs Amplitude Values

	Biceps				Vastus lateralis				Tibialis anterior			
	Median		Individual macro-MUAP		Median		Individual macro-MUAP		Median		Individual macro-MUAP	
Age	min	max	min	max	min	max	min	max	min	max	min	max
10-19	65	100	30	350	70	150	20	350	65	200	30	350
20-29	65	140	30	350	70	240	20	525	65	250	30	450
30-39	65	180	30	400	70	240	20	550	65	260	30	450
40-49	65	180	30	500	70	250	20	575	65	330	30	575
50-59	65	180	30	500	70	260	20	575	65	375	40	700
60-69	65	250	30	650	80	370	20	1250	120	375	45	700
70-79	65	250	30	650	90	600	20	1250	120	620	65	800

An important quantitative method for the study of the interference pattern (IP) is turns analysis. This is usually accomplished with a computerized EMG unit that has a special program to acquire the IP and analyze the signal for amplitude and turns. The IP recordings are made with standard concentric needle electrodes or monopolar electrodes. IPs are recorded at multiple sites within the muscle (Figure 1.59). The signal is then digitized and analyzed for the number of turns, a change in signal direction of 100 μV or more, and the amplitude of the potential difference between successive turns (Figure 1.60). Traditionally, these values were expressed in a plot of turns or amplitude versus percent of maximum force as measured by a strain gauge (Figure 1.61). The use of strain gauges to calculate maximum force and the percentage of force generated is technically demanding and cumbersome and limits the number of muscles that may be studied with this technique. Stalberg introduced the concept of a cloud of normal values, which represents a scatter plot of turns per second versus mean amplitude per turn (Figure 1.62). In this method, at least 20 different measurements are made at various levels of muscle contraction. Normal clouds vary with different muscles and change with age. An abnormal test requires two or more points out of 20 falling outside the normal cloud. Myopathies produce more turns and lower amplitudes and neuropathies produce fewer turns and higher amplitudes (Figure 1.63).

Nandedkar and colleagues recently introduced other parameters for turns analysis that includes upper centile amplitude measuring the amplitude of the 99th percentile of all amplitudes recorded in the IP, number of small segments (NSS) defined as the number of turns of 2 mV amplitude or less as an index of complexity of the IP, and activity defined as an index of the fullness of the IP. These parameters may also be expressed graphically

as clouds for normal values. Myopathies show a higher NSS and lower UCA, whereas neuropathies produce lower NSS and higher UCA (Figures 1.64 and 1.65). Other methods to analyze the IP have also been used such as Fast-Fourier Transformation with analysis of the power spectrum of the IP.

Figure 1.59 — Example of interference pattern recordings: (a) mild. (b) moderate. (c) maximal voluntary activation.

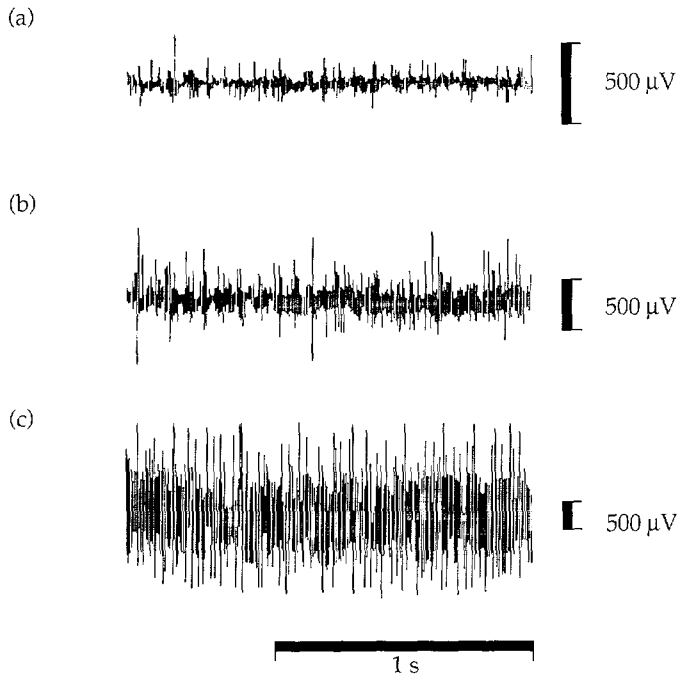

Figure 1.60 — EMG interface pattern showing five turns (T1-T5) that define four segments (S1-S4), whose durations (D1-D4) and amplitudes (A1-A4) are indicated.

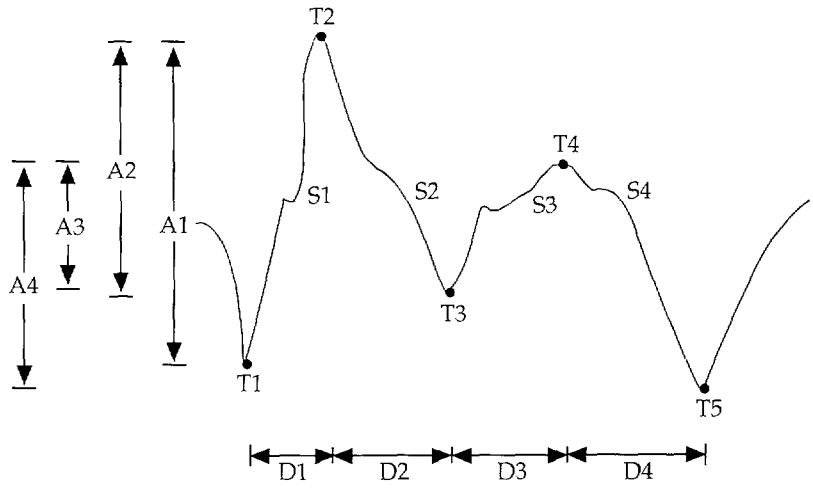

Figure 1.61 — Turns per 5s (left) and mean amplitude (right) as a function of force in percentage of maximum: (a) biceps. (b) brachioradialis. (c) triceps. The dashed line is the average of five normal subjects.

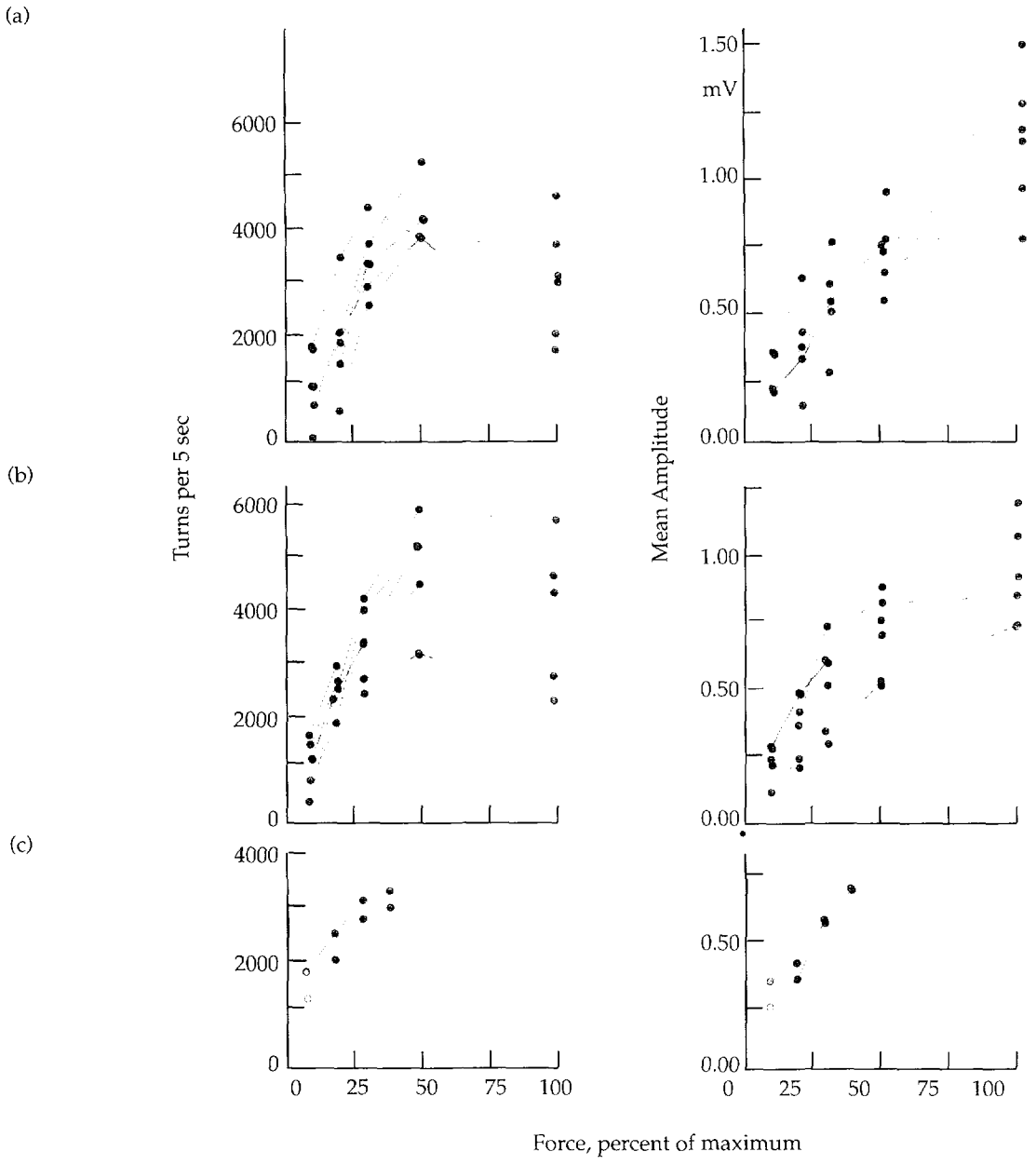

Figure 1.62 — Development of the normal cloud for turns and amplitude: (a) healthy females over 60 years. (b) linear regression and +/- SD of log amplitude versus log turns. (c) parts a and b redrawn. (d) normal limits obtained by setting upper limits on turns and amplitudes.

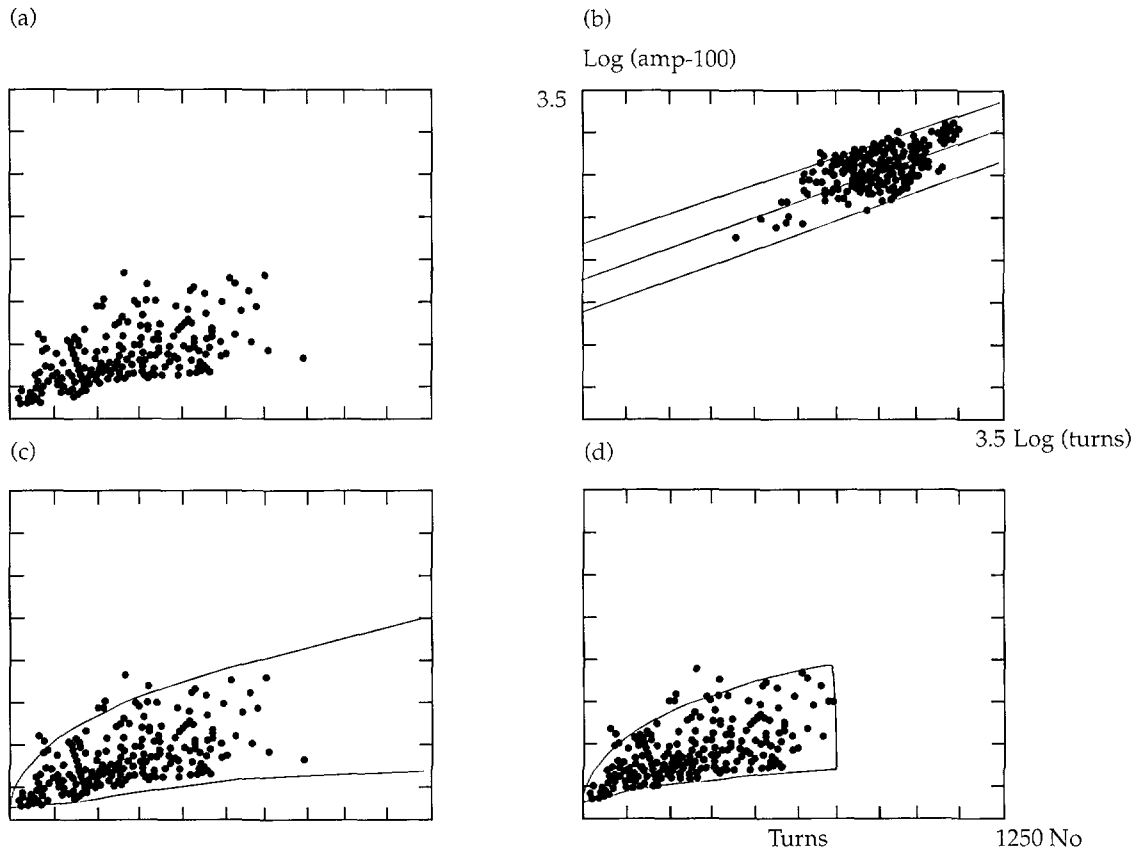

Figure 1.63 — Turns and amplitude values for two patients superimposed on normal limits.

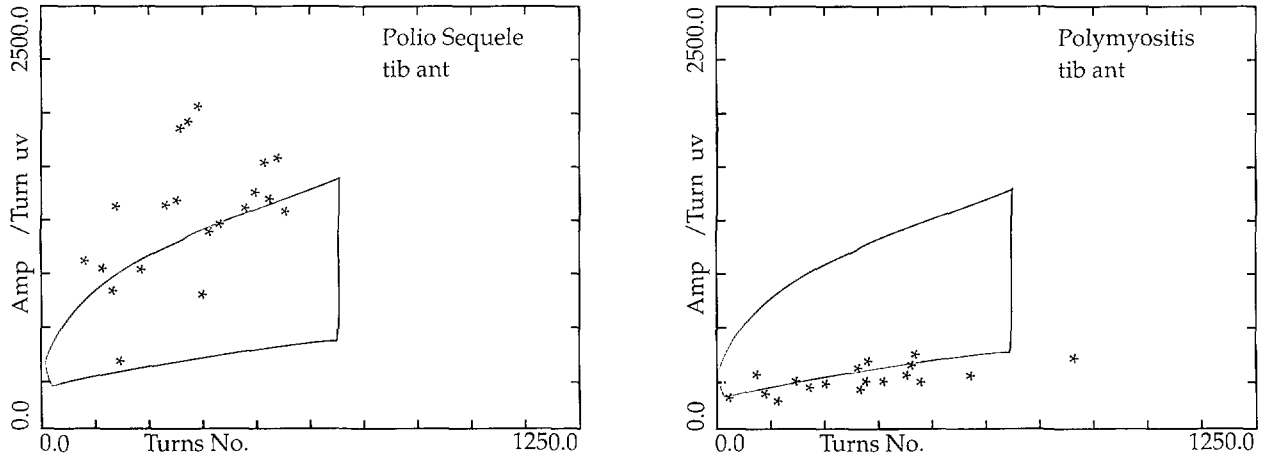

Figure 1.64 — Pooled data from IP studies in bicep muscles of seven female patients with myopathy.

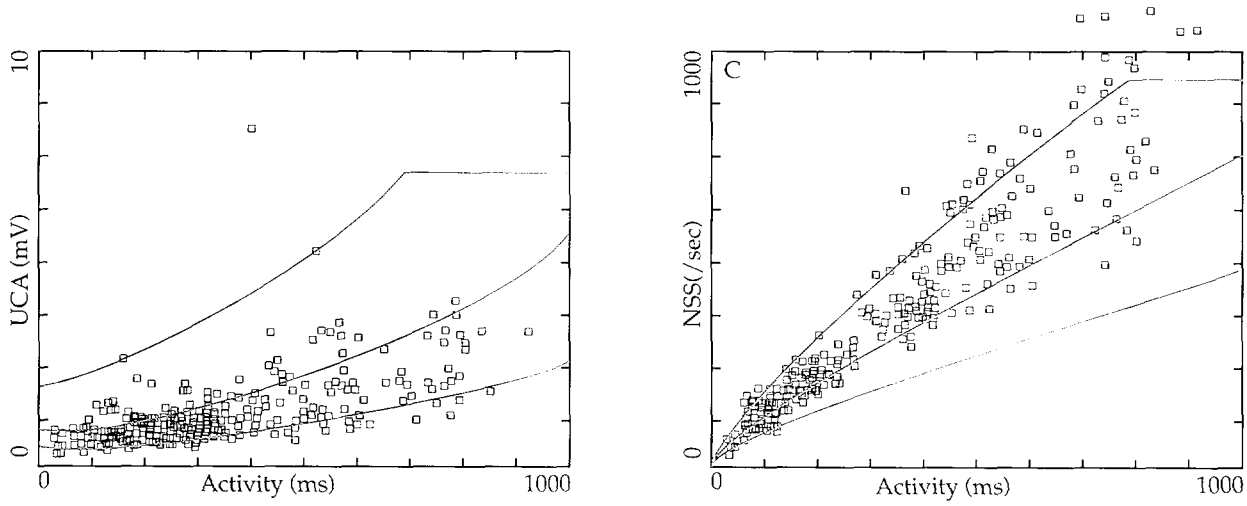

Figure 1.65 — Pooled data from IP studies in the bicep muscles of seven male patients with motor neuron disease.

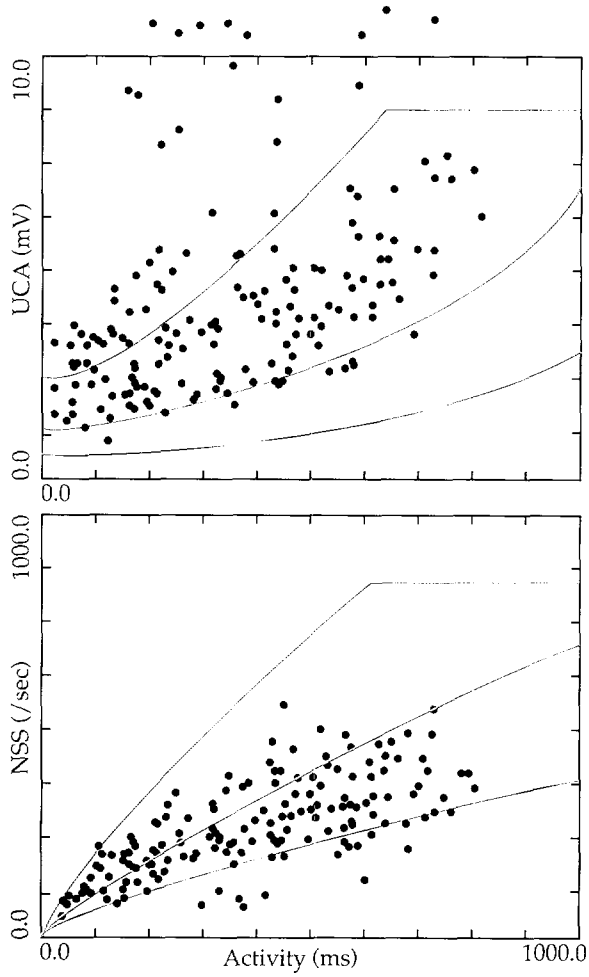

1.11 *Findings in Disease*

1.11.1 Hysteria/Malingering/Upper Motor Neuron Disease

The electrodiagnostic examination sometimes can be of substantial benefit in assessing patients with various non-PNS disorders. Because the motor unit and the primary sensory fibers are not affected, the motor and sensory NCS are completely normal. No abnormalities are seen on the NEE, except for the firing pattern. The MUAPs fire in significantly decreased numbers at a slow and often variable rate. If normal motor NCS amplitudes can be recorded from weak or paralyzed muscles, a problem with the AHCs and the peripheral motor nerve fibers derived from them can be excluded. This is particularly true if enough time has elapsed after onset of symptoms to exclude a proximal demyelinating conduction block from consideration.

1.11.2 Neuropathies

The electrodiagnostic examination is probably of greatest benefit to the clinician when it is used to assess patients with known or suspected disorders of the peripheral nerve fibers and their cells of origin. Abnormalities of these structures produce extremely variable electrodiagnostic findings, depending upon the particular component(s) of the PNS involved, their exact location (with focal lesions), the pathophysiology present, and the severity and duration of the process among other factors. Nonetheless, following the electrodiagnostic examination the clinician often can be provided with very useful information regarding the nature of the lesion (e.g., whether its probable pathophysiology is focal or generalized; if focal, its location, and severity). This information usually proves to be helpful in determining the necessity for additional diagnostic studies, in formulating the most appropriate approach to treatment, and in determining prognosis.

Overall, with neuropathies, axon loss occurs much more frequently than does demyelination. Hence, in NCS uniformly low amplitude or unelicitable motor and/or sensory responses are encountered far more often than are slowed latencies and CVs, or marked variation in amplitudes on stimulating at different points along the same nerve (due to conduction block).

A capsule review of typical findings seen with disorders at different points along the peripheral neuraxis follows.

Some diseases, such as poliomyelitis and amyotrophic lateral sclerosis (ALS, or Lou Gehrig's Disease), progressively destroy the AHCs in the spinal cord. The most common electrodiagnostic presentation is one or more low motor NCS amplitudes with completely normal sensory NCS amplitudes, along with normal latencies and CVs. On NEE, fibrillation potentials, fasciculation potentials, MUAP loss, and chronic neurogenic MUAP changes are often seen in widespread distribution (e.g., in multiple limbs).

With single-root lesions (e.g., those caused by a pinched nerve or slipped disc in the neck or back), the axon loss is usually minimal to modest in degree. Consequently, the NCS typically are normal — the motor NCS because not enough fibers have been destroyed to reduce their amplitudes, and the sensory NCS because the abnormalities are occurring proximal to the DRG, thus sparing the peripheral sensory fibers. The diagnosis, therefore, rests on NEE findings — specifically, on demonstrating fibrillation potentials and/or chronic neurogenic MUAP changes solely in muscles innervated by the involved

root. With multiple compressive root lesions, particularly when contiguous roots are affected (e.g., the left L5 and S1 roots), the motor NCS responses recorded from muscles supplied by the affected roots often are low in amplitude, but the sensory NCS remain normal. On NEE, fibrillation potentials, chronic neurogenic MUAP changes and prominent MUAP loss frequently are seen.

Plexuses are the intricate networks of nerve fibers interposed between the roots and the proximal peripheral nerves. They are thus situated proximally at the base of the neck and within the pelvis. With plexus abnormalities, the most common pathophysiology is one of axon loss. Consequently, motor and sensory NCS are usually low in amplitude, while the NEE shows fibrillation potentials, MUAP loss, and suggestive chronic neurogenic MUAP changes, depending upon the severity and the duration of the process.

With individual peripheral nerve lesions, electrodiagnostic studies can confirm that abnormalities are restricted to the nerve in question. The pathophysiology seen with the various mononeuropathies varies enormously. When studied early in their course (within approximately the first six to eight weeks after symptom onset), those that develop suddenly usually are manifested as either demyelinating conduction block or axon loss. Focal demyelinating lesions due to a single episode of nerve damage tend to resolve within the first 12 weeks or so after onset, usually within the first 6 to 8 weeks. Consequently, if electrodiagnostic studies are being performed on more chronic isolated peripheral nerve disorders, demyelinating conduction block is seldom seen and, instead, the process typically is completely that of axon loss.

With slowly developing peripheral nerve abnormalities and with those that have been present for several months, axon loss is the most common process, although demyelinating conduction slowing is sometimes seen. An example of the latter is carpal tunnel syndrome, the chronic entrapment of the median nerve beneath the transverse carpal ligament at the wrist. Prolonged median motor and sensory latencies (distal and peak, respectively) are the characteristic findings. Similarly, some ulnar nerve lesions at the elbow are manifested primarily by motor conduction slowing, with or without associated axon loss. For most other chronic focal peripheral nerve problems, however, the pathophysiology consists solely of axon loss. Thus, fibrillation potentials are seen in the muscles innervated by the damaged motor nerve fibers and, depending on severity, MUAP loss and suggestive chronic neurogenic MUAP changes are present, and the amplitudes of the motor and sensory NCS are diminished. In general, both NCS and the NEE must be performed for optimal assessment. The NEE may be the only component of the basic electrodiagnostic examination that is abnormal, with mild axon loss lesions affecting individual peripheral nerves, and typically, it is vital for localization of them. For example, if the median motor and sensory NCS responses are unelicitable in a limb, but all the other NCS studies are normal, the patient very probably has a median nerve lesion. Nonetheless, based on the NCS findings alone, the problem could be anywhere along the median nerve from its origin in the axilla down to the palm. However, the NEE may show abnormalities in all the muscles innervated by the median nerve in the forearm and hand, thereby indicating that the lesion is at or proximal to the elbow.

Many patients have a generalized disorder of their peripheral nerves, or polyneuropathy. These conditions have numerous causes. Some are inherited, but the majority are due to such diverse acquired entities as external toxins (e.g., arsenic), vitamin deficiencies, or metabolic disturbances (e.g., diabetes mellitus; uremia). Characteristically, the nerves of the lower extremities are affected more severely than are those of the upper and the process is more severe distally than proximally in a limb. The electrodiagnostic studies usually can confirm that multiple peripheral nerves are involved in multiple limbs, that a

distal to proximal gradient of abnormalities is present, and that the underlying pathophysiology is axon loss, demyelination, or a mixture of both.

1.11.3 Neuromuscular Junction Transmission Disorders

Disorders of the neuromuscular junction (NMJ) may be located at the postsynaptic site (muscle end-plate) or the presynaptic site (nerve terminal). The most common disorder of NMJ transmission is myasthenia gravis, a postsynaptic disorder of the Ach receptor molecules. Patients may show weakness of eyelids, ocular motility, speech, swallowing, neck muscles, and skeletal muscles of the extremities, including respiratory muscles. This is a disorder that expresses itself most clearly clinically and electrically in the fatigued state. The hallmark of the condition is the presence of Ach receptor antibodies directed against the Ach receptor molecules. These antibodies are detected in more than 90% of all myasthenia gravis patients.

In normal individuals, slow repetitive (2 Hz) stimulation of a motor nerve trunk results in uniform CMAPs recorded from the innervated muscle belly, reflecting the fact that every stimulus to the NMJ produces a maximal postsynaptic depolarization of the muscle fibers. This occurs in spite of the natural decline in Ach release at the presynaptic site, as the immediately releaseable pool of Ach is depleted. Enough Ach is always released to produce threshold depolarization of the postsynaptic muscle membrane in normal individuals (the so-called safety factor).

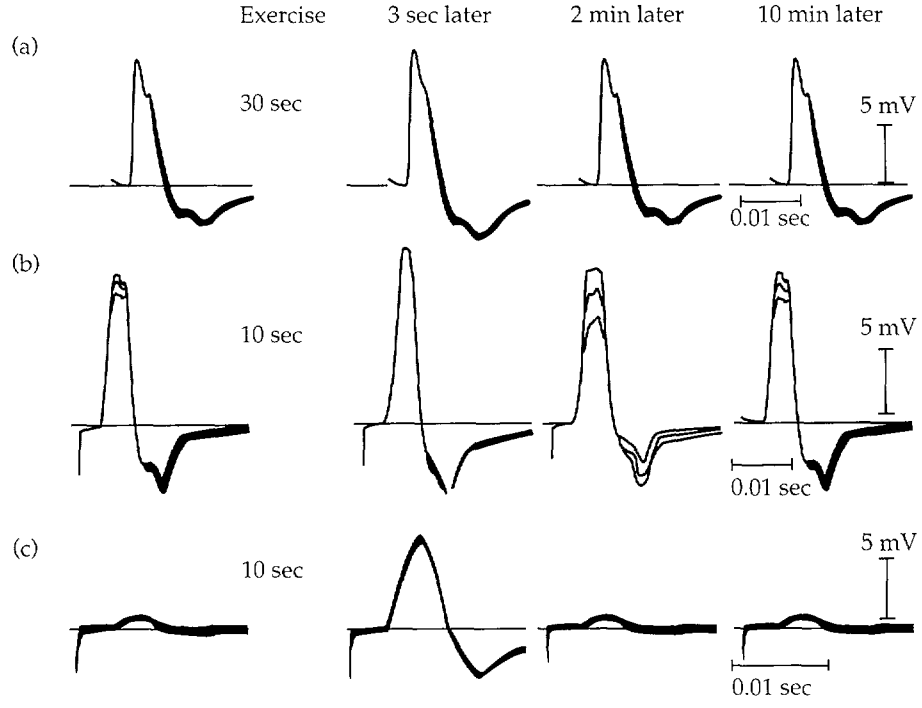

Figure 1.66 — Effect of exercise on the action potential of the hypothenar muscles evoked by maximal stimulation of the ulnar nerve at the wrist: (a) Responses of a normal subject. (b) responses of a patient with generalized myasthenia gravis. (c) patient with the myasthenic syndrome associated with a small cell bronchogenic carcinoma.

In myasthenia gravis, normal amounts of Ach are released but the Ach receptors are limited in number. Thus, as the released Ach naturally falls in a series of stimuli, at some point the existing receptors are underexposed to Ach, depolarization of the muscle membrane ceases, and contraction of that muscle fiber ceases. When this effect is summated over all the muscle fibers of a muscle belly, some NMJs being more severely affected than others, the net effect is a declining amplitude of the CMAP in a train of electric stimuli (Figure 1.66).

Brief forceful exercise produces a short-lived improvement in Ach release, thus repairing the safety factor and improving NMJ transmission. This phenomenon gives rise to a classic EMG picture of myasthenia gravis: with stimulation at rest, a decremental response is seen (Figure 1.66b). After brief forceful exercise when a new series of stimuli is delivered, the pre-existing decrement is lessened or completely repaired. Within two to four minutes after the exercise, an exhaustion phase is reached, when less than normal release of Ach takes place, exaggerating the decremental response when stimulation is performed at that time.

The NEE in myasthenia gravis shows a classic finding: motor unit instability. With repetitive firing of the same MUAP, one sees a moment-to-moment change in morphology, showing loss of turns, return of turns, or change in amplitude of the whole potential (Figure 1.67). This is the NEE correlate of decrement on repetitive stimulation. It reflects the intermittent loss of the safety factor at individual NMJs, producing blocked transmission and dropout of the muscle fiber action potential for that moment.

Figure 1.67 — Variation in motor unit potential amplitude in myasthenia gravis.

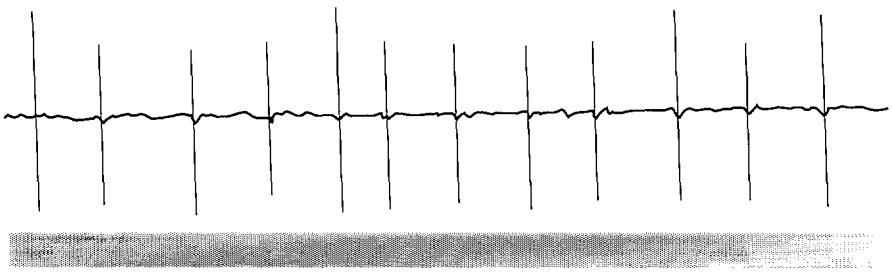

The classic clinical example of a presynaptic defect of NMJ transmission is the Lambert-Eaton syndrome (LES). A recently identified antibody is thought to act at the active zone of Ach release, preventing normal Ach transmission. The safety factor is thus lost and decremental responses to repetitive stimulation occur. Ach release is so impaired that the hallmark of this condition is very low amplitude CMAPs at rest. Brief forceful exercise transiently improves Ach release and increases the CMAP amplitude (Figure 1.66), due to calcium flux into the nerve terminal, a normal physiological event which facilitates Ach release. The EMG diagnosis of this condition depends on the identification of a low CMAP amplitude at rest following a single stimulus to the nerve trunk. After brief forceful exercise, a repeat single stimulus yields a CMAP amplitude at least 100% higher than the original. In patients unable to give strong exercise, tetanic repetitive stimulation at 20 Hz to 50 Hz can produce the same amplitude increase (Figure 1.68).

Figure 1.68 — Thenar muscle potential elicited by a train of stimuli 1 to 20 per second to the median nerve in a patient with the myasthenic syndrome.

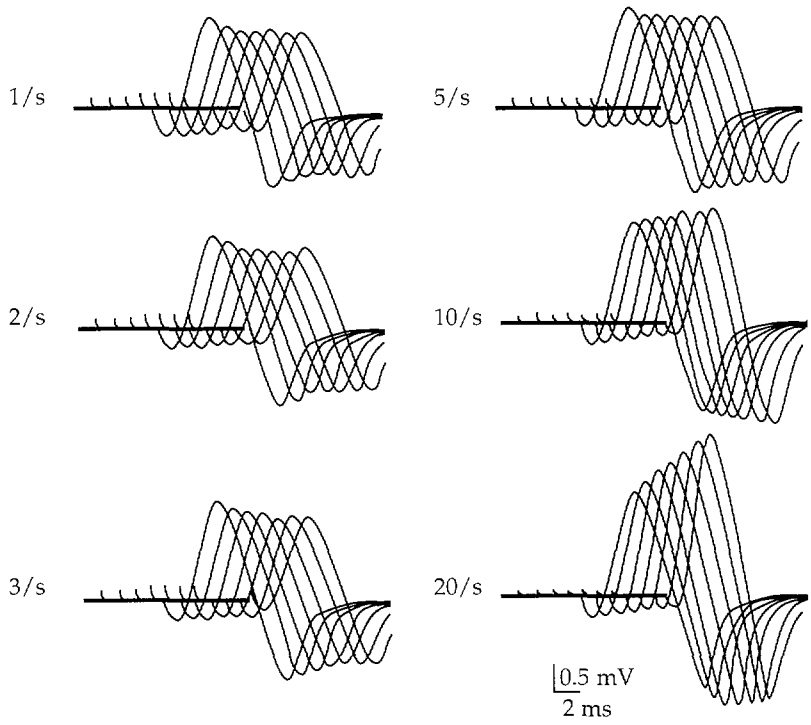

Concentric NEE and SFEMG show the classic features of defective NMJ transmission: MUAP instability and increased jitter, respectively.

1.11.4 Myopathies

Myopathies refer to the heterogeneous group of disorders that primarily affect muscle. These disorders range from severe inherited diseases of muscles, such as Duchenne muscular dystrophy, to the relatively mild myopathies associated with endocrine disturbances, such as steroid myopathy. The type of EMG findings encountered in the various myopathies depends largely on the pathology of the individual myopathy. Typically, sensory and motor NCS are normal. Notable exceptions are those rather severe myopathies associated with muscle cell degeneration and replacement with connective tissue. By virtue of damage to the muscle itself, motor NCS may display low amplitudes. However, distal latencies and motor conduction velocities remain normal. The myopathies that may produce such alterations in motor NCS include the muscular dystrophies and severe forms of myositis.

The principle EMG findings in myopathy are noted on the NEE. In those myopathies associated with muscle cell degeneration or necrosis, abnormal spontaneous activity can be recorded. In particular, fibrillation potentials are noted in these necrotizing myopathies, such as the progressive muscular dystrophies and myositis. The mechanism of fibrillation potentials in myopathy has been attributed to segmental necrosis of muscle

Figure 1.69 — (a) Motor unit potentials in Duchenne muscular dystrophy. (b) interference pattern at maximum voluntary contraction.

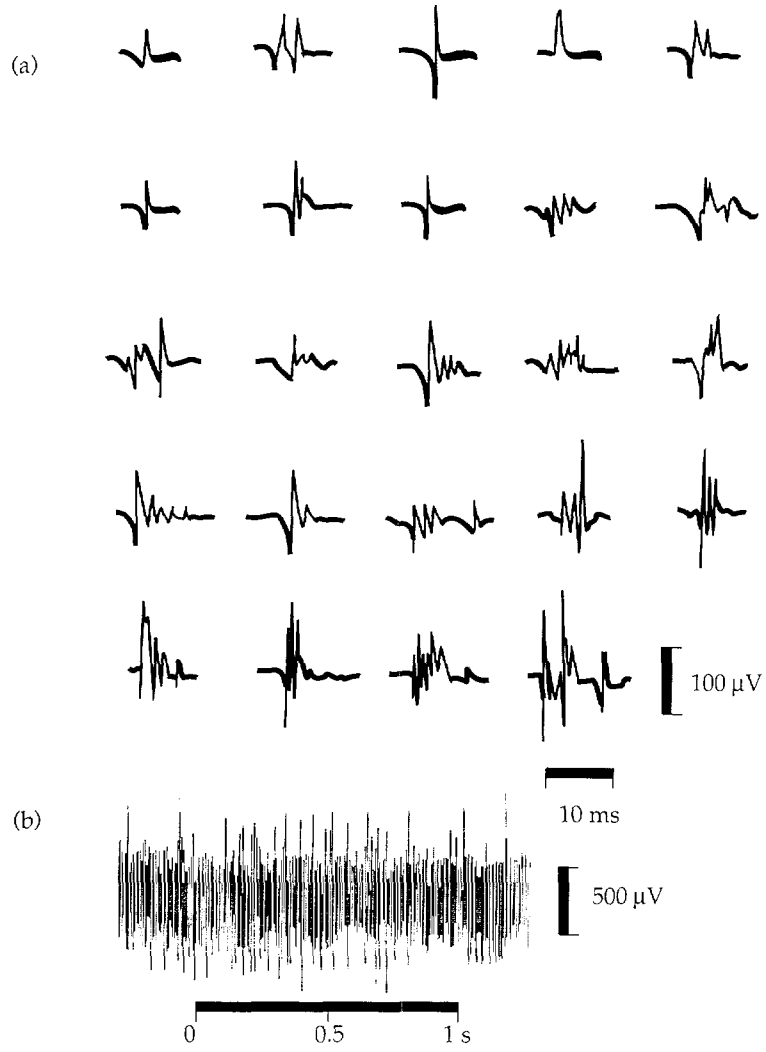

fibers that isolates part of the muscle fiber from its innervation. Thus, the muscle fiber becomes myopathically denervated. Fibrillation potentials in myopathies tend to occur in the axial and most proximal muscles first and are later noted in the more proximal limb girdle muscles, and sometimes in distal muscles. On some occasions fibrillation potentials are only encountered in the paraspinal muscles. In some necrotizing myopathies, such as inclusion body myositis, distal muscles may be preferentially involved, and thus the distribution of the fibrillation potentials follows the pattern of clinical involvement. Other forms of abnormal spontaneous activity, including myotonic discharges and complex repetitive discharges, may also be recorded in myopathies. Myotonic discharges are most prominent in the myotonic disorders such as myotonia congenita, myotonic dystrophy, and para-myotonia congenita. Myotonia, however, may also be seen in hyperkalemic periodic paralysis, adult acid maltase deficiency, hypothyroid myopathy, chloroquine

myopathy, diazocholesterol poisoning, and in some cases of polymyositis. Complex repetitive discharges may also be seen in the chronic myopathies, particularly muscular dystrophy and polymyositis/dermatomyositis.

The cardinal EMG features of myopathy are alterations in the morphology of the MUAP (Figure 1.69). Myopathies produce several alterations in MUAP morphology including a reduction in the duration, a decrease in amplitude, and an increase in the number of phases. These alterations appear to result from a random loss of muscle fibers and the variability of cross-sectional diameter of muscle fibers that typically occurs in myopathic disorders. Specifically, the increased polyphasia of the MUAPs may be related to loss of synchrony of firing of the individual muscle fibers within the motor unit. This may stem from variation in fiber size and altered muscle fiber conduction velocities. These MUAP alterations are preferentially recorded in the clinically affected muscles, typically, the axial and proximal muscles.

In addition to the alteration in morphology of the MUAP, interference and recruitment patterns may also be affected. In clinically weak muscles, early recruitment of MUAPs that is disproportionate to the degree of force generated may be observed. This is caused by the reduced size of muscle fibers and the reduced number of muscle fibers available to contribute to the force of contraction.

The typical alterations of the MUAP that occur in myopathies are nonspecific. Thus, it is strongly discouraged to use terms such as myopathic motor unit action potentials in referring to short duration, small amplitude, polyphasic MUAPs. Similar MUAP alterations may be seen as a consequence of reinnervation, demyelination of terminal nerve fibers in acquired demyelinating polyneuropathies, and disorders of neuromuscular transmission such as myasthenia gravis.

2.0 ELECTROENCEPHALOGRAPHY

The electroencephalogram (EEG) represents a technology that provides a real-time window of information on brain function. It transforms the minute electrical signals arising from synaptic activity in the brain into waveforms that map this activity over the surface of the skull. Unlike computer-aided tomography (CT) or magnetic resonance imaging (MRI), EEG records brain function, not its structure. It plays an important role in the diagnosis of diseases that affect the cerebral hemispheres such as epilepsy, stroke, tumors, infection, degenerative illnesses, and delirium. It is also used to investigate brain function in a variety of states, such as sleep sedation/anesthesia, coma, cognition, and as supportive evidence in the determination of death.

Over the past decade, the field of electroencehalography has flourished, providing clinicians with an impressive array of new technology to look directly at brain activity without the limitations of multiple-pen strip-chart recorders and signal distortion caused by the meninges, skull, scalp, and cerebrospinal fluid. Digital paperless EEGs allow investigators to sample brain activity over a broad spectrum of frequencies, manipulate these signals mathematically, and quantify temporal and frequency spectrum data for objective monitoring of brain function. Intracranial monitoring with electrodes implanted directly on the cortical surface, or inserted in the brain via depth wires, are reshaping our ideas on the generation of cerebral activity. These techniques allow mapping and localization of brain signals that are undetectable by the traditional scalp EEG. Electrical brain stimulation through these electrode arrays permits mapping of cortical function, a technique widely used in research and in conjunction with intracranial monitoring for the surgical treatment of epilepsy.

Evoked potentials (also called EP or evoked responses) provide information that complements the EEG. Evoked potential techniques map conduction of neuronal activity along neuroanatomical pathways in the peripheral nervous system (PNS) and central nervous system (CNS) in response to stimuli. The functional integrity of these pathways can be assessed, helping clinicians recognize disease states that interfere with conduction in particular places along these pathways. The signals measured by EP are very small and are detectable only by signal-averaging hundreds or thousands of responses to rapidly repeated stimuli. Examples of clinically useful EPs include: visual evoked potentials (VEP), which measure conduction along the visual pathways; brain stem auditory evoked potentials (BAEP), which test the integrity of the auditory pathways; and somatosensory evoked potentials (SSEP), which measure conduction over a distance of up to several meters between peripheral sensory nerves and the cortical neurons in the brain which perceive their stimulation.

Together, EEGs and EPs provide an expanding window on brain function. The following section presents the basic principles behind these technologies, techniques for their application, and a brief discussion of their use in clinical and research science.

Figure 2.1 — Synapse picture, close-ups showing synaptic cleft, and vesicles.

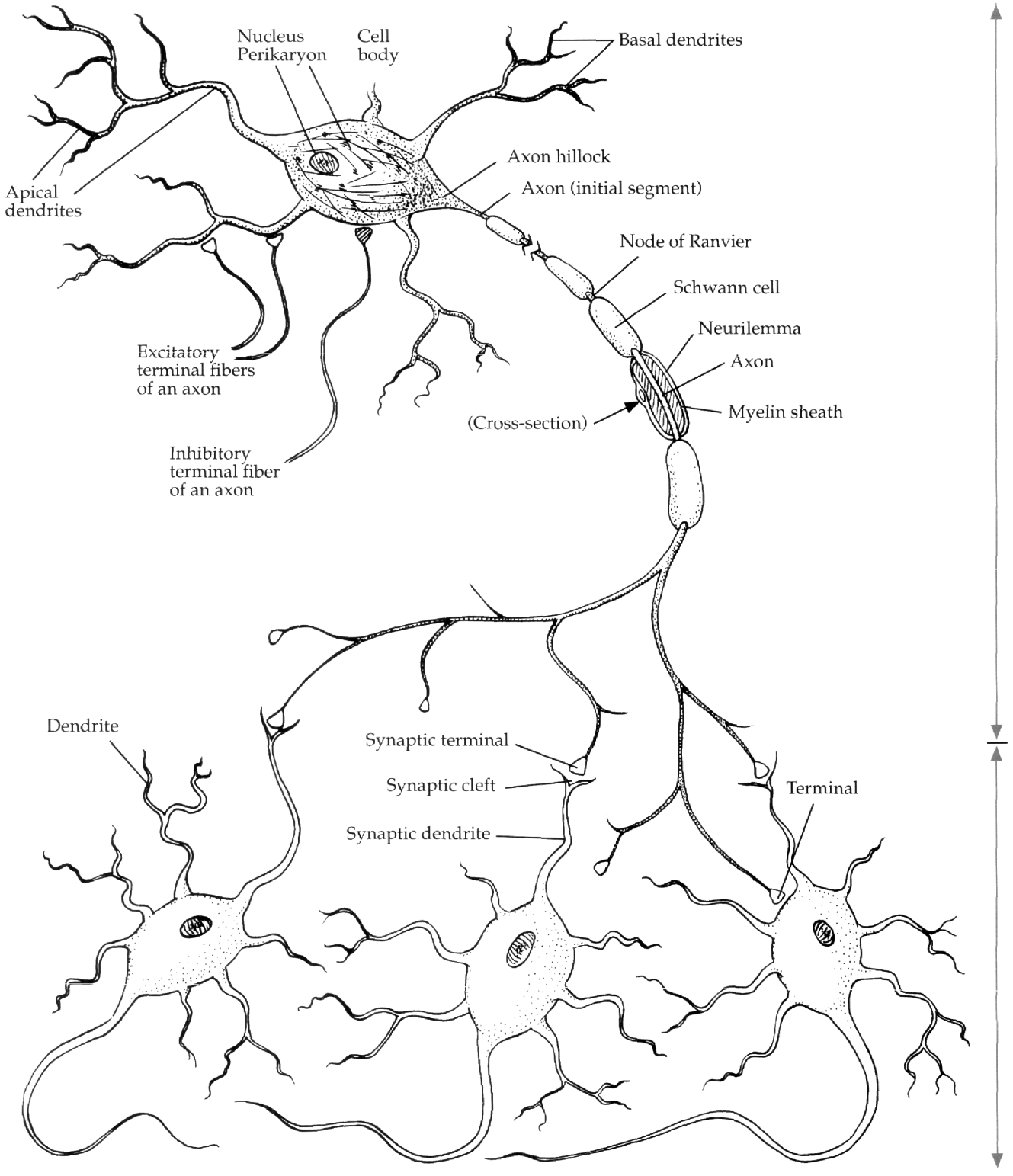

Figure 2.2 — Diagram of synaptic tree of cortical cell.

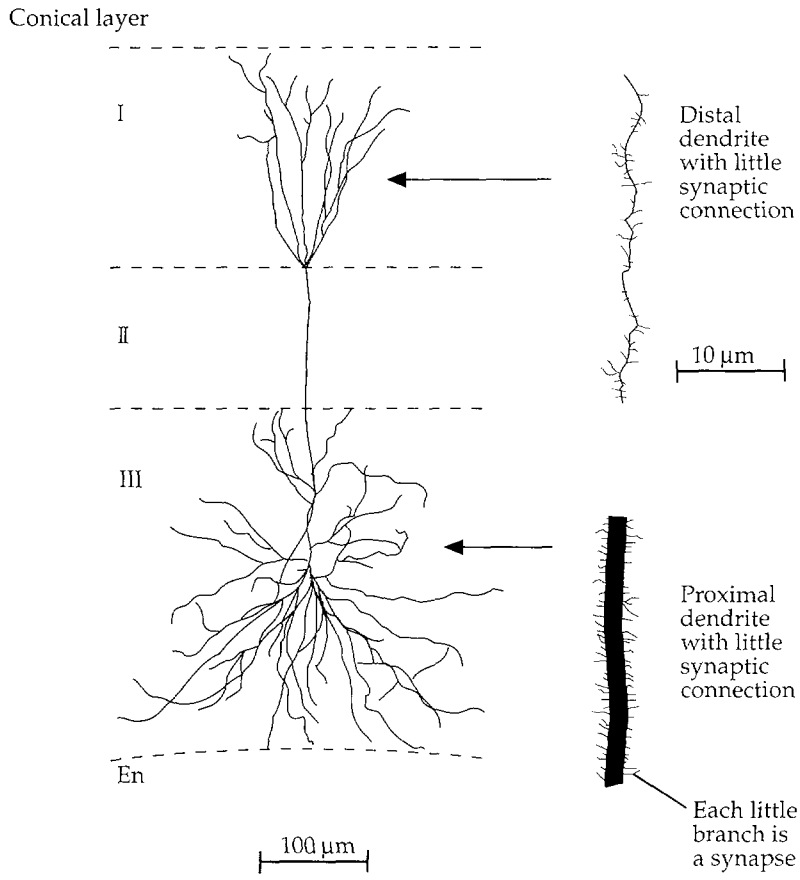

2.1 *The Living Cell as an Electrical Generator*

2.1.1 The Source of Electroencephalographic Potentials

Neurons communicate with each other through synapses, the spaces between one nerve cell and the beginning of another (Figure 2.1). Synapses include the presynaptic terminal of one cell, which in response to an action potential conducted along its length, releases small vesicles containing neurotransmitters that, in turn, bind to the membrane of the postsynaptic terminal of the target cell. This causes a change in membrane potential of the target neuron. Synapses can be excitatory, increasing target membrane potential (depolarization), or inhibitory, decreasing target membrane potential (hyperpolarization). In the brain, neurons may be stimulated by large numbers of synapses simultaneously (Figure 2.2). Changes in membrane potential from this activity are summed in the body of the target neuron (axon hillock region), resulting in postsynaptic potentials (PSPs) that are constantly changing. When membrane potential increases beyond some threshold value, ion

Figure 2.3a — Ion channels, cycle of depolarization.

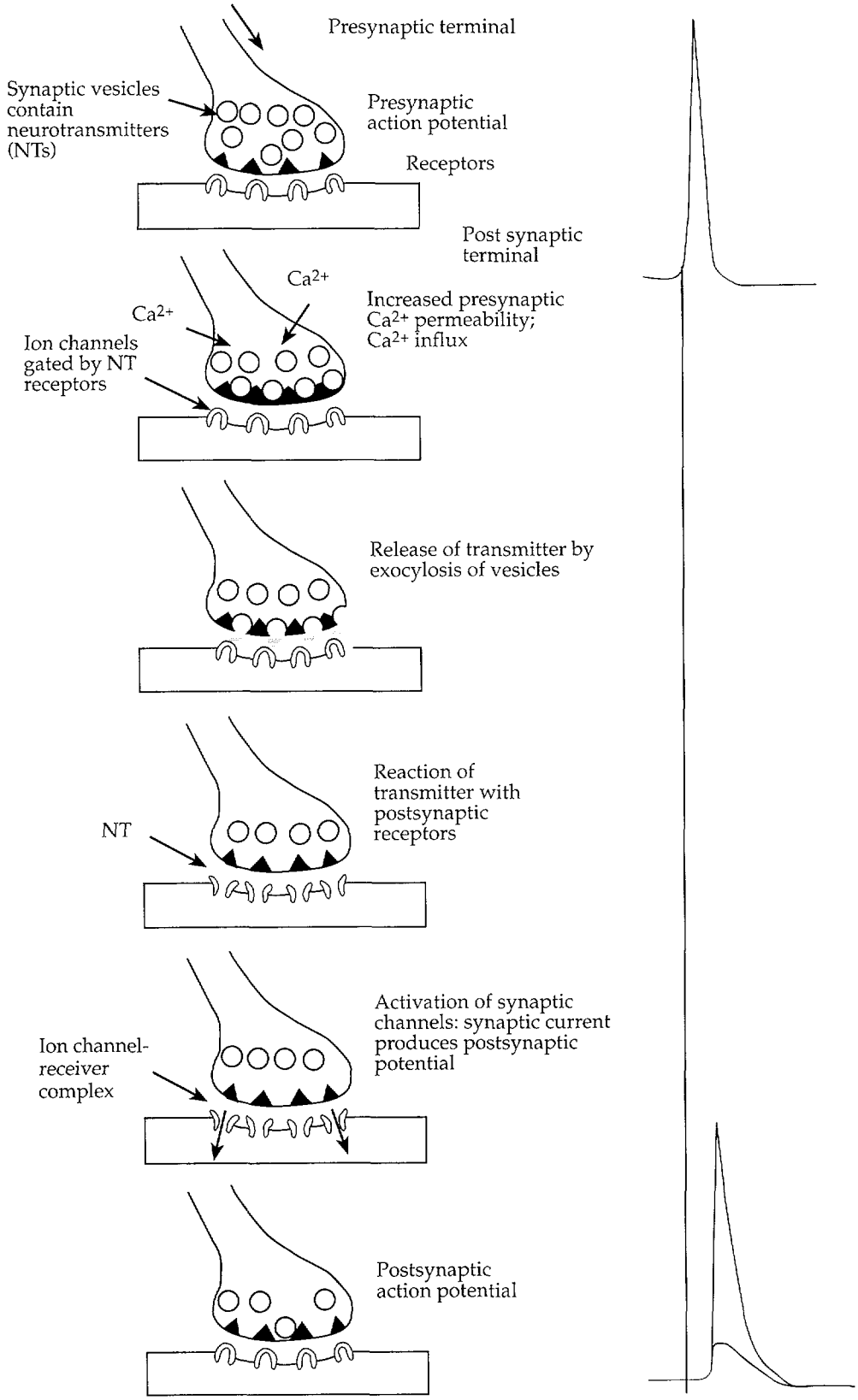

Figure 2.3b — Ion channels, cycle of depolarization.

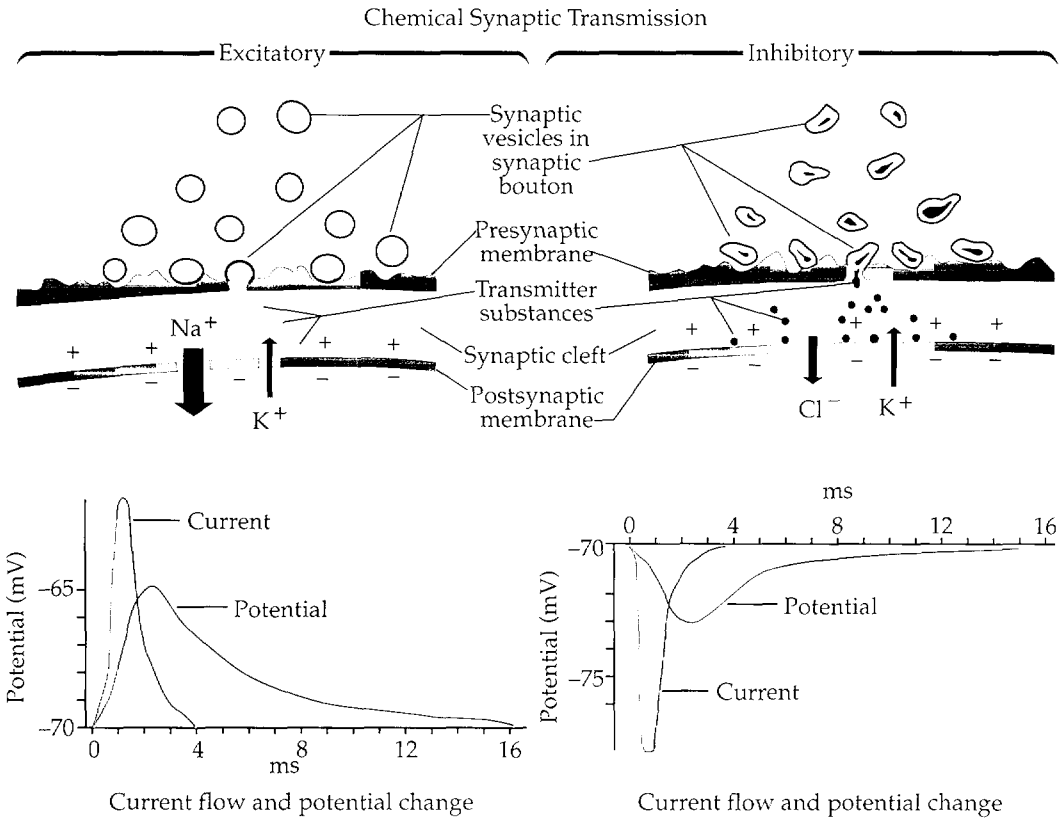

Figure 2.4 — Action potentials and post synaptic potentials.

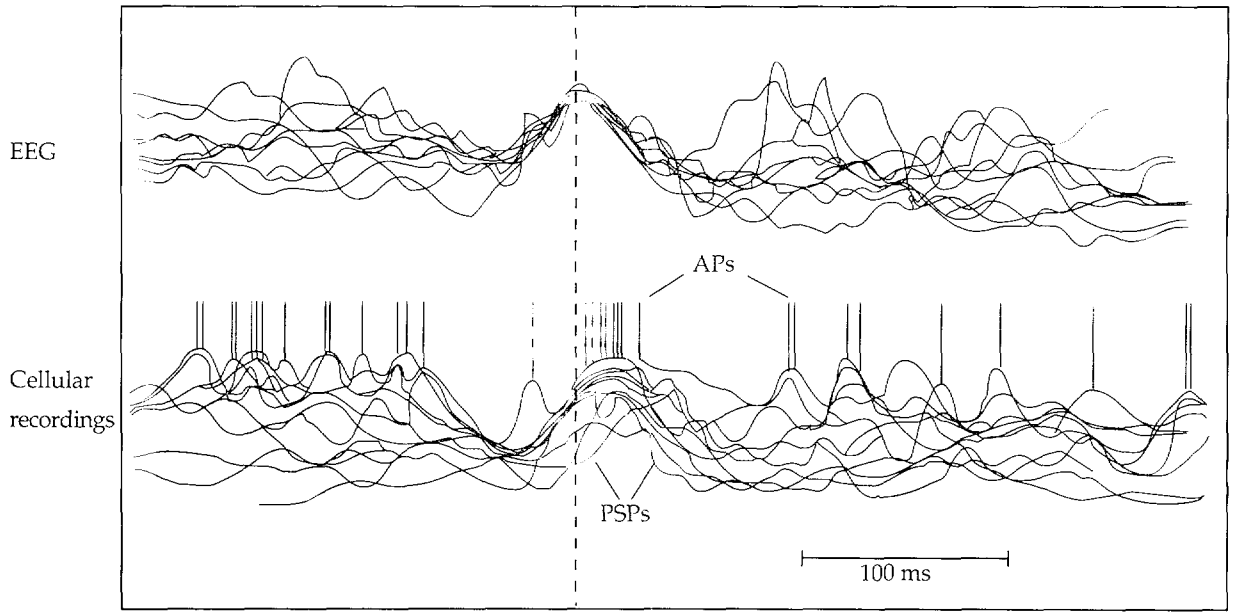

Figure 2.5 — Dipole figure from AEEGS.

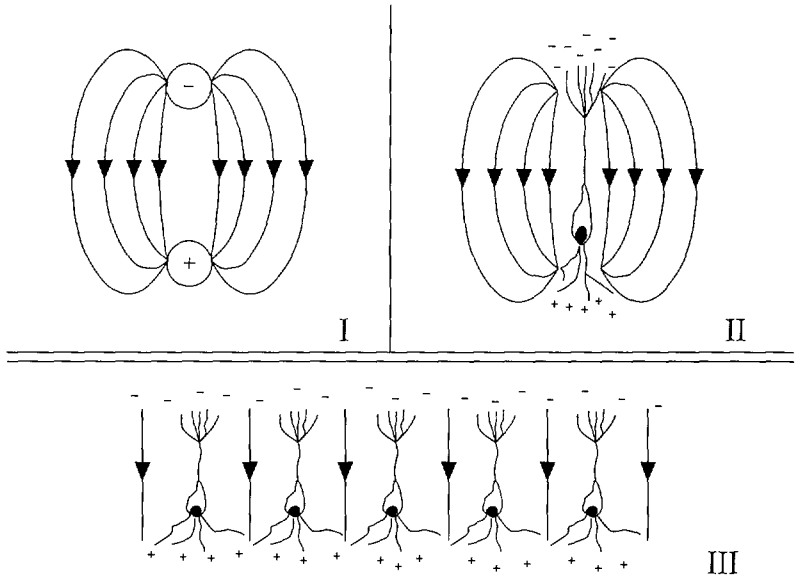

channels in the target cell membrane open, allowing the influx of sodium and calcium ions, and slightly later, an efflux of potassium ions, which results in the generation of an action potential. The action potential depolarizes the target cell, causing it to release neurotransmitters from its presynaptic terminals onto other cells (Figure 2.3b). The cycle then begins again after a brief recovery period during which ion balances are restored.[1]

Changes in membrane potential can be measured inside the cell with thin glass needle electrodes, in the extracellular space or on the surface of the volume containing the cellular preparation. Single sharp waves on the EEG are generated by PSPs from a large number of pyramidal neurons in layers three and five of the cerebral cortex thought to contain hundreds or thousands of neurons. The PSPs from these cells are summed together in the extracellular fluid around them and conducted through the volume of brain, cerebrospinal fluid (CSF), blood, bone, muscle, and skin that comprise the head, and into electrodes connected to the EEG machine. Individual action potentials are of higher voltage and generate larger peak currents than do individual PSPs. However, action potentials are short in duration and asynchronous; i.e., they do not occur exactly at the same time. This causes their effects to cancel each other rather than sum together, as do the longer duration PSPs. For this reason action potentials are not directly seen on the EEG (Figure 2.4).[2,3]

2.1.2 Dipoles and the Localization of Encephalographic Activity

Postsynaptic potentials that underlie EEG activity are synchronous, with a duration long enough to form carge separations that approximate dipoles. A dipole is composed of two equal and opposite charges separated by a small distance (Figures 2.5 and 2.6). By assuming that discrete EEG potentials arise from dipole sources (dipole approximation), generators of this activity can often be localized in the brain by using numerical methods of

Figure 2.6 —Dipoles made up of groups of pyramidal cells in cortex cause deflections on the surface EEG.

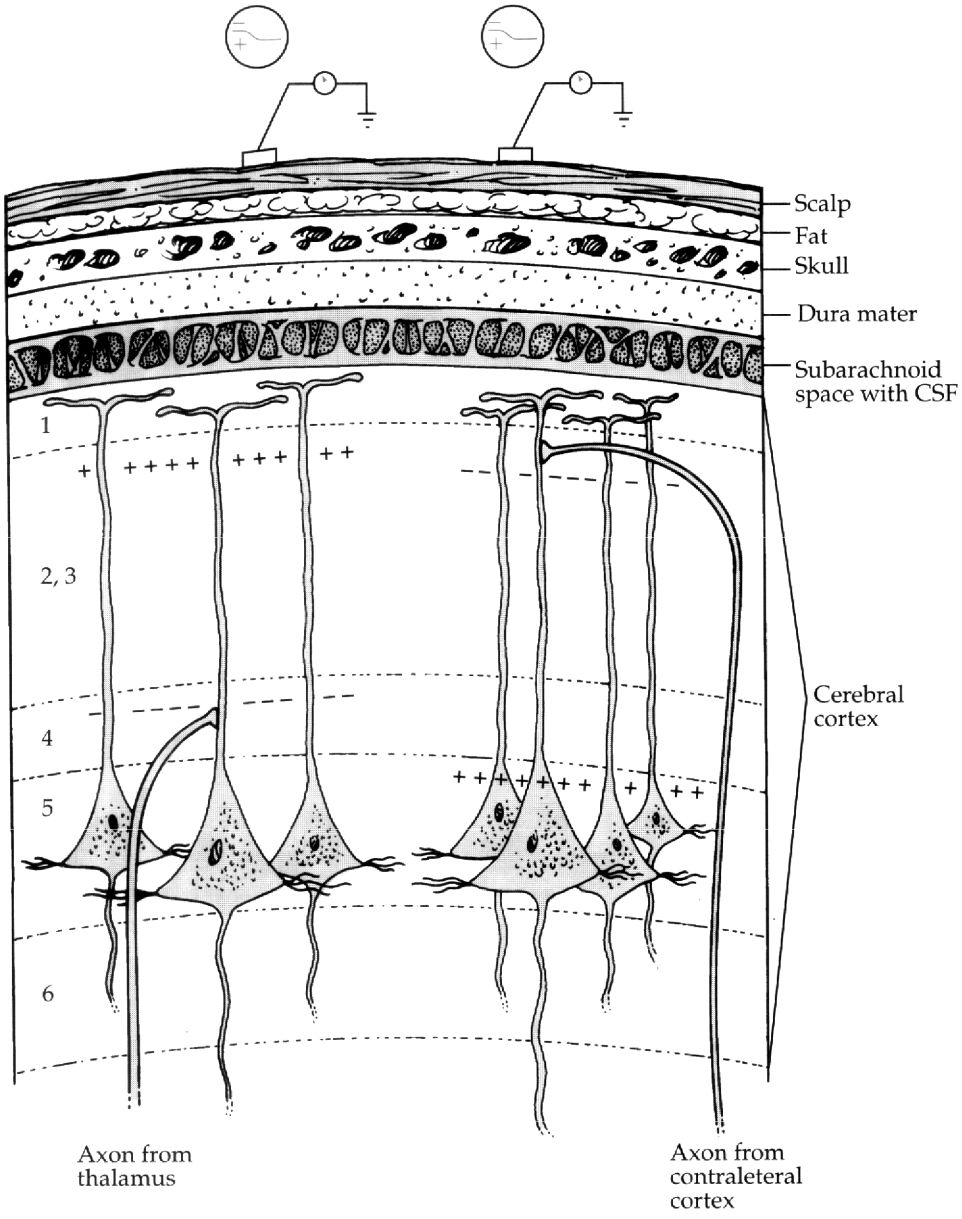

successive approximation (Figure 2.6).[4] The localization of a dipole source based solely upon the EEG it generates is called the inverse problem. Numerical methods are used because no one has yet devised a unique analytical solution to the inverse problem. Localization algorithms may assume that the head is a uniform spherical conductor and that EEG activity arises from point sources in the brain, both large assumptions that can lead to significant errors in source localization. Despite their flaws, approximate solutions to the inverse problem often provide useful clinical information. Finding a unique solution to the inverse problem is one of the great challenges facing neuro-electrophysiologists today (Figure 2.7).[5]

Figure 2.7 — The dipole field of a single seizure discharge mapped on the scalp.

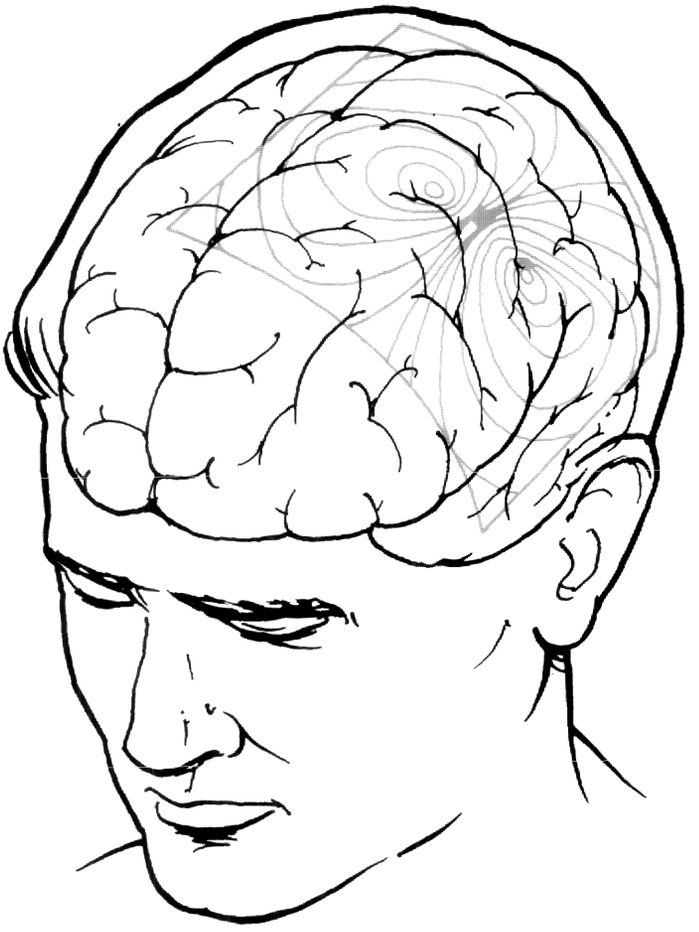

Figure 2.8 — Electrode-scalp interface (Req = resistance of electrolyte material between tissue and material, RD and CD = resistance and capacitance of electrode double layer, Rd and Cd = time and frequency-dependent diffusion impedance).

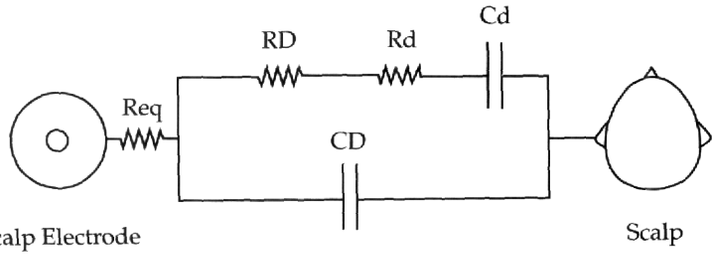

Figure 2.9 — Figure from Cooper, electrode responses/ properties.

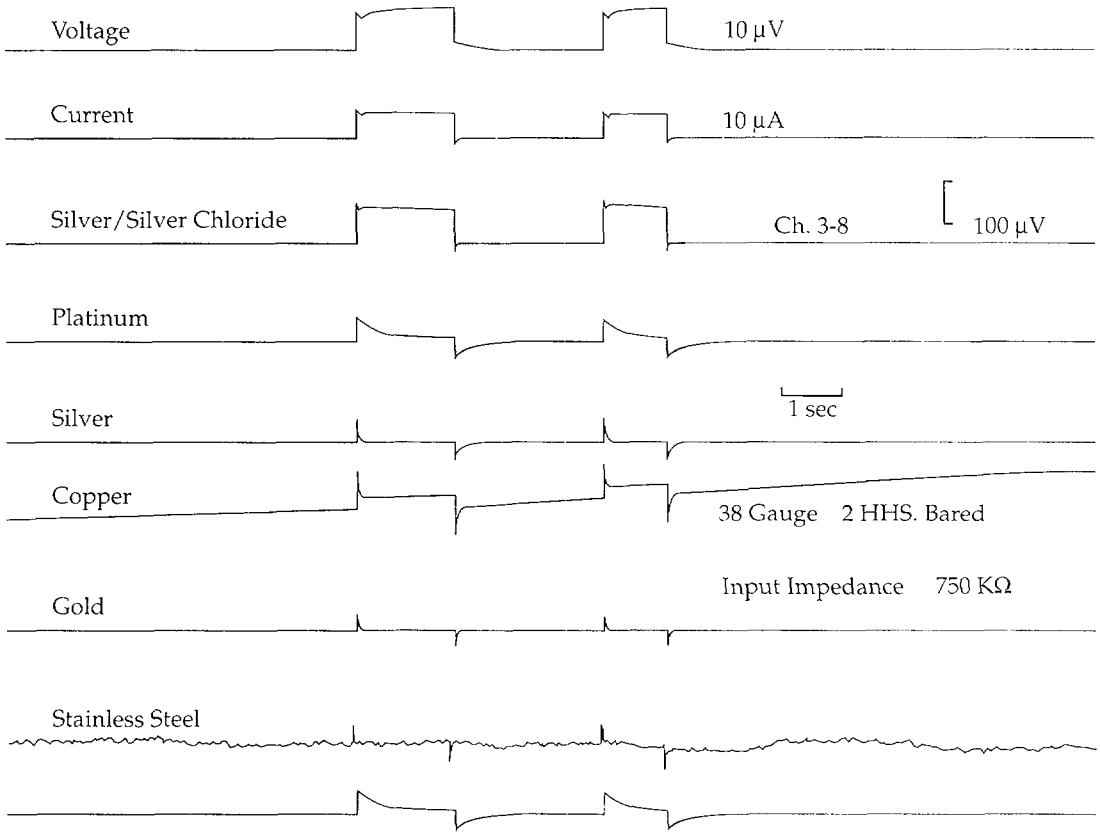

2.2 *Electrodes*

2.2.1 Noninvasive Electrodes

Standard noninvasive EEGs record the potential difference, or voltage, between two locations on the head, usually on the scalp or between one location on the head and a distant reference electrode. EEG signals usually range between 50 to hundreds of μV, with currents of several μA. Signals travel from the head to EEG machines via a number of different types of electrodes coupled to the scalp, or tissue of contact, in a circuit that has its own resistance, capacitance, and frequency-dependent impedance (Figure 2.8). The electrode-tissue interface consists of two layers of ions that allow electrons to pass from one side to another. Nonpolarized, or reversible, electrodes are composed of either noble metals like platinum, or from (or coated with) substances, such as silver chloride, that allow free exchange of ions with the salt-rich fluids surrounding body tissues. When contacting tissues, these nonpolarized electrodes have low electrode potentials; i.e., they pass little net current from electrode to solution, aside from the EEG signal.

Nonpolarized electrodes, in general, reproduce EEG signals more accurately than do electrodes that may become polarized. Polarized electrodes can have large electrode potentials compared to EEG signals. In the absence of an EEG signal, the electrode potentials

may pass substantial net currents into electrolyte solutions, which are large compared to signals measured by the EEG. This may cause substantial direct current signals that must be filtered out. While all electrodes can have some filtering effects on the EEG, nonpolarized electrodes may themselves have significant low-frequency filtering effects. The effect of different electrode materials on reproduction of a square-wave signal is shown in Figure 2.9.[6]

The usual noninvasive electrodes are shown in Figure 2.10.[7]

- **Cup electrodes** - Used for most routine recordings, cup electrodes comprise 4 mm to 10 mm-diameter chlorided platinum, gold or tin discs coupled to the scalp by a conducting paste or gel. The skin is first scrubbed with an abrasive compound to promote good electrical contact.

- **Subdermal electrodes** - Fine metal needle electrodes, 10 mm long and 0.5 mm wide, made from stainless steel or platinum, are inserted under the scalp (usually in unconscious patients) after cleaning the region with a presurgical scrubbing compound.

- **Clip electrodes** - Cup electrodes filled with conducting gel or paste, clipped to the ear lobes for referential recording.

2.2.2 Invasive Electrodes

The following electrodes, although somewhat invasive, are used in conjunction with scalp electrodes to detect signals from the inferior frontal or mesial temporal regions, areas that are often silent or poorly recorded on scalp EEG. The ability of these electrodes to detect seizure activity not seen on regular scalp EEG justifies the invasive procedures required for their insertion.

- **Nasopharyngeal electrodes** - Made from 10 cm to 15 cm-long segments of flexible insulated wire with an uninsulated 2 mm tip, the S-shaped electrodes are inserted into the nasopharynx and rotated outward to their position within 2 cm of the anterior mesial surface of the temporal lobes. These electrodes are rarely used for long-term monitoring because they are uncomfortable, show substantial respiratory artifact, and are poorly tolerated for longer than a brief outpatient recording.

- **Tympanic electrodes** - Thin stainless steel insulated wires with a 7 mm stainless steel, gold or platinum ball wrapped in felt at the end, are soaked in conducting solution and then inserted into the external auditory canal until the patient senses mild discomfort. The electrode is useful for recording from the mesial temporal lobes, but is rarely used.

- **Sphenoidal electrodes** - Thin, insulated stainless steel wires inserted into the temporal and masseter muscles between the zygoma and sigmoid notch of the mandible (about 1 cm in front of the ear lobe) to record from the anterior tip of the temporal lobe. These electrodes penetrate the skin so that the tip rests lateral to the foramen ovale at the lateral pterygoid plate.[8] Sphenoidal electrodes are the most commonly used invasive electrodes in inpatient epilepsy monitoring units because they are usually well-tolerated for days at a time and often detect temporal lobe spikes not seen on scalp EEGs.

Figure 2.10 — Types of non invasive and invasive electrodes.

Using Grass E5GH or E5SH electrodes with collodion

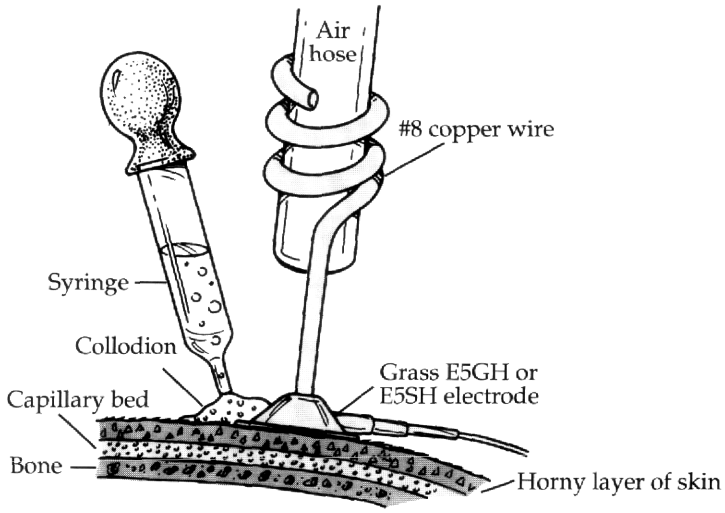

Site preparatation and insertion of subdermal invasive electrodes

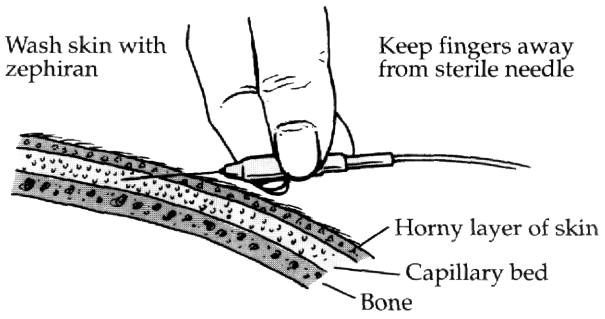

Subdermal invasive electrodes

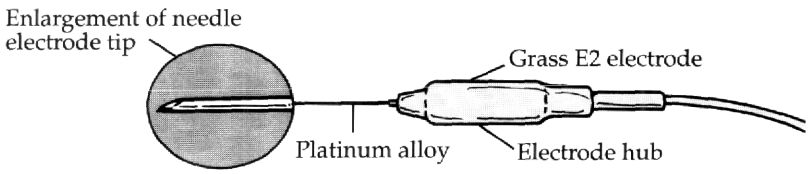

Grass model EPG-G nasopharyngeal lead

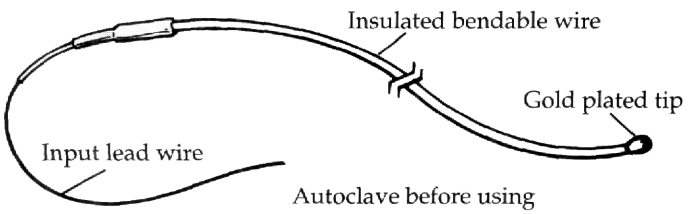

Typical sphenoidal electrode

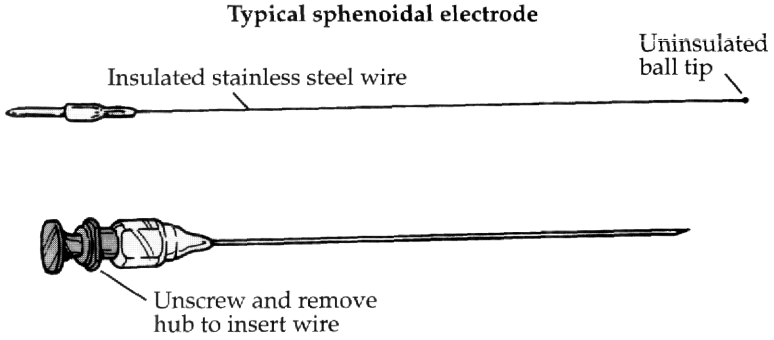

Figure 2.11 — Drawing of patient in a 24-hour video and EEG monitoring unit.

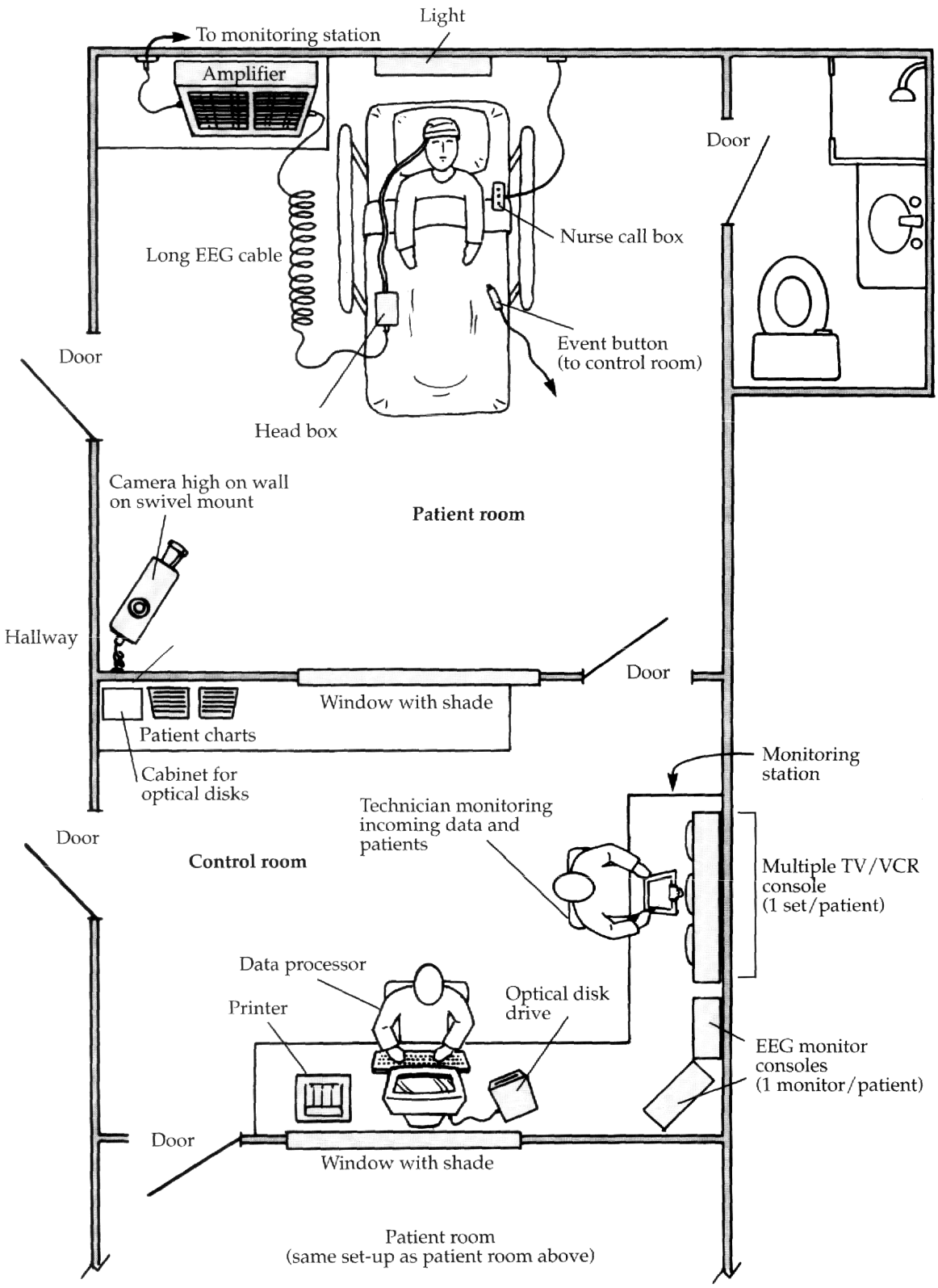

Figure 2.12 — Subdural grid and depth wires. Note: Similar connectors are used for all intracranial electrodes in the system shown. The number of connector contacts is equal to the number of contacts on the tress that is inserted into the tress that is inserted into the connector.

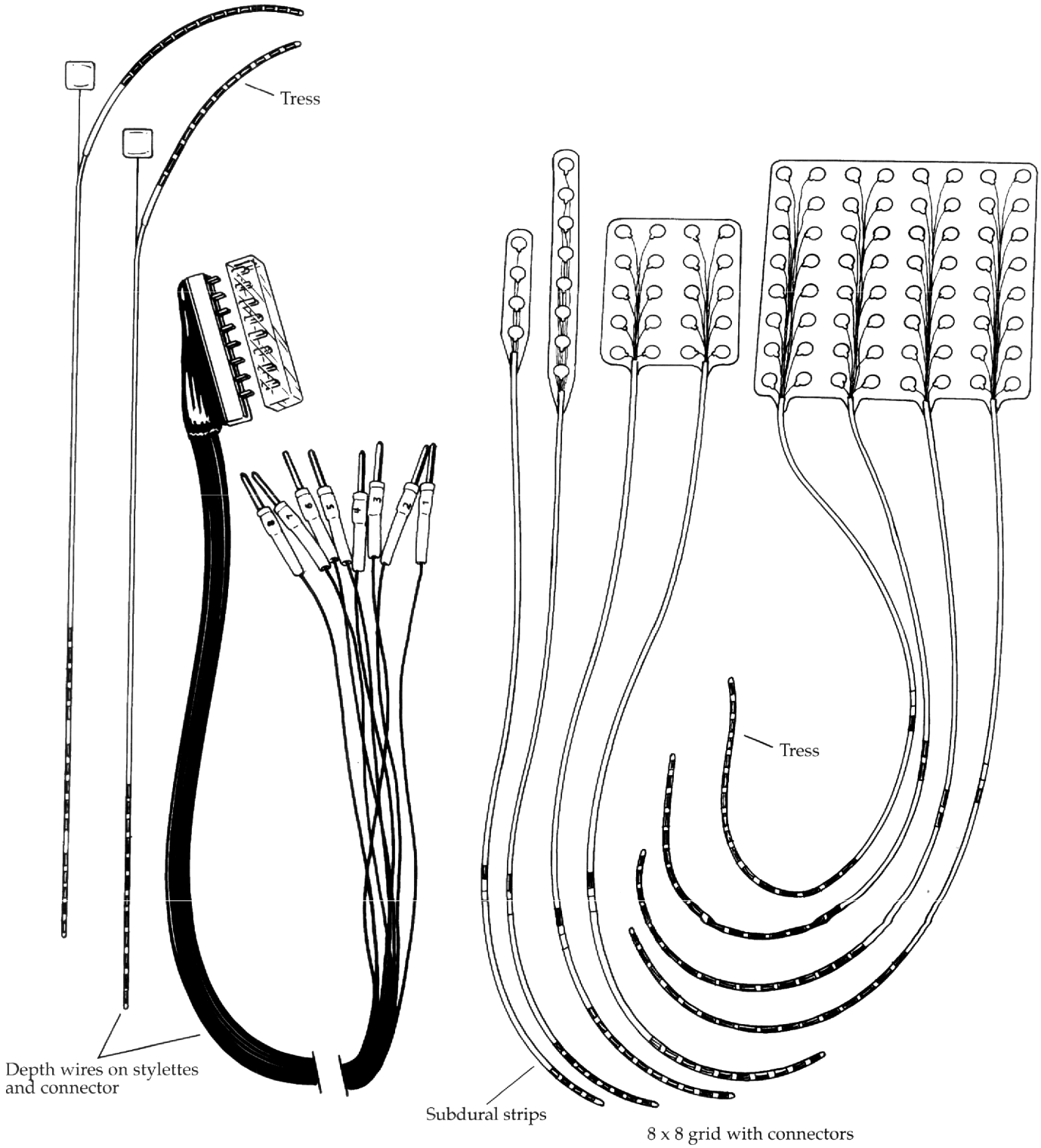

- **Foramen ovale electrodes** - Teflon-insulated, fine silver wires mounted on an insulated introducing wire that is inserted through the cheek, lateral to the corner of the mouth and under local or general anesthesia. The wire is advanced until it penetrates the subarachnoid space through the foramen ovale. These electrodes may have potentially increased sensitivity for temporal lobe discharges, but the technique is relatively invasive.

2.2.3 Intracranial Monitoring

Intracranial electrode arrays allow monitoring of cortical discharges directly from the brain without the distorting effects of the CSF, high-resistance skull, scalp, or dura. These techniques form the foundation of the modern surgical treatment of epilepsy. At first, invasive monitoring was performed only in the operating room at the time of surgery. Patients were anesthetized, sometimes lightly enough to allow them to respond to commands. Cotton wick electrodes were placed directly on the surface of the brain to map areas responsible for seizure activity. This procedure is called electrocorticography. Epileptogenic areas were then resected, with some attention given to sparing regions neuroanatomically known to serve vital functions, such as movement, sensation, vision, and speech.[5]

With the invention of new systems of implantable electrodes, patients now have arrays of electrodes implanted in an initial surgery, they are monitored for a period of days to weeks while the patient remains in the hospital (Figure 2.11). During this time, seizures are recorded and mapped to regions covered by the implanted arrays. Small currents are sometimes passed through adjacent pairs of electrodes (in subdural grids and strips only) while patients attempt to perform various motor, sensory, language, visual, and cognitive tasks. If these tasks are interrupted by the brain stimulation then that particular function is localized to the position of the stimulating electrode. Responses are recorded, mapping vital brain functions, and compared to the map of sources of seizure activity. During a second surgery, the electrode arrays are removed, along with epileptogenic tissue, sparing regions identified as critical areas by functional mapping.[9]

Intracranial monitoring techniques have improved success rates for the surgical treatment of epilepsy in appropriate candidates and have revealed a wide range of electrical activity in the brain that was previously undetectable by scalp EEG. These methods have demonstrated a large amount of variability in the location of vital cerebral functions, such as motor activity, sensation, language, and vision. Intracranial monitoring does have limitations, however, in that implanted electrodes sample only from regions adjacent to them, and may incorrectly localize epileptic sources due to sampling error.

The following brief summary discusses the most commonly employed intracranial electrodes and their intended use (Figure 2.12):[10]

- **Depth wires** - These arrays of stainless steel, gold, or platinum wires of different length are introduced into the brain stereotactically, with the help of a three-dimensional head-holding frame mounted onto the patient who is positioned in a CT scanner. Wires are placed through burr holes in the skull using a number of different strategies. In one commonly used technique, patients have three pairs of depth wires implanted, one each in the frontal lobes, hippocampi, and amygdala bilaterally. Different length wires in each insulated bundle allow simultaneous monitoring from deep structures, intervening white matter, and superficial cortical areas. These electrodes are often used for seizure localization when the scalp EEG is not diagnostic, particularly to determine the location of seizure onset, which seizure source is firing first, and from which side of the brain it fires.[11]

Figure 2.13 — Diagram of stimulation map.

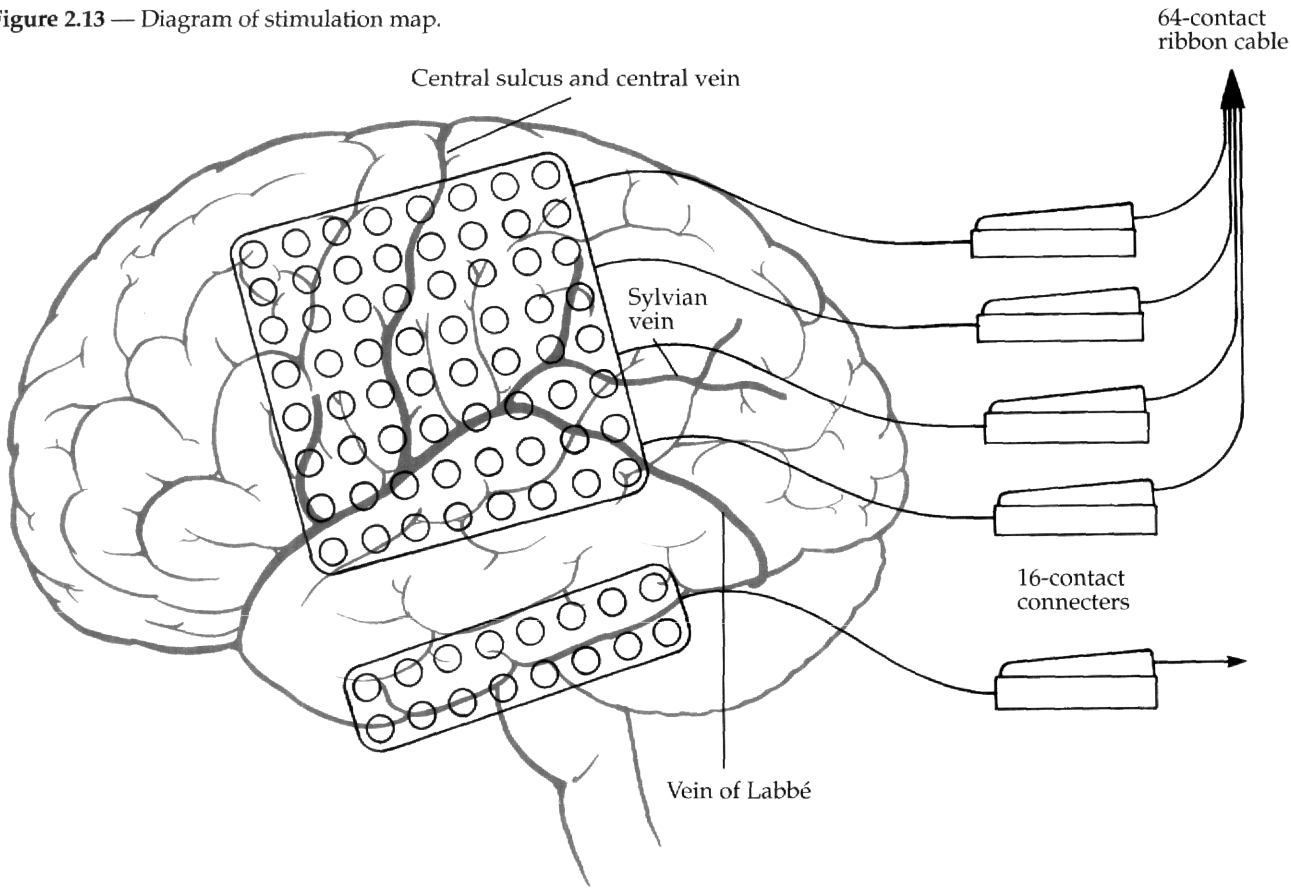

Figure 2.14 — Drawing of electrocorticographic halo used in electrocorticography.

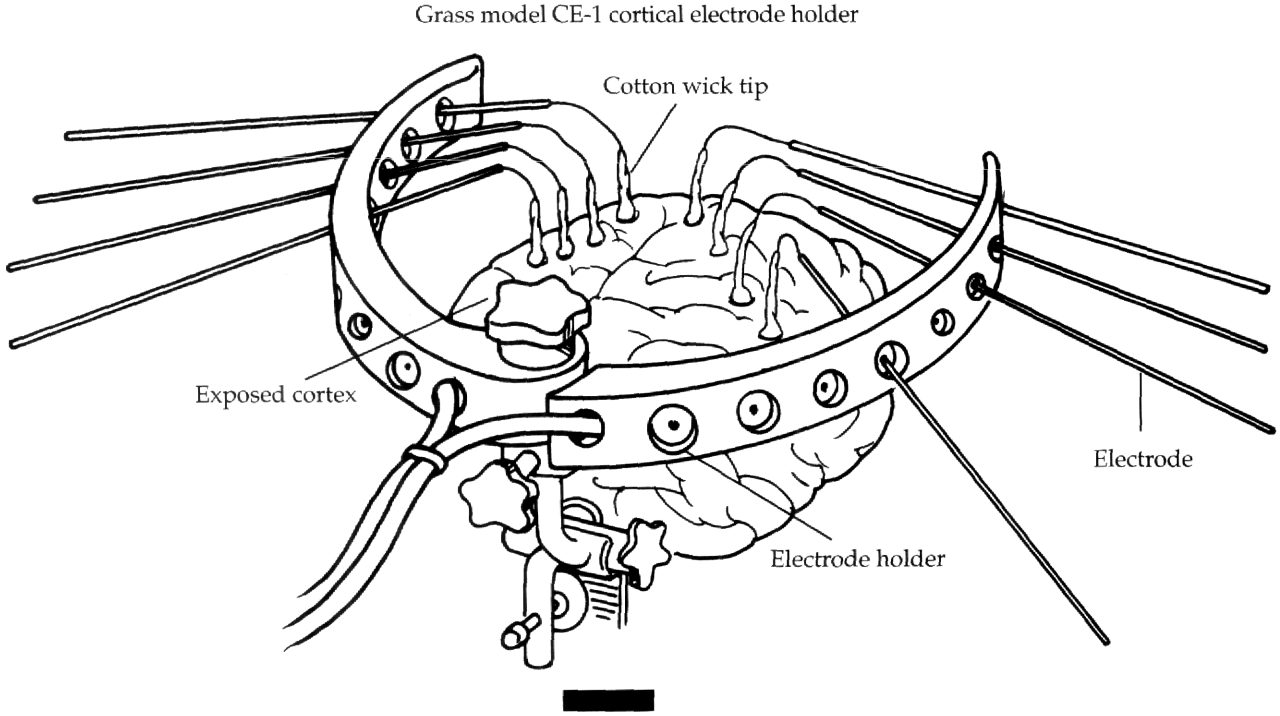

- **Subdural strips and grids** - These arrays of flat, 3 mm platinum or stainless steel discs are spaced 1 cm apart (on center) and imbedded in a sheet of plastic. The arrays are implanted directly on top of cortical regions of interest. Commonly used configurations include eight-by-eight grids (64 electrodes) and two-by-eight strips (16 electrodes), though other configurations are available. Grids and strips can be placed over many regions of clinical interest, including inferior frontal and basal temporal structures and in the interhemispheric fissure. Subdural electrodes are frequently used to conduct brain stimulation studies, to localize cerebral function, and to monitor a variety of EPs. Movable subdural grids have replaced arrays of cotton wick electrodes in electrocorticography in many institutions (Figures 2.13 and 2.14).

- **Epidural electrodes** - These sterilized peg or disc electrodes are implanted in the epidural space for monitoring. Their placement is slightly less invasive than the subdural electrodes, but the range of their placement is limited and they are not usable for brain stimulation because stimulation next to the dura usually causes pain.

2.3 *Impedance Checking*

The impedance of each electrode measures the quality of contact between the electrode and the tissue from which it is recording. High impedance indicates poor conductance of EEG signals. Impedance checking is used to determine which electrodes must be reapplied by the EEG technician. High-impedance electrodes detect low-amplitude noise signals more readily and are more likely to distort physiological signals. Accepted EEG standards require all electrode impedances to be checked at the beginning and the end of each recording and periodically when extended EEG recording is necessary (e.g., for hours or days at a time).[12] This accomplished through the electrode test switch which passes a small alternating current through each electrode and into the recording system (0.035 μA, 30 Hz sine-wave in the Grass Model 8 EEG machine). This small test current passes through the patient, but is felt to be too small to have any physiological effect, even when using intracranial electrodes. In most cases, the goal is to have impedances of less than 5,000 Ω, though in certain circumstances impedances of 10,000 Ω are acceptable if the impedances are similar in all electrodes paired together. In scalp recording, high electrode impedances may often be corrected by cleaning the skin with an abrasive cleaner, applying a new layer of conducting paste, or replacing the electrode. Other causes of high impedance include broken or frayed wires, faulty connectors, and machine malfunctions. High impedance in invasive electrodes usually relates to poor tissue contact, often because of suboptimal electrode placement or blood or other tissues or fluids interfering with the electrode-tissue interface. These problems are often not repairable without removing and replacing invasive electrodes, such as depth wires or subdural grids. Figure 2.15 shows the appearance of the output from sample electrode test channels with normal and high-resistance electrodes.

2.4 *Instrumentation*

Figure 2.16a illustrates a modern EEG machine with both analog and digital components (digital EEG is discussed below). Electrodes are electrically coupled to the brain or scalp by the appropriate conducting interface, as described above. They then plug into a jackbox

Figure 2.15 — Electrode test and EEG with high impedance channels.

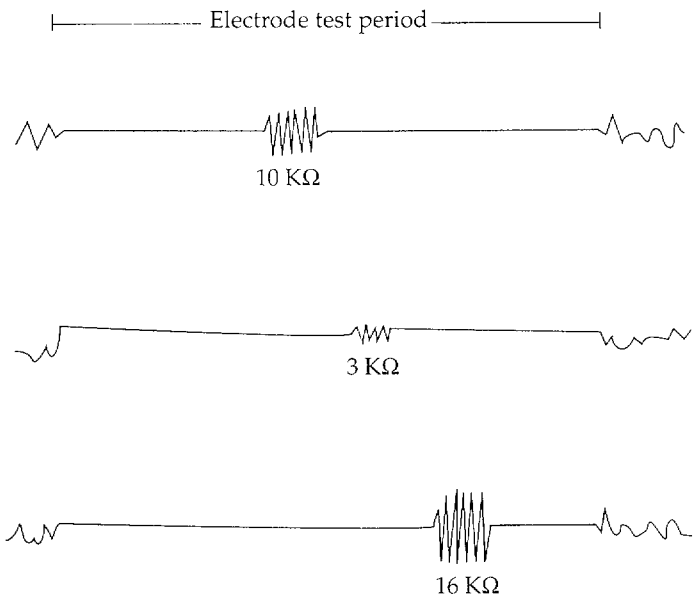

(also called a headbox) which conducts EEG signals to the EEG machine through a large multiconductor cable. Figure 2.16b depicts an analog 10 channel Grass EEG machine, one of the industry's standards in analog technology.

2.4.1 Montages

EEG electrodes are arranged on the scalp according to a standard, known as the 10-20 system, adopted by the American EEG Society.[12] This system calls for placement of electrodes at distances of 10% and 20% of measured coronal, sagittal, and circumferential arcs between landmarks on the cranium (Figure 2.17a). Electrodes are named according to their position on the head: Fp for frontal-polar, F for frontal, C for central, P for parietal, T for temporal, O for occipital. Odd numbers refer to electrodes on the left side of the head, even numbers to those on the right, and Z denotes midline electrodes. One electrode is labeled isoground and is placed at a relatively neutral site on the head, usually the midline forehead. A new montage convention has recently been introduced in which electrodes are spaced at 5% distances along the cranium. These electrodes are called closely spaced electrodes and have their own naming convention (Figure 2.17b).

EEG signals are transmitted from electrodes to the headbox, which is labeled according to the 10-20 system, and then to the montage selector. The montage selector on analog EEG machines is a large panel containing switches that allow the user to select which electrode pairs will have signals subtracted from each other to create an array of channels of output called a montage. Each channel is created in the form of the input from one electrode (called grid 1) minus the input from a second electrode (called grid 2). Montages are either

Figure 2.16 — (a) Schematic diagram of EEG machine.
(b) Grass EEG machine.

(a)

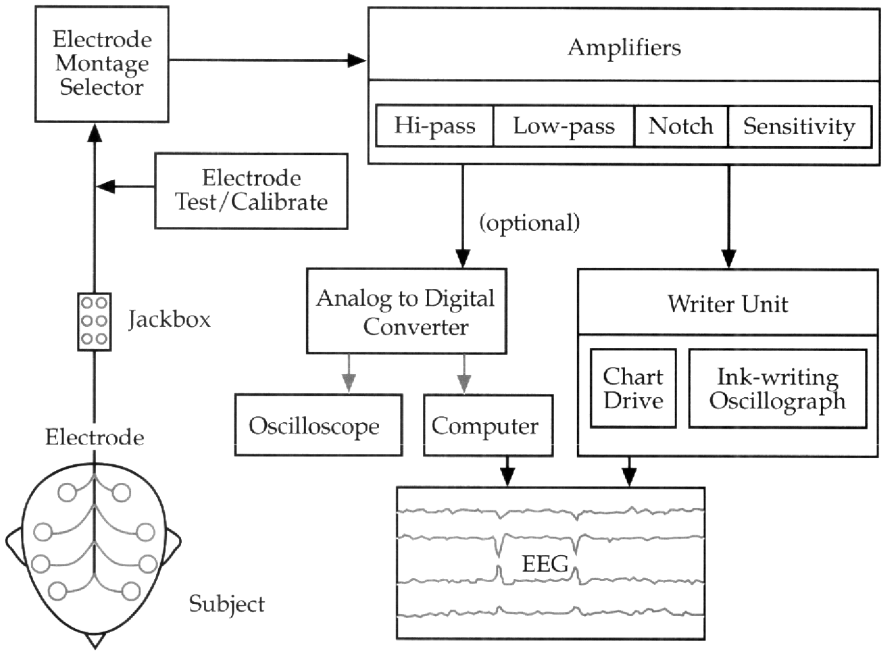

(b)

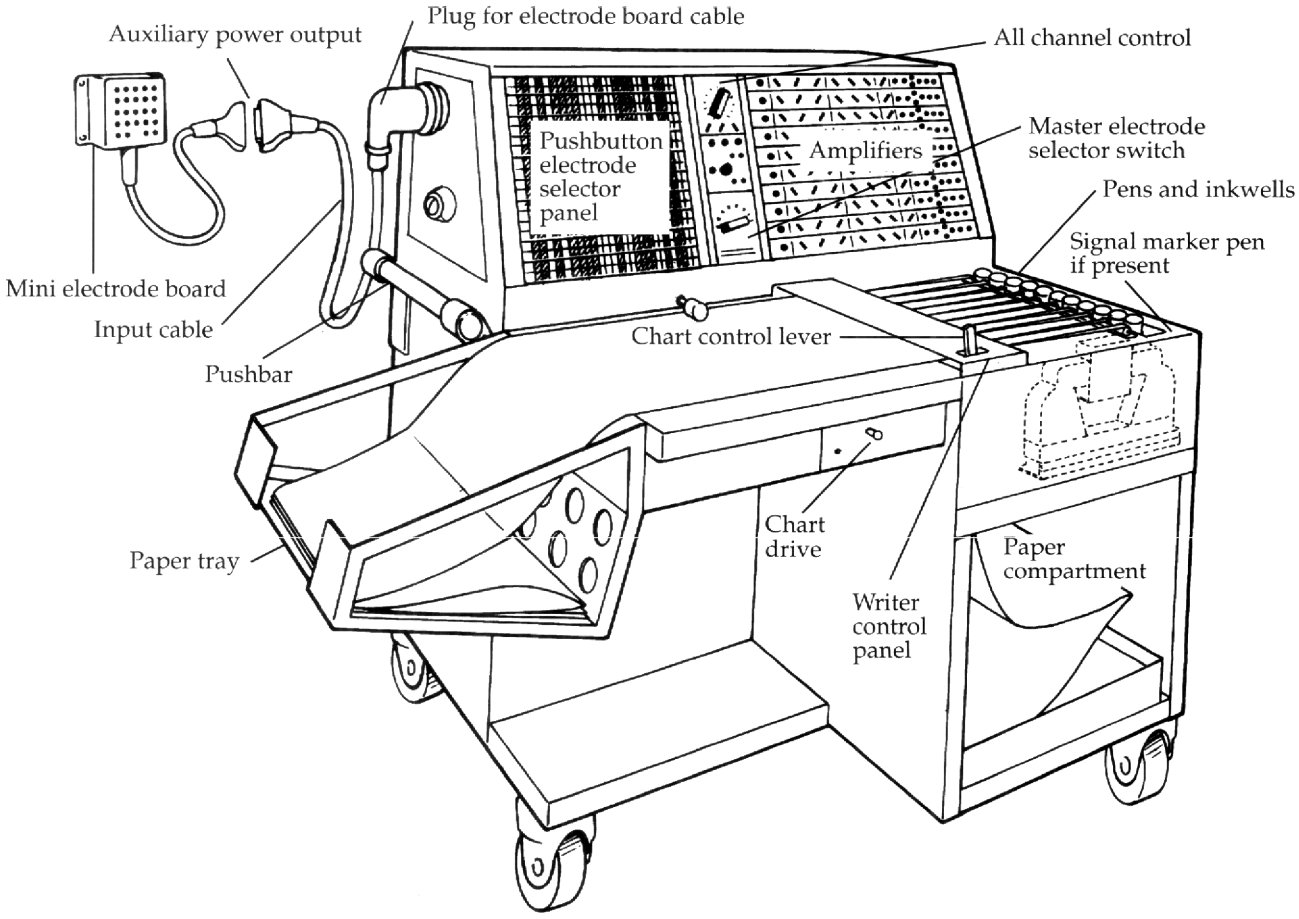

Figure 2.17 — (a) 10-20 system diagram. (b) Closely spaced electrodes.

(a)

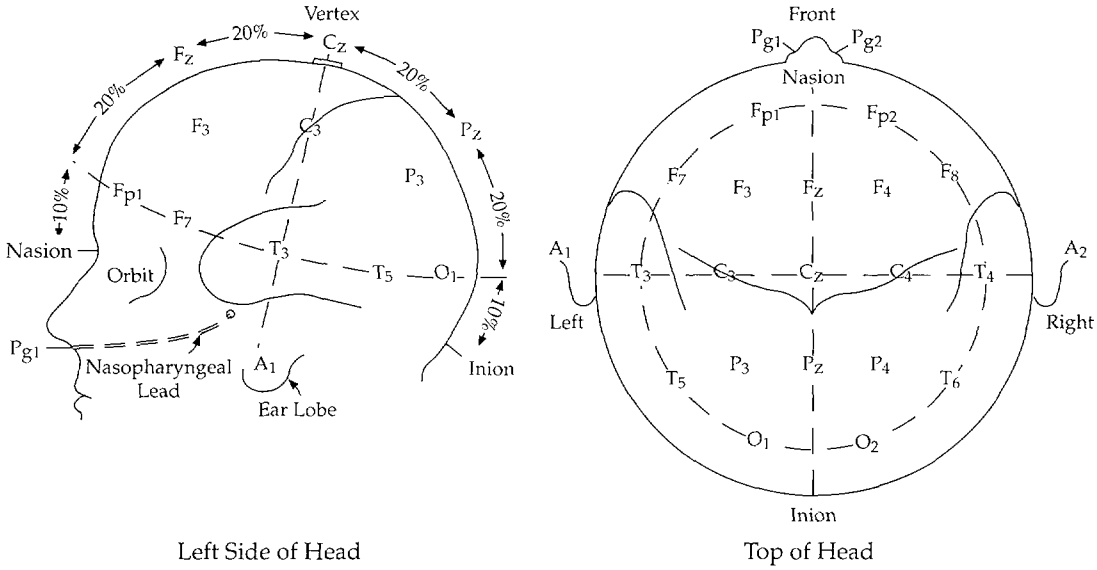

(b)

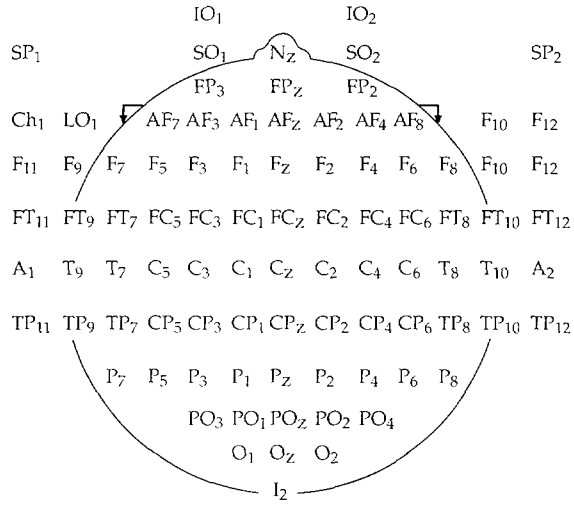

bipolar (made by the subtraction of signals from adjacent electrode pairs) or referential (made by subtracting the potential of a common reference electrode from each electrode on the head). In order to minimize noise, a separate reference is often chosen for each side of the head; for example, the ipsilateral ear. Bipolar and referential montages contain the same basic information that is transformable into either format by simple subtraction as long as all electrodes, including reference, are included in both montages and linked to one common reference. Many modern digital EEG machines record information referentially, allowing easy conversion to several different bipolar montages. Figure 2.18 shows some standard montages that may be mixed together for EEG recording. Figure 2.19 shows an example of remontaging, changing 16 channels of EEG channels between bipolar and referential montages.

The advantage of recording EEG in several montages is that each montage displays different spatial characteristics of the same data; e.g., how the potentials compare on the right versus left sides of the head or front to back. Referential montages best illustrate how a given potential is distributed over a large area of the scalp. The waveforms in each channel appear similar in this montage, but amplitudes vary with position. Peak activity can be localized to the channel in which the amplitude of activity is maximal. (Note: Amplitude is used here as a rough estimate of the gradient of the field mapped over the scalp. The potential is maximal where the peaks of the gradient fields are located.) Careful selection of the reference electrode is vital to good recording. If it is near the EEG activity of interest, the reference is said to be active or contaminated. All channels in the montage record the activity prominently, making localization difficult. Some disadvantages of referential recording include the fact that no single reference is appropriate for every situation. The recording montage must be changed, at times, depending upon what is being recorded. If the reference electrode is of high impedance, improperly placed, or disrupted, all of the EEG data for that montage is lost. Some adjustments used by electroencephalographers to minimize reference effects on the EEG include the placement of noncephalic references, common average references (taken by averaging the signals from all electrodes in the montage), weighted average references, and placement of the reference electrode at particular quiet sites, such as the mastoid processes, nose, or ears.

Bipolar montages measure the gradient of electrical potential on the head and aid in fine localization. For example, a bipolar montage may demonstrate exactly between which two electrodes the peak of potential is located. When the peak of potential passes beneath a bipolar chain of adjacent electrodes, a change in polarity and a phase reversal occur. These changes consist of a positive deflection in one channel and a negative deflection in an adjacent channel. The peaks of activity in each channel point at each other, localizing the peak of potential to the electrode in common between the two channels. For an example of a phase reversal localizing an epileptiform discharge, see Figure 2.30b, where the phase reversal over the F7 electrode identifies this region as the focus at the discharge. Standard EEG recordings should contain at least one section recorded in a longitudinal bipolar montage, one section in a transverse bipolar montage, and one section recorded in a referential montage. Examples of some standard montages and their output for a sample signal are displayed in Figure 2.19.[13]

Figure 2.18 — Electrode arrays commonly put together to form standard montages.

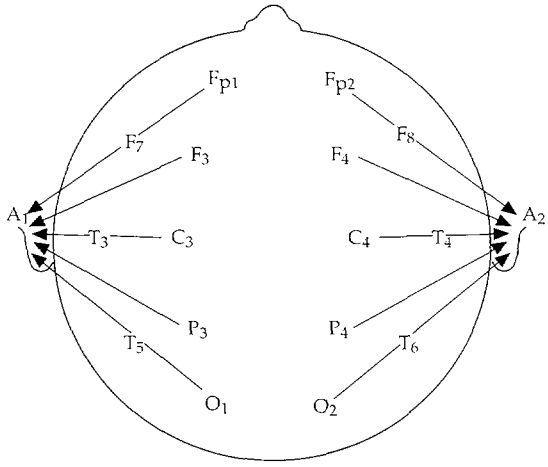

Referential

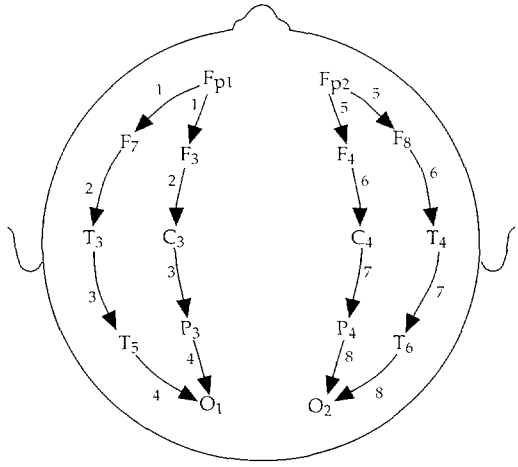

Longitudinal bipolar

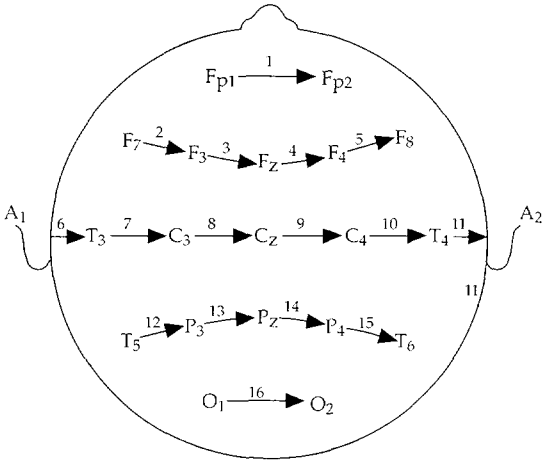

Transverse bipolar

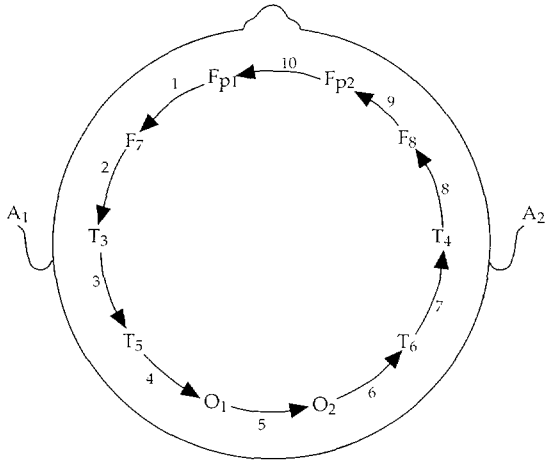

Circular bipolar

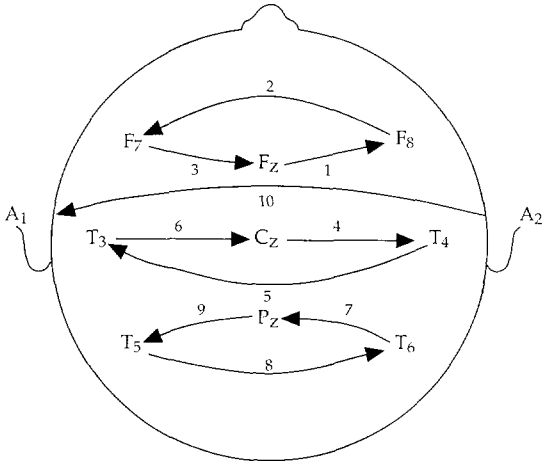

Transverse bipolar

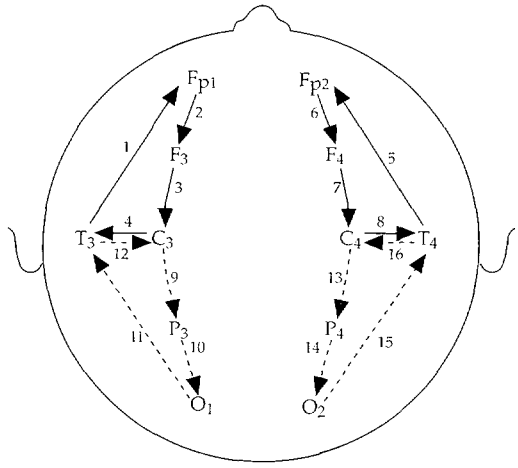

Bipolar–longitudinal and Gray-Walter montage elements

2.4.2 Amplifiers

Electrode signals are conducted to EEG amplifiers from the montage selector. The amplifiers are multicomponent devices that perform several important functions. First, the pair of electrodes set up in the montage selector panel are actually subtracted, with the resulting signals sent to an amplification stage that multiplies the voltage of the input signal. The amount of amplification is measured as the ratio of output voltage to the input voltage (V_{out}/V_{in}). Referred to as the gain of the amplifier, this is measured in dB. Gain in dB is defined as = $20 \times \log (V_{out}/V_{in})$. A tenfold amplification would then be equal to a gain of 20 dB. Since EEG amplifiers are differential amplifiers (they subtract two input signals and amplify their difference), a more important measure of their amplification is the common mode rejection ratio, or CMRR. The CMRR is defined as the amplification of the difference input divided by the amplification of the common input. It is measured by putting a signal into one input of the amplifier, with the other input connected to ground, and dividing this amplitude by the amplitude of the output voltage when the same signal is put into both amplifier inputs. Quality EEG amplifiers have CMRRs of greater than 10,000. CMRRs of 100,000 or more are common in other types of biological amplifiers. Amplifiers also have a dynamic range, that is a range of voltage that they can amplify and still faithfully reproduce variation in the signal. Voltages below the dynamic range will be lost in amplifier noise. Voltages higher than the dynamic range will saturate amplifiers, causing distortion in the signal and perhaps damage to the amplifiers. Typical CMRR amplification gains for EEG machines range from 5,000 to 100,000. Most electroencephalographers speak of amplifier gain in relation to its sensitivity to the EEG signal, measured in either mV/cm or μV/mm. The standard sensitivity for adult recordings is usually 7 μV/mm. Maximum sensitivity on standard EEG machines is 1 μV/mm.

After amplification, the signal from each channel is then passed through a voltage divider circuit that further adjusts the amplitude of the signal according to the settings of the sensitivity switch for each channel. The settings on these switches are altered by EEG technicians as necessary during recording so that tracings from individual channels are large enough to read easily but not so large that they run into the tracings of adjacent channels or clip the signal. As the sensitivity is set lower, the amplitude of the signal output to paper or computer screen is increased. Figure 2.20 shows a schematic of the voltage divider circuit used in standard EEG machine sensitivity switches. Figure 2.21 demonstrates the effect of changes in sensitivity on a typical EEG tracing.[7]

2.4.3 Filters

After amplification, each channel of EEG is passed through a series of filters designed to reduce sources of noise and artifact while sparing clinically important information as much as possible. Filters are made from combinations of resistors, capacitors, and, sometimes, using amplifiers as active filters. Typical EEG filters remove low frequencies (high-pass filters), high frequencies (low-pass filters), or specific frequencies (notch filters). Filters are defined by a number of characteristics, such as cut-off frequency (the frequency at which input amplitude is reduced by approximately 30% at output), roll-off [how "steeply" the filter attenuates input as a function of frequency (measured in dB octave)], and the filter frequency response curve (how the filter response varies with frequency). Basic principles of filters are shown in Figure 2.22. EEG filters should minimize amplitude and phase distortion. One such filter design, a Butterworth filter, is often used.

Figure 2.19 — Vertex waves in stage II sleep in several different montages (Sen = sensitivity, LF = low frequency setting, HF = high frequency setting, Notch-Out = notch filter is off, PS = paper speed in mm/sec).

(a) Transverse montage

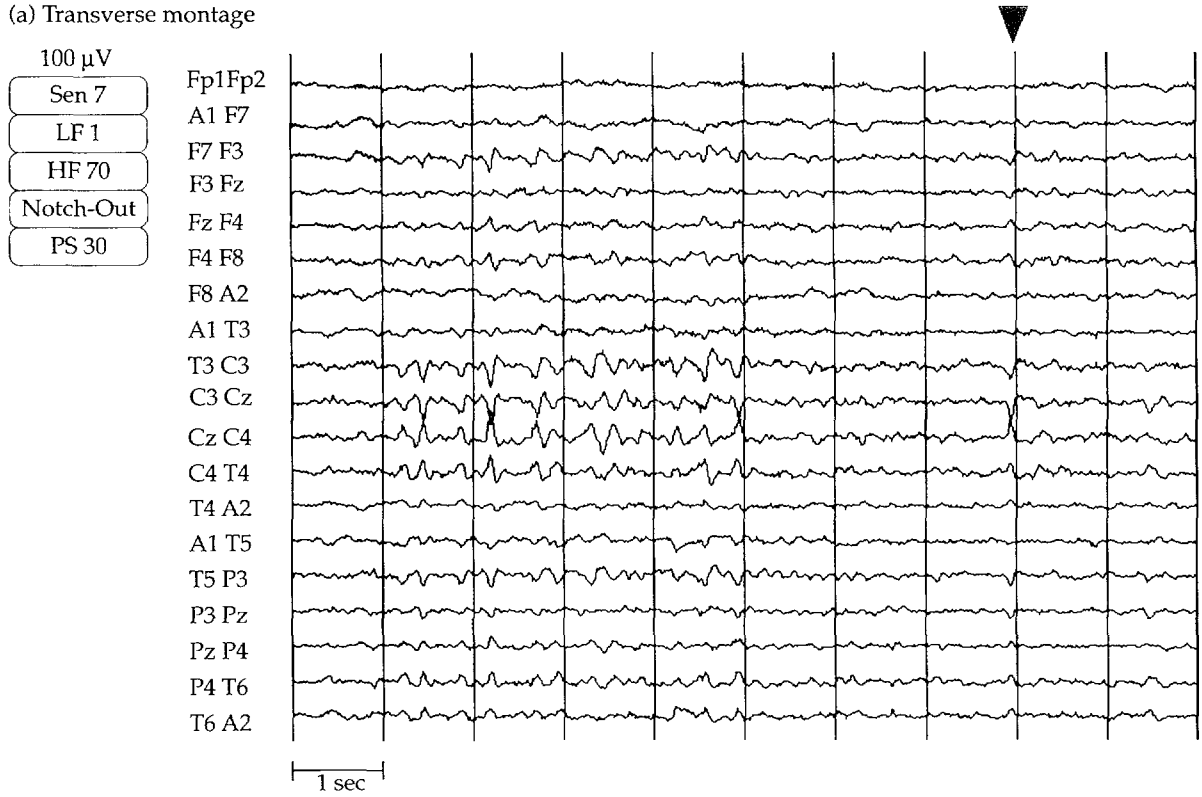

(b) Referential montage

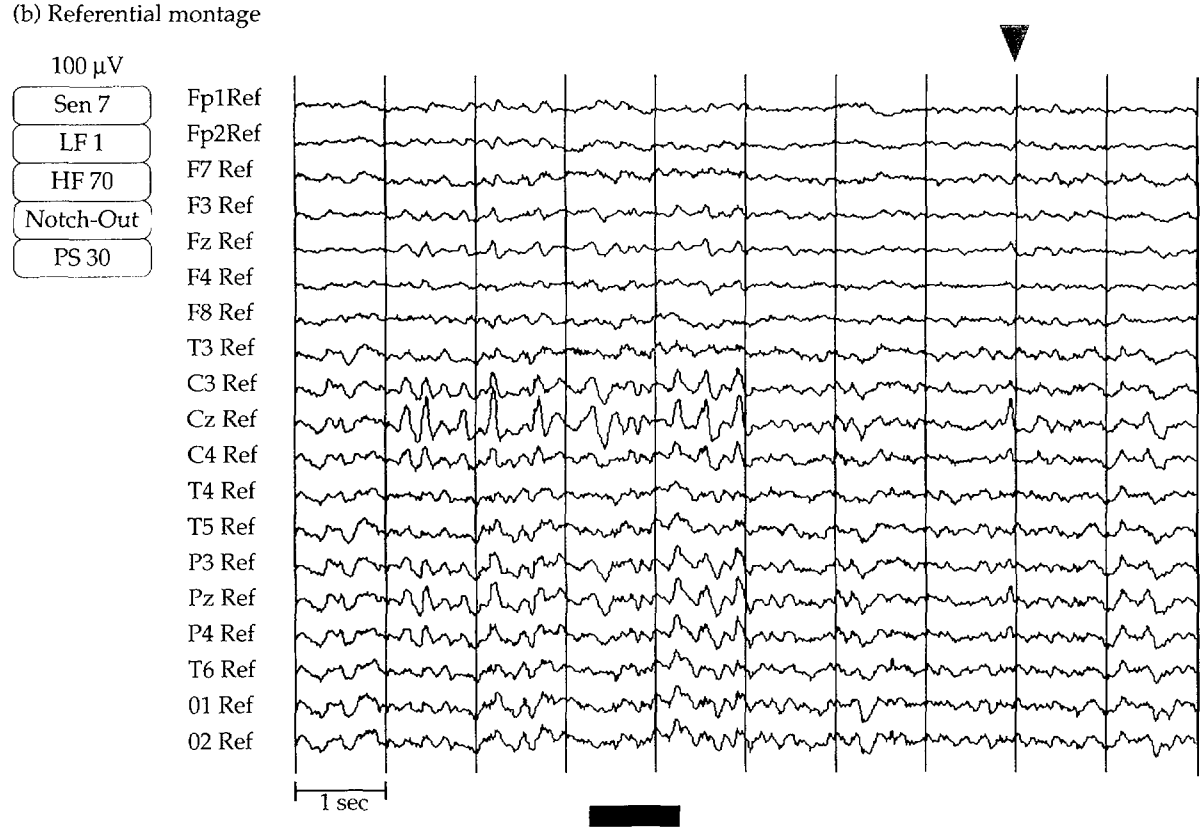

Figure 2.19 — continued

(c) Long itudinal bipolar montage

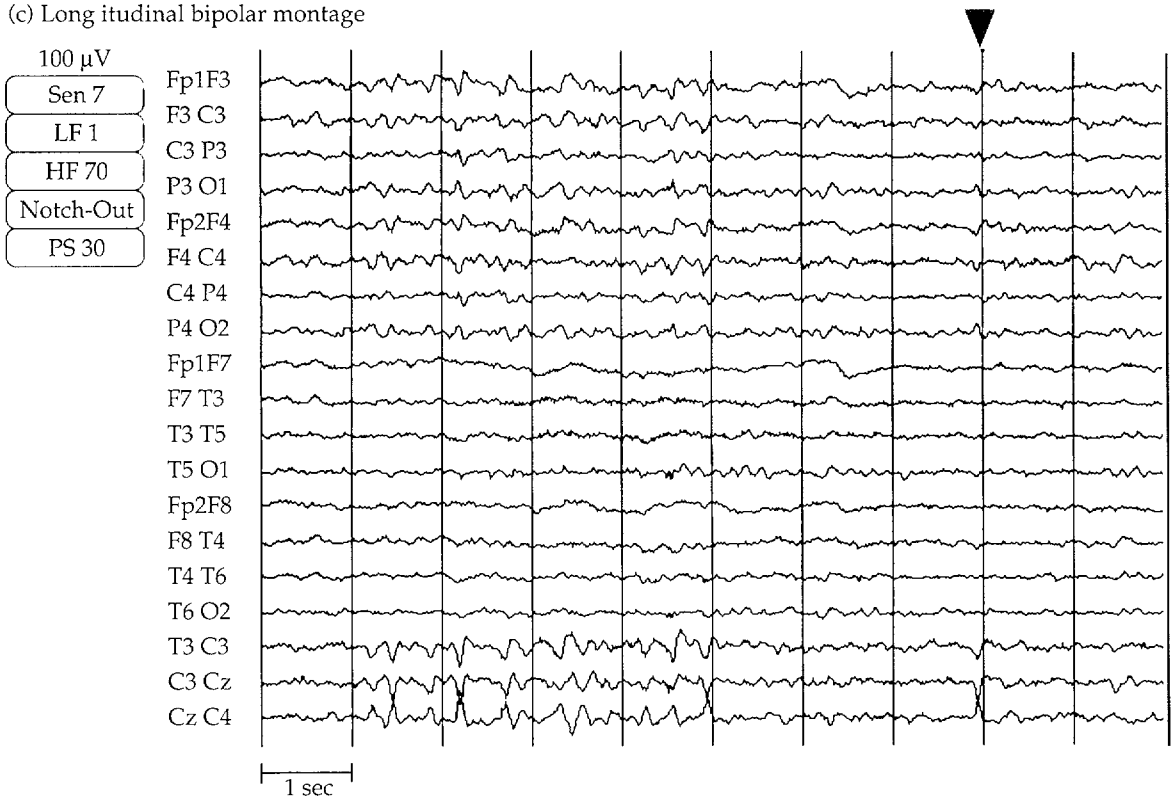

(d) Unipolar montage

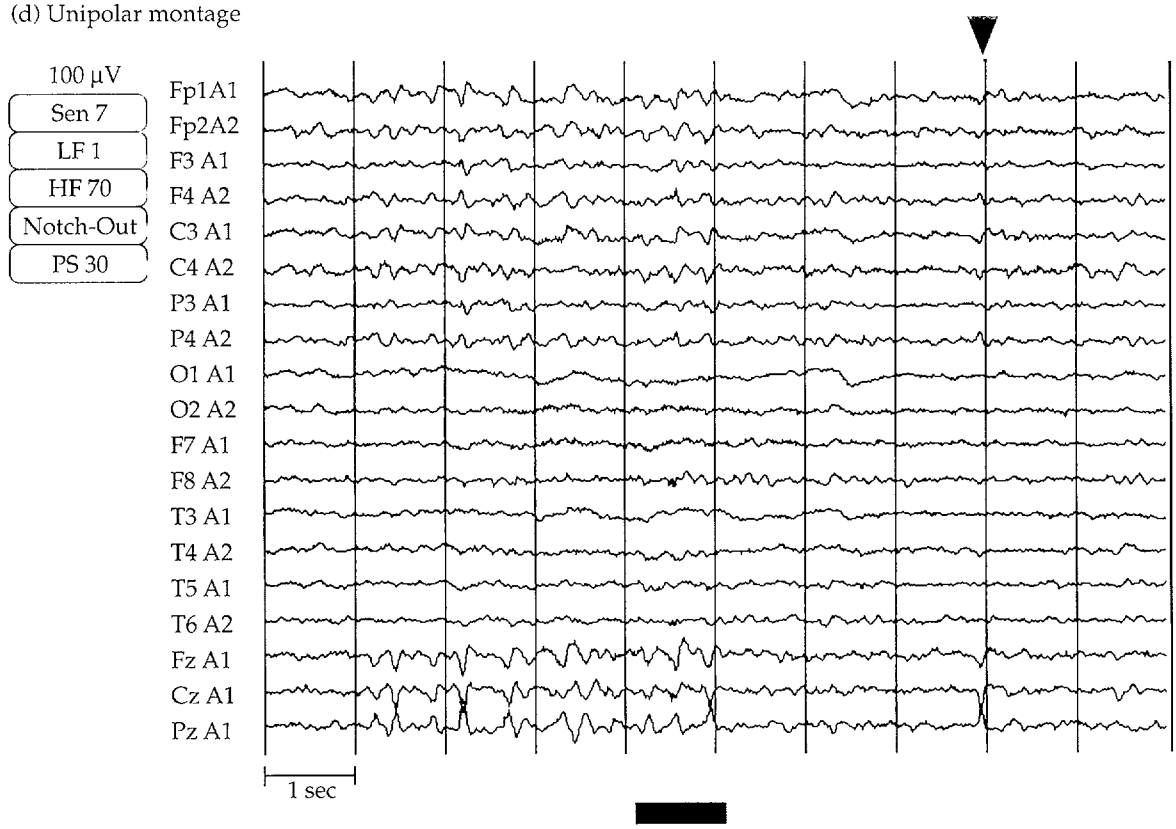

Figure 2.20 — Voltage divider circuit, used in the EEG machine sensitivity switch.

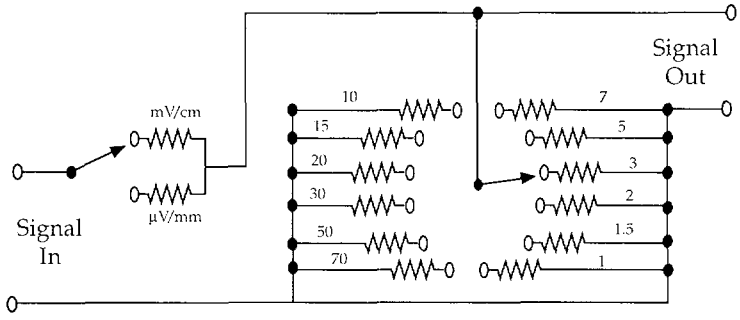

Figure 2.21 — Same EEG with different sensitivities.

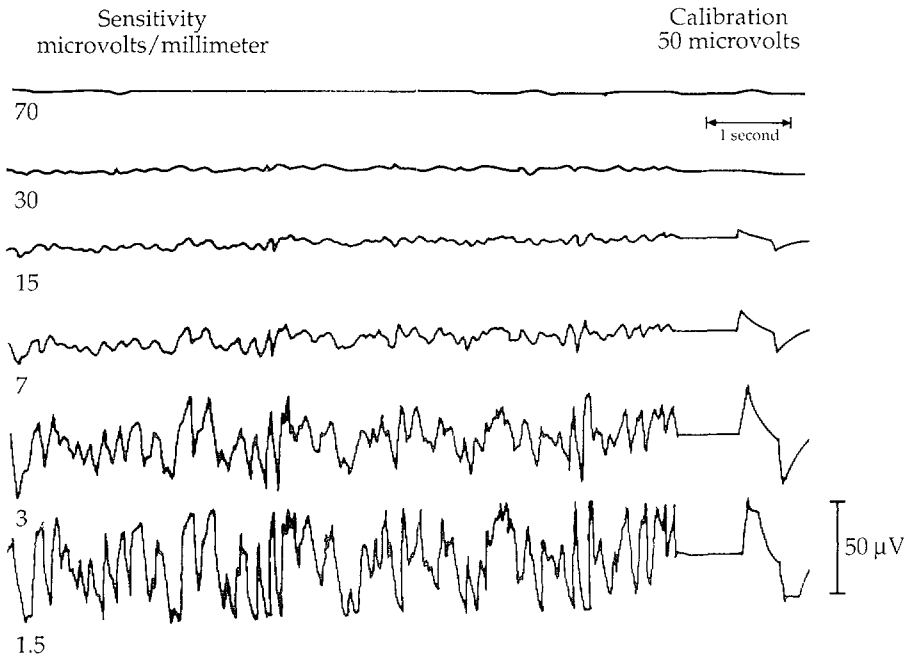

Filter settings are very important to the recording and interpretation of the EEG. For example, low-frequency oscillations from sweat artifact can be filtered out by low-frequency filtering (e.g., 1.0 Hz low-frequency cut-off). High-frequency muscle artifact can be reduced by high-frequency filtering (e.g., high-frequency cut-off at 35 Hz). The 60 Hz interference from power lines can be minimized by turning on the 60 Hz notch filter.

Improper filter settings can filter out vital information. For example, seizure discharges can be filtered out if high-frequency filters are set to remove muscle artifact. Filters shift EEG signals in time (phase shift), which may be important when trying to line up peaks in the EEG tracing. Typical low-frequency filters, depending upon the type of filter design used, advance a sinusoidal input signal by about 1/8 of a cycle at the cut-off frequency (phase shift of pi/4 or 45 degrees), and similar standard high-frequency EEG filters cause a delay of 1/8 of a cycle at the cut-off frequency (Figure 2.22d).[6] Figure 2.23

Figure 2.22 — Basic principles of filters: (a) low pass filter. (b) high pass filter. (c) effects of time constant. (d) effects of different filters (square waves and sine wave). (e) frequency response curves of typical EEG filters.

(a)

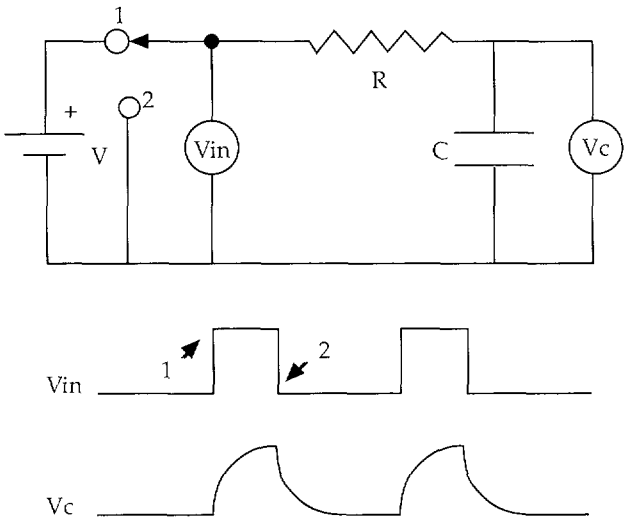

(b)

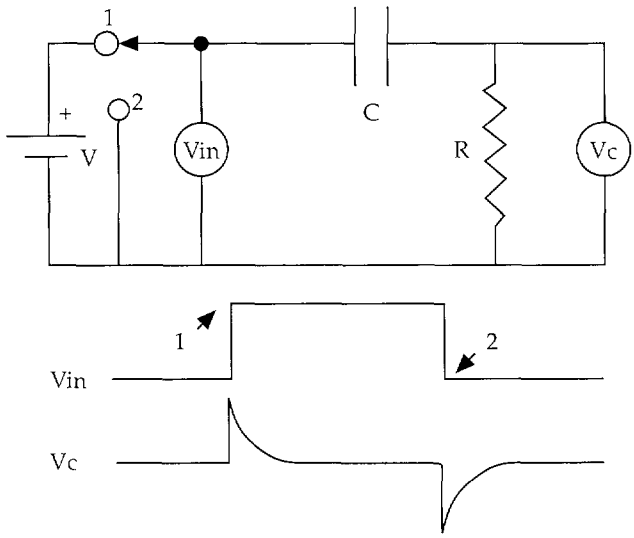

(c)

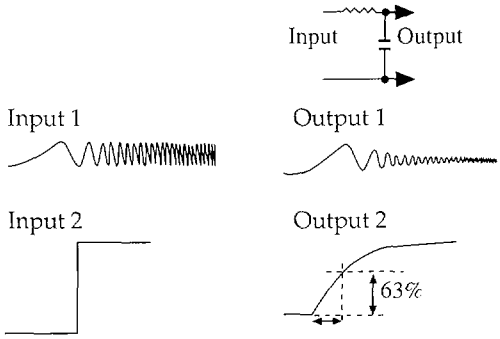

(d)

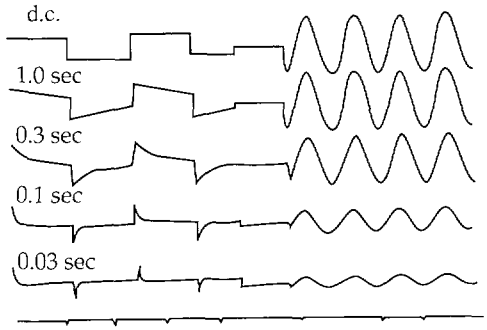

(e)

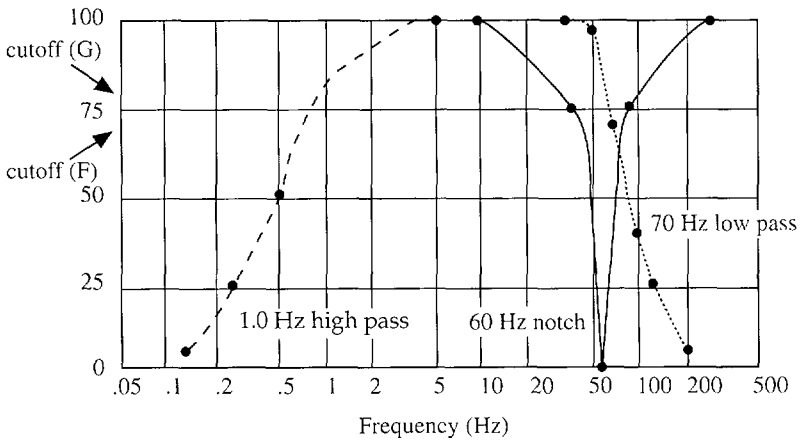

Figure 2.23 — Filtering effects on a section of EEG.

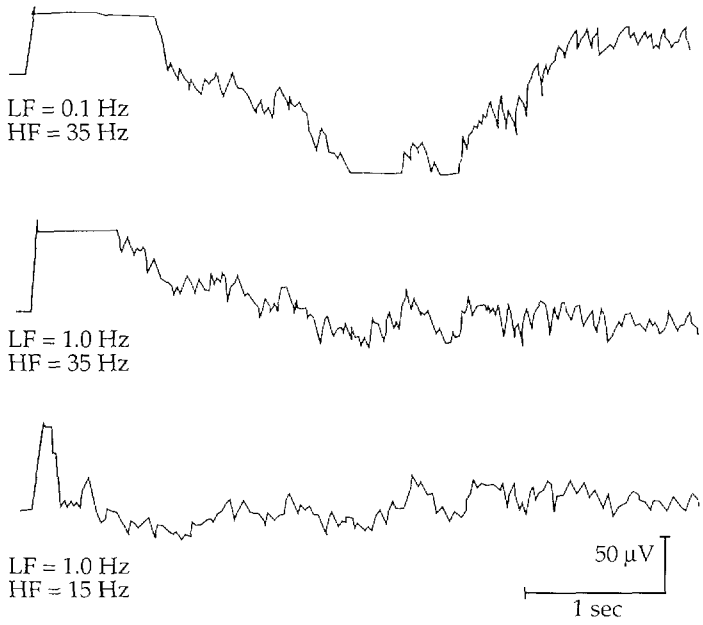

Figure 2.24 — Calibration test.

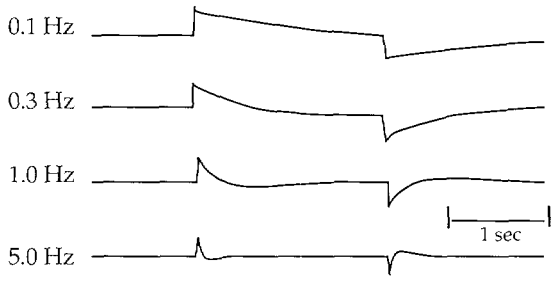

demonstrates some effects of filters on sample EEG output. The typical frequency range of standard EEG machines is from 0.1 Hz to 70 Hz, though newer machines allow the detection and filtering of frequencies up to several hundred Hz. This may have importance in some intracranial recordings. Another common artifact produced by filters is ringing. This comes from oscillations in filter output when subjected to sufficiently sharp inputs. These inputs provoke damped oscillations that can be mistaken for rhythmic brain activity.

2.4.4 Calibration

To ensure proper filter settings and uniform response, a calibrated square-wave input is sent through each channel via a built-in circuit. Calibration is performed at the beginning and end of each record, ensuring that the technician and reader set correct filters and sensitivities and that the pens are properly aligned. Figure 2.24 shows the same 50 μV calibration signal passed through four different frequency filters. Calibration is still performed in newer digital EEG machines. However, this is often performed by internal software using a known calibration signal.

2.4.5 Chart Recorders

After filtering, montaged EEG signals are then output to a strip chart recorder that consists of a series of pivoting pens coupled to galvanometers, one set for each channel, that move up and down in a smooth, continuous (analog) arc in response to voltage changes. Pens print EEG onto standard paper that, when run at the standard speed of 30 mm/second, displays 10 seconds of EEG per page. The paper has dark vertical lines marking each second at this standard speed and lighter vertical lines marking every 200 ms. The EEG convention is to record positive voltage changes as downward waves and negative voltage changes as upward waves. Strip chart recorders also have a frequency response limited to approximately 90 Hz, due to a fixed mechanical response time of the pens and because the pens move in an arc rather than up and down. A number of artifacts may result from these limitations; for example, an arc is printed on paper rather than a vertical line in response to a very fast change in voltage.

2.5 *Digital Electroencephalography Technology*

With the widespread use of high-speed digital technology and analog-to-digital converters (A - D converters), analog EEG technology is rapidly being overtaken by digital computers. Digital EEG allows quantitative manipulation of EEG data, permits flexible filtering and multiple montages to be employed for a single data set, and employs frequency analysis and powerful data display, such as topographic display of EEG power spectra.

The first generation of digital EEG machines are essentially the same as analog machines up to the point at which the electrical signal is sent to the strip chart recorder. At this point, signals are passed to an A–D converter. This device samples the voltage and holds a numerical value for each channel many times per second (first-generation devices sample around 200 samples per second or 200 Hz) and then stores the numerical value for the voltage at each time on a computer storage medium, such as a hard disk drive, floppy disk, optical disk, or magnetic tape. Analog to digital converters are usually available as circuit boards that plug into most commercially available computers. They are distinguished by their design for data sampling, the number of input channels, the resolution of each channel, and the throughput of the converter. Strategies for data sampling range from boards that sample each channel in turn, and stagger them in time (it takes at least a few ms to collect and transfer each sample), to sample-and-hold devices which sample sequentially and then align data points in time, to devices that sample all channels simultaneously.

Converter resolution is a function of how may bits the converter uses to resolve the signal. The more bits a converter has, the higher its voltage resolution (precision). Most A–D converters have an 8- or 12-bit precision. A bit is a numerical place in the binary system. A 4-bit converter allows a numerical resolution of $\pm 2^4$. Like filters, A - D converters have a dynamic range and require that input signals be within a certain span of voltages. For example, if a 12-bit A–D converter can accept input voltages between -1000 μV and +1000 μV, it can divide the 2 mV dynamic range into 4096 segments, having a resolution of 2/4096 = 0.488 μV. This does not mean that a sinusoidal EEG signal of 0.488 μV can be resolved. The total number of samples a converter can store per second, including all channels, is called the converter throughput. For example, an A–D converter with a throughput of 10000 samples per second might be used to sample and store 10 channels of data at 1000 Hz each, or 2 channels of data at 5000 Hz each. The total throughput is the same in both cases. Throughput, usually a limitation imposed by hardware, is a function of all of the items mentioned above and the time required for a single-sample, hold-and-

Figure 2.25 — Digital sampling diagram; samples signals then shows improved resolution of simple waveform with increased sample rate.

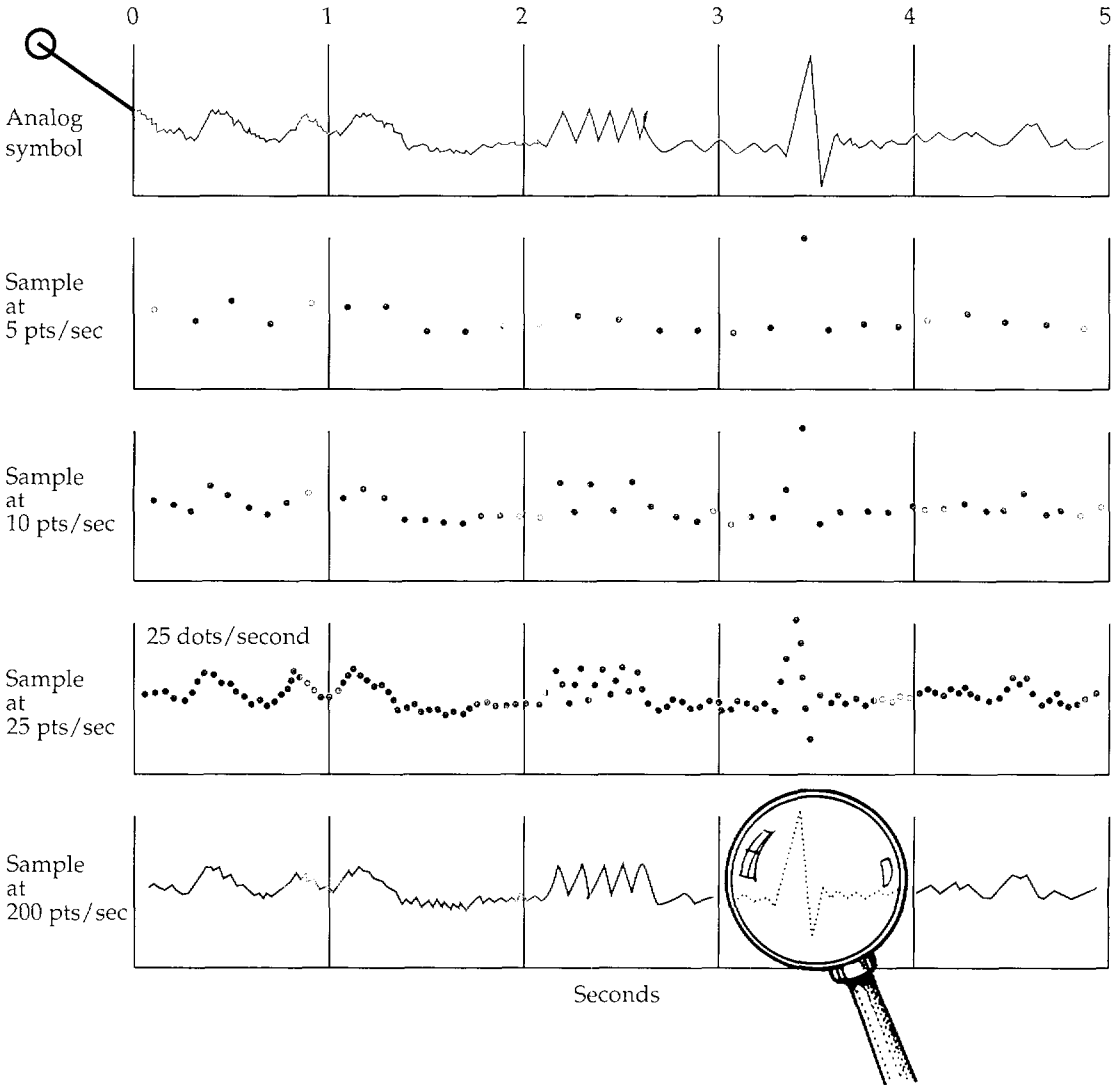

Figure 2.26 — Simple diagram of aliasing. The 80 Hz signal is sampled too slowly, giving the appearance of a 20 Hz signal when the points are connected.

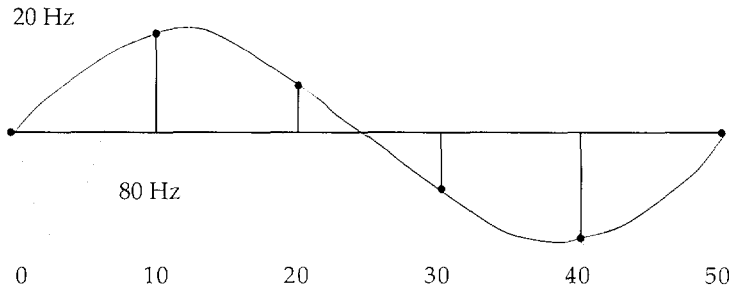

record operation. In general, the higher the throughput and the greater the precision of an A–D converter, the greater the cost. In practice, the main factor that limits the collection of information in digital EEG is storage capability. Typical digital systems store 20 channels of EEG sampled at 200 Hz per channel. This corresponds to 4000 numbers per second. If each number is represented as 2 bytes of storage, this is 8000 bytes per second. A typical 30-minute EEG would then contain $144x10^5$ bytes, or 14.4 million bytes (14.4 Megabytes) of information. Because of this storage requirement, optical or tape drive storage mediums are necessary. This points out another advantage of digital EEG: it is cheap, reliable, and does not create the enormous paper waste that results from standard paper EEG records. In addition, the high rate of data transfer from A–D hardware to computer disk storage (e.g., hard disk drive) is another factor that limits the amount of data that can be acquired per second.[14]

The most recent generation of EEG machines take advantage of very high-speed computer processing and new high-speed A–D converter technology. All signals are recorded in a referential montage using a single reference. Other montages are displayed at the push of a button, through transformation of the referential digital signal. In another improvement, digital EEG is recorded broad band, that is, with filters open to a much wider range than the usual 0.1 Hz to 70 Hz, so that signals up to several hundred Hz can be resolved. This is especially important in intracranial monitoring, where it has recently been found that, at the onset of some specific seizure patterns, substantial activity appears in the range over 100 Hz. This may give clues to the neurophysiological basis of onset of these seizures.[15] This information would be lost without the ability to digitally sample EEG signals broad band. Any required filtering to reveal clinically important phenomena can be performed with "post-hoc" digital filtering, leaving the original broad-band signal untouched.

Once EEG signals are digitized, this information can be manipulated mathematically (e.g., remontaged), before it is output to a paper strip chart recorder or plotted on the screen of a computer monitor. The EEG tracing becomes a table of evenly spaced numbers stored in a computer rather than an ink line drawn on a long sheet of paper. At standard paper speeds and magnification, the digitally sampled signal appears identical to the standard strip chart record. If the time scale on the computer display is decreased, displaying a very short period of time, the discrete nature of the digital signal, with spaces between data points, can be appreciated (Figure 2.25). When the digital signal is output to a strip chart recorder, the pens connect the closely spaced data points, eliminating the gaps between them. The pens then interpolate between the points. Computer algorithms exist that can interpolate between data points if necessary.

Several important rules exist that must be followed when digitally sampling the EEG or any other signal. Some of these rules are: 1) an adequate sampling rate must be used to resolve the signal; 2) amplifiers must have sufficient sensitivity and CMRR to detect and amplify the signal; 3) the A–D converters must have a linear response over the dynamic range of the signal; and 4) the A–D converters must have adequate resolution to faithfully reproduce the signal. The adequate sample rate, as stated in Nyquist's theorem, is a very important principle in digital EEG. Nyquist's theorem states that a given signal must be sampled at a rate of at least twice the highest frequency you wish to resolve, preferably slightly higher, to avoid distorting the signal. For example, to duplicate the standard EEG frequency range of 0.1 Hz to 70 Hz, one must digitally sample each channel at least 140 times per second. If this rule is not followed, the record may demonstrate aliasing, the display of a fraction of the high frequencies in the input signal as low frequencies, and may introduce distortion in all frequency ranges (Figure 2.26). High-frequency filters are also important in preventing aliasing because they reduce the contribution of signals above the Nyquist frequency that may be aliased by digital sampling.

Figure 2.27 — EEG components: (a) alpha; (b) beta; (c) theta; (d) delta.

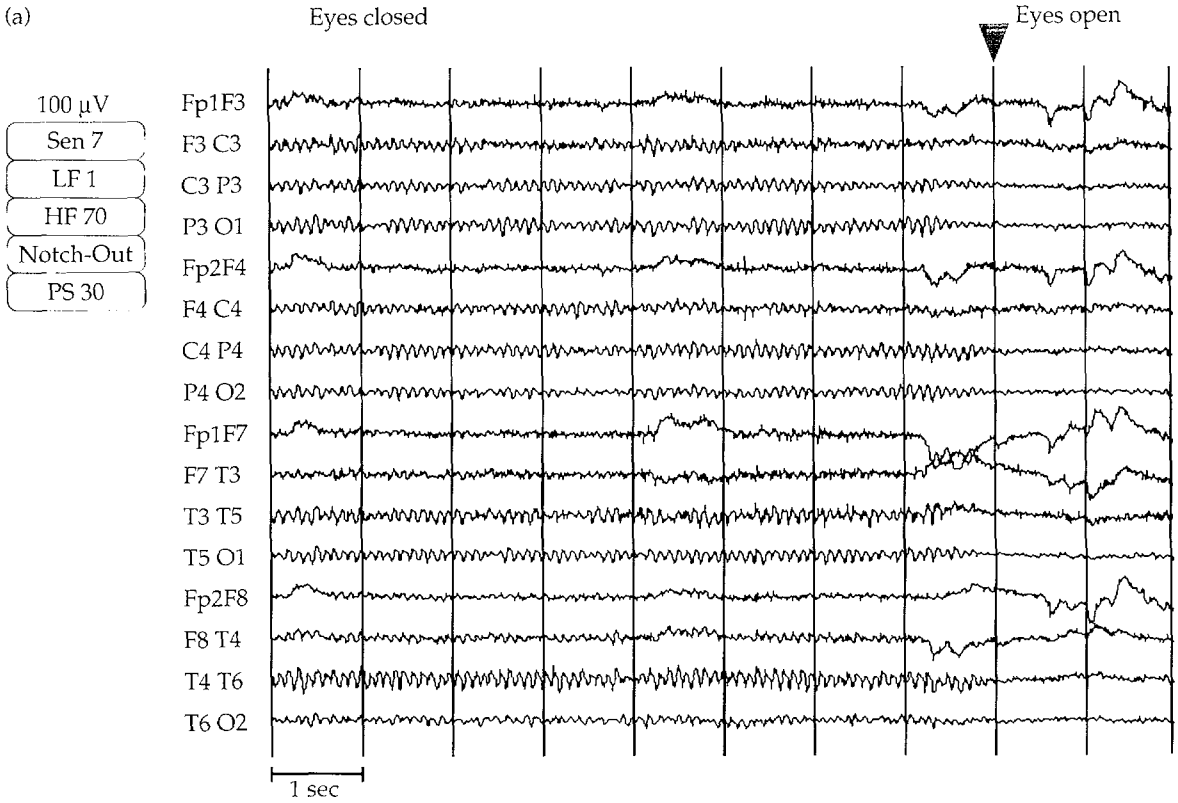

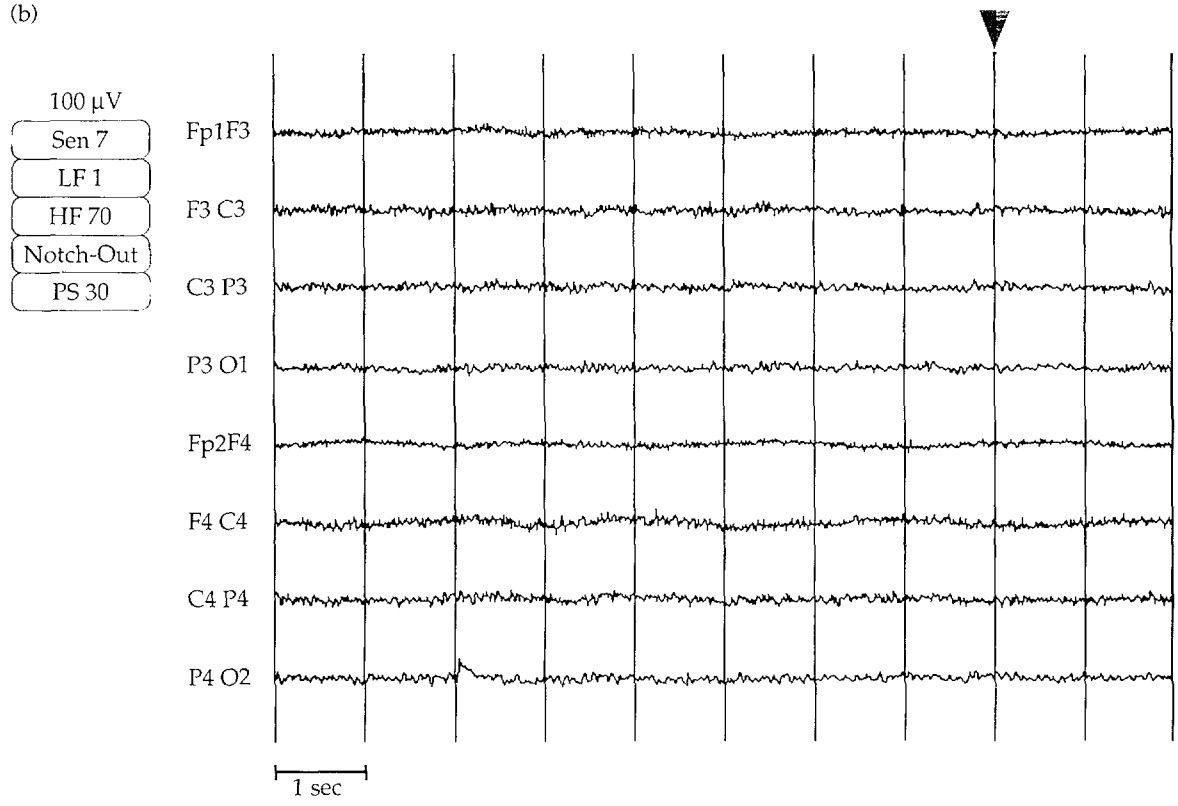

Figure 2.27 — continued.

(c)

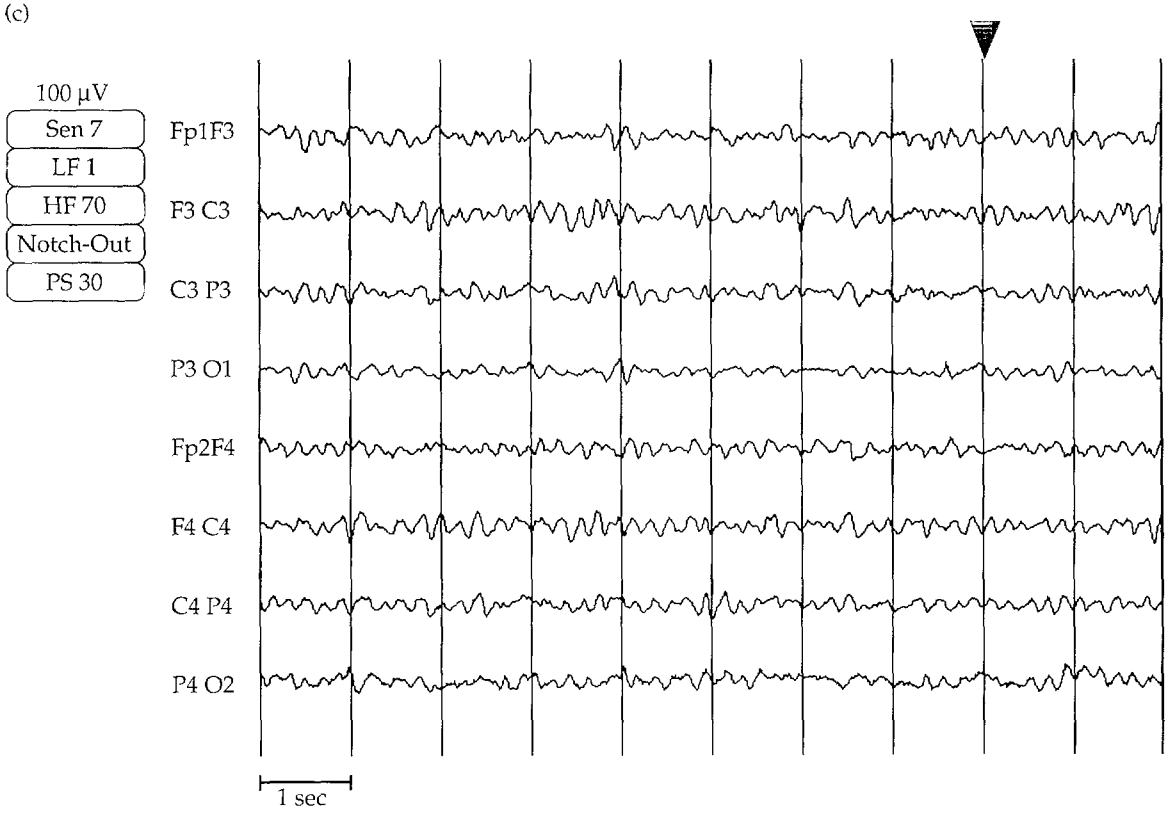

(d)

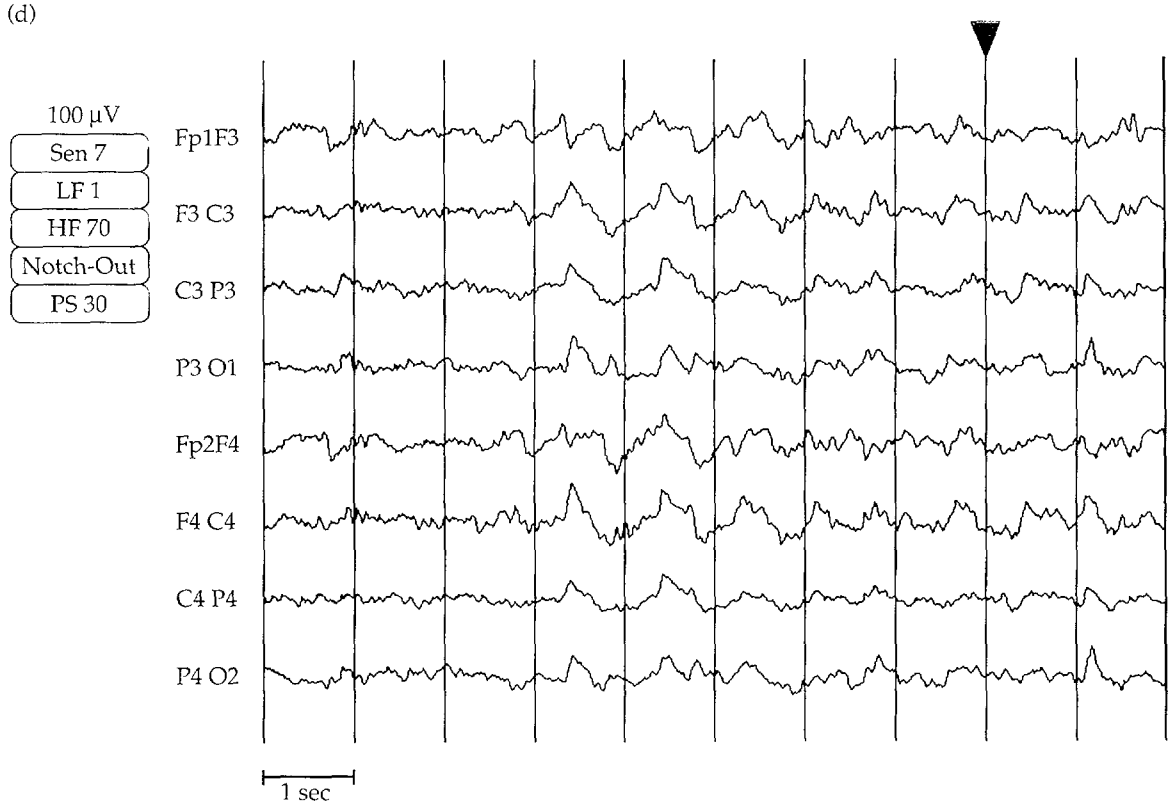

Figure 2.28— Sleep: (a) vertex wave. (b) sleep spindles. (c) k-complex: vertex wave plus spindles.

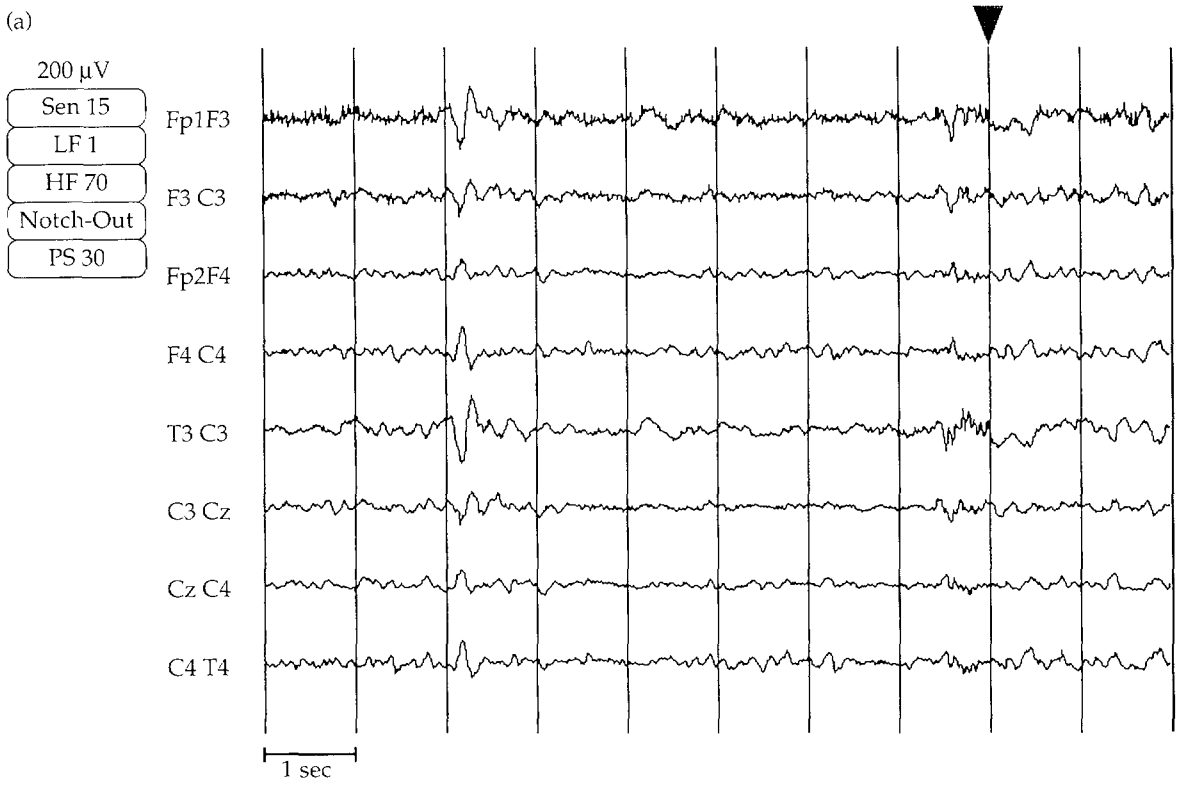

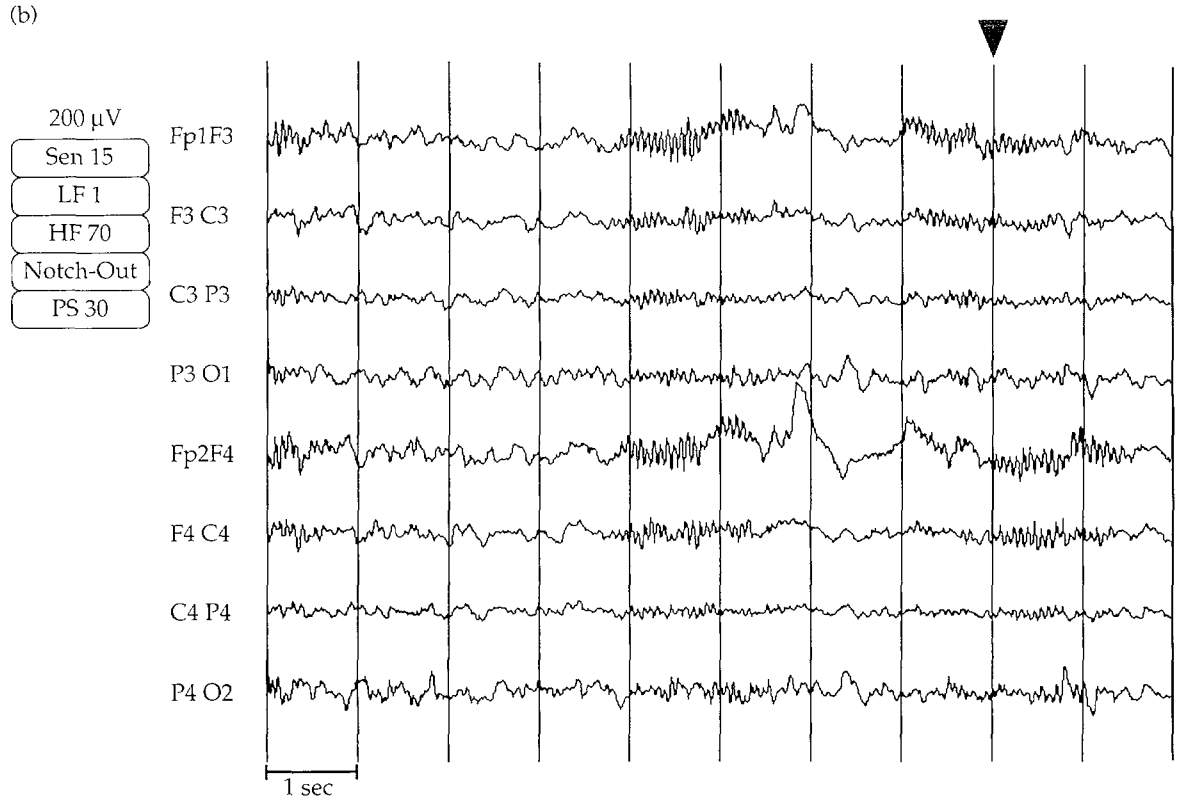

Figure 2.28 — continued.

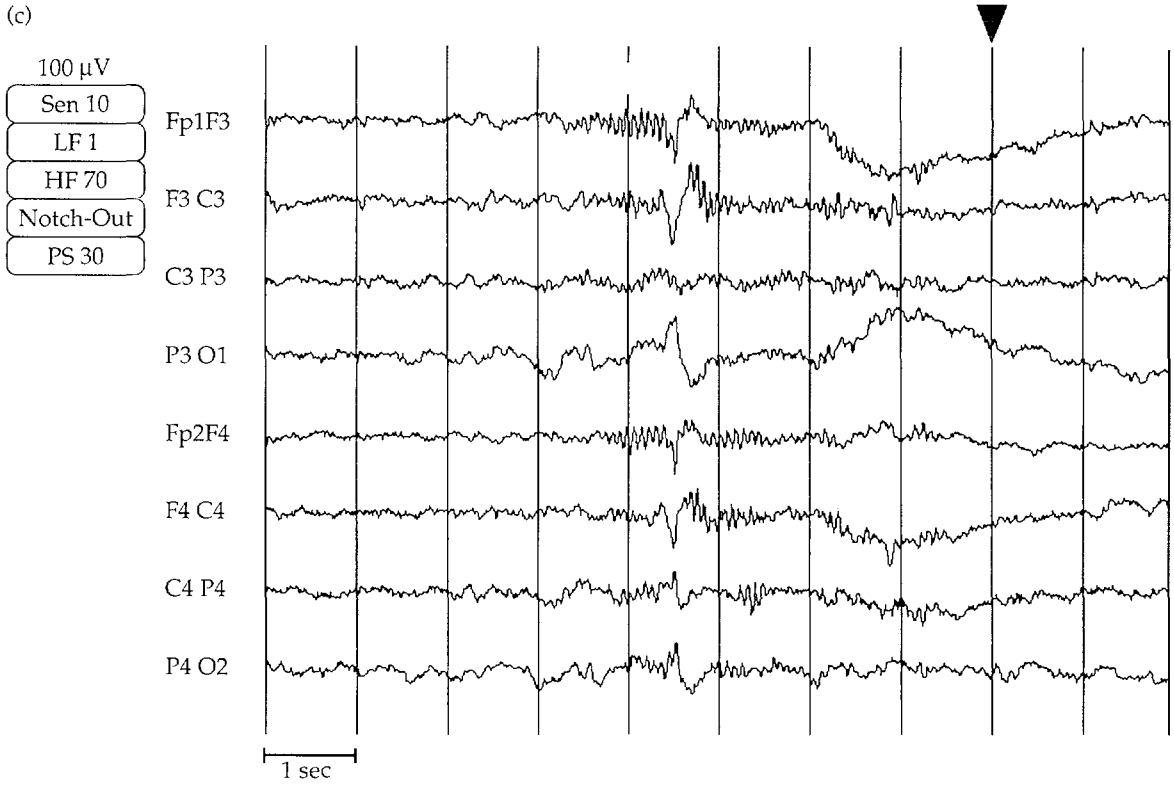

2.6 *Clinical Signals*

2.6.1 Normal Electroencephalography

Normal scalp EEG is an electrical signal that contains both frequency and spatial information. Its main components are activities in four major frequency ranges named alpha (usually posterior maximum at 8 Hz to 12 Hz), beta (usually anterior at > 12 Hz), theta (usually widespread at 4 Hz to 7 Hz), and delta (normally seen during drowsiness and sleep at < 4 Hz) (Figure 2.26). A wide range of normal exists in the EEG. However, normal records are usually continuous, symmetric, show standard reactivity in response to specific states such as eye opening, repetitive movements of the extremities, drowsiness, sleep, hyperventilation, and photic stimulation, and do not display any of a number of clearly abnormal patterns.

The EEG evolves with age and changes most rapidly in infancy. It becomes slower in the second and third decades of life and then reaches a plateau for most of adult life, with the exception of mild slowing in old age. Neonatal EEG is a fascinating subject with a complexity beyond the scope of this discussion. Changes occur so rapidly in the EEG of infants, particularly premature infants, that an experienced electroencephalographer can estimate the age of the infant from the tracing alone, up until an age of about 8 weeks postterm, to within several weeks.

A normal posterior basic EEG rhythm begins to develop about 3 to 4 months post-term, starting at a frequency of 3 Hz to 4 Hz. By one year post term, this rhythm is approximately 6 Hz and is 8 Hz by three years. After reaching 8 Hz, the posterior basic rhythm has reached the alpha frequency range and is called the occipital alpha rhythm. The rate of increase slows from this point on, reaching an adult average of 10 Hz by age 13 or 14. Occipital alpha activity increases with eye closure and slows with drowsiness, decreased cerebral perfusion, toxic and metabolic disorders, and focal lesions. It usually increases in amplitude over the nondominant occipital region, due to slightly decreased skull thickness on this side, and is occasionally not detectable in some normal individuals. The alpha rhythm is maximal over the occipital area in 65% of adults and widespread in 32% of adults. Slowing of the posterior basic rhythm is one of the first EEG signs of diffuse cerebral dysfunction.

Beta activity usually occurs with the frontal-central maximum. It may be seen in three specific bands: ". . . a common 18 Hz to 25 Hz band, a less common 14 Hz to 16 Hz band, and a rare 35 Hz to 40 Hz band."[16] A focal decrease in beta activity may be the first subtle sign of cortical injury, such as results from trauma or stroke. Focally increased beta activity on the scalp may result from skull defects (called a breach rhythm), since high-frequency activity is preferentially filtered out by the skull. Generalized increased beta activity may result from the administration of agents affecting the CNS, such as general anesthetics, benzodiazepines, alcohol, barbiturates, or opiates. Low voltage with globally increased beta activity has also been reported in various chronic disease states, such as alcoholism, chronic opiate abuse, and HIV infection.

Theta and delta activities are variable in their amount and location and may change dramatically with state of consciousness. Theta activity, normally widespread, may increase in voltage, rhythmicity, and prominence with sleep (hypnagogic theta), awakening, and with hyperventilation. These EEG changes occur more dramatically in children. Theta activity also increases in toxic and metabolic encephalopathies and with focal cortical injury. Variable amounts of delta activity occur normally in children such as posterior slow waves of youth, and during sleep. Stages III and IV of sleep are defined by the amount of delta activity present; 25% to 50% and greater than 50%, respectively.

Mu rhythm is a normal variant pattern that usually continues during wakefulness, within 1 Hz to 2 Hz of the alpha rhythm and centered over the motor cortex (Rolandic area) unilaterally or bilaterally. It is recognizable because it disappears with repetitive limb movements or when subjects think about moving a limb.

Other common normal EEG patterns include positive occipital sharp transients of sleep (POSTS), benign epileptiform transients of sleep (BETS), vertex waves, sleep spindles, and k-complexes, all of which indicate sleep (Figure 2.28).

2.6.2 Common Abnormal Patterns

Many common abnormal patterns include significant asymmetries in the EEG between homologous areas. Such a pattern can take the form of focally increased or decreased amplitude, frequency or rhythmicity, including the alpha rhythm, beta activity, or persistent focal slowing in the theta or delta ranges. These changes are frequently seen in focal cerebral injuries, such as those due to stroke, trauma, focal infectious, or neoplastic lesions.

Figure 2.29 — FIRDA.

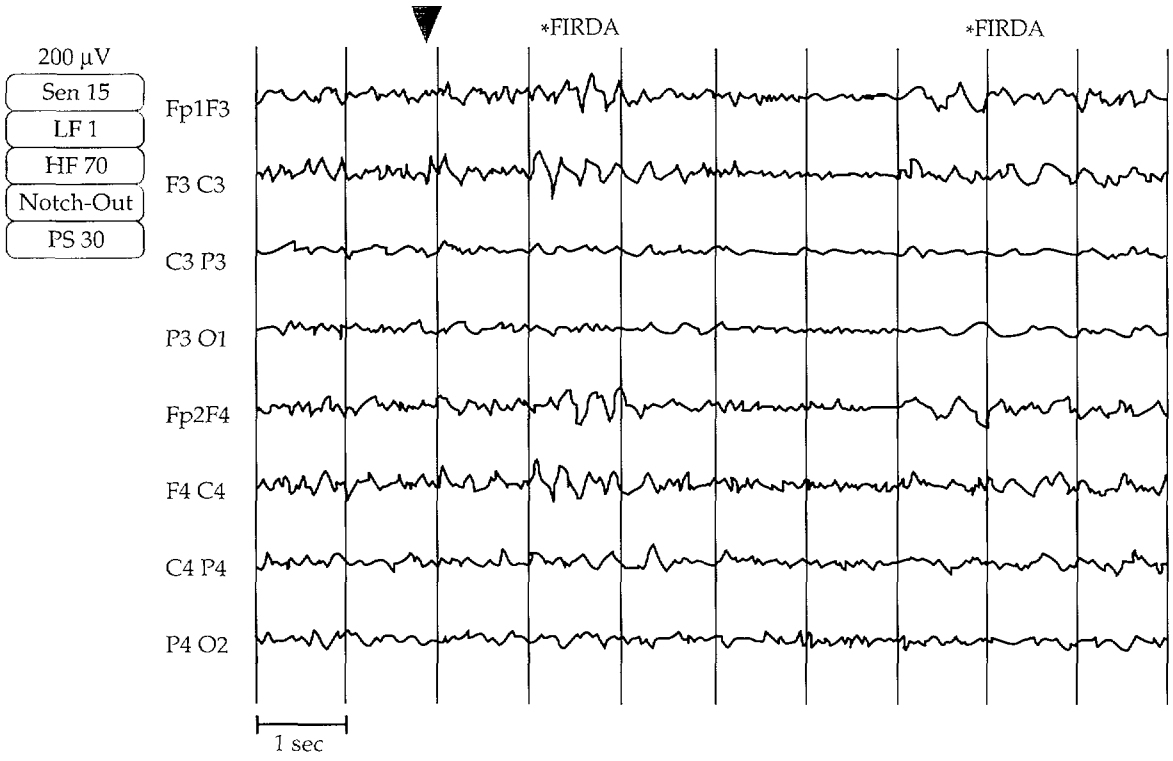

Slowing is one of the most common manifestations of cerebral dysfunction. When focal, it usually indicates localized pathology, such as stroke, infection, trauma, or tumor. When generalized, slowing may indicate intoxication, such as observed with drugs of abuse, or overdoses of prescribed medications, metabolic disorders (such as hepatic or renal failure), or electrolyte disturbances. Slowing may appear in the form of increased theta or delta activity, a decrease in the amount or distribution of beta activity, or just slowing of the posterior basic rhythm. Toxic and metabolic encephalopathies may also be present with characteristic EEG patterns, such as triphasic waves, commonly seen in hepatic and renal failure, and frontal intermittent rhythmic delta activity (FIRDA), seen in hydrocephalus, in some toxic/metabolic processes, and in hydrocephalus (Figure 2.29).

Other important abnormalities in the EEG correspond to the diagnosis of epilepsy and specific epileptic syndromes. Focal seizure disorders can arise from any region of the cerebral cortex, most commonly from the temporal lobe (complex partial seizures). The EEG may demonstrate focal slowing, focal spikes (duration $\leq$ 70 ms), or sharp waves (duration up to 150 ms to 200 ms) over the region of the epileptic focus (Figure 2.30). Continuous rhythmic spiking may identify focal seizures, and spike and slow-wave patterns may be present in individuals with certain types of primary generalized seizure disorders (e.g., absence epilepsy) (Figure 2.31). Many other abnormal patterns exist that may be seen on routine electroencephalograms.

Figure 2.30 — (a) Focal spikes over the left parietal area with left temporal spread. (b) Two left temporal spikes. (c) Focal slowing over left hemisphere.

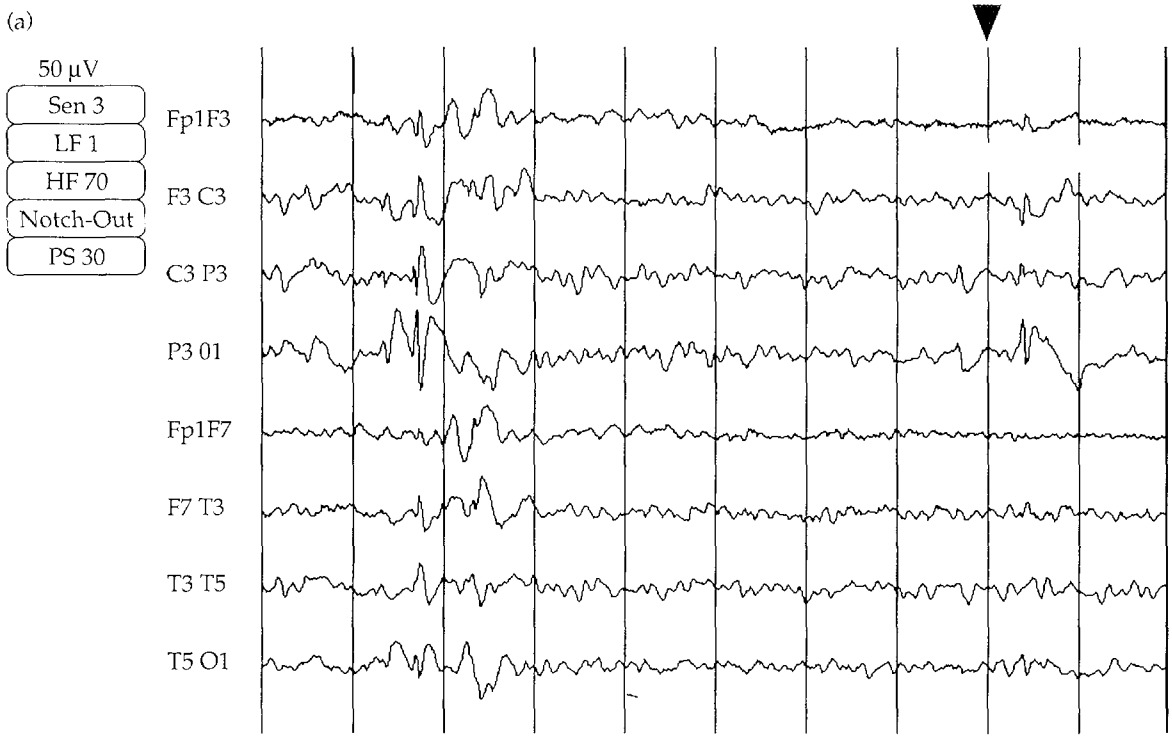

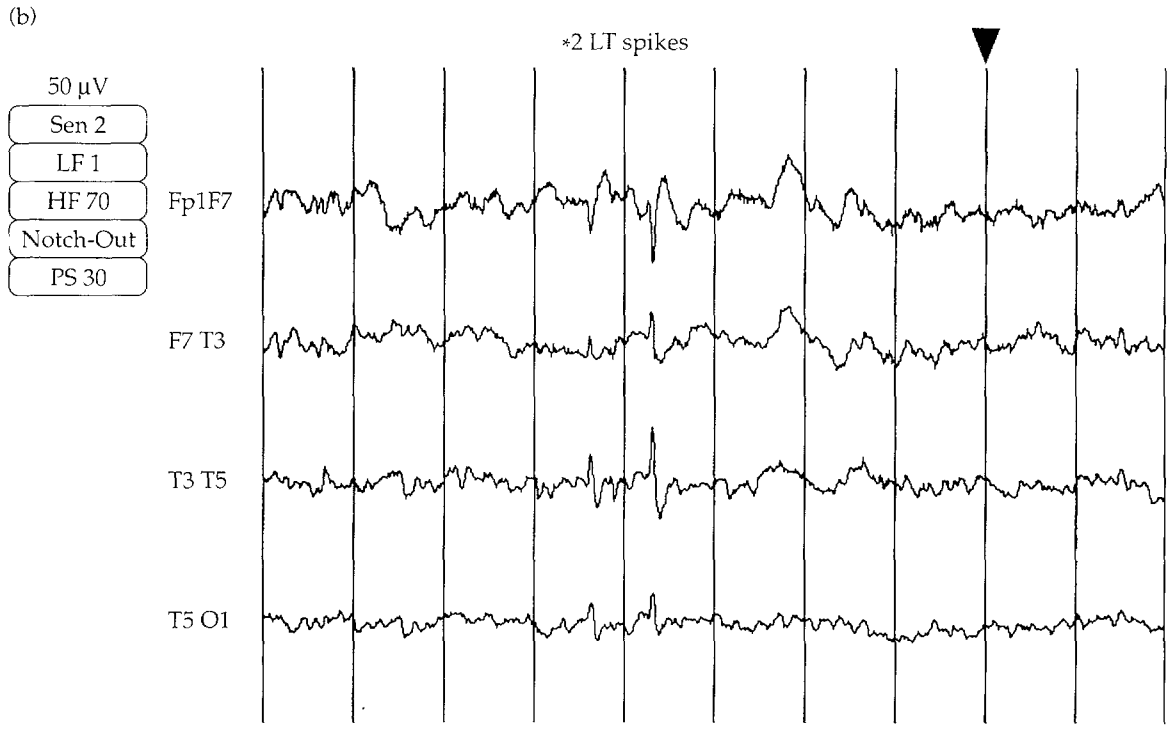

Figure 2.30 — continued.

(c)

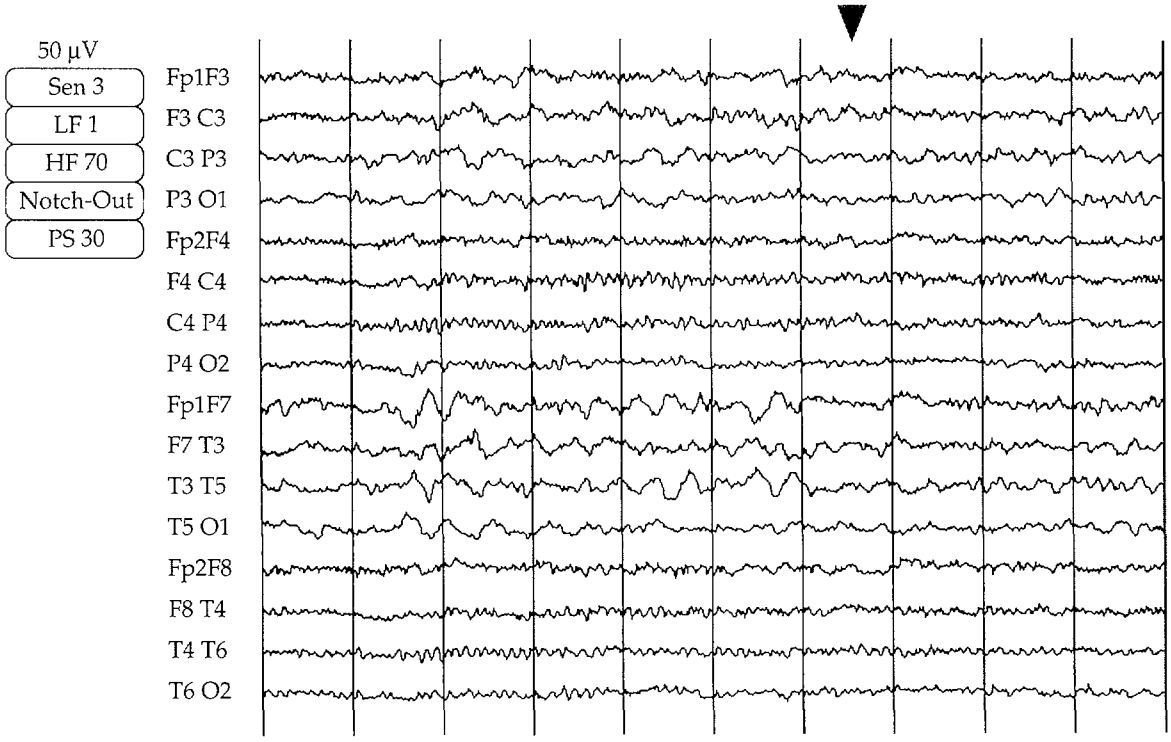

Figure 2.31 — Spike and slow wave discharge typical of absence epilepsy.

(a)

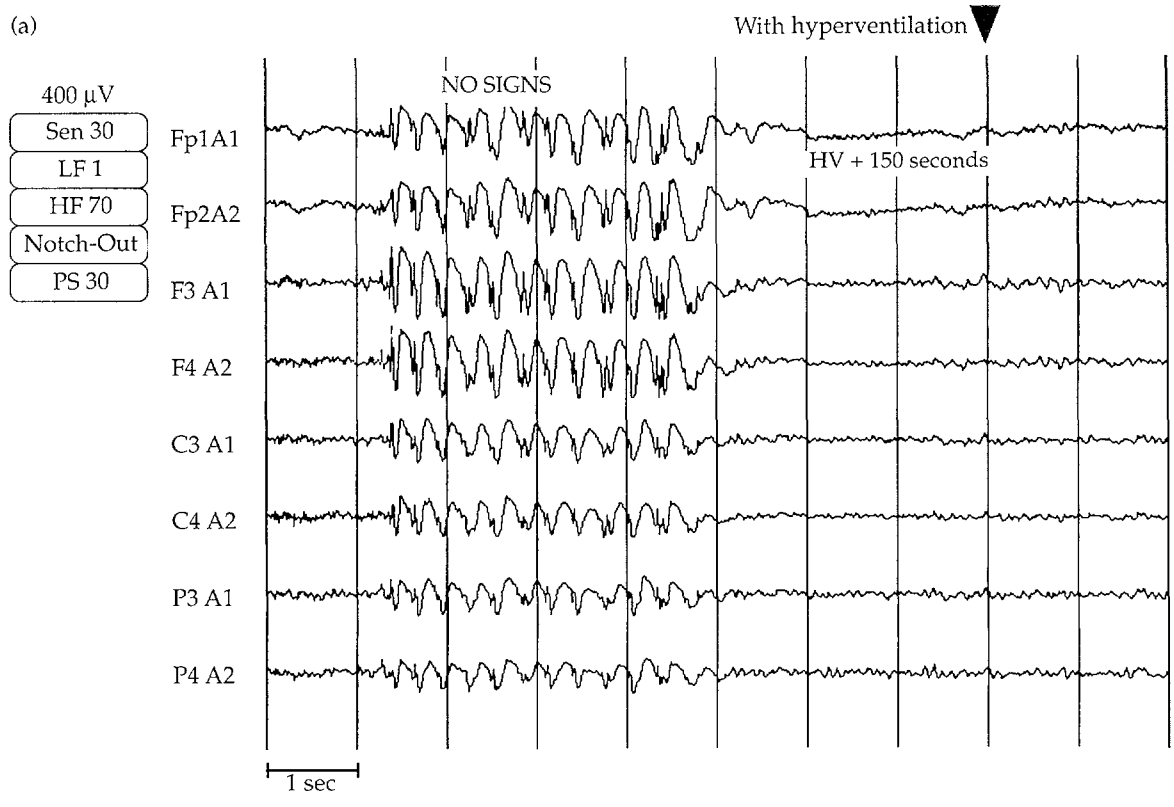

Figure 2.31 — continued.

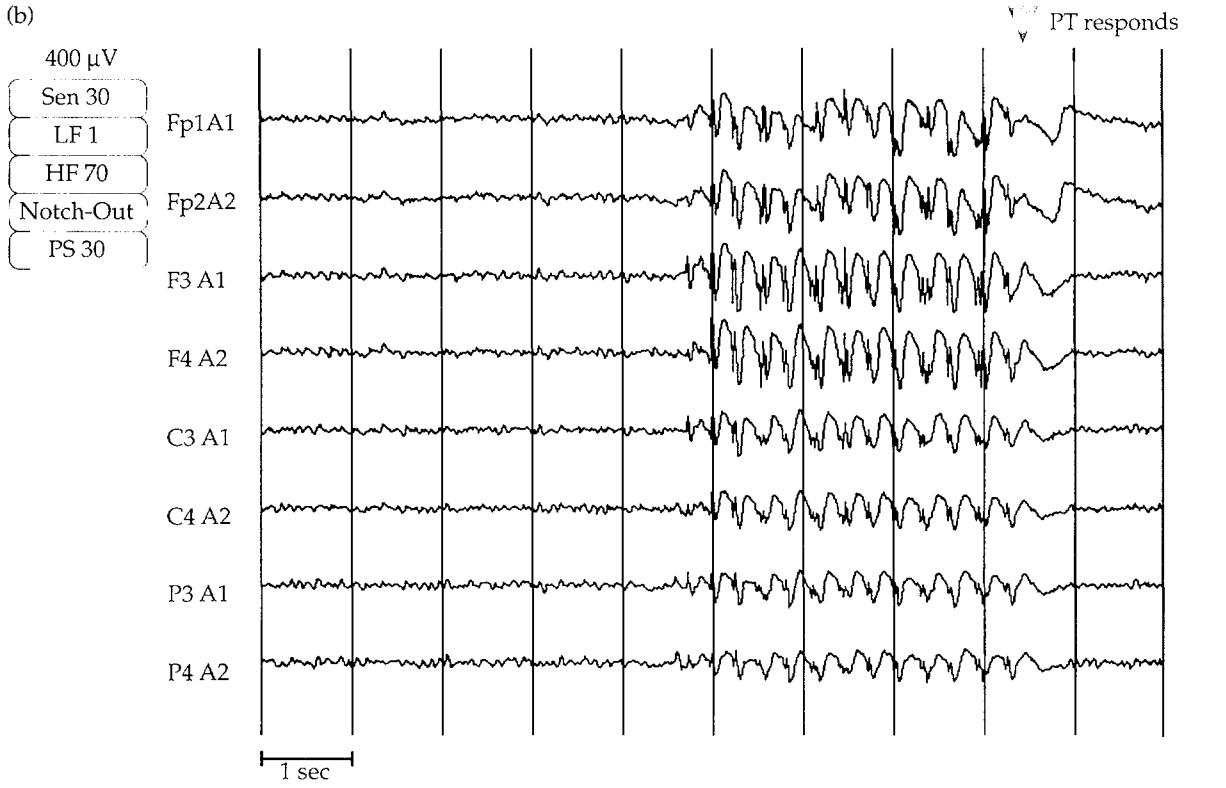

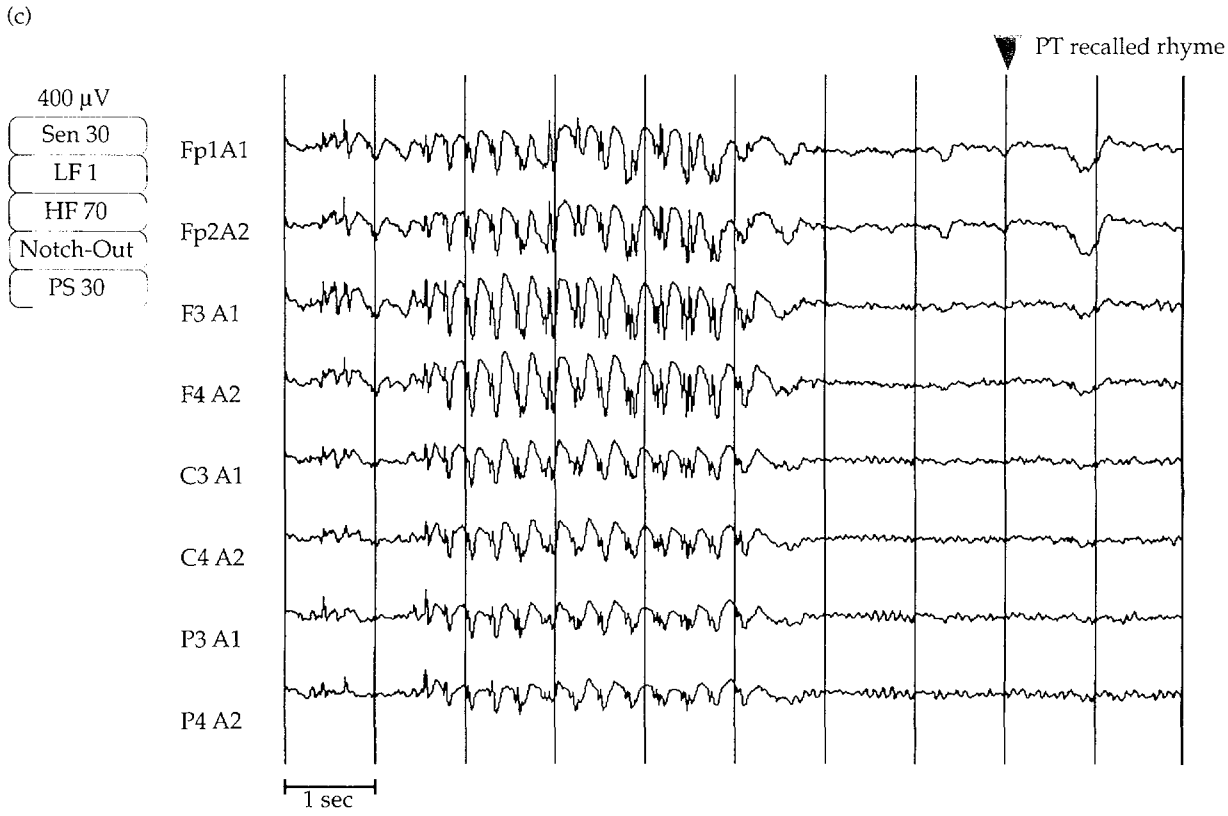

2.6.3 Artifacts

It is important to be familiar with common sources of artifact in the EEG because, along with normal variant patterns, artifacts are one of the most common reasons for incorrect record interpretation. Artifacts can be divided up into two major categories, physiological and nonphysiological. Common physiological artifacts are demonstrated in Figure 2.32a and include: eye blinks; muscle activity; movement; and sweat artifact arising from skin.

Figure 2.32b demonstrates common appearances of nonphysiological artifacts including: electrode pops; wire movement artifact; 60 Hz power line interference; high-frequency artifact resulting from electrical instruments used during surgery (in this case an electrosurgical device); and artifacts arising from other devices used in the medical setting (e.g., intravenous infusion pumps).

The most difficult artifacts to detect appear as irregular signals mimicking abnormal EEG activity, such as epileptiform discharges. Artifact identification is a skill that requires many hours of training reading EEGs. Even experienced electroencephalographers can misinterpret physiological-looking artifacts from time to time.

2.7 *Processed Electroencephalography: Monitors and Methods*

Digital EEG provides clinicians and investigators access to a variety of techniques for quantitatively measuring brain function. Some of these techniques are used to localize electrical activity to a particular region of the brain. Other methods follow trends in the EEG over time, such as slowing or sharp activity, and are used to correlate these trends with important clinical changes in the patient's condition.

2.7.1 Domains: Time, Frequency and Fourier Analysis

Digital EEG signals can be processed in several ways. In the time domain, statistics on segments of the EEG can be compiled, such as the mean voltage, number of times the signal crosses zero, standard deviation, and variance of the signal. Using these and other measured parameters, segments of the EEG can be compared to one another statistically, using such techniques as coherence, crossed spectral density, etc. In the frequency domain, the EEG is decomposed into its basic frequency components and the amount of power in each frequency band is measured, yielding a frequency spectrum. This allows comparison of selected components of the EEG, such as the alpha rhythm, frontal slowing, or beta activity between individuals, in different circumstances, and over time.[14]

The basis of frequency domain analysis is Fourier's theorem, which states that any waveform may be exactly represented as the sum of a number of sine-waves of different frequency, phase, and amplitude. When added together, these data reproduce the waveform. If the frequency range (bandwidth) of the waveform being analyzed is unlimited, then the number of sine-waves (or series) required to reproduce the waveform is infinite. If the frequency bandwidth is limited, such as from 0.1 Hz to 70 Hz in the standard EEG, then a finite number of sine-waves may be utilized. In practice, digital processing makes use of an algorithm called the Fast Fourier Transform (FFT) which operates on discrete segments of the EEG and yields a set of numerical coefficients that can reconstruct the

Figure 2.32 — (a) Eye blinks, sweat, muscle, movement; (b) pops, 60 Hz, other artifacts.

(a)

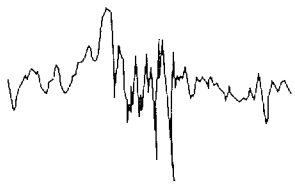

Frown

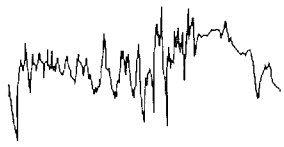

Teeth gritting

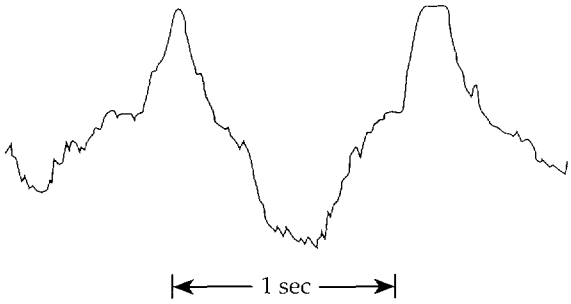

Eye blinks. Chart speed = 30 mm/sec.

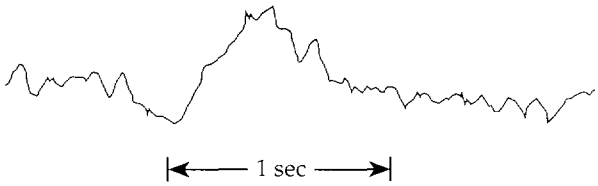

Movement artifact. Chart speed = 30 mm/sec.

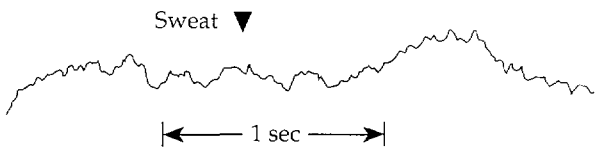

Sweating artifact. Chart speed = 30 mm/sec,

(b)

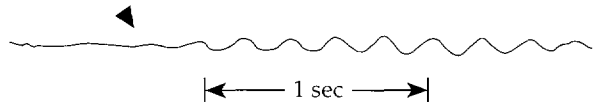

Wiggling respirator hose. Chart speed = 30 mm/sec.

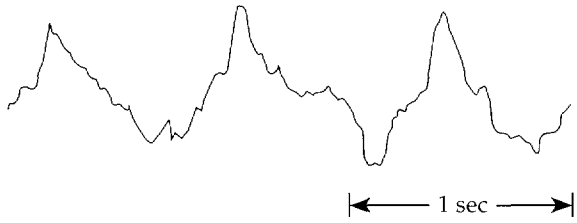

Loose Electrode. Chart speed = 30 mm/sec.

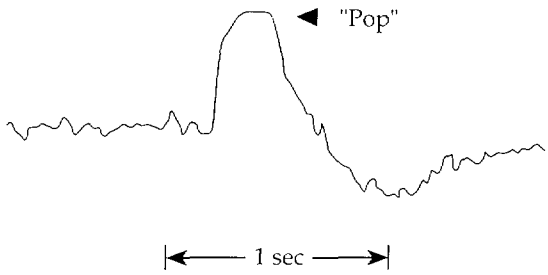

Electrode "Pop". Chart speed = 30 mm/sec.

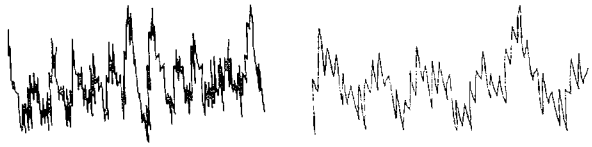

Chart speed = 30 mm/sec.
ESU interference

Chart speed = 30 mm/sec.
60 cycle interference

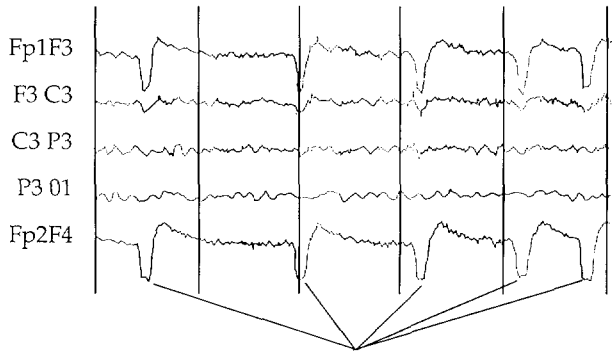

Example of clinical eye blinks

waveform when multiplied by the appropriate sine and cosine functions. The frequency spectrum is computed for each discrete segment of EEG. Connections between adjacent segments of EEG are mathematically smoothed so as to create a continuous waveform when the FFT coefficients are used to reconstruct the signal. The output of the FFT algorithm is a set of coefficients, two for each frequency component in the signal's spectrum. One coefficient is multiplied by the cosine or amplitude portion of the component (A), and the other is multiplied by the sine or phase portion of the component (B), yielding the phase portion of the component. Each component in the FFT series can be represented as:

$$A \cos (wt) + i\, B \sin (phi) \qquad \textbf{Equation 2.1}$$

where

w	=	angular frequency of the component,
A	=	an FFT coefficient
B	=	an FFT coefficient
phi	=	the phase angle of the component
i	=	the imaginary number sqrt(-1).

The number of frequency components and pairs of FFT coefficients necessary to represent a given waveform is a function of the highest frequency (F) to be resolved and the sample rate (SR) is used. The FFT requires the number of points (N) processed in a given segment of EEG to be a power of two, commonly 256, 512, or 1024. If, for example, a sample rate of 256 Hz is chosen (SR=256), then the maximum frequency that can be accurately resolved is 128 Hz. If a window of 1024 points is taken (N=1024), this is equivalent to a 4-second segment of EEG on one channel. The number of pairs of FFT coefficients required to represent N samples is N/2, and the resolution of the signal is SR/N=256/1024, or 0.25 Hz. This means that the FFT algorithm will generate a pair of coefficients for each incremental frequency of 0.25 Hz from 0.25 Hz to 128 Hz. Figure 2.33 illustrates the decomposition of an EEG waveform into its basic frequency components and then displays them as a frequency spectrum, a diagram that shows the different frequency components of a given waveform, and how much power (in this case voltage) is present at each of these frequencies (Figure 2.33). Once the frequency spectrum of a given segment of EEG has been calculated, a number of techniques are available to display this information as it is distributed in space over the head or in time.

Figure 2.33 — Section of EEG. (a) a typical waveform broken down into its frequency components. (b) frequency spectrum for the waveform in (a).

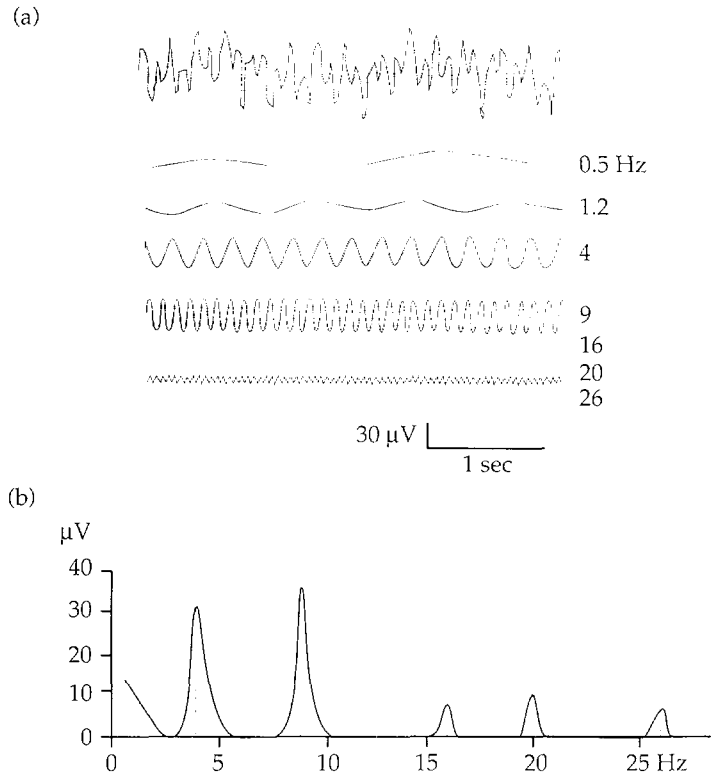

2.7.2 Brain Mapping

Several types of brain mapping using EEG serve patient care and research. Only two types will be discussed here: spatial mapping of EEG data over the scalp surface, and source analysis. In spatial EEG mapping, a number of types of data may be displayed, including frequency components of the EEG, electrical potential fields, current density, or gradient fields of particular events recorded on the EEG. The example of topographical mapping of EEG frequency data, popularized by the commercially available BEAM (brain electrical activity mapping), will present the general concept. In this display method, EEG data is divided into basic frequency bands such as alpha, beta, theta, and delta by taking the FFT of the data. The power in each band is calculated over each electrode in the EEG montage and the frequency data is displayed on a topographical map of the scalp for each electrode. Frequency data at locations between electrodes is interpolated between electrodes using one of a variety of algorithms, so that the actual display represents only in part the actual EEG data. Each frequency band is assigned a color, or shade of gray, and is displayed over the scalp map so that the intensity of the color in the display corresponds to the amount of power in that frequency range. In this way, the frequency spectrum of the EEG is easily visualized, changing in activity over particular regions of the head. The EEG may be broken down into as many frequency bands as is useful for the particular application of the technique. Figure 2.34 shows a gray-scale example of the output from a typical BEAM program during a number of states of consciousness and cognitive tasks.[17]

The source analysis type of brain mapping is used to predict the location of sources of abnormal electrical activity in the brain, such as seizure discharges or particular kinds of EPs. In this technique, a discharge is recorded over the scalp and the amplitude and location of the discharge at each electrode is recorded. This data is placed into a mathematical model that moves an imaginary electrical dipole around in a simplified, usually spherical, theoretical model of the brain. The field of the imaginary dipole is calculated at a given position and then compared with the electric field map actually recorded over the scalp. The cumulative error between the real and imaginary signal is calculated and the imaginary dipole is moved to another position, searching for the imaginary dipole location that minimizes the error between the real and imaginary signal. The imaginary dipole moves along a path of decreasing error until some arbitrary minimum error threshold is met, localizing the dipole source of the scalp electrical activity.

Source localization models of this type contribute to EEG research, but their accuracy is limited by broad assumptions made about the shape, uniformity, and conductivity of the brain and about the number of sources from which the activity emanates. In reality, epileptiform activity is thought to be generated by volumes of tissue. Finally, these techniques use the method of progressive approximation to find a solution to a problem not analytically solvable. Such techniques may yield a local minimum as a solution, and miss a better answer elsewhere on the surface of possible solutions. These techniques provide researchers with tools for mathematically localizing seizure foci in patients with epilepsy and potentially for the experimental localization of sources of particular brain functions. They are currently being investigated and refined, and some groups are beginning to experiment with these methods for potential routine clinical use.

Figure 2.34 — BEAM-type brain map.

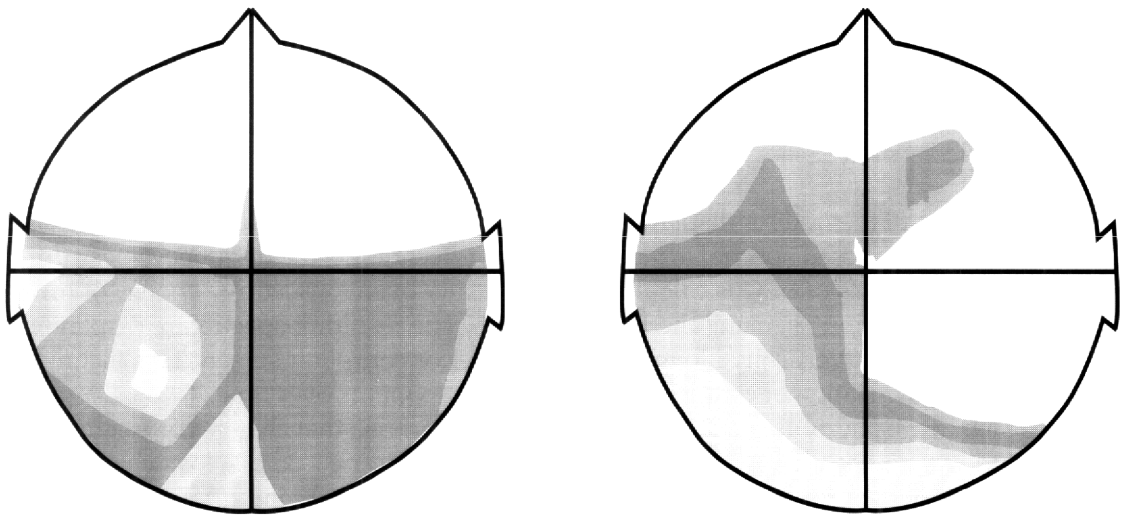

Figure 2.35 — Compressed spectral array data displayed on a head map.

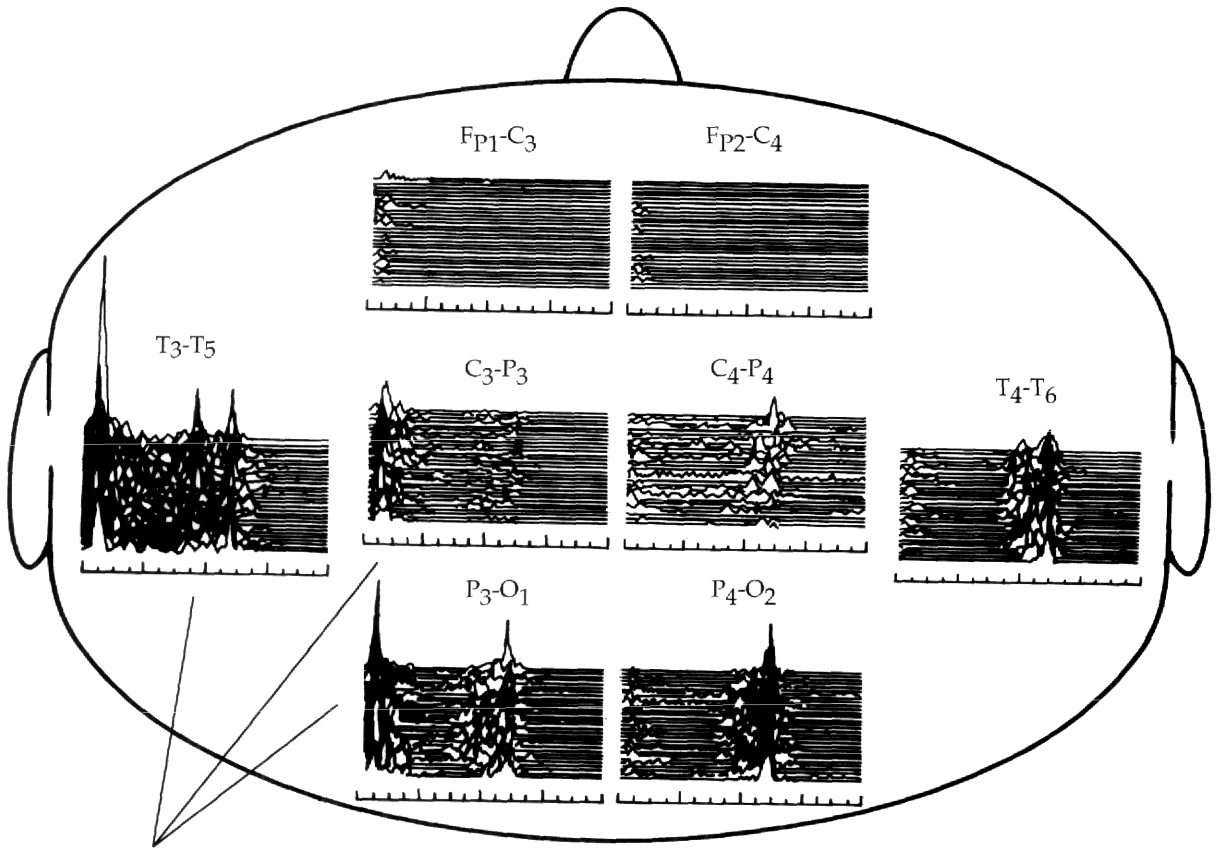

2.7.3 Compressed Spectral Array

One useful method for displaying changes in the frequency spectrum of the EEG over time is the compressed spectral array (CSA). In this technique, the frequency spectrum of one or more channels of EEG is calculated periodically over consecutive epochs of time, such as every five minutes, using the FFT algorithm. The resulting spectra are displayed in a cascaded format vertically along a chart recorder or computer screen. This technique allows easy identification of changes in frequency components over time. Two CSA plots, one for each hemisphere, are usually displayed side by side, so that changes or trends in frequency spectra may be compared between hemispheres. Figure 2.35 displays changes in the EEG spectrum over time in a patient with ischemia over the left temporial area.[18]

2.7.4 Zero Crossing Analysis

Another method sometimes used to characterize the frequency content of the EEG over time is called zero crossing analysis. This method marks each point at which the EEG

waveform crosses the zero voltage line. The time between adjacent marks is measured and the equivalent frequency of the half-wave so defined is calculated. A histogram of the measured frequencies is then constructed, revealing the relative frequency content of the waveform. Since many portions of the EEG waveform do not cross the zero line, another form of zero crossing analysis marks the local extrema of each portion of the waveform. The time between each adjacent pair of extrema is measured, yielding the relative frequency content of the waveform. When local extrema are used, in this first derivative form of zero crossing analysis (the first derivative of the waveform is zero at the extrema), amplitude information on each portion of the waveform can be compiled. Scientists have different opinions about which applications are better served by frequency analysis or zero crossing analysis. Both methods are under current study for EEG monitoring applications.

2.7.5 Clinical Use

The EEG is one of the only clinical tools available to assess brain function in real time. It monitors normal brain function, such as in staging sleep in studies evaluating patients for sleep disorders. The EEG is also used to detect evidence of cortical injury early, while it may still be reversible. Such applications include continuous EEG monitoring during procedures, such as carotid endarterectomy or coronary artery bypass grafting (under investigation). The EEG can often detect and characterize a number of toxic, metabolic, or degenerative states, and help differentiate them from psychiatric disorders. For example, if a patient is exhibiting activity that appears to be delirium or seizure activity and the EEG is normal, then a psychogenic cause for the patient's disorder must be considered. The EEG can also detect acute cortical injury before it is detectable by MRI or CT scanning. It is used for finding evidence of a focal seizure disorder, and for categorizing a number of epileptic syndromes whose treatment and prognosis often depend upon the EEG findings. The EEG can also prove a very useful adjunct to the physical examination in the determination of clinical brain death. In critically-ill patients who cannot be moved from intensive care units, in patients who have suffered severe head trauma, or in those whom neuromuscular blockade has made the neurologic examination useless, the EEG may be the only tool available to assess the patient's progress and function. In experienced hands, the EEG is an extremely useful clinical tool. As with other technologies, the clinical utility of the information provided by this technology is only as good as the indications for each specific study and the quality of the study interpretation.

2.7.6 Applications of Processed Quantitative Electroencephalographic Monitoring

2.7.6.1 Bedside Electroencephalographic Monitoring

Bedside EEG monitoring (other than for epilepsy) has a variety of clinical applications, particularly when using compressed spectral array display or time domain analysis. Stroke patients, postoperative neurosurgical patients, head trauma, and those with other intracranial disease processes can be monitored, often in intensive care units, to detect

trends in the EEG that may predict clinical change. A focal or generalized shift of power in the spectrum toward lower frequencies or diminished amplitude of the waveform may indicate progression of the disease process and predict deterioration of the patient's condition before it becomes clinically detectable. This may promote early intervention in the management of cerebral edema, evolving stroke or other potentially life-threatening processes at a time when treatment may make a difference. Patients in this setting are often sedated or unresponsive, so that the neurological examination is lost, making bedside EEG monitoring potentially even more useful.[19]

2.7.6.2 Perioperative Monitoring

Perioperative monitoring is used to detect cerebral ischemia during and after surgery before it results in a fixed and lasting deficit. One use currently under investigation is intraoperative EEG monitoring during carotid endarterectomy. Carotid endarterectomy is a procedure in which the internal carotid artery (ICA) that supplies blood to the ipsilateral eye and anterior cerebral hemisphere is clamped, opened, and cleaned of usually hard circumferential atherosclerotic plaque thought to cause ischemia or emboli in tissue. EEG monitoring is used primarily when the carotid artery is clamped in preparation for opening the vessel. If the EEG shows $\geq 50\%$ slowing or loss of amplitude over the cerebral hemisphere supplied by the vessel, the clamp is removed and a shunt is placed that allows blood to flow around the surgical site to the brain during the surgical procedure. While on-line EEG analysis is sufficient for monitoring during this procedure, CSA display may prove an easier and more compact method of displaying monitoring data.[20]

Perioperative EEG monitoring has also been applied to patients having coronary artery bypass graft surgery (CABG). Changes in EEG amplitude and frequency spectra have been observed with changes in bypass pump perfusion pressure during surgery. This implies that an intraoperative EEG in patients on coronary artery bypass may have some correlation with brain function. This is an area that requires further study. Investigation is ongoing using EEG to manage depth of anesthesia during surgery. Neural networks and spectral analysis are new processing tools used for this application.

2.7.6.3 Automated Analysis of Sleep

Patients with disorders of sleep and wakefulness are frequently studied using polysomnograms (or sleep studies). These assessments are performed in laboratories where patients are monitored for one or more nights while they sleep. A number of physiological parameters are measured, depending upon the patient's complaint, and may include: several channels of scalp EEG, respiratory effort, oxygen saturation, electromyogram (usually recorded from axial muscles and the tibialis anterior), electro-oculogram (records eye movements), ECG, esophageal pH (to monitor for esophageal reflux of gastric contents), and nocturnal penile tumescence (recording nocturnal erections in male patients under evaluation for impotence). Each of these signals may be digitized, displayed in a variety of manners (e.g., CSA), and entered into a computer program that detects patterns characteristic of the different stages of sleep and specific sleep disorders. For example, in obstructive sleep apnea, sleep is disrupted by frequent periods of ineffective respiratory effort accompanied by a drop in blood oxygen saturation and arousal from sleep. Sleep is

disrupted so frequently that these patients spend abnormally little time through the night in slow wave and rapid eye movement (REM) sleep. They feel tired throughout the next day and frequently fall asleep for brief periods during the daytime. A number of commercially available sleep analysis software packages are currently on the market. These programs continue to improve in their accuracy of detection of significant events in non-EEG monitors and in their ability to summarize the amount of time spent in the different stages of sleep as better algorithms evolve. Prior to the development of automated sleep analysis packages, collation of sleep data had to be performed by technicians pouring over eight- to ten-hour continuous paper recordings of the parameters listed above. Many laboratories still use this manual system, awaiting better automated algorithms. Figure 2.36 depicts a typical polysomnogram tracing in a patient with obstructive sleep apnea.

2.7.7 Epilepsy Monitoring

One of the most widespread uses of digital EEG, at present, is in the detection, localization, and treatment of patients with intractable epilepsy. Intractable patients are admitted to epilepsy monitoring units (EMUs) where they are continuously followed with scalp or invasive EEGs and by video cameras, so that their behavior can be correlated with the EEG. These methods are used because behavioral manifestations of seizures often correlate with the location of seizure onset in the brain.[21] Seizures, interictal activity, and behavioral spells are recorded and processed to determine the type of seizures and their location in the brain. This information is used to direct the patient to specific treatment for his or her disorder. In patients who do not respond to maximal medical therapy and have no contraindications, surgical removal of the origin of seizure activity, or focus, is often pursued. Many patients with intractable seizures have poorly localized seizures, or seizures emanating from areas adjacent to vital regions of the brain that cannot be safely surgically removed. These patients frequently undergo invasive monitoring with depth electrodes placed in the brain stereotactically through burr holes in the skull, or subdural electrodes laid overtop the cerebral cortex and beneath the dura placed during an open craniotomy.

Epileptiform activity is localized by finding the origin of interictal spikes (discharges that occur between seizures) and seizure onset in ictal recordings. There are times when clinical seizure activity precedes epileptiform activity on the recorded EEG, indicating that the true seizure focus is in a location not detectable by whatever electrodes are being used. This type of sampling error is one of the most challenging problems facing epileptologists in epilepsy surgery centers.

Once a seizure focus has been identified the patient is evaluated to determine whether or not the area involved in seizure generation is responsible for a vital function, such as motor control, vision, language generation, or comprehension. This is done by localizing language via an intra-carotid amobarbital test known as the Wada test, after Dr. Juhn Wada, to determine language dominance or codominance; formal cognitive function testing to map particular patterns of cognitive function and dysfunction; and brain stimulation mapping to pinpoint specific functions in the region of the epileptogenic focus around intracranial electrodes. If patients are properly selected for seizure surgery, moderate to good improvement in seizure control can be expected in approximately 70% of patients treated with this modality.

Figure 2.36 — Polysomnogram showing obstructive sleep apnea.

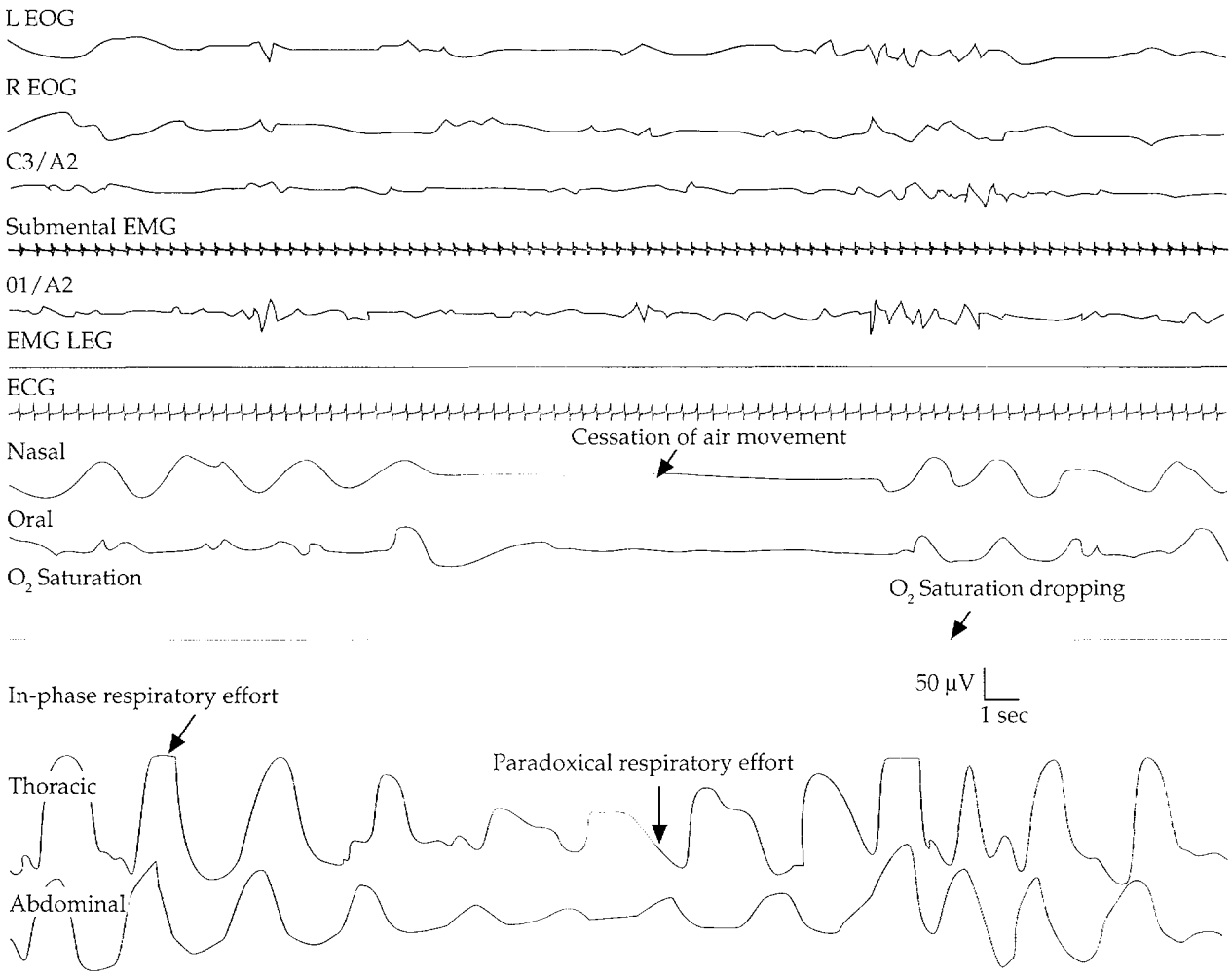

2.8 Current Research

EEG research is currently expanding on a number of levels. On the cellular level, investigators are recording and modeling intracellular and extracellular potentials in networks of cells in animal hippocampal slice models of epilepsy.[22] These models additionally provide a way to investigate the mechanisms underlying a generation of EEG potentials. In medical practice, clinician-scientists are monitoring a rapidly growing number of patients with intractable seizures using intracranial electrode arrays in the pursuit of surgical treatment for their epilepsy. This provides a direct cortical correlation in awake functioning patients to the scalp recordings that have been performed over the past 60 years.

In the field of neuroscience, a tremendous effort is underway to put into understanding the mechanisms of epilepsy on the level of single cells, neurotransmitters, ion chan-

nels, and even the genes involved in the generation of seizures. Work continues in neurophysiology that explores simple animal models for keys to the driving forces behind postsynaptic potentials and the generation of simple local electrophysiological electrochemical rhythms. In the fields of engineering, mathematics, and computer science, a number of investigators world-wide are pursuing modeling of the EEG and source localization, with particular emphasis on developing robust solutions to the dipole inverse problem. Engineers focus more and more on digital signal detection and processing techniques, including areas of neuronal networks and chaos theory, to glean more information from broad-band digital recordings. An offshoot of this work, the area of automated EEG analysis, offers a potential useful aid to the continuous monitoring of patients in epilepsy monitoring units. Finally, ongoing clinical studies continue to expand our clinical knowledge, characterizing the EEG in particular disease states, using it to predict outcome and to decide which therapies will be most useful, particularly in the arena of epilepsy surgery. The field continues to flourish now more than 60 years after its first description by Hans Berger.[5]

3.0 EVOKED POTENTIALS

Conduction along the sensory and motor pathways of the nervous system can be measured electrically by placing electrodes over relevant neural structures. The recorded neural signals, when coupled to an eliciting sensory stimulus or movement, are called evoked potentials (EP) or evoked responses. EP signals clinically evaluate the integrity of various segments of the sensory or motor-conducting pathways. The latency of EP voltage changes measures the conduction velocity between various neural structures. For example, following stimulation of the median nerve at the wrist, neural responses are recorded over large nerve bundles in the shoulder (the brachial plexus) as well as from the scalp, from the cervical spinal cord, upper brain stem, and the sensory parietal cortex (Figure 3.1). Slowed conduction between the point of median nerve stimulation and the brachial plexus suggests abnormal peripheral nerve function. Slowed conduction between the brachial plexus and upper cervical cord indicates abnormalities in the spinal roots or central nervous system (CNS) sensory pathways (Figure 3.2).

The most frequently used EPs for clinical testing include brainstem auditory evoked responses (BAERs), visual evoked responses (VERs), and somatosensory evoked potentials (SEPs).

Figure 3.1 — Somatosensory EP recordings during median nerve stimulation.

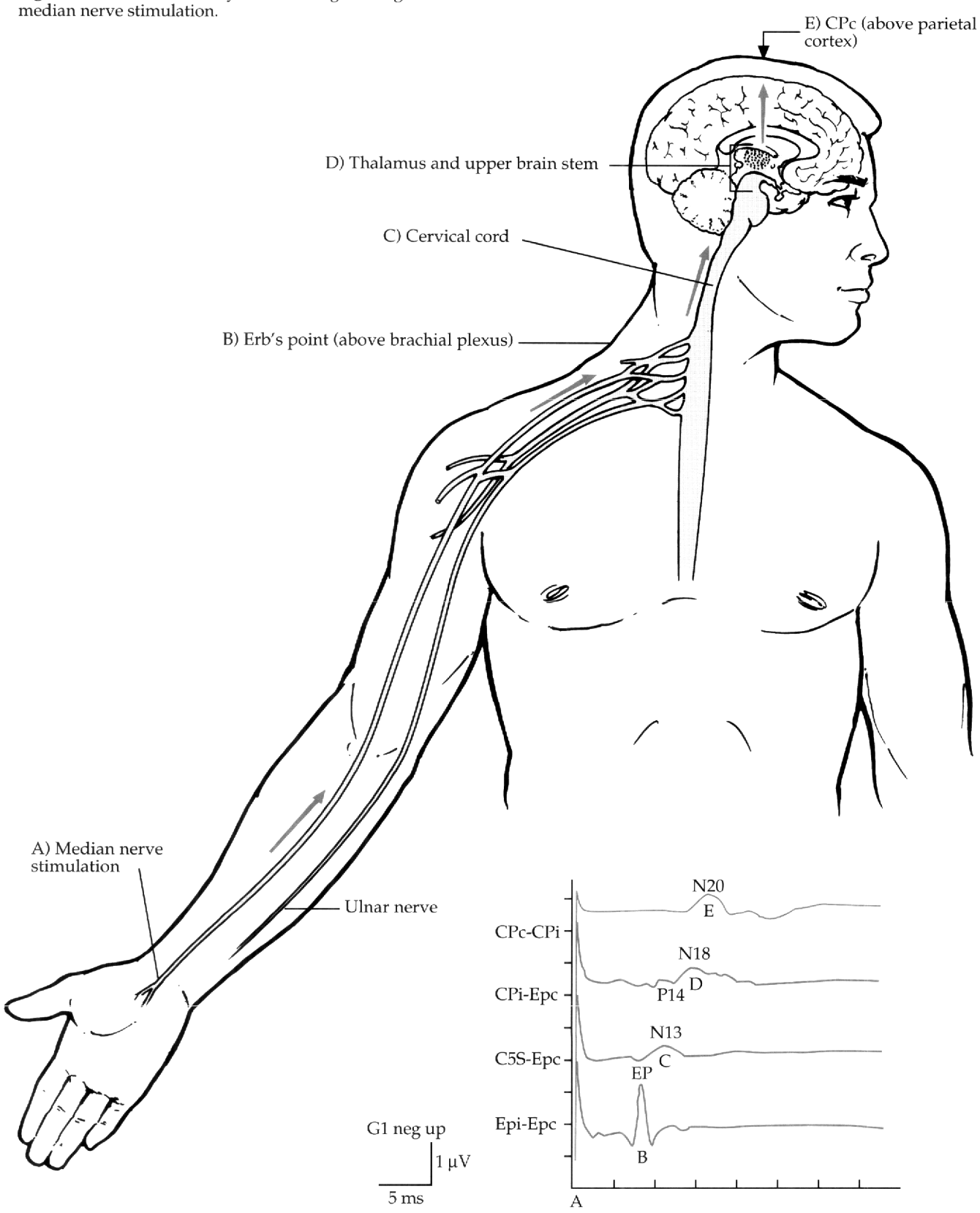

Figure 3.2 — Abnormal arm somatosensory EP. Prolonged EP-N13 interval demonstrates a sensory conduction abnormality between the brachial plexus and upper cervical cord.

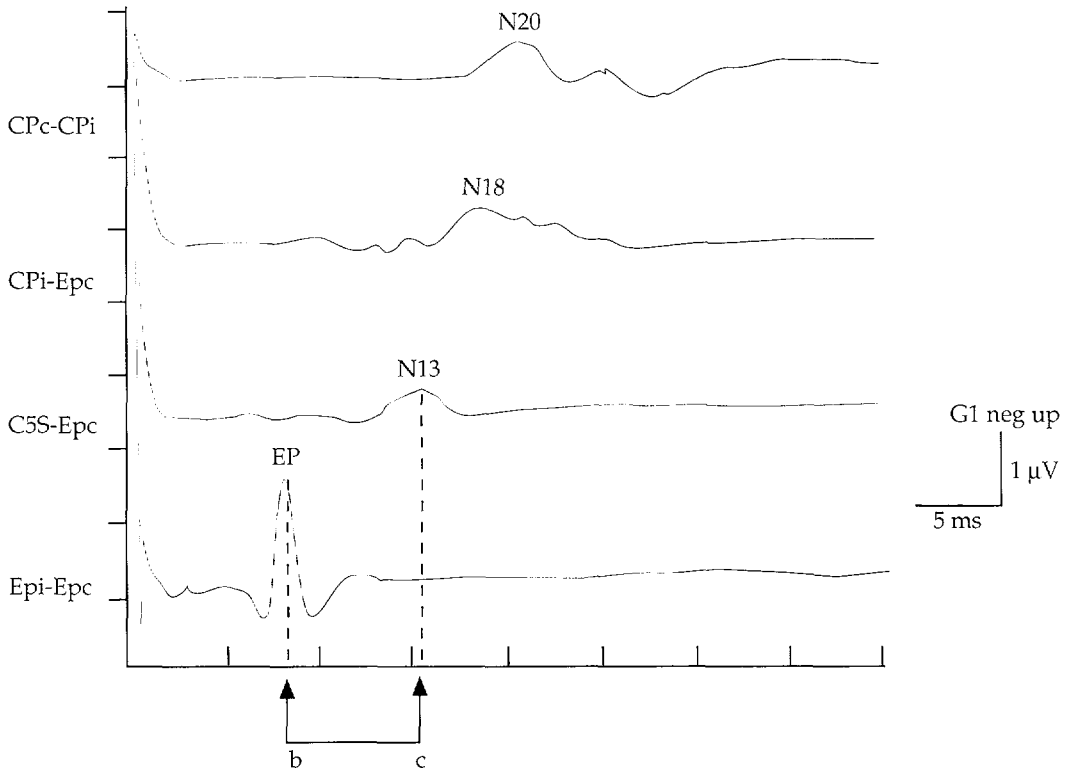

3.1 Averaging

When recorded from the skin, EPs are very small, typically 0.2 μV to 5 μV in amplitude, and are often overshadowed by background electroencephalographic activity, with its usual amplitude of 20 μV to 100 μV and by other sources of electrical noise. Muscle activity, movement, ECG, ocular potentials and nonbiologic artifact such as 60 Hz line voltage all can mask neural signals of interest. To reduce unwanted noise, recording segments synchronized to eliciting stimuli are averaged across multiple trials. Since the background EEG and other unwanted signals often appear irregular, or do not synchronize to EP stimuli, they are markedly reduced by averaging. For example, exposure to tone pips produces a series of brainstem and cortical electrical responses less than 5 μV in amplitude when recorded from the skin. Such low-amplitude responses cannot be detected following a single tone or even after averaging 16 auditory responses. Averaging 64 or more trials, however, demonstrates brain activity associated with auditory processing (Figure 3.3).

In general, averaging reduces noise proportionately to the square root of the number of trials.

$$\text{signal/noise} \propto \sqrt{\textit{number of averaged trials}} \qquad \textbf{Equation 3.1}$$

EP amplitudes often measure 1/10 the amplitude of background EEG and other unwanted signals. To obtain an EP response two times greater in amplitude than background noise, a 20-times enhancement of signal-to-noise is necessary (Equation 3.1) and 400 trials are required ($20 = \sqrt{400}$).

Figure 3.3 — Auditory event-related potentials (ERPs): noise reduction and improvement in signal/noise with increasing number of averaged trials.

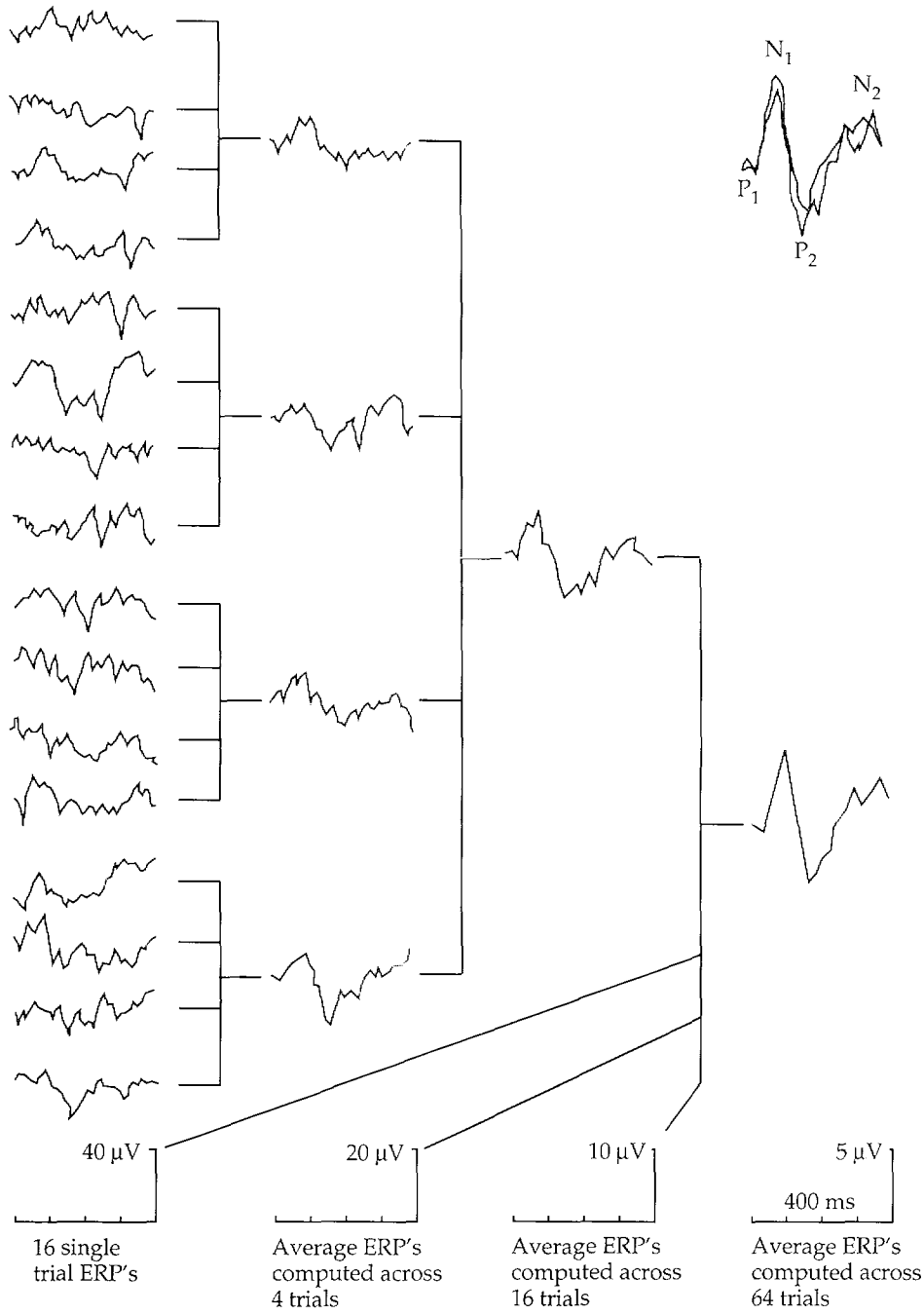

Because improvements in signal-to-noise ratio are inversely logarithmic, most of the improvement in signal-to-noise ratio occurs within 40 to 100 trials (Figure 3.4). The number of trials needed to reliably detect EPs, however, also depends on the amplitude of expected EP signals and the amount of noise. When EP signals are very low in amplitude, as with the SEPs, or when large amounts of high-amplitude noise are present, such as when a restless patient produces muscle, ocular, and movement artifact, large numbers of trials (500 to 1000) may be required.

Other techniques, including signal filtering and aperiodic averaging, can enhance EP detection. The rhythmical posterior alpha rhythm (8 Hz to 12 Hz) and semirhythmical temporal theta rhythm (4 Hz to 7 Hz) are normal EEG patterns that may coincide with EP stimulation cycles and obscure EP responses. To minimize interference from rhythmical EEG, the EP stimulation can be performed aperiodically or at rates that do not coincide with normal rhythmical EEG activity.

Screening individual trials can remove large-amplitude sources of noise such as movement artifact. Trials containing waveforms with high root-mean square (rms) or high peak- to-peak voltage amplitudes can be manually or automatically screened so that fewer averages may be used to resolve EP signals. For example, if biologically relevant signals measure less than 20 μV, automatic screening of trials with waveforms >40 μV may effectively screen contaminated trials in which a subject moved, blinked, or produced other unwanted signals. A table of waveform rms or peak-to-peak amplitudes and number of trials can be used to determine appropriate levels of noise screening to obtain a reasonable number of trials for averaging. Amplitude screening or filtering is often performed automatically in commercial EP systems.

On-line or intermittent cumulative averages can also be used to monitor testing to detect sources of artifact prior to completing an examination. For intraoperative monitoring of neural structures, trend analysis can be useful. Traveling averages of the *n*th most recent block of trials can demonstrate recent changes in EPs to determine effects of surgery on structures. Some commercial EP machines also plot changes in latency between serial EP studies in order to detect trends in peak latency.

3.2 *Evoked Potential Amplitude*

The EP amplitude is generally a less useful measure of neural integrity than latency because small variations in EP latency (latency jitter) and technical recording variations reduce the amplitudes of averaged EP. In general, the effect of latency jitter on averaged amplitude resembles a high-frequency filter—the amplitude of narrow waveform peaks is reduced more than the broadly contoured waveform peaks (Figure 3.5).

Evoked potentials are technically challenging to record. Amplitude abnormalities are often due to technical difficulties and are not related to physiologic abnormalities. Recording impedances over skin, bone and tissues can vary markedly, even with appropriately applied electrodes, and may produce amplitude variations.

The EP amplitudes may also fluctuate due to changes in the effective intensity of the eliciting stimuli. Amplitudes of BAERs recorded during right and left ear stimulation may change because of alterations in the position of external auditory meatus earphones. Minor changes in visual fixation may reduce VEP amplitudes.

Marked amplitude reductions or side-to-side amplitude asymmetries are most significant for relatively hard-wired portions of the nervous system, which have small expected latency fluctuations. Right-to-left asymmetries in amplitude of BAERs, SEPs, and VERs greater

Figure 3.4 — The signal/noise ratio of EP is improved with increasing numbers of averaged trials. For example, when signal amplitude is 1/10 amplitude of noise.

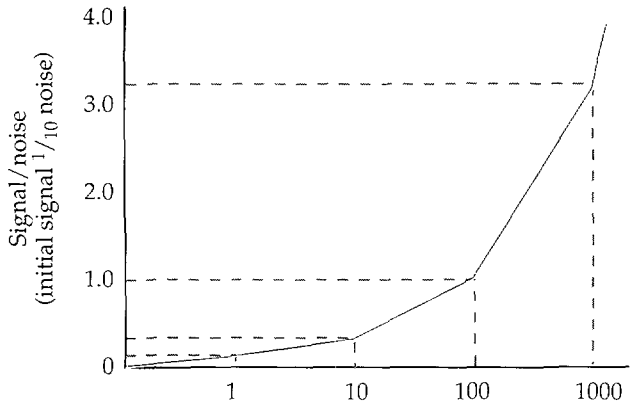

Figure 3.5 — Effects of latency variation on the amplitudes of averaged waveform peaks.

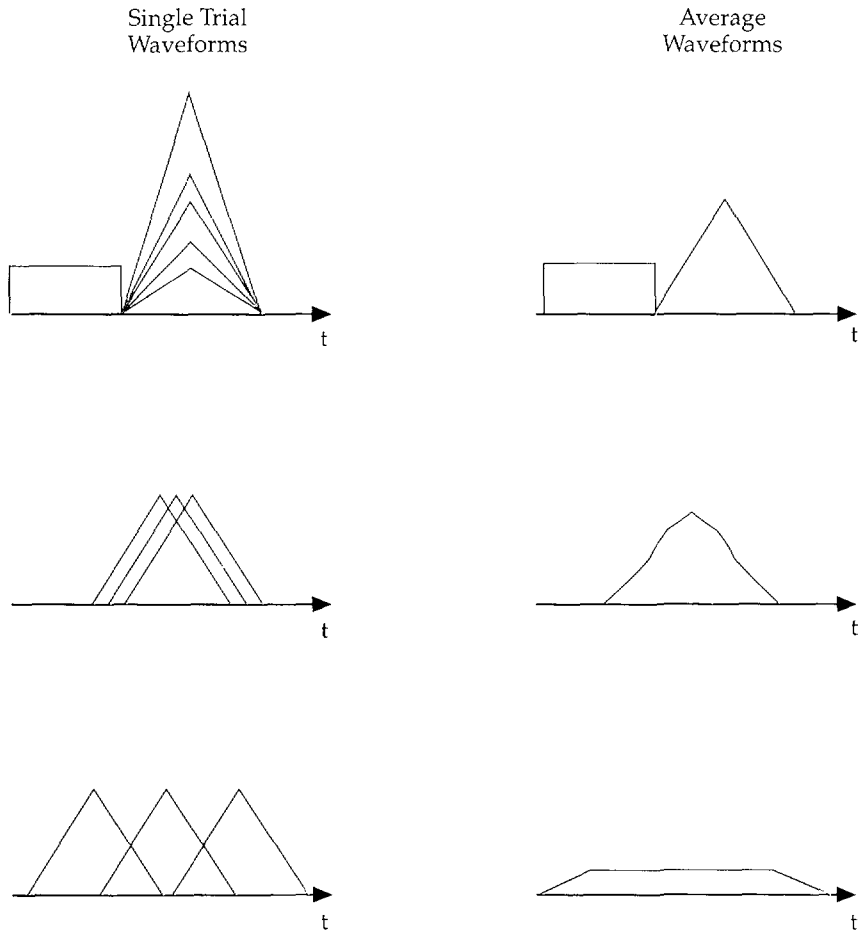

than 50% are often significant. So, for example, the ratio of the amplitudes of BAER peaks I and V (wave I/wave V) usually varies no more than 50% between the right and left ears.

3.3 *Evoked Potential Latency*

Although many EPs are generated by postsynaptic potentials, the latency of the EP is largely determined by the rate of action potentials conducted along fast-conducting myelinated axons. Large myelinated axons conduct action potentials rapidly by saltatory conduction; that is, action potentials jump along nodal gaps between myelinated segments. A major clinical use of the EP is to detect abnormalities in conduction along myelinated neuronal pathways. VERs and BAERs are sensitive indicators of demyelination produced by multiple sclerosis. Neuronal injury can also prolong latencies. EP latencies, however, are often normal unless most of a neural pathway is damaged. Tumors involving visual pathways in the cortex usually damage only a portion of visual fibers, so the VERs often have normal latency. Compression of the auditory nerve by an acoustic neuroma tumor, however, almost always produces an abnormal auditory EP response.

Only a limited amount of variation occurs between normal subjects in the latency of EP responses. Abnormal EP latencies for individuals are usually defined as latencies prolonged 2.5 or 3 standard deviations (SD) from group norms. Normal means and standard deviations must be established for individual laboratories using EPs recorded from 30 or more normal subjects. Long-latency EPs elicited by psychological responses to stimuli, called event-related potentials (ERPs), vary more in latency than do short-latency EPs such as BAERs. Careful experimental controls are needed to elicit replicable ERP responses.

3.4 *Evoked Potential Recording*

Important biophysical principles in recording EPs include the concepts of EP generators, near- and far-field recording, and dipole models. Normal and abnormal latency and voltage ranges must also be recognized since these parameters determine recording requirements. In order to correlate EP signals with underlying anatomic systems, it is also important to know the conducting pathways for the visual, auditory, somatosensory, and motor systems.

3.4.1 Evoked Potential Generators

The EPs over peripheral nerve and white matter tracts in the spinal cord and brain are generated by compound action potentials and post-synaptic potentials.[23] The EPs over fiber tracts consist of localized potential gradients called near-field potentials and more broadly distributed far-field potentials.[24] Near-field potentials are usually recorded as triphasic waves and are thought to represent traveling waves from compound action potentials propagated along fiber tracts. Electrodes must be placed adjacent to the neural sources to detect the steep potential gradients of near-field potentials. Far-field potentials have broader fields that are detected by electrodes placed farther from the anatomic source. Far-field potentials appear to measure variations in local geometry that produce impedance changes, such as when a fiber tract exits a tissue compartment.

Like EEG, EP signals in cortex are due to summated postsynaptic activity from clusters of related neurons called generators. Neuronal action potentials are larger than postsynaptic potentials, but are poorly synchronized and rapid (often 1500/second) and are usually not detected by the macro-electrodes used for clinical EP recording.

Figure 3.6 — The size of brain electrical sources and their distance from the scalp influence the attenuation of modeled dipoles recorded from the scalp.

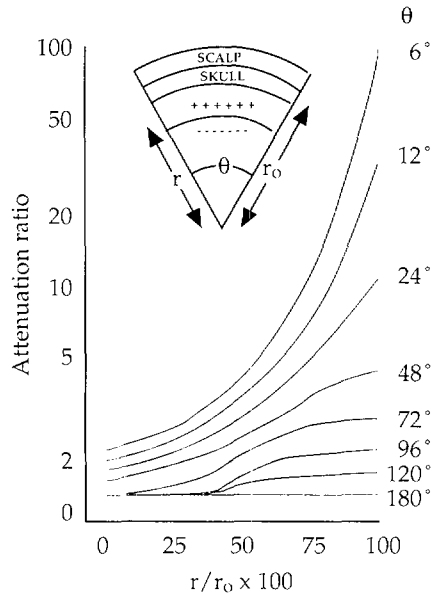

Figure 3.7 — Modeled effect of dipole orientation and depth on recorded scalp amplitude.

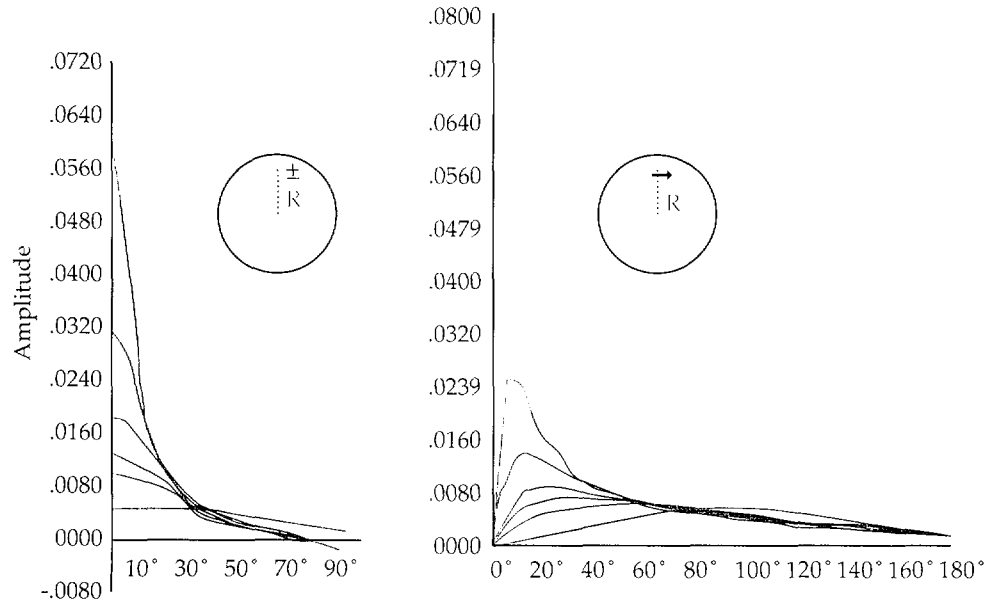

In many cases, the exact neural generators of EP waveforms have not been discovered and some EPs may, in fact, represent summated activity from multiple structures. Approximate locations for several EPs have been determined via direct brain recordings performed during surgery and by correlating the effect of isolated neural lesions on EP components. For example, wave VI in the BAER is located in the upper brain-stem, but has not been precisely localized to the medial geniculate or other auditory structures.

The electrical fields produced by some EP generators can be modeled as electrical dipoles. Dipole fields, along with the conformation of conducting structures, often explain the distribution of electrical fields recorded on the skin. For example, stimulation of the right retinal field activates right occipital regions and produces a P100 response, which is maximally recorded on the scalp over the contralateral (left) visual cortex. This apparently paradoxical localization relates to the placement of visual regions in the mesial occipital cortex so that P100 projects maximally contralaterally.

The orientation of cortical generators and their distance from the scalp also influences the amplitude of EP responses. Generators distributed over a large region of cortex are only slightly attenuated by transmission through the CSF, meninges, skull, and scalp (Figure 3.6). Transversely oriented or small, deep sources, however, are difficult to detect from electrodes placed on the skin (Figure 3.7).

3.4.2 Recording Techniques

Evoked potential recording was developed in the 1940s by Dawson and others when it was found that rapid electronic averaging allowed detection of small neural signals recorded on the skin. Computerized digital signal processing has recently improved the recording and analysis of EP.

Modern digital EP recording devices consist of sensory stimulators, recording amplifiers with analogue filters, an analogue-to-digital converter, a digital signal averager, and a display and storage system. A key component that differentiates EP systems from digital EEG recorders is a device which triggers recording sweeps synchronized to sensory stimulation or motor responses. A typical digital EP system is shown in Figure 3.8.

The voltages and latencies of EP responses vary significantly between different sensory modalities, requiring different recording parameters for various EP tests. Recording windows of two to three times normal latencies are usually needed to detect prolonged waveforms. EP cortical responses are elicited 30 ms to 40 ms following ankle (tibial nerve) stimulation, approximately 10 ms following auditory click stimuli, and approximately 100 ms after visual pattern stimulation. Thus, a minimum recording period of approximately 60 ms is needed for recording leg SEP, 15 ms for BAERs, and 250 ms is necessary for VER recording.

Voltages for various EPs range from approximately 0.1 μV to 100 μV. In the United States negative voltage is usually plotted upward for VER and SEP, while positive voltage is plotted upward for BAERs (there are different conventions in Europe). Negative peaks are labeled N and positive peaks are labeled P. The current convention is to number EP components sequentially or to label them by their typical latency. Typically, the major VER response to pattern stimulation is a positive, approximately 100 ms waveform peak, which has been labeled both P1 and P100. The BAERs are labeled I through VI. It is important to remember that terms such as P100 do not imply exact latencies, but are merely labels. A visual EP response is called a P100 response, even though it occurs at 95 ms.

Figure 3.8 — An EP recording system.

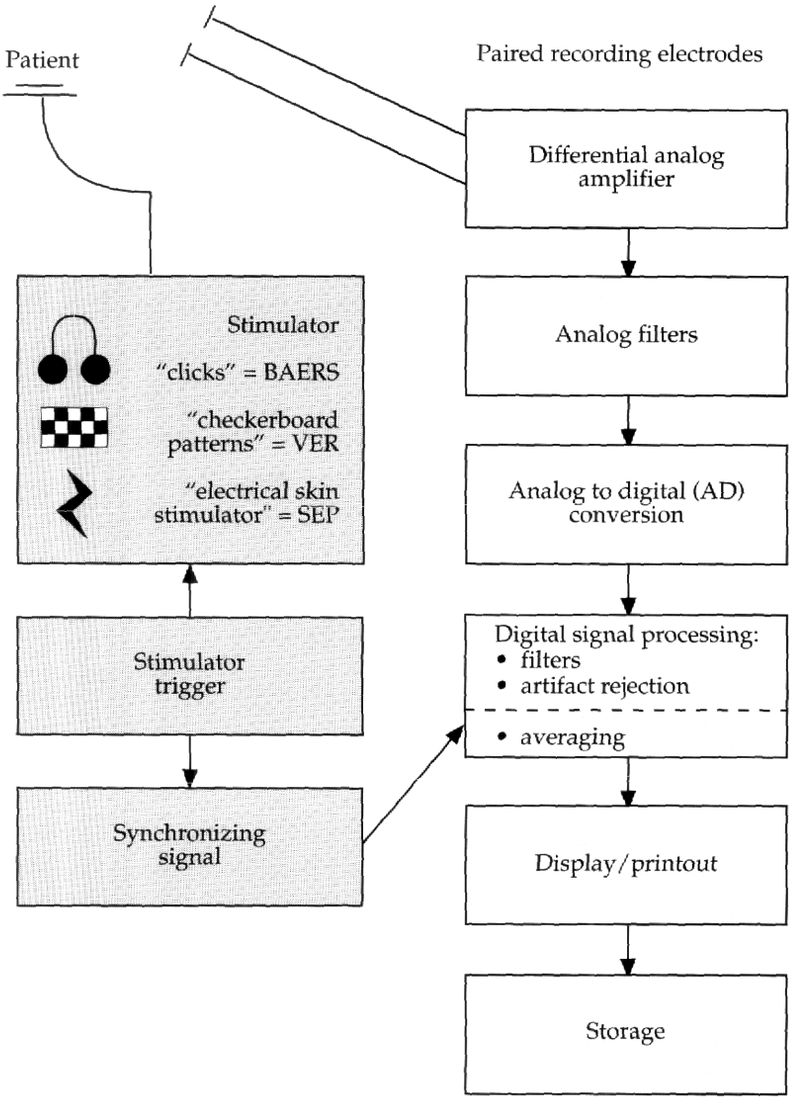

3.4.3 Digital Sampling

Since many EP components are of short duration, about 2 milliseconds to 1 second, rapid sampling rates are needed to digitally record EP. A high-frequency (low-pass) analog filter must be used when acquiring signals and the sample rate must be set at least two times the highest frequency present to avoid distortion due to aliasing (the Nyquist effect). Usually, the sample rate is adjusted to provide approximately 4 to 10 data points per wave. Consequently, digital sample rates must be several times the period of the waveforms of interest. To digitally record EP waveforms of 10 ms (.01 second) duration, for example, 1000 samples/second are required (10 samples per .01 second).

The amplitude of EPs are normally measured on a vertical scale with sample points measured as bits on a logarithmic resolution scale. Resolution of voltage is usually sufficient with 8-bit recording, although 10- to 16-bit amplifier A – D systems are becoming available.

A sample-and-hold function may be needed to maintain synchronized averaging if recording multiple channels with A – D serial data conversion. One recent development is the use of EP collectors that provide simultaneous recording with multiple channels employing different time and voltage scales and sample rates. This allows the concurrent EP monitoring of several systems, such as BAERs and SEPs, which have different time and amplitude scales. This type of monitoring is clinically useful for simultaneous monitoring of somatosensory and auditory structures during surgery.

3.4.4 Filters

Band-pass filters, comprising combined high-pass and low-pass filters, are used to improve EP signal detection. High-pass filters stabilize recording baselines, prevent amplifier blocking due to high amplitude signals, and reduce low-frequency activity which occurs below the expected power spectrum of EP. Low-pass filters eliminate high frequency activity above clinically-important EP ranges. Cut-off frequencies of low-pass analog filters should be adjusted to no higher than one-half of the digital sampling rate to avoid distortions due to aliasing (the Nyquist effect). A high-frequency cut-off of 100 Hz to 200 Hz could be used for 400/second sampling. A notch filter can be used to minimize line frequency (60 Hz) interference. In the operating room, however, artifact may produce recording oscillations called ringing if a notch filter is used. It is important not to use filters in the range of the EP of interest because they can both attenuate EP responses and alter the latency of EP responses. High-pass filters may advance the apparent latency of slow waves, while low-pass filters may delay apparent peak latencies. A variety of analog and digital filters are available. EP data is collected using analog filters. The data may then be further processed following A – D conversion by using digital filters.

3.4.5 Evoked Potential Recording of Specific Neuroanatomic Systems

General guidelines for recording EP have been developed based on the expected latencies and amplitudes of the visual, auditory, and somatosensory systems (Table 3.1).

Table 3.1 - Recommended Recording Parameters

	Number of Channels	Band Pass	Sweep Length	Typical Number of Trials
VER (VEP)	≥4	1 Hz to 100 Hz (-3 dB)	250 ms	100 to 500
BAER (BEAP)	≥2	10 Hz to 3000 Hz (-3 dB)	15 ms	1000 to 4000
SEP (SSER)	≥4	30-3000 Hz (-6 dB)	40 ms (arm) 60 ms (leg)	200 to 4000
ERP (EP) (P300)	≥3	0.3 Hz to 100 Hz	600 ms to 1000 ms	200 to 400

3.5 Visual Evoked Response

3.5.1 Anatomy

Visual information is conveyed from the retina to occipital lobes via optic nerves, optic chiasma, and lateral geniculate bodies (Figure 3.9). Visual evoked response peaks typically recorded following pattern-reversal stimulation are N75, P100, and N145 over the occiput. The P100 response is the most consistent peak and is normally maximal over midoccipital recording sites.

Figure 3.9 — Visual evoked response recording.

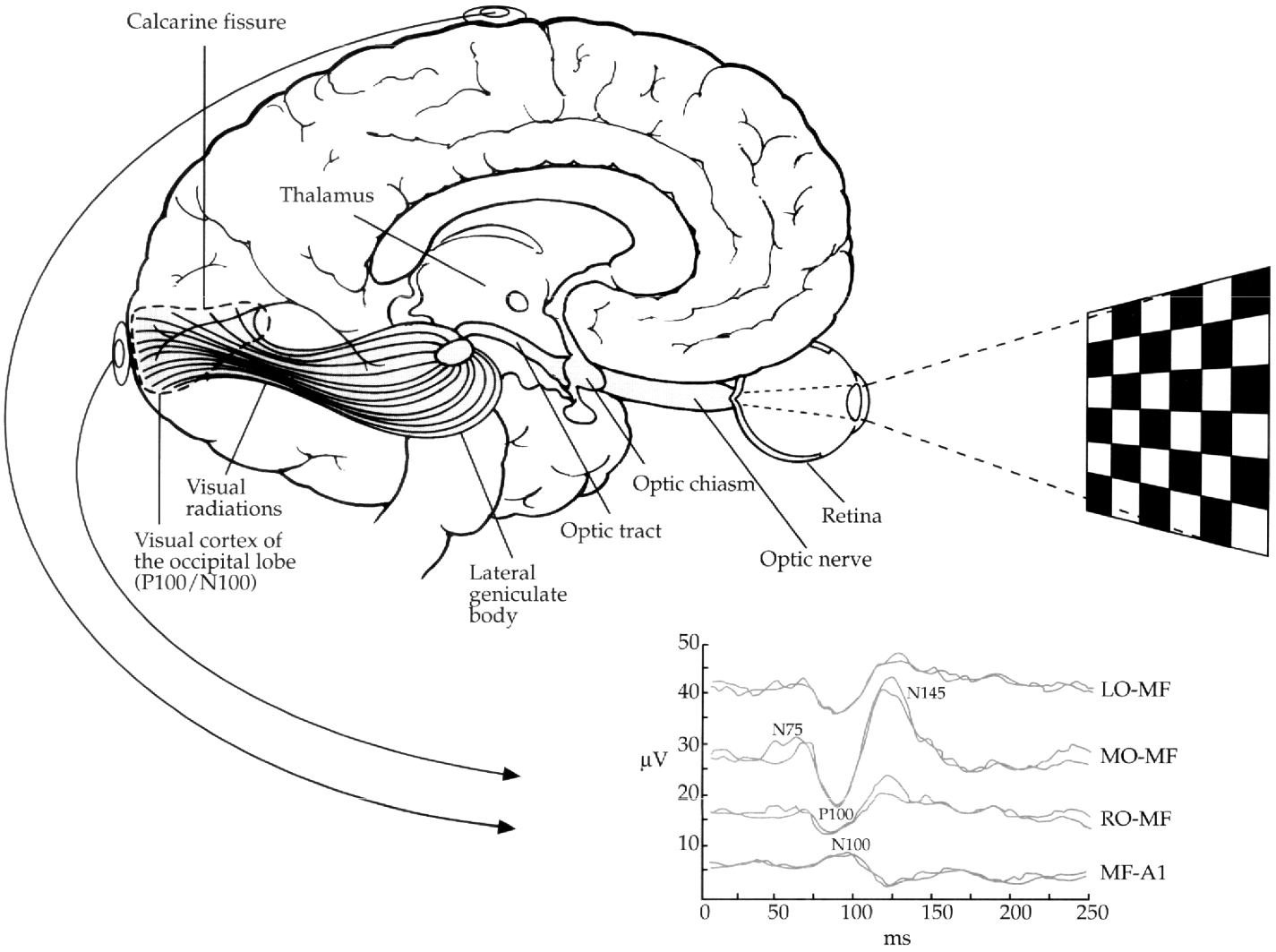

3.5.2 Recording Methods

When recording VERs, a reversing checkerboard pattern is used to stimulate the visual system. This stimulus maintains constant luminosity during stimulation. A visual strobe light stimulus is used for patients who cannot focus on a screen, such as patients with severe refractive impairment, uncooperative or comatose patients, and infants or young children. During strobe stimulation, the latency of peaks varies among patients. Often, only the presence or absence of a response can be evaluated using strobe stimulation.

The distance between the subject and a reversing checkerboard pattern and the check size influences visual responses. This distance is expressed as the visual angle which equals the check width divided by the distance, or B = arctan W/D. For small angles, B = 57.3 (minutes) × [W (mm) ÷ D (mm)]. Smaller checks, ranging from 12 degrees to 16 degrees, stimulate central vision more selectively than do larger checks.

Luminosity directly influences amplitude and latency of VERs, and thus is kept constant. Luminosity is expressed in candela/meter^2 (meters squared). Typically, black and white patterns are turned repeatedly on and off or preferably reversed, so that black and white checks alternate with constant luminosity. Pattern contrast equals the maximum minus the minimum luminosity times 100, divided by the maximum plus the minimum luminosity. Stimulus rates should usually be less than four per second to avoid steady-state stimulation (e.g., one stimulus every 100 ms would produce overlapping P100).

3.5.3 Recording Montage

It is recommended that the VER be recorded using a minimum of four channels with electrodes placed according to the Queen Square System montage:[25]

- Channel 1: left occipital to midfrontal = LO - MF
- Channel 2: midoccipital to midfrontal = MO - MF
- Channel 3: right occipital to midfrontal = RO - MF
- Channel 4: midfrontal to ear/mastoid = MF - A1

3.5.4 Clinical Applications

Most clinical VER testing is performed with monocular stimulation. Monocular stimulation largely screens for ipsilateral prechiasmal lesions (retinal and optic nerve abnormalities) or bilateral hemisphere disturbances. To screen for optic nerve demyelination due to optic neuritis, each eye is stimulated using pattern reversal checks. A delay in the P100 response in either eye is suggestive of an optic nerve abnormality, although a lesion between the retina and chiasm or both hemispheres is still possible (Figure 3.10). An electroretinogram can determine whether a VER abnormality may be due to retinal disease.

Hemifield stimulation, the testing of either the right or visual field, tests for abnormalities in one cerebral hemisphere. Approximately 20% of cortical visual fibers remain ipsilateral. They primarily include the mesial fibers. Hemifields can be tested with slight lateral gaze fixation, such as visual fixation one check over from a centerpoint. Currently, hemifield testing has limited clinical applications.

Important clinical uses of VER are screening for: multiple sclerosis and other demyelinating disorders; optic nerve injury after compressive injury from trauma, hemorrhage, or tumor; hysterical blindness; and, visual function in patients who cannot be tested directly, such as those in coma, infants, or uncooperative patients.

Figure 3.10 — Abnormal visual evoked response due to delayed P100 response during pattern stimulation of the right eye.

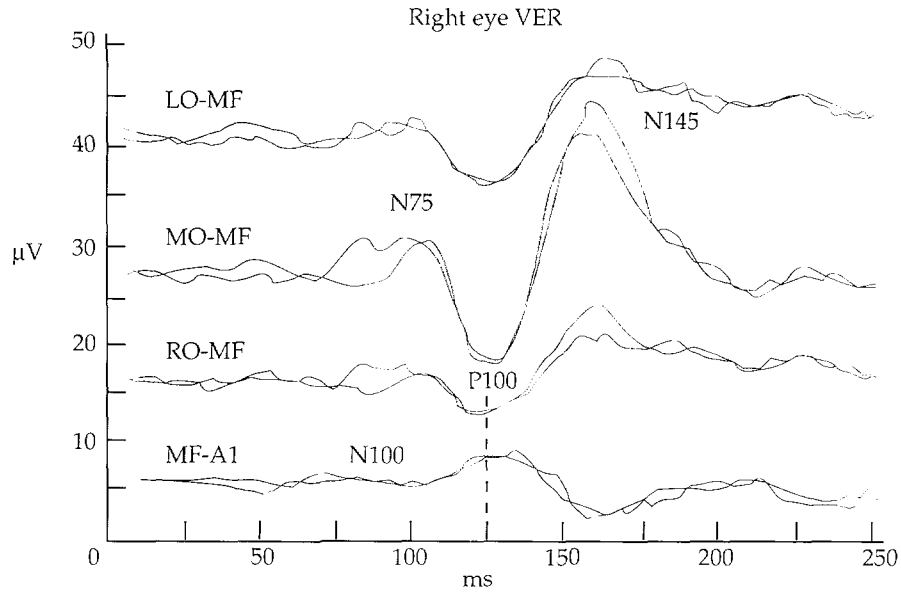

3.6 *Brain Stem Auditory Evoked Responses*

3.6.1 Anatomy

BAERs evaluate the function of several levels of the peripheral and brain stem auditory system, including auditory nerves, the pons, and mid-brain (Figure 3.11). Only the approximate locations of several of the BAER generators are known. Approximate generators of waveforms include: spiral ganglion and auditory nerve near the cochlea (wave I); proximal auditory nerve (wave II); ventral cochlear nucleus or superior olivary complex in the pons (wave III); superior olivary complex and inferior lateral lemniscus (wave IV); lateral lemniscus in the lower mid-brain (wave V); and upper mid-brain, possibly medial geniculate (wave VI). Interwave latencies serve as useful indices of the integrity of these different brain stem levels. A prolonged latency between waves I to III suggests an abnormality between the proximal auditory nerve and the pons, while a prolonged latency of conduction between waves III to V may represent an abnormality between the pons and mid-brain. Absence of wave I, if not due to technical factors, is usually due to a peripheral hearing disturbance.

Figure 3.11 — Brain stem auditory event related responses following auditory stimulation.

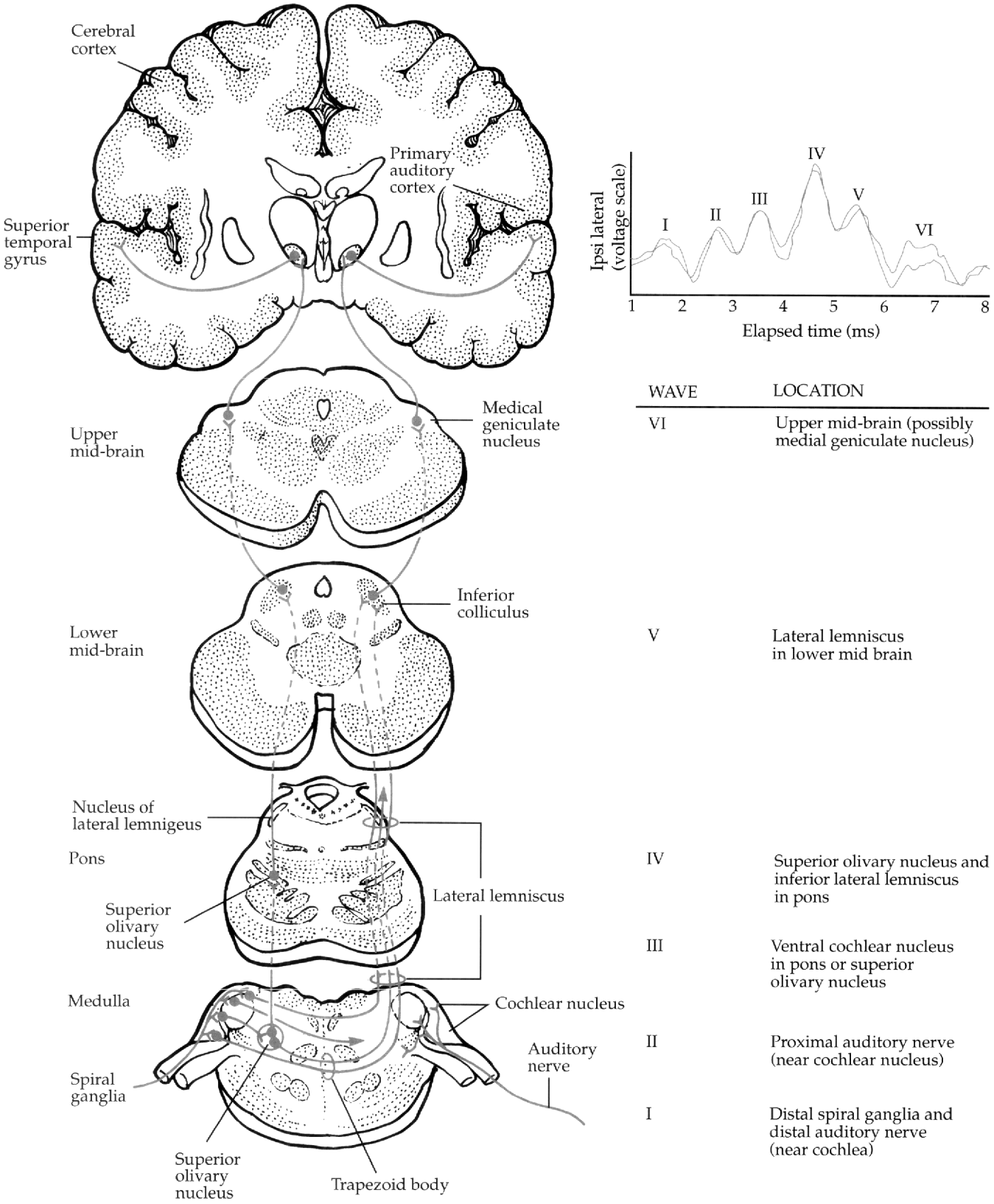

WAVE	LOCATION
VI	Upper mid-brain (possibly medial geniculate nucleus)
V	Lateral lemniscus in lower mid brain
IV	Superior olivary nucleus and inferior lateral lemniscus in pons
III	Ventral cochlear nucleus in pons or superior olivary nucleus
II	Proximal auditory nerve (near cochlear nucleus)
I	Distal spiral ganglia and distal auditory nerve (near cochlea)

3.6.2 Recording Methods

Monaural broad frequency clicks, usually 100 μsec rectangular pulses, are typically used to elicit short-latency BAERs. Tone pips are used for some applications. White noise (40-100 dB) is used to stimulate the contralateral ear and to mask the effects of bone conduction between the contralateral ear and the tested ear. The initial pressure wave of clicks can be negative (rarefaction clicks) or positive (condensation clicks). Rarefaction clicks often produce a larger wave I than condensation clicks, and the remaining peaks may also be sharper. Thus, rarefaction clicks are used for clinical testing. Alternating rarefaction and condensation clicks are not employed because the two together elicit waveforms that may vary in latency and cancel each other. A maximum stimulations rate of 8 to 10 stimuli per second is typically used, because peak amplitudes often decrease at higher rates.

Testing is usually performed with stimuli 30 dB to 40 dB above hearing sensation threshold. Sound intensity is calibrated in several ways, including: dB peak-equivalent sound pressure level (dB pe SPL), using a reference level of 20 Pa or 0.0002 dyne/cm sq; normal hearing level (dB NHL) for a group of control subjects; and the sensation level (dB SL) for individual test subjects.

3.6.3 Recording Montage

The recommended montage for the placement of EEG electrodes is:

- Channel 1: Vertex-ipsilateral ear or mastoid (Cz-Ai or Mi).
- Channel 2: Vertex-contralateral earlobe or mastoid (Cz-Ac or Mc).

3.6.4 Clinical Applications

BAERs are used to test the integrity of the auditory nerve (CN VIII), pons, mid-brain, and auditory pathways. Brainstem lesions may occasionally spare auditory pathways and preserve BAERs. In most patients, however, brain stem lesions due to stroke, tumor, trauma, multiple sclerosis, and hemorrhage are not discrete and involve auditory fiber pathways. BAERs are sensitive screens for detecting acoustic neuromas. BAERs are also sensitive for detecting neural demyelination due to multiple sclerosis and other disorders such as pontine myelinolysis. Concussive injuries may influence BAERs, but these abnormalities cannot reliably be detected in individual patients.

BAERs are useful screens for abnormal increases in hearing threshold (decreased acuity) in patients who cannot be tested with standard audiometry. The appearance of wave V serves as an indicator of the auditory threshold. Auditory screening with BAERs is often performed in infants who are at risk for hearing impairment, including premature infants, infants who have suffered meningitis, and patients exposed to ototoxic antibiotics.

3.7 *Somatosensory Evoked Potentials*

3.7.1 Anatomy

Stimulation of the median, tibial, and other nerves elicits neural responses in the proximal spinal nerve roots, spinal cord, brain stem/thalamus, and the parietal cortex. The sensory

portion of these nerves includes large myelinated fibers that project to the posterior column of the spinal cord. Sensory fibers decussate and cross in the lower brain stem and then project to the contralateral medial lemniscus in the brain stem and to the sensory thalamus and sensory parietal cortex. Anatomic correlates for EP elicited by median nerve stimulation are: Erb's point (brachial plexus), N13 (upper cervical spinal cord), P14 (caudal brain stem medial lemniscus), N18 (multiple sources in upper brain stem and possibly thalamus), and N20 (somatosensory parietal cortex). Somatosensory pathways for the median nerve and typical normal SEP are shown in Figure 3.1. The EP responses elicited with stimulation of the posterior tibial nerve in the leg are: LP (lumbar cord), N34 (multiple sources in upper brain stem and possibly thalamus), and P37 (somatosensory parietal cortex). Somatosensory pathways for the posterior tibial nerve and typical SEPs are shown in Figure 3.12.

3.7.2 Recording Methods

Transcutaneous stimulation employs stimulating cathode and anode placed over a nerve. A ground electrode is placed on a limb between a distal stimulation site and the more proximal recording site. Stimulation intensity is set to above the motor threshold. Rectangular, monophasic stimulation pulses are used. Pulse width is typically 100 μsec to 300 μsec with rates of 3 Hz to 5 Hz. Contact impedance is preferably less than 5000 Ω to reduce discomfort.

Either constant-current or constant-voltage stimulation is used. Recording is typically performed over the structure of interest (e.g., brachial plexus at Erb's point above the clavicle).

3.7.3 Recording Montages

Four, and preferably eight, channels are necessary to record the SEP. Recommended electrode montage for the median and tibial nerves SEPs are:

Median Nerve SEP:

- Channel 1: Erb's point ipsilateral to stimulation reference (usually contralateral Erb's point); EPi-REF.
- Channel 2: cervical spine (C5)-reference; C5S-REF.
- Channel 3: centroparietal scalp ipsilateral to stimulation (CPi=halfway between C3 or C4 and P3 or P4)-reference; CPi-REF.
- Channel 4: centroparietal scalp contralateral to stimulation - centroparietal scalp ipsilateral; CPc-CPi.

Tibial nerve SEP:

- Channel 1: thoracic spine (T12) reference (usually iliac crest or midthoracic area); T12S-REF.
- Channel 2: midline frontopolar scalp (Fpz)- cervical spine (C5S); Fpz-C5S.
- Channel 3: midline centroparietal scalp (Cpz) frontopolar scalp (Fpz); Cpz-Fpz.
- Channel 4: ipsilateral centroparietal scalp (Cpi) frontopolar scalp (Fpz); CPi-Fpz.

Figure 3.12 — Somatosensory evoked potential responses following leg stimulation.

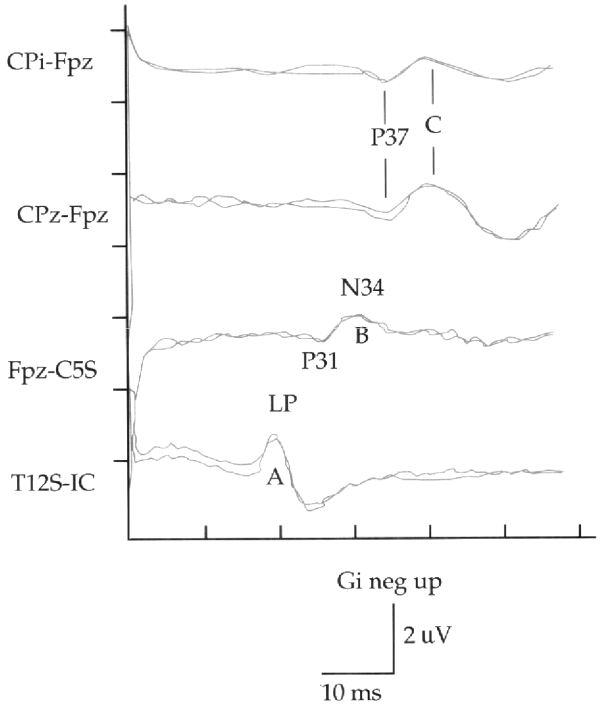

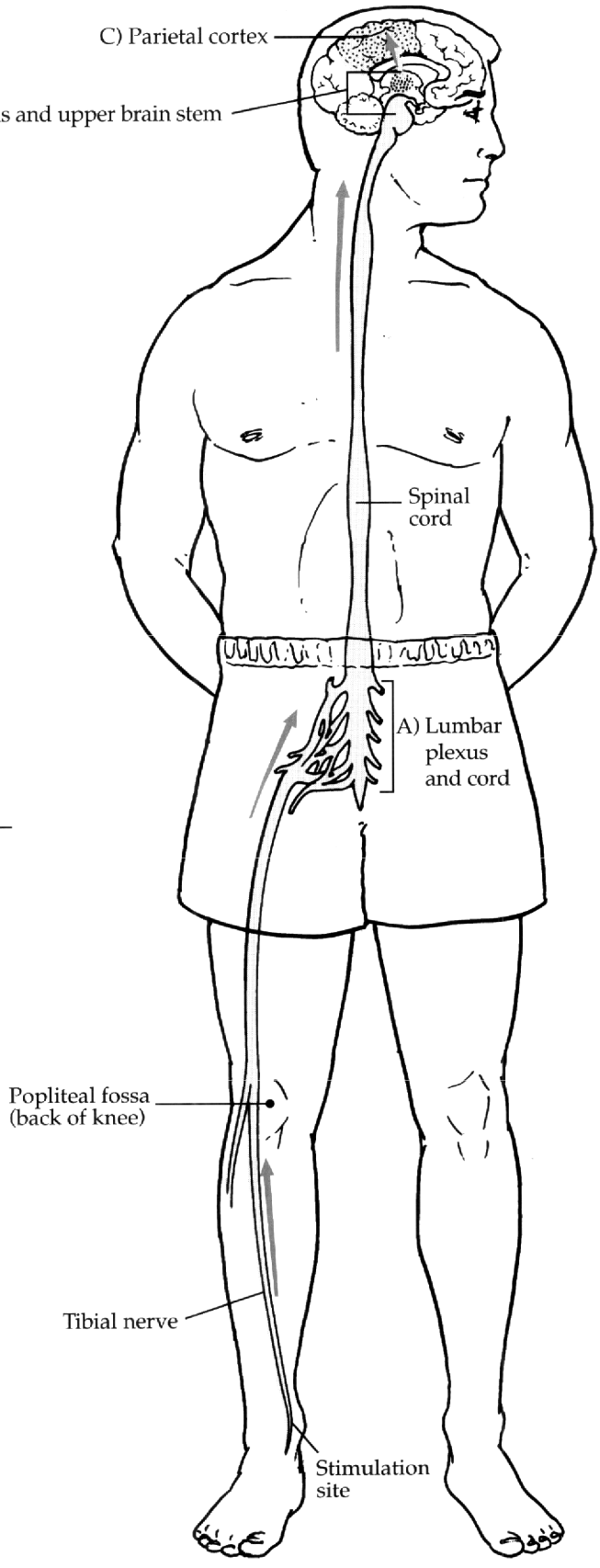

3.7.4 Clinical Applications

SEPs serve to screen for neural conduction abnormalities in the large fiber sensory system in the posterior spinal cord, brain stem medial lemniscus system, and sensory parietal cortex. Figure 3.1 illustrates a normal median nerve SEP. Figure 3.2 presents an example of an abnormal arm SEP in the EP-P/N13 segment due to an injury between the brachial plexus and cervical spinal cord. Since SEP responses can only be reliably detected at a few points along the entire sensory conduction system, localization of SEP abnormalities is often imprecise. A SEP abnormality between the lumbar potential and upper brain stem response with tibial nerve stimulation cannot further localize the abnormality between these distant structures. SEPs are particularly sensitive to demyelinating disorders such as multiple sclerosis, transverse myelitis, and adrenoleukodystrophy. SEPs are also useful screens for spinal cord and brain stem injury such as that due to trauma, myelopathy and ischemia. SEPs may be useful for demonstrating normal function in patients with hysterical paralysis and sensory deficits and in determining the prognosis in coma. The absence of brain stem and cortical SEP responses correlate with an outcome of death or vegetative state in coma.[26]

3.8 *Intraoperative Monitoring*

In the operating room, electrodes can be placed adjacent to conducting structures and EP can be used to monitor the integrity of the spinal cord, proximal nerve roots, and other structures during the surgical procedure. During scoliosis repair, for example, the spinal cord may be injured when the spine is straightened. An abnormal tibial SEP can alert the surgeon that spinal cord compression has occurred, allowing spinal retraction to be reversed before permanent damage results.

Intraoperative EP monitoring can aid in other surgeries that risk injury to the spinal cord, including resection of spinal cord tumors, major abdominal vascular surgery, and repair of spinal deformities. The posterior spinal cord sensory pathways monitored by SEP may remain intact, however, despite paralyzing injury to the anterior spinal cord motor pathways. Motor EPs using electrical and magnetic spinal cord stimulation are under investigation to test spinal cord motor function more directly during surgery.

Figure 3.13 represents an example of spinal cord SEP monitoring. Normal tibial nerve SEPs are lost when the spinal cord is traumatized by the passage of a sublaminar wire. The SEPs partially return following several interventions, including increasing blood pressure, increasing hypothermia, and the administration of steroids.

Intraoperative monitoring is also used to assess hearing and facial motor function during posterior fossa or lateral skull surgery. Hearing and facial strength can sometimes be preserved by monitoring the BAERs along with facial electromyography during the removal of acoustic neuroma and tumors adjacent to facial and auditory nerves.

3.9 *Event-Related Potentials*

Evoked potentials recordings measuring long-latency perceptual and cognitive processing in the brain are called event-related potentials (ERP). ERP are later in latency than sensory EP and correspond to mental operations involved in various perceptual and cognitive tasks. One of the largest and most easily elicited ERP response is called the P300. This is an approximately 200 to 600 msec positive response elicited by changes in a stimu-

Figure 3.13 — Intraoperative spinal cord monitoring using leg SEP, (a) passing sublaminar wires; (b) spinal cord struck with wire, SEP signal lost; (c) end of surgery, SEP signal recovers.

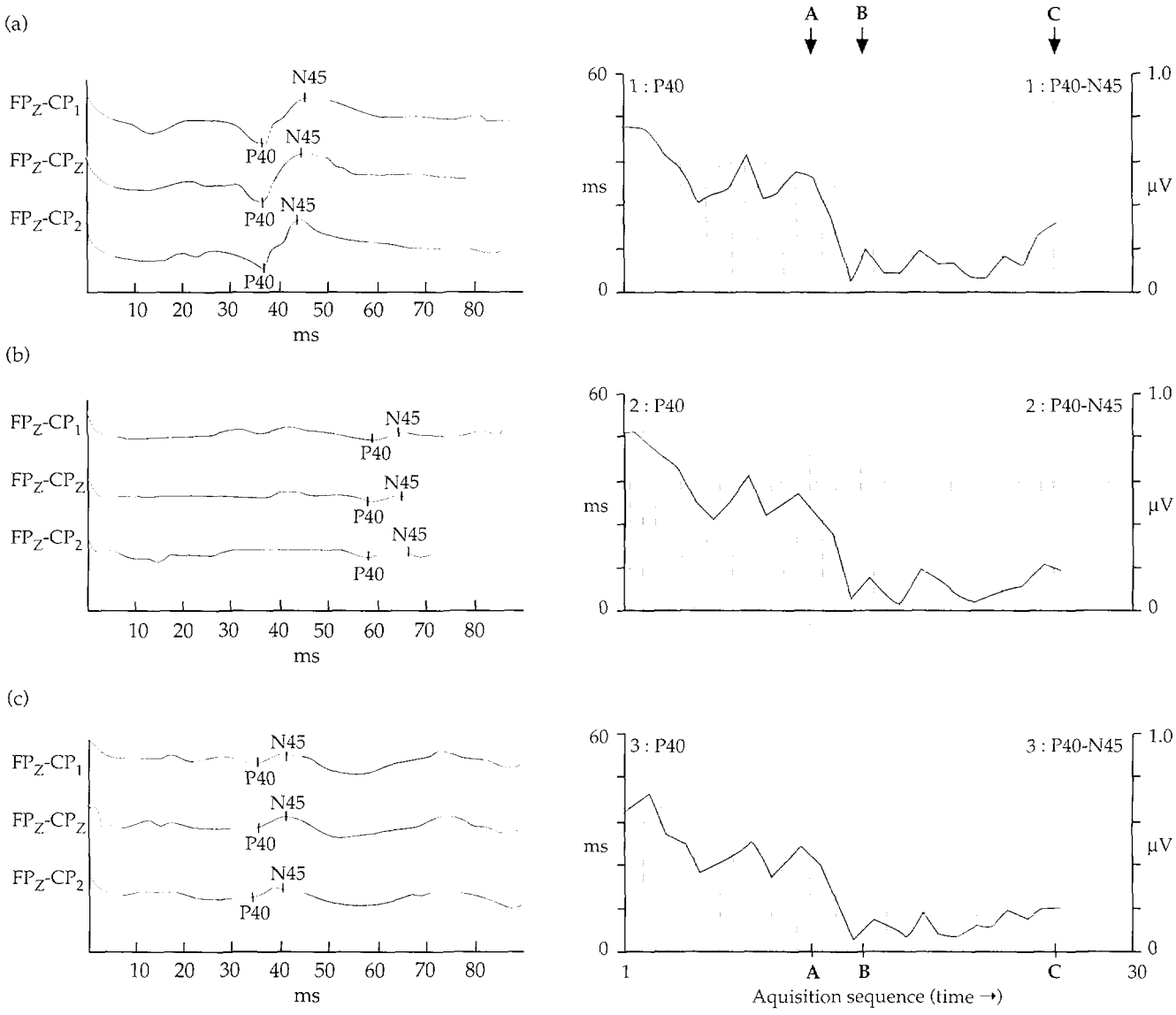

Figure 3.14 — *Event-related potential recording: a large positive shift in brain electrical activity (P300) appears during exposure to an infrequent stimulus.*

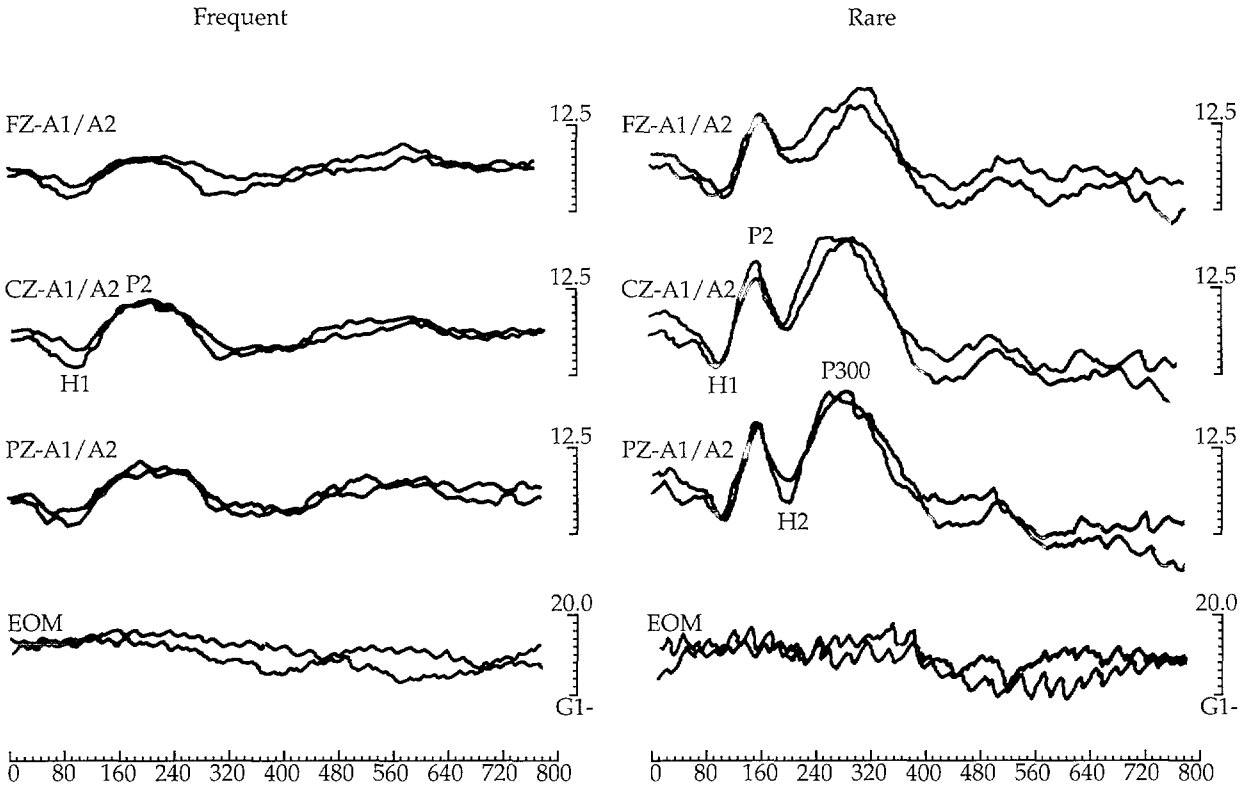

lus train during an attended task. A common paradigm for eliciting P300 activity is the oddball task: an enhanced positive response (P300) is elicited when repeated visual or auditor stimuli are interrupted by a novel stimulus (Figure 3.14). P300 is best seen when ERP waveforms recorded during high probability (standard) stimulus conditions are subtracted from ERP recorded for the low probability (non-standard) stimulus conditions. P300 is under evaluation as a clinical test to screen for changes in cerebral function.

A major difficulty in using ERP clinically to screen for cognitive abnormalities is that ERP latencies vary considerably between individuals. These individual variations often make it difficult to differentiate patients who have P300 abnormalities from normal subjects. Despite these limitations, however, ERP are useful for evaluating serial cognitive changes in patients, particularly when a treatment intervention has occurred. ERP have been used successfully to monitor patients with AIDS dementia, dyslexia and other cognitive disorders.

Another major use of ERP are investigating the sequence of mental processes engaged by various mental tasks. Attention, orientation, and memory are among the cognitive processes being investigated using ERP recordings.

4.0 INTRAOPERATIVE BRAIN MONITORING USING ANALOG AND COMPUTER-PROCESSED EEG

4.1 *Background*

During the past decade, new microcomputer technology has resulted in improved intraoperative monitors that allow safer anesthetic and surgical management of patients. Among the most significant are a new generation of brain monitors that can have a dramatic impact on the administration of anesthesia and reduction of surgical risks.

Neurophysiological monitoring during major surgery and anesthesia has become an essential element of the anesthesiologist and surgeon in the operating room (OR) and Intensive Care Unit (ICU) environments. Changes in the electroencephalogram (EEG) and evoked potentials (EPs) can be easily displayed and quantified by high-technology, microcomputer-assisted brain monitors for rapid on-line interpretation. The intent of this section is to introduce the basic principles and theories of intraoperative brain monitoring, and the interpretation of spontaneous and computer-processed EEG during general anesthesia and major surgery. A number of practical strategies have been implemented for incorporating computer-processed brain monitors into the anesthetic and surgical arenas for adult and pediatric cardiac, vascular, neurological, and orthopedic surgeries.

Modern anesthesiology has slowly begun to stress the importance of applying intraoperative brain monitoring techniques to assess the effects and depth of anesthesia, to prevent awareness, and to recognize and prevent anesthetic and surgical complications.[27,28] While the accelerated development of microprocessor technologies has fostered an extraordinarily rapid growth in EEG as well as multimodality EP and transcranial Doppler (TCD) monitoring devices for application during anesthesia and surgery, the primary advances afforded by commercial and academic research have included: (1) easier-to-interpret, computer-transformed images of the EEG, EP, and TCD signals, and (2) quantification and computer-processed indices for on-line clinical assessment as well as for subsequent statistical analyses.

Historically, interest in the EEG patterns associated with anesthesia is as old as the discovery of the EEG itself; however, there is still no universal adoption of a monitoring technique or of criteria for its neural end-point by anesthesiologists and surgeons. Although the brain is the major target organ of anesthetic drugs, ironically this organ system has been largely ignored for routine monitoring during anesthesia and major surgery. This has been repeatedly ascribed to numerous reasons including: (1) large, bulky, expensive equipment; (2) the need for experienced personnel to operate the equipment and interpret the signals; (3) the difficulty of recording the EEG in an electrically hostile environment; and (4) the inexact relationship between EEG changes and anesthetic drugs, and effects of surgical procedures. Recently, concerns such as cost, degree of user friendliness, validity, and reliability have been successfully addressed by a highly competitive commercial market, making routine application of this technology substantially easier and more practical.

The primary clinical outcomes for which modern intraoperative EEG technology has made significant contributions include: 1) brain monitoring for drug administration in order to determine depth of anesthesia or to tailor drugs to a predefined neural effect for a variety of anesthetic end-points; and 2) recognizing and/or preventing perioperative ischemic insults. These issues are addressed below.

Figure 4.1 — Digital power spectral analysis and various types of computer-enhanced displays of the analog EEG.

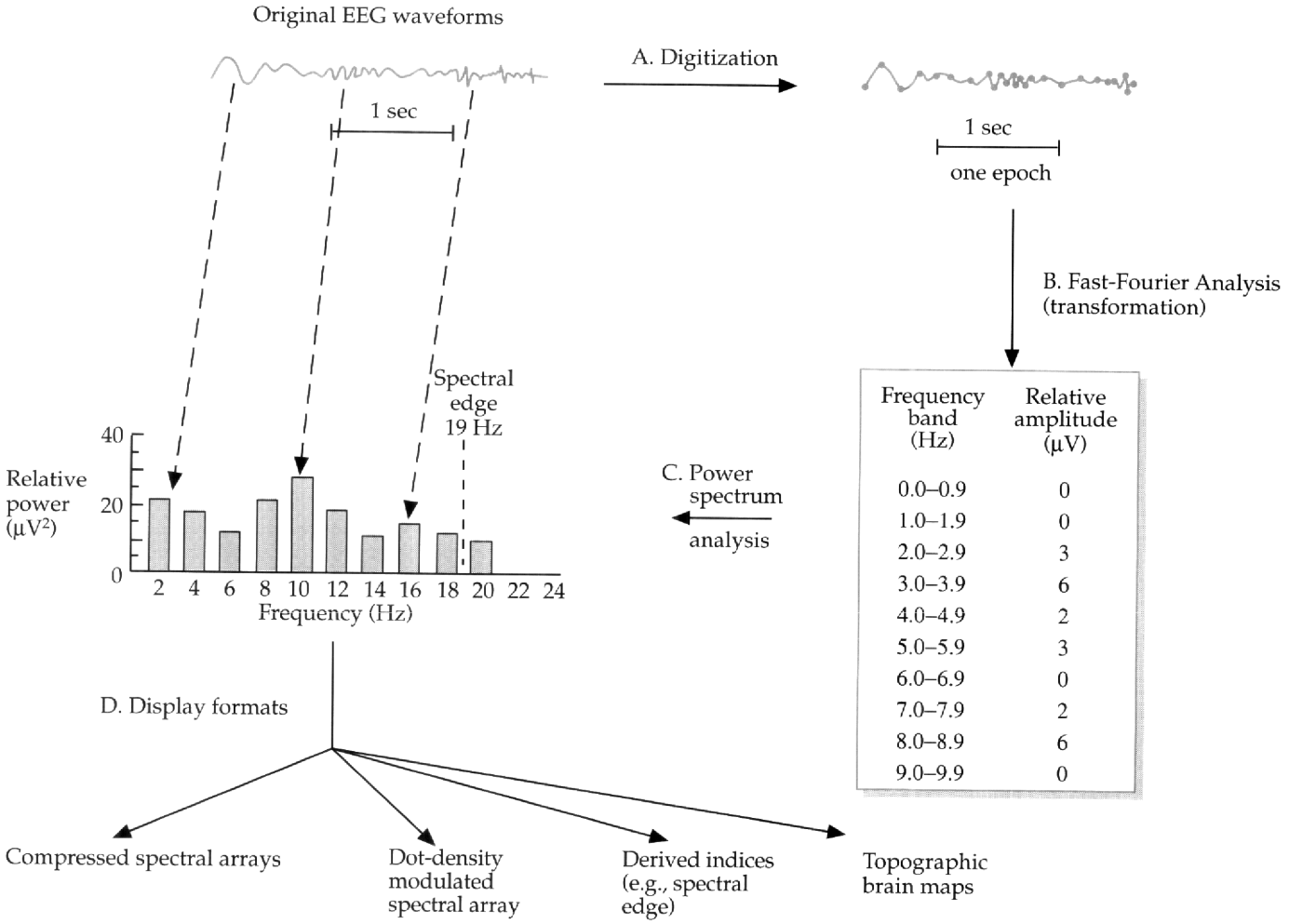

4.2 Digital Power Spectral Analysis, Derived Measures, and Computer-Enhanced Displays

The EEG is classically defined as the spontaneous (analog), scalp-recorded electrical potentials of the cortex, the continuous "roar" or "noise" of the brain.[29] More specifically, these gross potentials are the composite (spatial and temporal summations) of negative and positive waves resulting from graded summations of excitatory and inhibitory postsynaptic potentials in millions of cortical neurons, primarily layer III pyramidal cells. For descriptive purposes, a sample or epoch of EEG may be divided into two general types of activity: (1) ongoing background activity, and (2) activity representing either event-related changes or transients which appear suddenly and are of relatively short duration. These and other issues are discussed in Section 2.0.

Figure 4.2 — Mathematical and display techniques used to generate the compressed spectral array format.

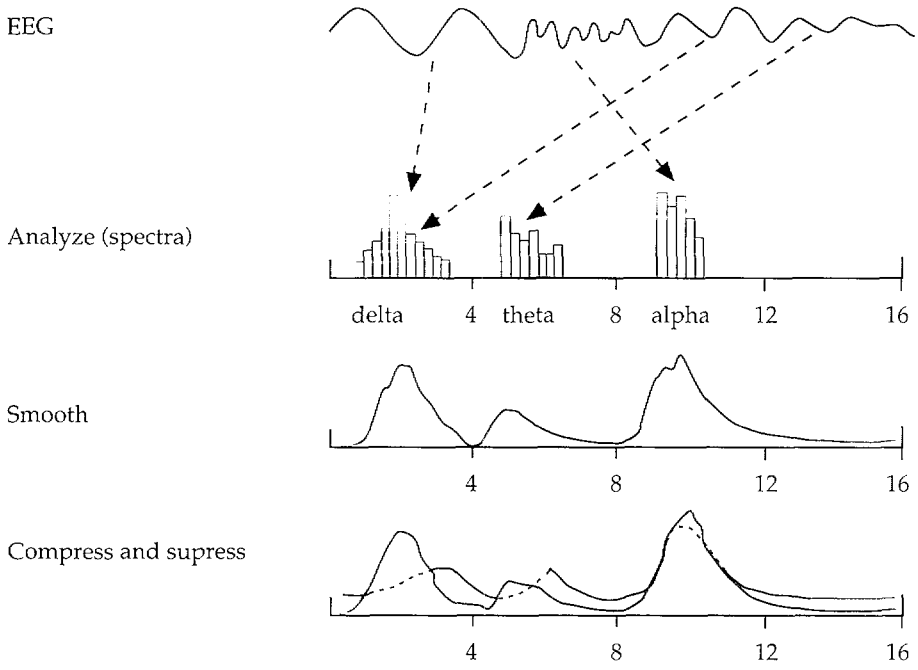

Figure 4.3 — (a) CSA display created from spectral analysis of the raw data shown at the bottom; (b) conventional trace or epoch of the analog EEG for alpha activity recorded from a single channel over the posterior brain.

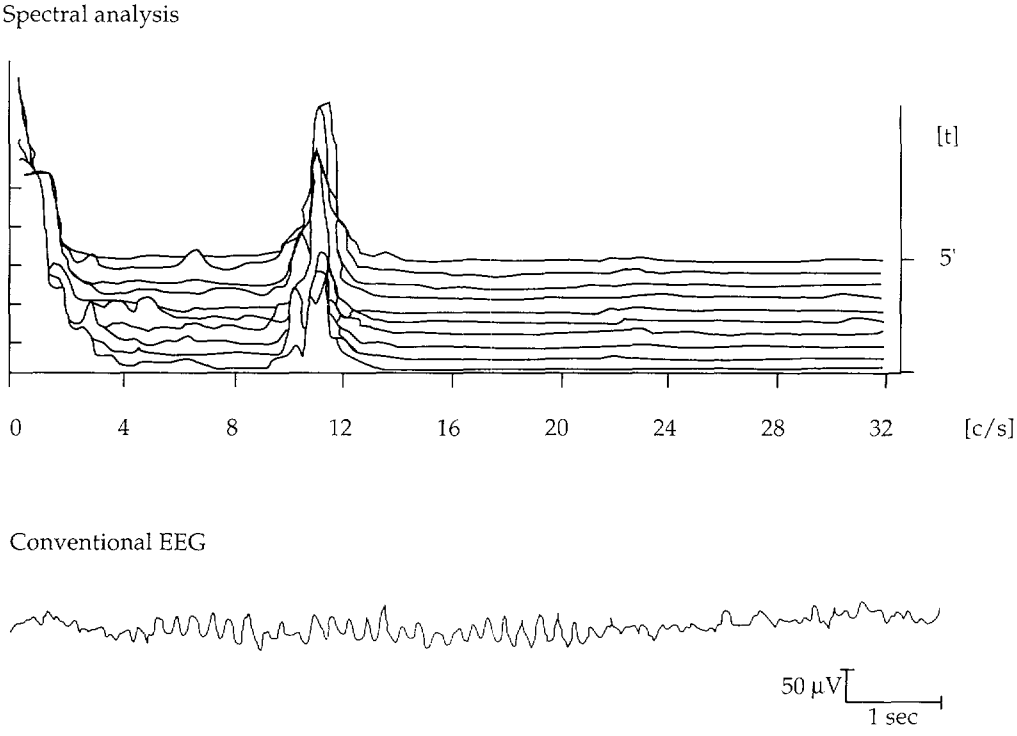

Assessment of the frequency and amplitude of the EEG is crucial for rapid and accurate interpretation; however, such assessment is quite difficult using the analog signal and naked eye. Thus, several methods have been developed to extract and present the frequency and amplitude information in simple, visually-enhanced formats that are useful to the clinician.

The schematic shown in Figure 4.1 depicts the process of digital power spectral analysis (DPSA) of the analog EEG and of the various types of computer-enhanced visual displays of the mathematically transformed or Fast-Fourier transformed (FFT) data. In general, spectral analysis transforms the analog EEG signal recorded on the time axis into a signal displayed on the frequency axis (Figure 4.1, a to d). Furthermore, it is the most common form of computer-processed EEG; almost all commercially-available devices employ this type of analysis. In Figure 4.1:

a. The first process, **signal amplification** and **filtering,** is not shown and can occur at several stages of computer-assisted EEG analysis. The next process is to **digitize an artifact free signal,** (i.e., the analog or continuous signal is separated into discrete elements).
b. **Fast-Fourier transformation** of the digitized EEG waveform is a mathematical transformation of a complex waveform (defined as any waveform having varying frequency and amplitude content) into simpler, more uniform waveforms (such as different sine waves of varying amplitudes).[30] For power spectral analysis, an epoch of EEG is typically broken down into component sine waves at intervals of 0.5 Hz over a range of 1 to 32 Hz.
c. The **power spectrum** is then calculated by squaring the amplitudes of the individual frequency components. Thus, the EEG signals recorded on the time axis are transformed and displayed on the frequency axis.
d. Several different **display formats** have been developed for visually enhancing the computer-processed power spectrum, such as: (1) the compressed spectral array (CSA);[31,32] (2) the dot-density modulated spectral array (DSA);[33] and (3) color-scaled, topographic brain maps.[34]

These computer-enhanced images can give the user an impression that each anesthetic drug or combination of agents or that each surgical event may produce its own signature or fingerprint in the EEG profile. For CSA and DSA display formats, brain power (μV^2) and time are plotted against frequency.

In the CSA display format, a series of computer-smoothed spectral arrays are stacked vertically, with the most recent EEG event at the bottom and the oldest at the top. Peaks appear at frequencies which contain more power or make larger contributions to the total power spectrum. Since the origin of the plot shifts vertically with time, this produces a pseudo three-dimensional graph (Figures 4.2 and 4.3). Because data can be obscured by the hill-and-valley format, another method for displaying power spectra (DSA) was developed (Figure 4.4). This format displays a power spectrum as a line of variable intensities and/or densities with successive epochs again stacked vertically as in the CSA plots. Areas of greatest density represent frequencies which make the greatest contribution to the EEG power spectrum. A major advantage of the DSA format is that no data is hidden by the peaks as in the CSA display. The methods by which commercial instruments perform the above-mentioned steps are all relatively similar. The major differences among instruments are in display formats, derived measures, storage, and statistical processing capabilities.

Figure 4.4 — Snapshot of the pre-anesthesia baseline EEG displayed as a gray-scaled DSA along with the spontaneous waveforms recorded by the 2-channel Cerebro-Trac 2500 PLUS.

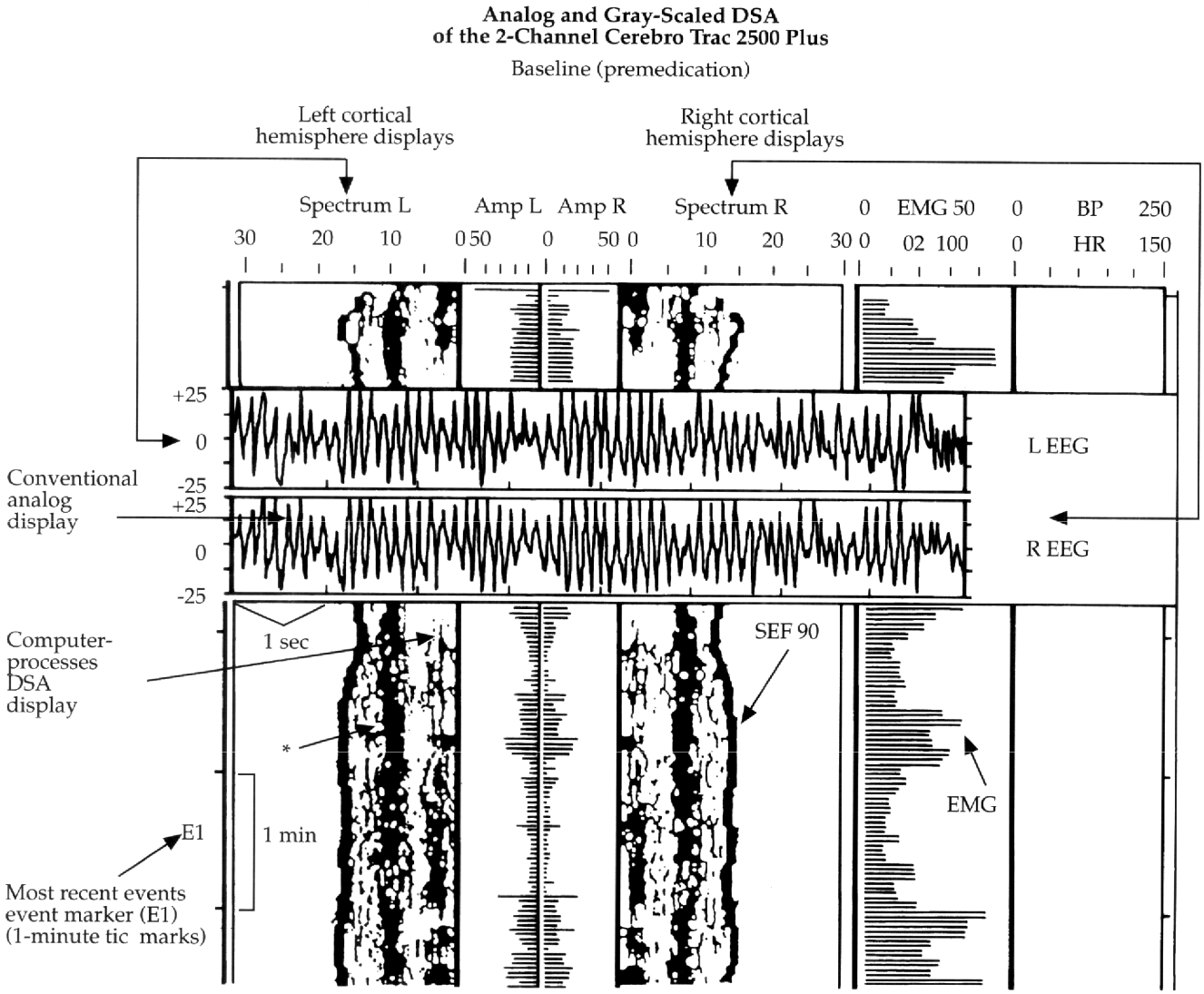

SEF 90	spectral edge frequency, 90%
AMP	EEG amplitude (AMP)
EMG	spontaneous frontalis EMG (EMG)
S_pO_2	oxygen saturation (0_2)
MAP	mean arterial pressure (BP)
HR	heart rate (HR)

Event: holding area baseline (premedications, MS; 0.1 mg/kg; Scopolamine, 0.005 kg/mg; Diazepam 0.15 mg/kg)

Analog display: with eyes closed, characteristic alpha rhythm (8-10 Hz)

DSA display: dominant narrow alpha band (*) at 8-10 Hz with SEF=17 Hz for each hemisphere.

Figure 4.5 — A generic CSA format with SEF indicated by a discontinuous line of box markers which track along the highest visible frequencies of the power spectrum. Typically, the SEF is the value below which is contained 95% or 97% of the brain power for a given spectral array of analyzed EEG.

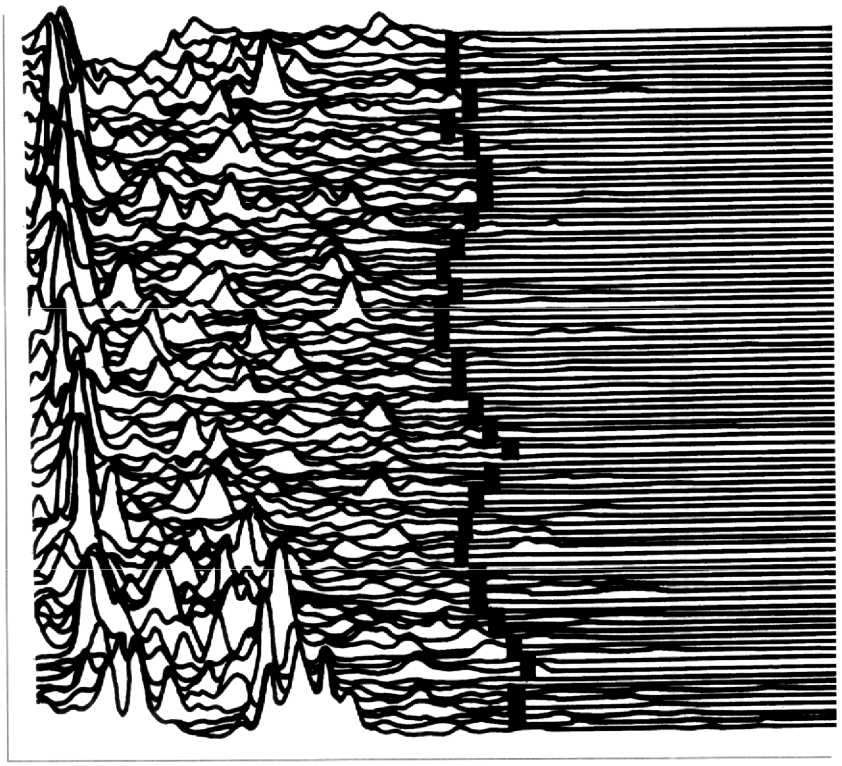

4.2.1 Brain Power, CSA/DSA Formats, and Spectral Edge Frequency

Perhaps the most informative, reliable, and widely used techniques in routine clinical practice today for displaying brain power across the EEG spectrum are the CSA or DSA formats, with derived indices such as spectral edge frequency (SEF95 or 97), mean or median frequency, peak power frequency, power band ratios, coherence, asymmetry and magnitude estimates [e.g. peak-to-peak or RMS amplitude (μV), and absolute (μV^2) or relative brain power ($\mu V^2\%$)]. DSA displays include two varieties: gray- or color-scaled densities. To further simplify and/or assist the display of the entire power spectrum of the EEG, the DSA and CSA formats use a single number, the SEF, for any given epoch (Figures 4.1, 4.4, and 4.5).[35]

From a qualitative perspective, SEF is the highest visible frequency component of the EEG spectrum. Quantitatively, SEF is calculated typically as the frequency below which 95% (SEF95) of the total brain power is contained. The SEF is, thus, a derived index of cortical activity that compresses the entire EEG waveform into a single number for clinical

Figure 4.6 — A compressed spectral array showing the sinusoidal variation in the inspired concentrations of halothane.

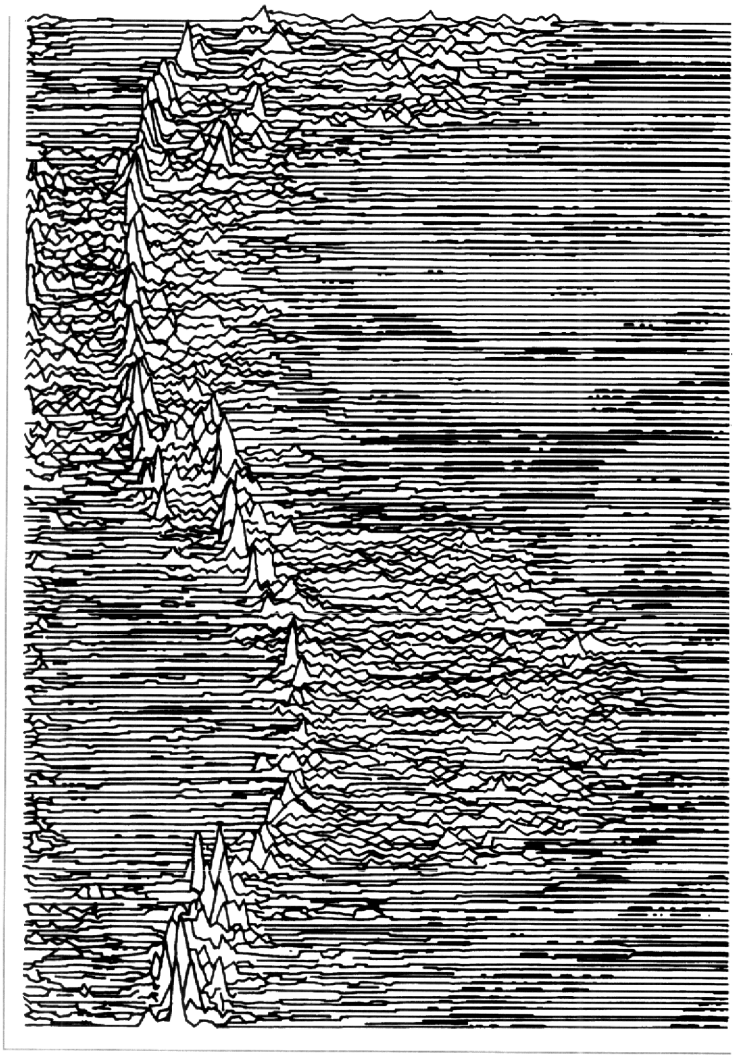

judgments and statistical analyses. Changes in the power spectral analysis and derived measures such as SEF have been shown to correlate in a rather orderly and predictive fashion with: (1) depth of anesthesia and concentration of agent for a variety of drugs (e.g., halothane[36] and serum concentrations of thiopental, fentanyl and alfentanil);[37,38] (2) awareness levels;[27] (3) hemodynamic response to laryngoscopy;[39] and (4) tailoring induction doses of narcotics to a predefined neural fingerprint.[40-42]

Figure 4.6 shows a remarkable correspondence in the variation of the brain power displayed as a compressed spectral array and the sinusoidal variation in halothane concentration.[36] The sine wave period was 31 minutes with trough and peak concentrations of 0.42% and 2.94%, respectively. As halothane was decreased there was an increase in brain power in the higher frequencies (more hills) and a decrease of the lower frequencies (less hills). As halothane was increased, brain power shifted to the lower frequencies in the spectrum and was represented by an increase in peaks.

Figure 4.7 — (a) Analog EEG stages for fentanyl and alfentanil inductions; (b) time course of spectral edge and serum fentanyl concentrations. Fentanyl infusion rate = 150 μg/min; (c) time course of spectral edge and serum alfentanil concentrations. Alfentanil infusion rate = 1500 μg/min (solid bar). Note the inverted spectral edge axis.

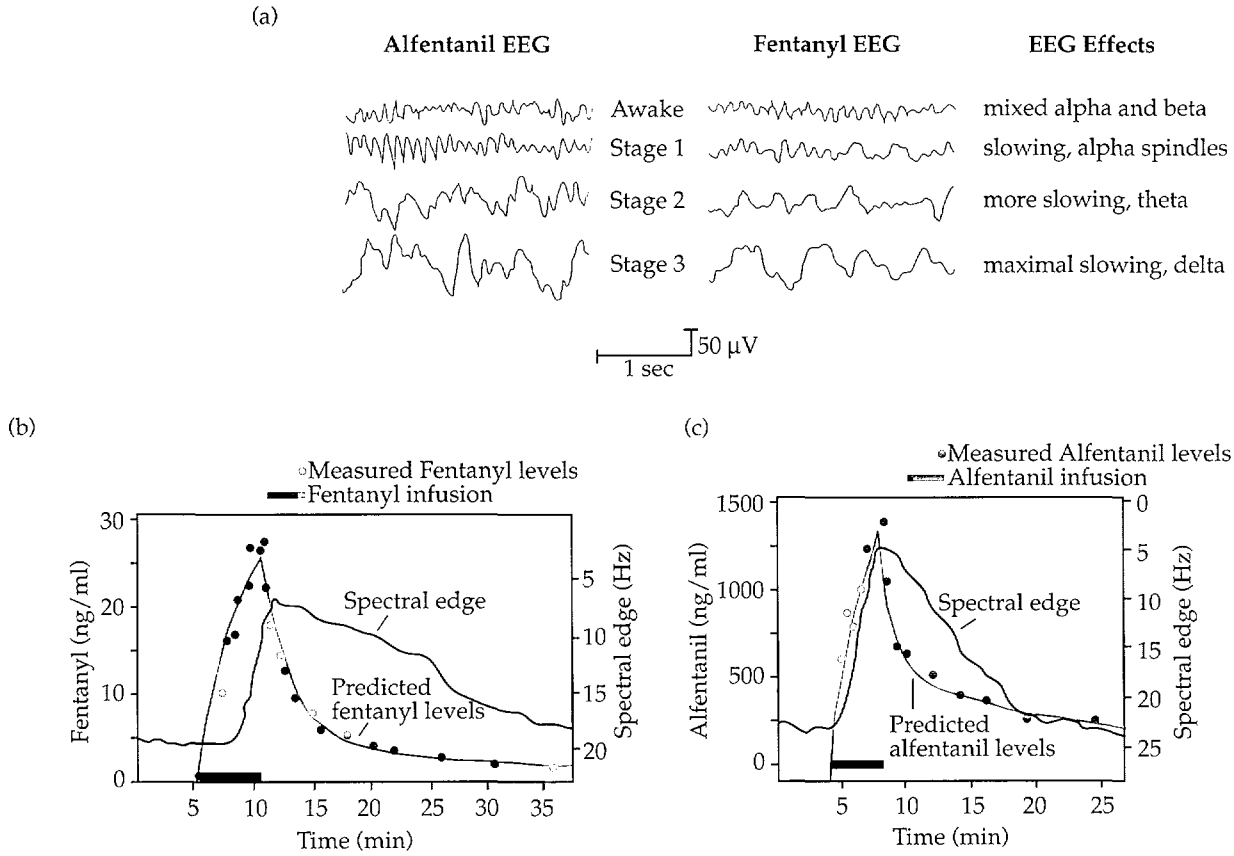

Figures 4.7a, b, and c illustrate a similar correspondence between SEF and induction doses of synthetic opioids. Figure 4.7a shows the changes in the analog EEG signal with anesthetic induction using alfentanil and fentanyl, respectively. Figures 4.7b and 4.7c illustrate the correspondence between SEF values and changes in serum concentrations of each anesthetic drug.

In part, the criteria for clinical recognition of anesthetic effects, particularly an induction end-point, are dependent on preferences for type of computer-generated and trended indices. However, a general picture has begun to emerge about the induction effects of opioids based on the digital power spectrum of the EEG, and, thus, some of the criteria for the clinical recognition of a primary, or predefined, induction end-point for neural activity. Although the single most important or exact subset of derived measures has yet to be clinically identified, it is apparent that dynamic and consistent changes in enhanced, visual displays, and derived indices afforded by DSPA in general, have proven to be sensitive for assessing the EEG effects of drug administration.[37,38,43]

Of the computer-derived indices of the power spectra which compress the power spectrum of the EEG into a single or unitary descriptor or activity measure (e.g., peak or

mean frequency, magnitude indices, power band ratios), SEF has received substantial support as a useful clinical index of anesthetic depth. For example, threshold doses of opioids have been determined for adequate anesthesia based primarily on power spectral analysis of the delta bandwidth and SEF.[37,38,43] This is presented in greater detail in the section on synthetic opiates.

Lastly, recent criticism has been raised about the appropriateness of the mathematical basis for applying spectral analyses to processing analog EEG. Spectral analysis assumes an independent relationship among its sine wave components. Since electrical brain waves such as the EEG exhibit nonlinear behavior and intercomponent relationships, an alternative form of processed analyses called bispectral analysis has been recently applied with interesting success in studies of anesthetic drug effects. Bispectral analysis measures the potential interactions between the waves to determine whether dependent components are present. For example, if two fundamental waves are generating a harmonic, then the harmonic's frequency is equal to the sum of the frequencies of these fundamentals and the phase of the harmonic is equal to the sum of the phases of its fundamental components. Thus, bispectral analysis quantifies the phase coupling between every possible frequency pair combination and their sum in order to determine if the component waves are harmonics or fundamentals. Recent studies have demonstrated that bispectral analysis may enhance the overall value of computer-processed EEG as a depth of anesthesia indicator[44] and provide additional information about anesthetic depth at incision when compared to conventionally processed EEG parameters such as SEF and median frequency.[45,46]

4.3 Anesthetic Drug Effects

Hans Berger, the father of modern clinical electroencephalography, was the first to describe the effects of drugs (e.g., cocaine, phenobarbital, chloroform, and scopolamine) on the human EEG. Although numerous studies and reviews have concentrated on the EEG changes associated with anesthesia, the normal practice of modern anesthesia involves polpharmacy or the use of a combination of anesthetic agents for premedication and balanced anesthesia.[47] For example, most patients are premedicated prior to surgery and the administration of general anesthesia. Thus, the EEG effects often observed and assessed are not necessarily the effects on background rhythms typically associated with each drug alone.

This section will focus on the changes in the analog and computer-processed EEG which are associated with general anesthesia, particularly induction. Although each anesthetic agent produces a characteristic pattern in background rhythm, several general stages can be defined based on clinically defined and electroencephalographically defined changes (Figure 4.8).[48] In Figure 4.8 the alpha rhythm typifies the relaxed, conscious state. With light levels of anesthesia, the alpha rhythm gives way to a faster rhythm in the beta range. As this excitement phase is passed with increasing levels of anesthesia, wave frequency decreases until a delta pattern prevails. If further CNS depression occurs, the waveforms become more complex with a clear persistence of slow waves. At even deeper levels, alternating periods of electrical silence are interrupted by bursts of high voltage activity known as burst suppression. At the deepest level of anesthesia, total electrical silence, or an isoelectric EEG, is reached.

Figure 4.9 shows a comprehensive summary of the distinct, definable stages of anesthesia based on traditional clinical parameters such as respiration, pupil size, and various reflexes as compared to those which can be determined by EEG changes. The stages of in-

Figure 4.8 — A diagram of the average changes in the patterns of the EEG with increasing depths of anesthesia.

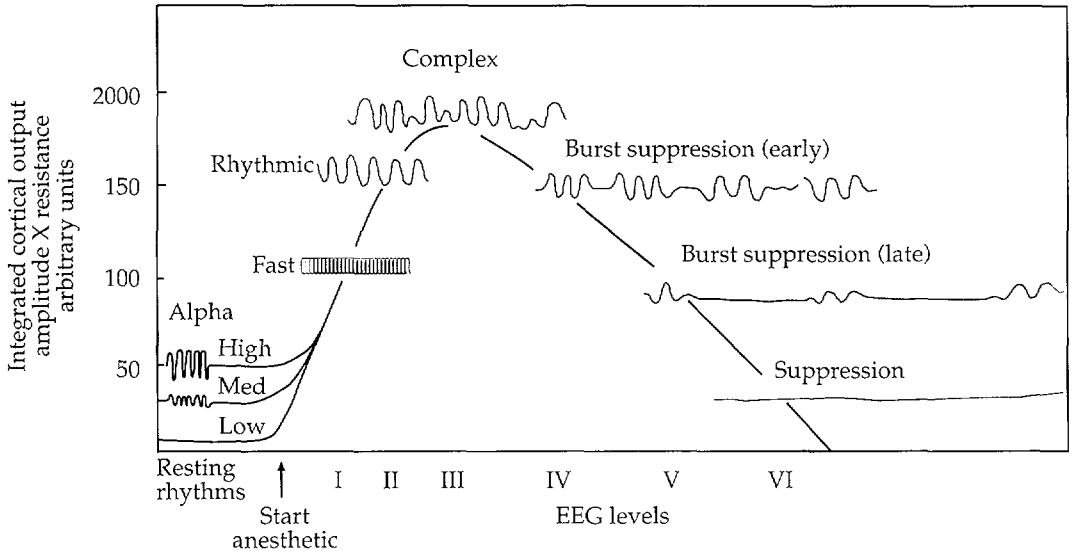

Figure 4.9 — Characteristic clinically-defined and encephalographically-defined changes according to the effect of the individual stages of anesthesia on the central nervous system.

Stages of anesthesia as determined clinically		EEG characteristic findings	
Initial state – awake		Alpha (8-12 Hz)	None
		Normal	
I		Alpha-reduction	Light cortical depression, euphoria, loss of powers of discrimination
		Stage of activation	
II		Beta (13-30 Hz)	Cortical depression, unconsciousness, dominant subcortical hypersensitivity
		Stage of falling asleep	
III	1	Delta-Theta (0.5-8 Hz) I beta (13-30 Hz)	Subcortical light depression
	2	Delta-Theta (0.5-8 Hz)	Intense: mesencephalon dominates, onset of depression of medulla spinalis
		Surgical stage of sleep	
	3	Delta-Theta (0.5-3 Hz)	Onset of mesencephalon depression
	4	Delta-Theta (0.5-2 Hz) Burst-supression	Onset of pontine depression
		Surge of narcotic deep sleep	
IV		Suppression	Depression of the medulla oblongaia, collapse of vegetative function
		Surge of complete narcotic deep sleep	

Figure 4.10 — Progressive changes in the analog EEG after barbiturate (thiopental and pentothal, respectively) anesthesia.

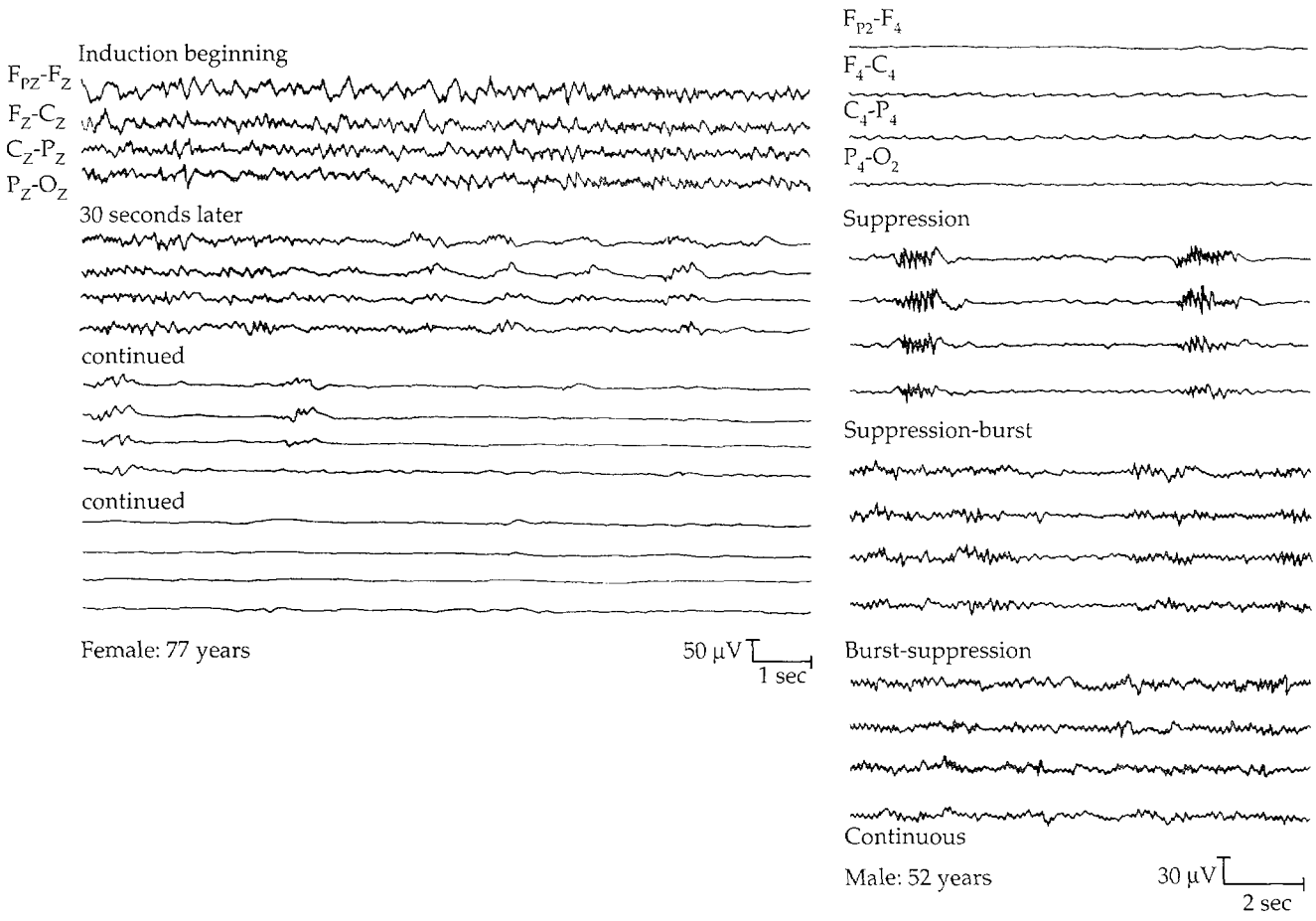

duction of anesthesia to progressive deepening and its termination were defined by Guedel in 1920 according to clinical parameters which resulted in stages I to IV.[49] Subsequent investigators have staged anesthesia based on EEG changes and correlated these to the clinical stages (e.g., Kugler in 1966 developed stages A to F).[50]

Induction of anesthesia is a complex and dynamic cascade of pharmacological and physiological events clinically defined by a loss of consciousness and associated changes in cardiovascular and respiratory function. The state of general anesthesia is described as hypnosis, analgesia, amnesia, and muscle relaxation. This state may be produced by a single drug or a combination of multiple drugs. The induction effect of any general anesthetic is often evaluated by a loss of consciousness, eyeball motion and position, pupillary size, conjunctival ejection and tearing, together with changes in respiratory pattern and responses to verbal commands. These clinical signs are complemented by other continuously monitored, noninvasive and, where appropriate, invasively measured cardiovascular and respiratory variables. However, because the major target organ of general anesthesia is the brain, an adequate definition of induction with any anesthetic drug should also include an assessment of cerebral function.

General anesthetic agents may be separated into six classes; some of their effects on the EEG will be briefly reviewed here:[47]

- Barbiturates
- Nonbarbiturate induction agents (e.g., etomidate, propofol)
- Potent inhalation agents
- Nitrous oxide
- Synthetic opiates
- Benzodiazepines

4.3.1 Barbiturates

Short-acting barbiturates, most commonly sodium thiopental, are used for induction of anesthesia and not for maintenance anesthesia. These agents possess excellent hypnotic properties, but do not possess analgesic or muscle relaxant properties, or have weak muscle relaxant properties, at best. Barbiturates may also be used in a therapeutic fashion during surgery, taking advantage of their ability to decrease intracranial pressure, cerebral blood flow, and cerebral metabolism (or oxygen demand). Thiopental causes a biphasic effect on the EEG which is dependent on dose and speed of administration. Initially there is an increase in fast activity, particularly in the frontal brain, or a disinhibition phase. As dosage is increased, the EEG slows in frequency and increases in amplitude. This transition phase is associated with complete loss of consciousness. At higher doses, burst suppression develops and further increases lengthen the periods of flat EEG until the EEG becomes completely isoelectric. As barbiturate levels decrease, the EEG patterns reverse in the manner described above. Figures 4.10 and 4.11 show a typical barbiturate induction profile for the analog signals and the computer-processed EEG displayed in both CSA and DSA formats, respectively.

Recent evidence has generated heightened interest in the possible role of barbiturates in the protection of the brain during cardiac surgery involving cardiopulmonary bypass procedures.[51,52] Although the traditional form of cerebral protection during cardiopulmonary bypass is hypothermia, there are several high-risk periods when hypothermia is not present: at the initiation of bypass, aortic cannulation, and weaning from bypass. It is during these periods that the brain is invariably normothermic and vulnerable to embolization. Clinical application of barbiturates during normothermic and hypothermic cardiopulmonary bypass procedures have been shown to reduce neuropsychiatric complications. The EEG is used to titrate the dose of thiopental to a burst suppression or isoelectric pattern such as the one shown in Figure 4.10.

4.3.2 Nonbarbiturate Induction Agents

Propofol is an ultrashort-acting intravenous, sedative-hypnotic that produces a dose-dependent CNS depression. It has a reputation for producing a smooth level of anesthesia. It is used for both induction and maintenance of general anesthesia. The EEG patterns produced by propofol are similar to those of thiopental as dose is increased. Levels appropriate for maintenance anesthesia produce a frontally dominant, regular, slow, delta rhythm with superimposed waxing and waning 8 to 11 Hz activity. Higher doses produce burst suppression which may progress to an isoelectric EEG. Propofol has the obvious advan-

Figure 4.11 — Typical induction profiles shown in the CSA and DSA formats following barbiturate (225 mg) and forane (1.5%) anesthesia using the Sentinel IV by AXON, Inc. (increase in beta brain power = *; increase in theta/delta brain power = **).

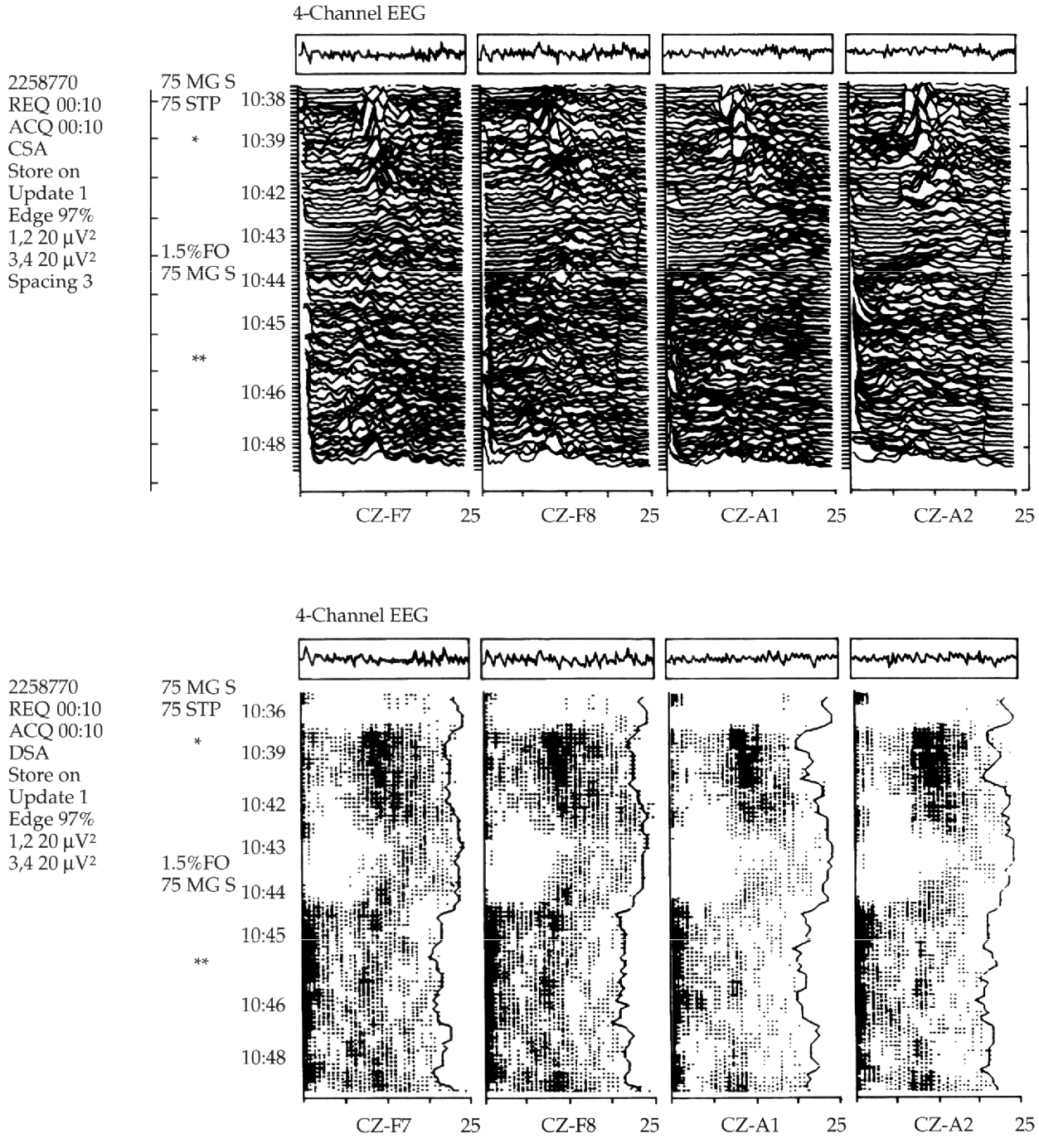

Figure 4.12 — Characteristic analog EEG patterns associated with forane anesthesia.

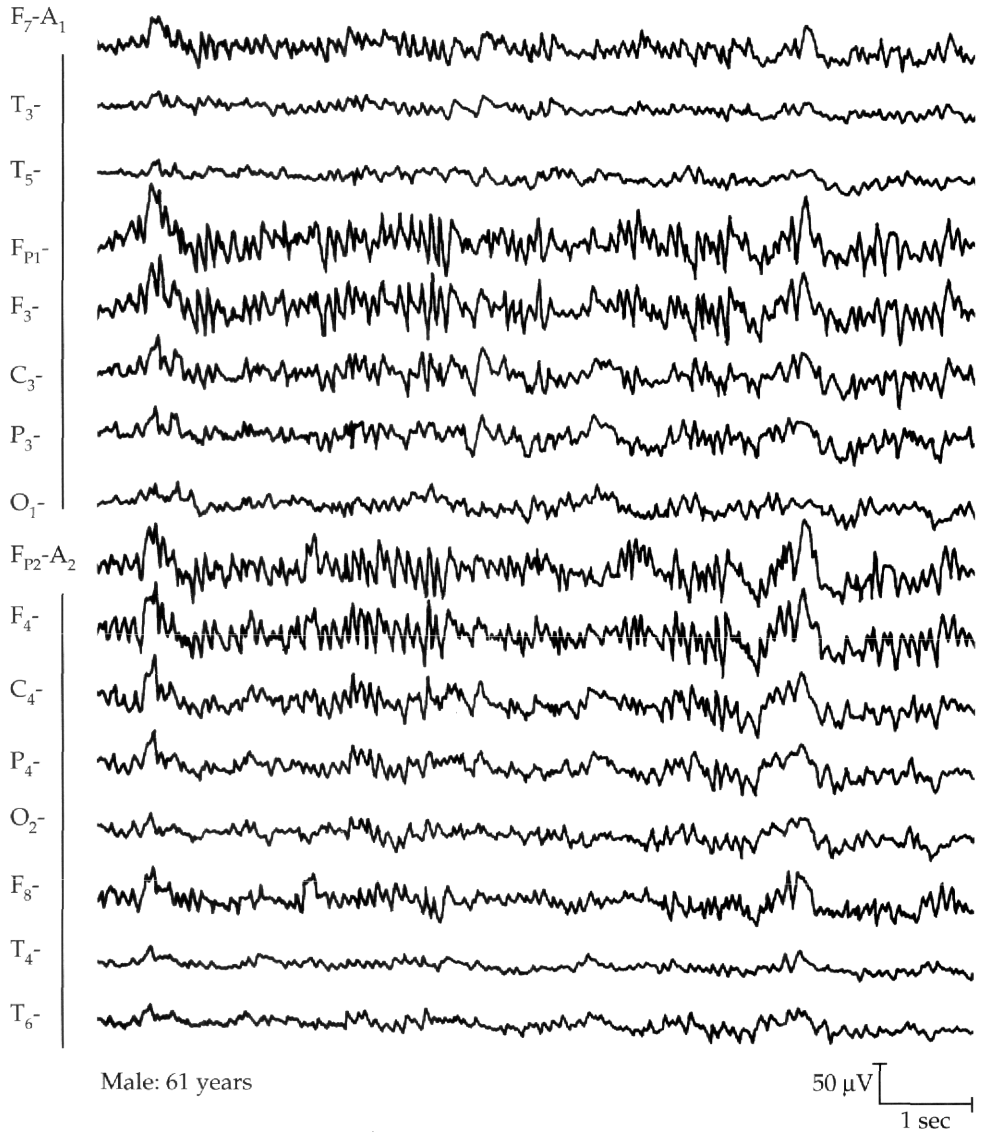

tage of rapid elimination, so that recovery of the EEG following discontinuance of propofol is more rapid than with barbiturates.

Etomidate is a potent nonbarbiturate hypnotic with anticonvulsant properties. It is particularly desirable for patients with poor cardiovascular reserve. Following etomidate induction, changes in the EEG pattern occur in four characteristic stages and are similar to those observed with barbiturates. Initially, alpha amplitude is increased and is mixed with theta activity; the second stage is a mixture of theta and delta activity; in the third stage there is the appearance of continuous delta; and the fourth stage is one characterized by burst suppression activity. Recovery from etomidate anesthesia, like propofol, is also much faster than from barbiturates.

Figure 4.13 — Typical CSA induction sequence with inhalational anesthetics (e.g., halothane 1%). Initial loss of alpha activity with activation of beta activity (20 to 28 Hz) and later theta/delta activity dominate.

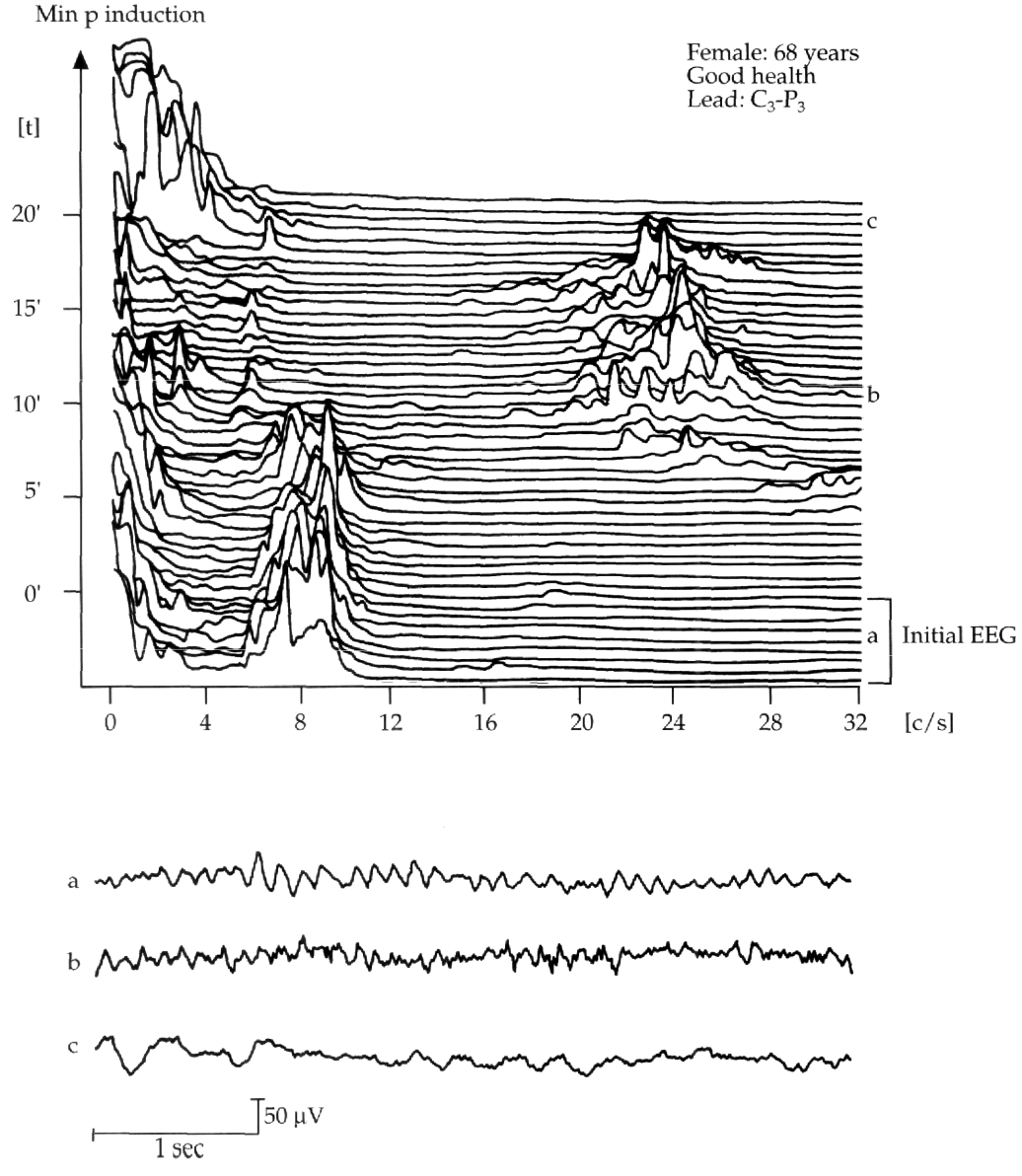

4.3.3 Potent Inhalation Agents

The potent inhalational agents include halothane, enflurane, and isoflurane. These agents are vaporized and delivered at potencies described by a clinical measure known as the minimal alveolar concentration (MAC). MAC is the alveolar concentration at which 50% of the patients move in response to surgical incision or standard stimulation. It takes about 30 minutes of administration for the brain concentrations to approximate the inspired gas

level indicated on the anesthesia machine. Recent developments in anesthesia equipment provide end-tidal concentration measurements of inhalational anesthetics in the alveoli, which is considered an equilibrated site and thus an appropriate indication of the brain's concentration.

Halothane, which was the first modern anesthetic gas, causes progressive EEG frequency slowing and amplitude decreases that are proportional to increasing concentration. It is rarely used in contemporary surgery, particularly for adults, because of risks related to drug-induced hepatitis. With halothane in the absence of nitrous oxide, the EEG pattern observed during the loss of consciousness is an increase in the frequencies between 10 to 20 Hz. At MAC levels greater than 1, progressive EEG slowing occurs. Halothane has an antiepileptic effect with concentrations as high as 4 MAC needed to produce an isoelectric EEG. Nonspecific generalized EEG slowing has been demonstrated to persist 7 to 14 days following anesthesia.

Enflurane, like other inhalation agents, initially induces fast EEG activity. At inspired concentrations of 1 MAC, large amplitude, 7 to 14 Hz waves appear. Increasing concentrations produce further slowing until slow waves predominate. At levels of EEG suppression epileptoid bursts suddenly appear. Abnormality in the EEG pattern may persist up to 30 days following general anesthesia.

Initially, isoflurane produces an increase in the faster frequencies (15 to 30 Hz), particularly the frontal areas. At the time unconsciousness occurs, slow waves (2 to 4 Hz) become mixed with fast activity. At approximately 1 MAC, large 4 to 8 Hz waves dominate the EEG pattern. Between 1 and 2 MAC burst suppression occurs with complete suppression at levels around 2.5%. Elderly patients, as compared to younger patients, show a greater proportion of time in electrical silence when burst suppression occurs.

At sub or minimal MAC anesthetic levels, a similar symmetrical EEG pattern is produced when using any of the potent inhalational agents.[52] EEG patterns associated with three phases of anesthesia have been described: induction, steady-state subMAC levels, and supraMAC concentrations. With induction, an initial characteristic drug-induced beta activity tends to be maximized anteriorly. As induction proceeds, beta activity becomes more widespread, increases in amplitude, and slowing in frequency towards the alpha range occur. It is during this phase and before a steady state that a faster rhythm may be intermixed with a burst of high-amplitude intermittent rhythmic delta activity, usually frontal (FIRDA). At lighter levels of steady-state anesthesia, a characteristic widespread anteriorly maximum rhythmic pattern (WAR) is seen usually in the lower beta and alpha ranges.

This pattern slows with increasing anesthetic concentrations. Other patterns in addition to WAR activity may be present such as anteriorly maximum, intermittent slow waves (AIS) or widespread persistent slow waves (WPS). At concentrations above MAC it has been reported that these agents begin to present their unique EEG effects. With enflurane a spike and wave activity may develop around 1.5 MAC. At further increases to 2 to 3 MAC, a pattern of bursts of high voltage spikes are often separated by periods of relative inactivity. When these higher concentrations are accompanied by hyperventilation, seizures are produced. Halothane has an antiepileptic effect with concentrations as high as 4 MAC needed to produce an isoelectric EEG. Isoflurane also produces an antiepileptic effect with a burst suppression pattern at 1.5 MAC and complete isoelectric EEG between 2 and 2.5 MAC levels. Figures 4.12 and 4.13 show typical analog and CSA profiles for induction effects following potent inhalation agents.

Figure 4.14 — Gray-scale DSA profile of high-dose fentanyl induction effect for a 76 year-old male for CABG surgery. (a) Analog traces for the left and right cortical hemispheres; (b) DSA plot for preinduction premedication; (c) shift in dot density to a dominant delta band; and (d) neuromuscular blockage is acheived.

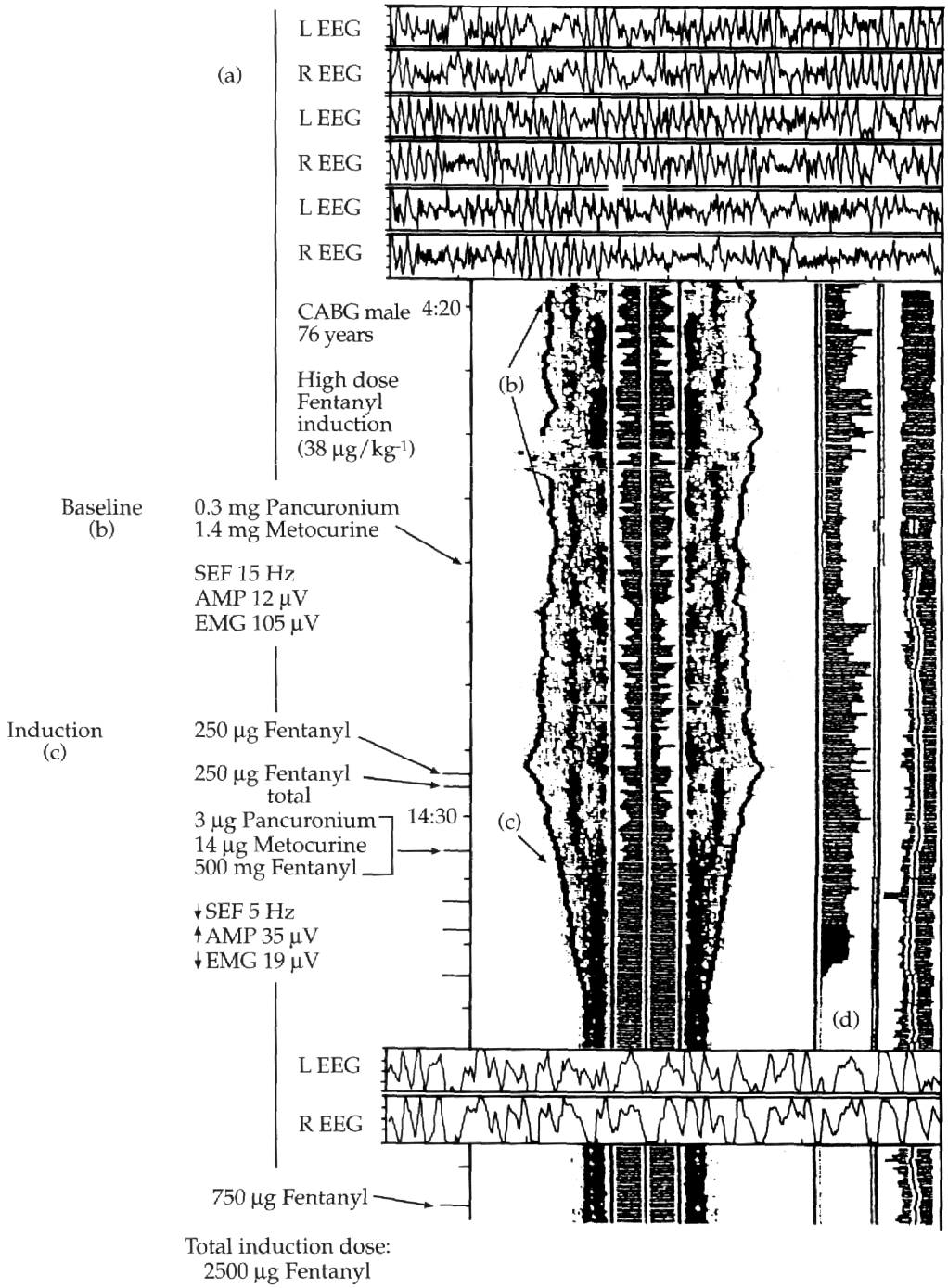

4.3.4 Nitrous Oxide

Nitrous oxide administered as 80% N_2O and 20% O_2 without other anesthetic drugs produces relatively weak effects on the EEG as compared to the awake state. The changes consist mostly of high-amplitude, slow-wave activity. These changes do not correlate well with depth of anesthesia. Burst suppression is never reached with increasing concentrations. When additional anesthetic agents are added, they usually dominate the pattern.

4.3.5 Synthetic Opiates

There is the well established practice of using rapid-acting synthetic opioids (such as fentanyl and sufentanil) during cardiac surgery, because these anesthetics minimize hemodynamic instability while producing a relatively rapid induction of anesthesia. In particular, high-dose fentanyl induction, which is defined as an intravenous dose exceeding 25 mg/kg (or an equipotent dose of other opioids such as sufentanil), has gained widespread popularity for cardiac surgery involving cardiopulmonary bypass procedures. The data also show that a fentanyl/pancuronium combination affords the greatest hemodynamic and electrocardiographic stability without producing myocardial ischemia as compared to other combinations of opioid anesthesia and neuromuscular blocking drugs (e.g., sufentanil and vecuronium).[54] Several studies have directly focused on assessing the induction effects of synthetic opioid anesthesia on both the analog and computer-processed EEG.[40,55,56] Furthermore, even a few reports have prescribed or established clinically effective and practical criteria and strategies for administration of these opioids during induction based on EEG changes: fentanyl and alfentanil;[37,38] small doses of sufentanil (5 to 13 mg/kg) and fentanyl (0.5 to 1.3 mg/kg);[43] high-dose (>25 mg/kg) fentanyl;[40,41,57] and very high dose (75 to 100 mg/kg) fentanyl.[58]

The main outcome of these studies has been the description of a neural fingerprint using computer-processed EEG clinically applied to tailor high-dose opioid induction effects to individual needs during cardiac surgery. At the global electrophysiological level, conventional multichannel EEG analysis of analog waveforms indicates that anesthetic induction begins with the appearance of diffuse theta and some delta which is maximal frontally.[55] Within 1 to 2 minutes following the emergence of an irregular bifrontal delta, global and more synchronous monomorphic delta activity may prevail, depending upon dose and the individual. Over the next 2 to 5 minutes the global EEG pattern evolves and stabilizes into a more polymorphous or irregular slow-wave activity, comprised mostly of delta waves.

Figure 4.14 shows typical 2-channel analog and gray-scale DSA patterns with SEF95 and RMS amplitude represented in trended and digital formats that developed with high-dose fentanyl induction (range = 26 mg/kg to 82 mg/kg; x = 40 mg/kg). In general, high-dose fentanyl produced remarkably consistent and homogeneous EEG changes. Within 2 to 3 minutes after the initial induction bolus (usually 250 to 500 mg), the analog EEG changed quite abruptly and distinctively from an admixture of small to medium amplitude, moderate-to-fast frequency waves (mainly alpha and beta), to larger amplitude, broader waves until there was a dominant slow-wave activity, mostly delta. The transition phase from a heterogeneous EEG profile at preinduction to a homogeneous and diffuse pattern of delta at postinduction rarely exceeded about 2 minutes at doses of 250 to 750 mg. In many cases, the immediate postinduction analog waveforms were monomorphic, exhibiting an almost sine wave morphology at a single delta frequency. This pattern generally evolved and stabilized into a more irregular or polymorphous delta activity.

The changes at induction, manifested in the enhanced visual images and derived measures provided by computer-processed EEG, exhibited a statistically significant bilateral and symmetrical: decrease in SEF90; increase in EEG amplitude; and, shift in dot-density, usually from a dominant alpha and/or beta band to a dominant, extremely dense delta band.

In regards to opioid anesthesia using a continuous infusion technique, Scott and coworkers, defined threshold doses of fentanyl and alfentanil based on the correlation between changes in SEF95 and serum concentrations of those agents.[37] For example, threshold doses of 600 to 825 mg and 6000 to 9000 mg for fentanyl and alfentanil, respectively, were reported to produce an EEG profile characterized by a dominant diffuse delta with a SEF95 of <4 Hz and amplitude of >50 μV. These findings show a significant relationship of delta power spectra associated with opioid-induced EEG changes and age.[38] The dose requirements for comparable EEG changes decreased by 50% for both fentanyl and alfentanil from ages 29 to 80 years.

A clinically acceptable range for SEF90-97, indicating adequate opioid anesthesia with hemodynamic stability for cardiac patients, ranges from 4 to 12 Hz, based on several different devices which use different filters and power spectrum algorithms. However, the clinically acceptable values for a particular brain monitor are always dependent on within-subject baselines and may exhibit a significant degree of variability. A recent report by Sidi and colleagues suggests that cardiac patients tolerated a SEF95 of 10 Hz during high-dose fentanyl anesthesia with cardiovascular stability and no increased incidence of awareness.[57] Using a periodic analysis, Smith and co-workers,[58] reported a decrease in SEF95 from 17.8 Hz to 7.9 Hz following very high-dose fentanyl (93 mg/kg).

Taken together, a number of studies using digital power spectral analysis involving periodic analysis reported that the greatest mean maximum power value occurred in the delta bandwidth (<4 Hz) following opioid anesthesia.[40,43,55,56] In particular, Bowdle and Ward reported that maximal delta power was achieved within 4 minutes after 7 to 10 mg/kg of fentanyl and 1.0 to 1.3 mg/kg of sufentanil.[43] Interestingly, this occurs prior to maximum serum concentrations. Furthermore, values for the potency ratio of sufentanil: fentanyl have ranged from 1:5 to 1:11 using various strategies. However, by superimposing the dose versus brain power or SEF (response) curves, a potency ratio of sufentanil: fentanyl have ranged from 1:5 to 1:11 using various strategies. By superimposing the dose versus brain power or SEF (response) curves, a potency ratio of 1:8 for sufentanil:fentanyl occurred. Thus, one description of the neural effects of synthetic opioids at the molar level involves a dynamic and significant increase in brain power for particular bandwidths (most strongly, delta) at the expense of decreasing the power in others (alpha, beta). In addition, this is sensitive to brain topography, opioid, dose, and age. It is clear that the traditional idea that anesthesia involves just a generalized dampening, depression, or deactivation of cerebral function is invalid, and that its very definition is open to debate and progressively changing. Bovill and co-workers,[59] and others have suggested that the neurophysiologic mechanism of opioid anesthesia involves a blocking of afferent input, not generalized depression.

Thus, by using changes or patterns in the power spectrum of the EEG as a common induction end-point, one of the primary goals of anesthesia may be partially achieved. That is, each patient's separate pharmacokinetic and pharmacodynamic components for that individual's dose requirements for providing stable anesthesia can be more easily managed. Several different strategies for tailoring drug dosage to individual patient requirements based on a common EEG end-point have been routinely employed during cardiac surgery. One of the most recent and controversial involves maintaining a steady-

Figure 4.15 — Typical effects of valium on the analog EEG. Note the excessive beta activity in the frontal channels for each hemisphere.

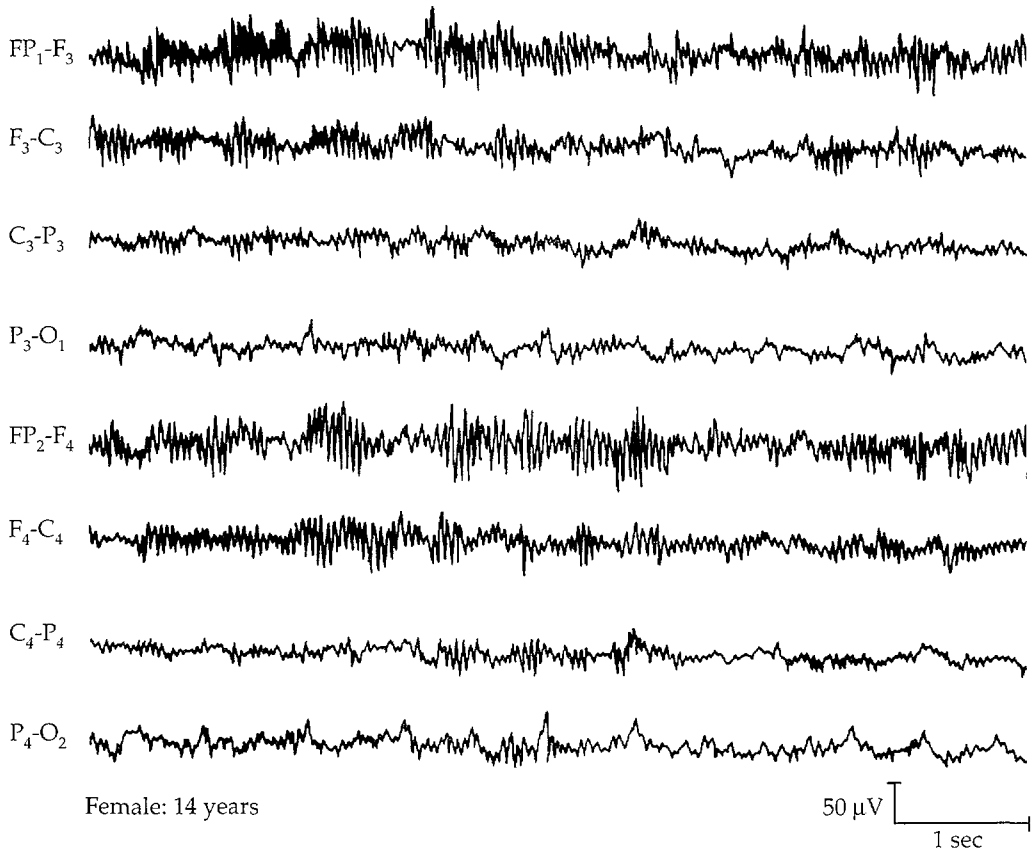

state condition of burst/suppression or isoelectric EEG induced by barbiturate protection during cardiopulmonary bypass procedures.[51,52] Another involves using a predefined neural end-point based on power spectral analysis as a primary "gauge" of opioid induction.[37,38,40,41] Findings have been presented which strongly suggest that as experience and confidence grew with computer-processed brain monitoring for a desired EEG end-point based on power spectral analysis (e.g., DSA profiles, SEF95, and RMS amplitude), fentanyl dosage was significantly reduced by 23% at induction without changes in hemodynamic stability and awareness. Thus, a particular pattern of computer-processed neural effect (Figure 4.13) became a primary desired goal in clinical assessment and regulation of anesthesia, as well as re-emergence from it.

4.3.6 Benzodiazepines

Benzodiazepines are commonly used for sedation and the production of amnesia. The most common uses of these agents are either for premedication or as adjuncts to other anesthetic agents. Diazepam represents the classic example. In general, at low doses, benzodiazepines produce a marked increase in frontally dominant beta activity. Figure 4.15

Figure 4.16 — Typical CSA profile following premedication with diazepam. The initial power in the alpha range is rapidly replaced by an increase of activity in the beta and theta ranges. The accentuation of theta activity shows the tranquilizing component of the substance, while the activity in the beta band corresponds to psychic indifference.

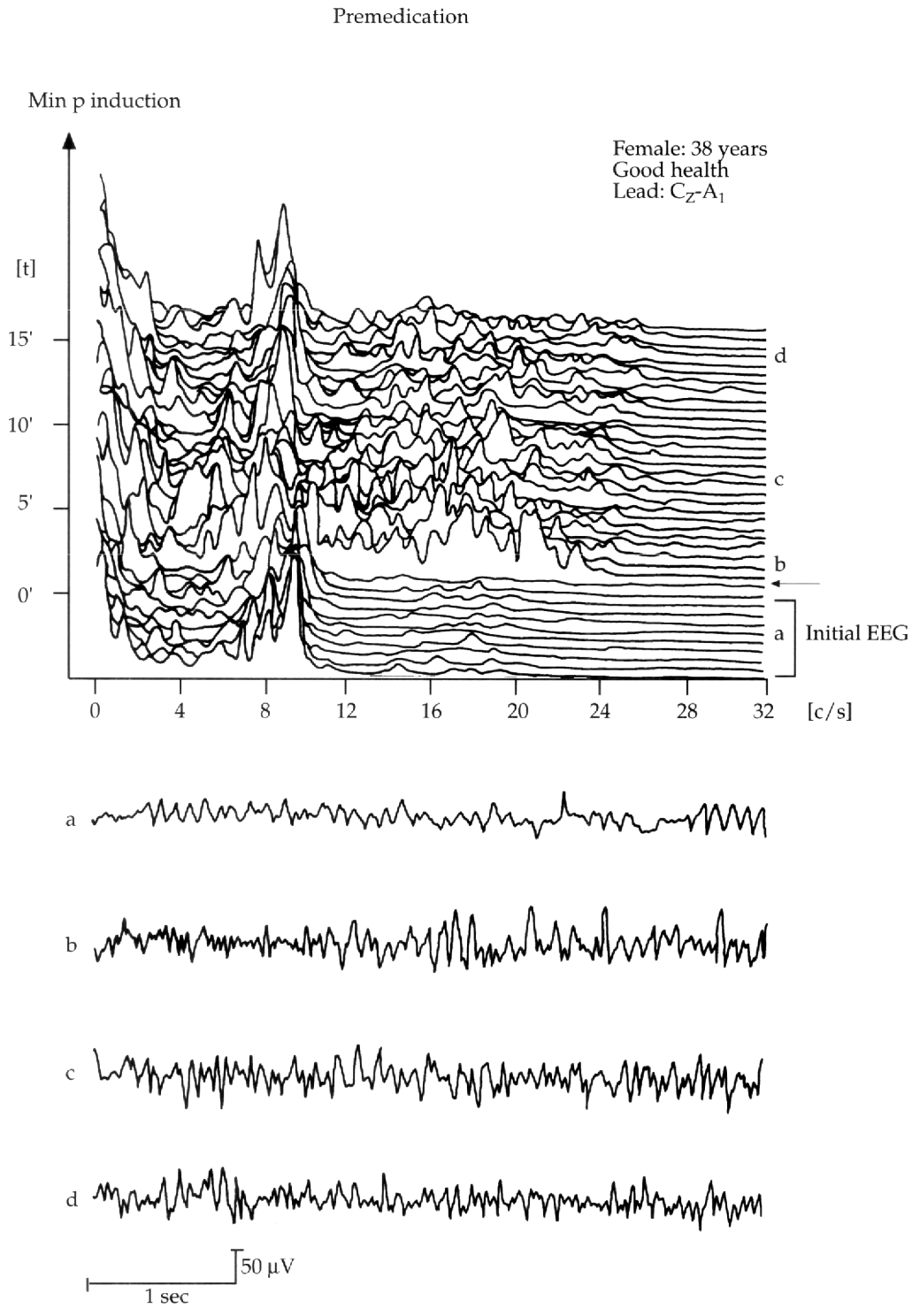

shows a characteristic example of the analog EEG effects of diazepam, and Figure 4.16 documents the effects as displayed by a CSA format. In the CSA profile shown in Figure 4.16, the accentuation of theta corresponds to the tranquilizing effects, while the beta activity reflects the psychic indifference. Midazolam is a recently released benzodiazepine used for intravenous sedation, premedication and induction of general anesthesia. With sedation there is an increase in high-frequency activity, particularly from 13 to 30 Hz, which is most evident over the frontal cortex, with a simultaneous decrease in occipital alpha. It has been recently reported that a beta 1/alpha ratio (13.5 to 20 Hz/8 to 13 Hz) derived from the power spectrum could be used to identify periods of amnesia.[60]

A major advantage of a premedication/induction regime combining benzodiazepines (such as midazolam) and synthetic narcotics (such as fentanyl or sufentanil) is the putative synergistic effect on the level of amnesia and analgesia. However, hypoxemia and apnea following sedation or hypotension on induction has been associated with concomitant benzodiazepine and narcotic use. Although the EEG effects of these drugs have been studied individually, little is known about the EEG patterns associated with their concomitant use. Figure 4.17 presents the DSA profile of high-dose narcotic and high-dose benzodiazepine induction during cardiac surgery.

4.4 EEG Monitoring During Carotid Endarterectomy Surgery

Carotid endarterectomy (CEA) is a surgical procedure designed to reduce the incidence of stroke in patients with carotid occlusive disease. Specifically, this technique prevents emboli or occlusion of a common carotid artery bifurcation containing significant atheromatous plaque. The surgery involves adequate exposure of the distal common carotid artery, carotid bifurcation, and the internal carotid artery well beyond the upper end of the plaque. The common external and internal carotid arteries are then clamped in order to perform the arteriotomy and endarterectomy (plaque removal). A shunt or conduit may be placed between the distal common and internal carotid arteries because of reduced blood flow to the brain. Several aspects of controversy about this surgery have emerged. One involves the routine use of shunting. Another addresses the importance of assessing the sensitivity and specificity of various brain monitoring techniques to reduce cerebral ischemia, particularly during cross-clamping and shunting procedures.

CEA remains the most commonly performed noncardiac vascular surgery in the United States.[61] Analog and computer-processed EEG and somatosensory evoked potential (SEP) monitoring during CEA are well established as sensitive monitors of ischemia, particularly as an assessment of cerebral collateral circulation during temporary occlusion and shunting of the carotid artery. In addition, it is generally recognized that arterial embolism from the carotid to the brain represents a major mechanism for stroke. A recently introduced adjunct technique for intraoperative brain monitoring is the use of Doppler ultrasound (transcranial Doppler) in detecting gas and/or formed-element emboli from thrombus or plaque material. Monitoring strategies should incorporate a multimodality approach that utilizes the simultaneous combination of at least two of the above techniques: either multichannel (at least four) EEG and TCD or median nerve SEP (mnSEP) and TCD monitoring.

Figure 4.17 — A DSA profile with corresponding analog waveforms showing three distinct "signatures" associated with induction of anesthesia: premedication baseline, midazolam induction phase, and fentanyl induction phase.

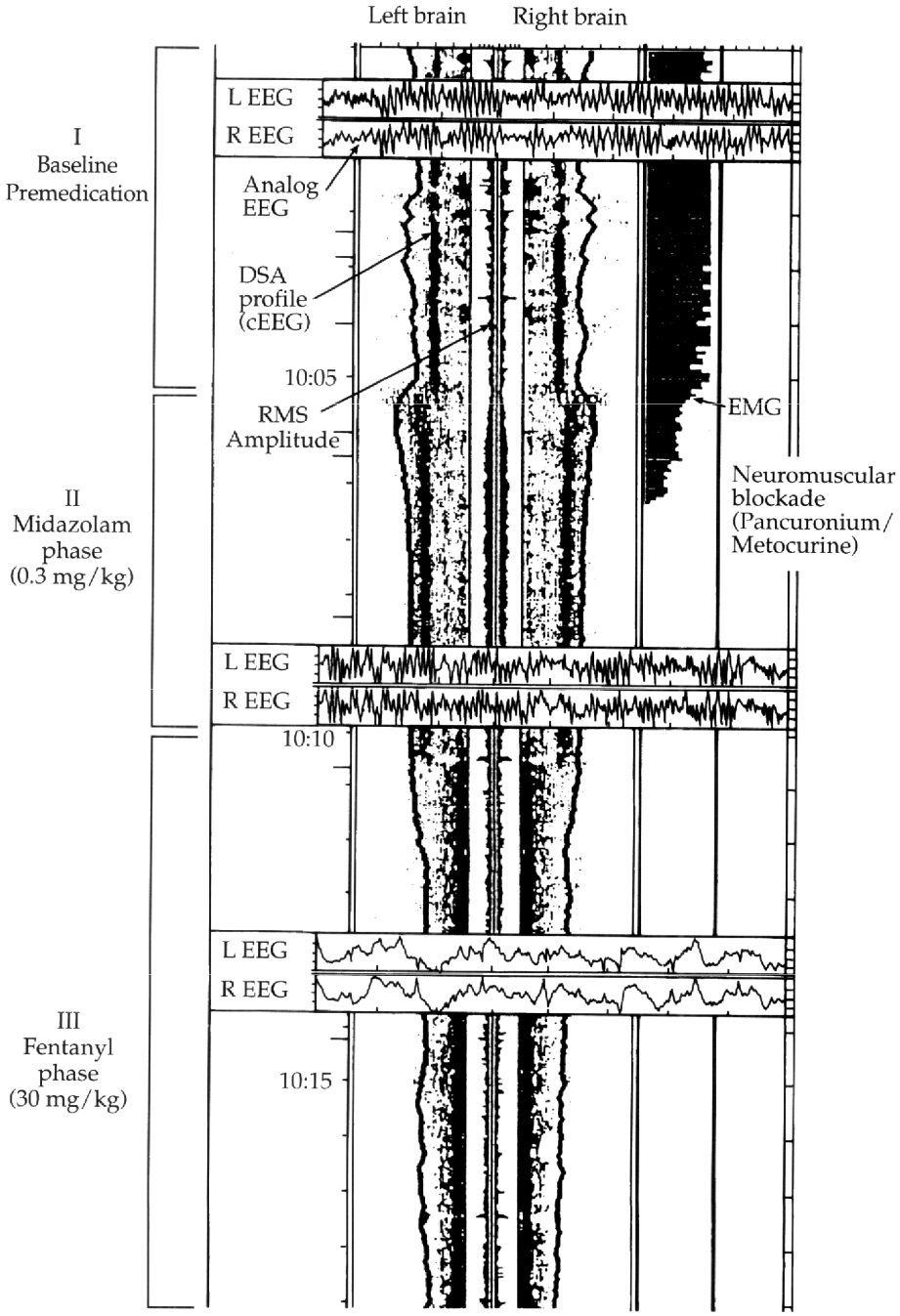

Figure 4.18 — Ischemic insult to right cortical hemisphere 20 seconds after cross-clamping of the right internal carotid artery as determined by multi channel, analog EEG recordings.

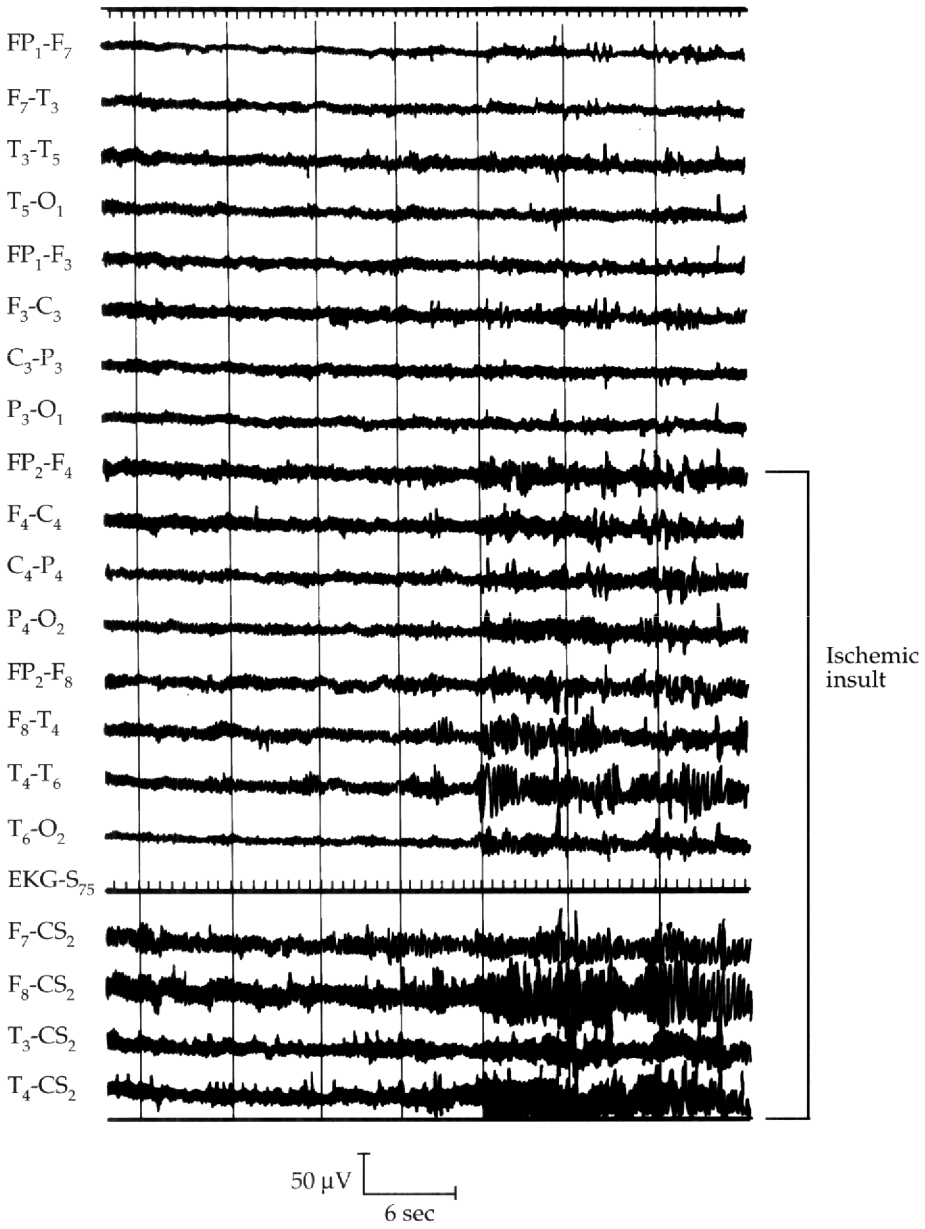

4.4.1 EEG Changes Associated With CEA

EEG changes have been reported in 9.8% to 31% of patients after mechanical occlusion of the carotid prior to arteriotomy,[62-65] with the majority of these clamp-related changes occurring within one minute following clamping.[53] Of patients exhibiting clamp-related changes of the EEG, 80% appear within the first minute; 50% appear within 20 seconds. Major changes begin earlier; more than 80% of these occur within the first 20 seconds.

Figure 4.19 — Moderate to severe ischemic insult to the left cortical hemisphere after cross-clamping the left carotid artery as determined by multi channel, analog EEG recordings. The EEG changes were characterized as major, exhibiting a greater than 50% attenuation of all activity across all frequencies.

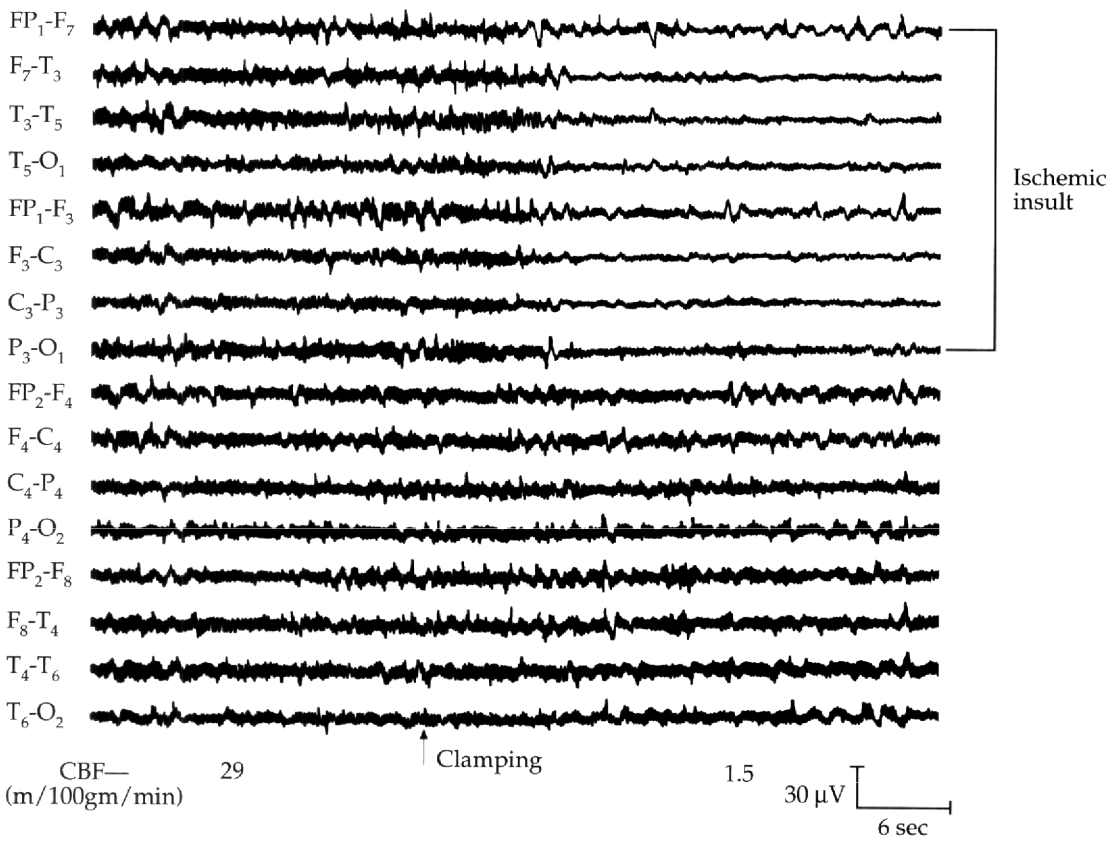

The characteristic EEG alterations due to ischemia range from subtle EEG changes, such as a minimal increase in slower frequencies and mild loss of beta activity, to a complete loss of all detectable electrical activity.[64,65] The EEG amplitude may increase (e.g., high-amplitude slowing phenomenon, Figure 4.18) or decrease (Figure 4.19). Increased delta activity is almost always associated with decreased amplitudes of higher frequency activity. Frequency and amplitude changes are usually ipsilateral to the occlusion, although bilateral changes may occur with severely compromised collateral circulation.[65] Unilateral changes occur more than twice as often as bilateral changes. After shunt placement, focal EEG changes typically resolve in 2 to 7 minutes, although longer times may be required.[66] According to Sharbrough and co-workers, approximately 1% of CEA patients that develop persistent focal EEG changes during CEA are associated with a neurological deficit immediately postoperatively.[67] These changes are probably caused by embolic phenomena.

Some centers have characterized EEG changes associated with cross-clamping as either minor or major. Major clamp-related changes were defined as changes producing: at least 75% alternation of all activity and/or a two-fold or greater increase of less than 1

Hz delta activity.[67] A moderate change was attenuation of nondelta activity to about 50% of preclamp levels and/or an obvious and persistent increase of delta activity at greater than 1 Hz.[53] Approximately 15% to 20% of patients experience major focal changes.[64] Shown in Figure 4.20 is an example of severe ischemia episodes as detected by computer-processed EEG.

Proponents of selective (or EEG-determined) shunting argue that the major disadvantages of routine shunting are an increased potential for embolic phenomena and the increased technical difficulty in performing the endarterectomy itself.[68] It has been reported that only 20% to 30% of patients require shunting and that EEG-determined shunting would significantly reduce the risks of cerebral embolism.[64,65] If intraoperative ischemia is detected with EEG during trial clamping prior to shunt insertion, it can be easily reversed with shunt insertion. Mayo Clinic policy has been to place a shunt whenever visible EEG change occurs or whenever cerebral blood flow with clamping drops below 18 to 20 ml/100g/min.[53,63] About 45% of Mayo Clinic's patients require shunts using these criteria.

In conclusion, recent reports indicate that 2% to 20% of patients having a CEA experience a stroke.[69] The main factors contributing to this outcome include: 1) hypoperfusion during cross-clamping; 2) air or particulate emboli occurring during shunting procedures, and reperfusion of the carotid; 3) reperfusion cerebral hyperemia; and 4) postoperative emboli (e.g., debris remaining in the vessel or clot formation at the operative site). Several intraoperative brain monitoring techniques have been utilized for assessing cerebral blood flow and embolic phenomena, and thus reduce the above risks associated with CEA. These include: 1) EEG; 2) SEP; and, more recently, 3) TCD.

4.4.2 Benefits of Continuous Monitoring

In summary, EEG monitoring during CEA is beneficial for:

- Detection of occlusion-associated ischemia.
- Assessment of anesthetic level (e.g., level of anesthesia or dosage of barbiturates necessary for burst suppression as a means of brain protection during shunting procedures).
- Detection of hypotension (or, more generally, to evaluate requirements for blood pressure control).
- Detection of hypoxia.
- Detection of shunt malfunction or patency of the shunt during cross-clamping.
- Determination of selective or EEG-determined shunting.
- Monitoring for delicacy of surgical manipulation of tissue (e.g., dissection and clamp preparations around carotid).
- In general, a more thorough and careful surgical intervention that would not have been provided in the absence of monitoring.

4.5 *Monitoring During Cardiac Surgery Involving Cardiopulmonary Bypass Procedures*

Cardiac surgery utilizing cardiopulmonary bypass procedures consists of a cascade of dynamic surgical and anesthetic events. In 1990, an estimated 400,000 open-heart surgeries were performed in the United States alone (American Heart Association, 1993). The in-

Figure 4.20 — Severe ischemic episode during shunt placement and removal as shown by CSA displays generated by the Sentinal IV by AXON, Inc. Note the abrupt decrease in SEF97 (*) in both frontal channels with some decreases in the posterior channels as well. The left internal carotid was completely occluded; the right internal carotid artery had a >90% high-grade stenosis.

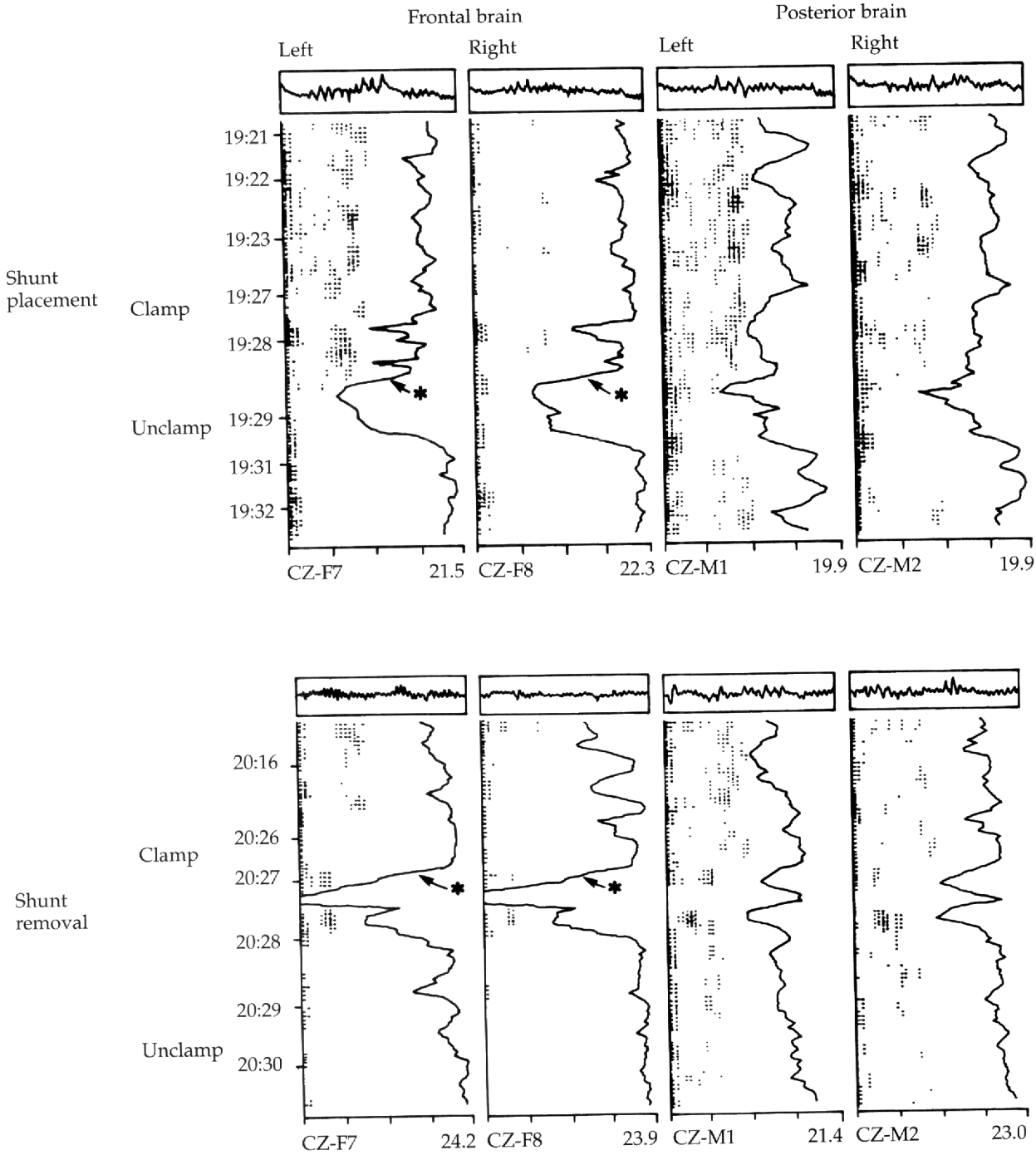

Figure 4.21 — This bar plot graphically depicts the effects of high-dose narcotics on the SEF95 values and root-mean-square amplitude before and after anesthetic induction for each cortical hemisphere. Also, note the inverse relationship between these two derived measures of the EEG.

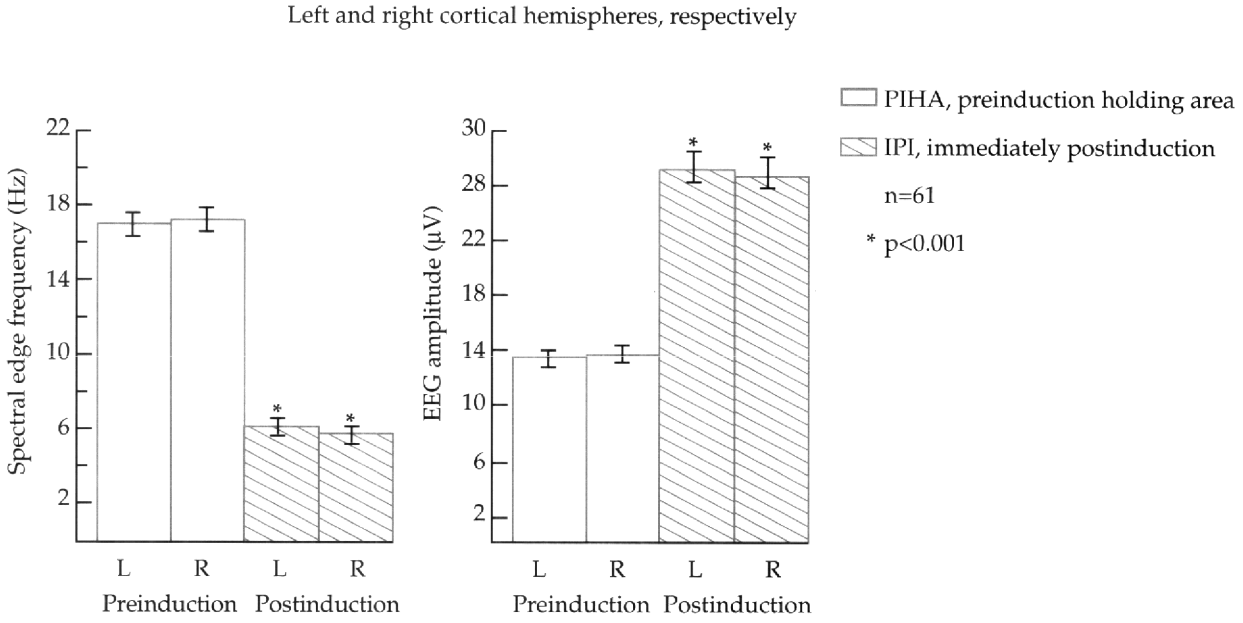

cidence rates of early (<14 days) postoperative neurological and/or neuropsychological complications range from 0% to 100% with the most commonly reported range being 35% to 50%.[70] Although many of these psychological/neurological problems appear to resolve, reports on permanent residual problems have ranged from 5% to 50%.[71]

Although St. Kubicki, *et al*, first used EEG monitoring routinely in open-heart surgery with cardiopulmonary bypass over 25 years ago, brain monitoring has not yet become a routine tool in the repertoire of every cardiac anesthesiologist.[72] Several attempts have been made to present an easy-to-use brain monitoring atlas of various patterns of analog EEG and DSA displays associated with cardiac surgery.[73-76] Portions or snapshots of the continuous analog EEG and computer-processed EEG profile were chosen primarily to represent routine and critical anesthetic or surgical events. The spectrum of EEG events documented and analyzed directly address such issues as: (1) level of anesthesia; (2) functional classification of anesthetic drugs; (3) recognition and prevention of anesthetic and surgical mishaps; (4) hypoxic and ischemic insults on the EEG; (5) quantification of the EEG for statistical analyses and its clinical relevance to critical anesthetic and surgical events; and (6) systems integration of neural, respiratory, and cardiovascular data.

The results of several studies will be briefly reviewed here. The first involved documenting and analyzing the neural induction effects of high-dose synthetic opioid (fentanyl) anesthesia using power spectral analysis to generate DSA displays and derived measures such as SEF (Section 4.3.5).[40] Figure 4.4 shows an example of pre-anesthesia baseline measures, while Figure 4.14 shows anesthetic induction effects as reflected in a snapshot of the analog DSA-displayed EEG generated by the 2-channel Cerebro-Trac 2500 PLUS with frontalis EMG, mean arterial pressure (MAP), SaO_2, and heart rate (HR) concurrently trended with the neural data.

Figure 4.22 — Developed by CNS, Inc., this is a trend of the power drop index which demonstrates a diffuse drop in power as compared with baseline during cardiopulmonary bypass procedures for cardiac surgery. This patient suffered from a diffuse encephalopathy postoperatively.

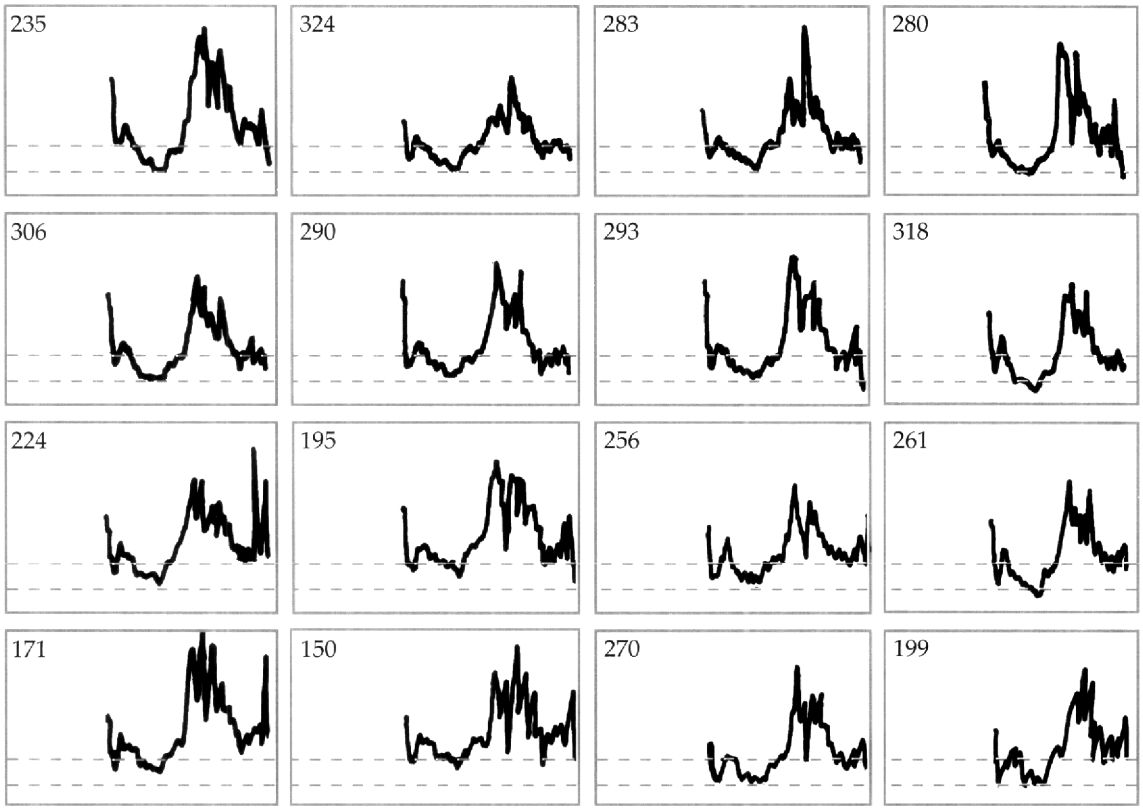

Figure 4.21 graphically depicts the opioid induction effects (see Figure 4.14) observed in each cortical hemisphere for SEF and EEG amplitude (AMP) following high-dose fentanyl anesthesia (25 mg/kg, fentanyl) for 61 CABG patients. Two measures were taken for paired t-test comparisons: preinduction in the holding area (PIHA) and immediately postinduction (IPI) but before intubation.

There was a significant inverse relationship between SEF and AMP for the four measures taken (rho = 0.96, $p < 0.01$). At induction there was a dynamic reversal in the relationships between the mean values for SEF and AMP in which SEF significantly decreased to nearly one-third of the preinduction values, while AMP more that doubled (paired t-tests, $p < 0.02$). In addition, there was a rather abrupt shift in dot-density of the DSA from moderate-high frequencies to a narrow, dense band appearing within the delta range (<4 Hz).

The second study involved using these DSA fingerprints as a predefined neural endpoint of anesthetic induction.[41] A comparison of the average dose of fentanyl (mg/kg) administered as the total induction dose, and across the entire case, was made between the first 25 and last 25 cases of a series of 92 CABG cases performed over a 14-month period. In Group I, clinical decisions by the anesthesiologist for dosage were not routinely based

on brain monitoring, while in Group II, dosage was influenced directly by monitoring the analog EEG, computer-processed EEG in DSA format, and derived indices like SEF. Both groups were similar with respect to age, weight, proportions of males and females, and severity of illness, and also involved the same four cardiac anesthesiologists. Patients in Group II whose anesthetic doses were determined solely or in part by brain monitoring received significantly smaller amounts of fentanyl, both at induction and across the entire surgery (23% less). SEF was significantly higher during both periods for Group II as compared to Group I, which is in accordance with less drug administration. The typical induction effect for high-dose opioids has been described previously. Briefly, both groups showed similar induction profiles which were characterized by a significant bilateral and symmetrical: (1) decrease in SEF; (2) increase in EEG amplitude; and (3) shift in dot-density to a dominant delta band, as described in the first study.

The next studies utilized a preselected, computer-defined baseline to make intraoperative interventions. Aron, and co-workers, undertook a two-part study to monitor 16 channels of computer-processed EEG during hypothermic cardiopulmonary bypass procedures in order to: (1) determine if computer-processed EEG measures correlated with neurological outcome, and (2) compare neurological outcome in a similar group of patients who had received intraoperative interventions based on the identified characteristics.[77] The first part of the study involved data acquisition and analysis of online information in an easily interpretable format. Part two of the study involved intraoperative intervention during sustained power drops and a comparison of neurological outcomes between the two groups.

A power drop index (PDI) was calculated and compared to baseline measures. The PDI was specially developed for use during cardiac surgeries employing cardiopulmonary bypass procedures. The power trend display (Figure 4.22) shows the drop in power below the baseline power level at each channel site. This display is based on a comparison to the baseline. Each box on this display corresponds to one channel site, looking at the top of the patient's head with the nose at the top of the screen and the occipital area at the bottom of the screen. This display updates from the right, moving across the screen to the left with each update. The top line of each box represents 100% of the baseline power level at that channel site. Within each box are two dotted lines which serve as markers to determine the severity of the power decrease. The bottom dotted line is positioned at 10% of the baseline power level. If the graphical representation of the power drop crosses this dotted line, that indicates a 90% decrease in the level of power below the baseline level at that channel site. The top dotted line is adjustable and represents the level at which the PDI begins to accumulate.

The PDI is a numerical indicator of the severity and duration of the decrease below the baseline power level. The individual PDI for each channel is located in the upper left-hand corner of each box. The PDI is calculated by considering how far the power level drops below the baseline power level and how long the power level stays decreased. The greater the decrease in power, and/or the longer it lasts, the higher the PDI. The PDI will start accumulating when the power level being recorded at any channel site drops to less than 40% of the baseline power level at that same channel site. Thus, the overall PDI gives an indication of the severity of power decrease over the entire head.

In part one of the study, 44% of the patients who were brain-monitored without intervention developed new global deficits. In part two, patients who were brain-monitored with interventional criteria showed a significant decrease in new global neurological deficits. The incidence was only 5%.

Figure 4.23 — CIMON display of the Spectrum 32 by Cadwell, Inc. Within the upper portion of each box, the unprocessed EEG segment from the most recent 2.5-second epoch is shown. Color-coded moving window averages are represented below the waveform as a stack of poker chips. The newest average is inserted at the bottom of the stack with the oldest simultaneously removed from the top, causing time to scroll upward. This display depicts marked EEG changes of 2-3 standard deviation increases (yellow) or decreases (blue) from the reference self-norm baseline obtained during surgery.

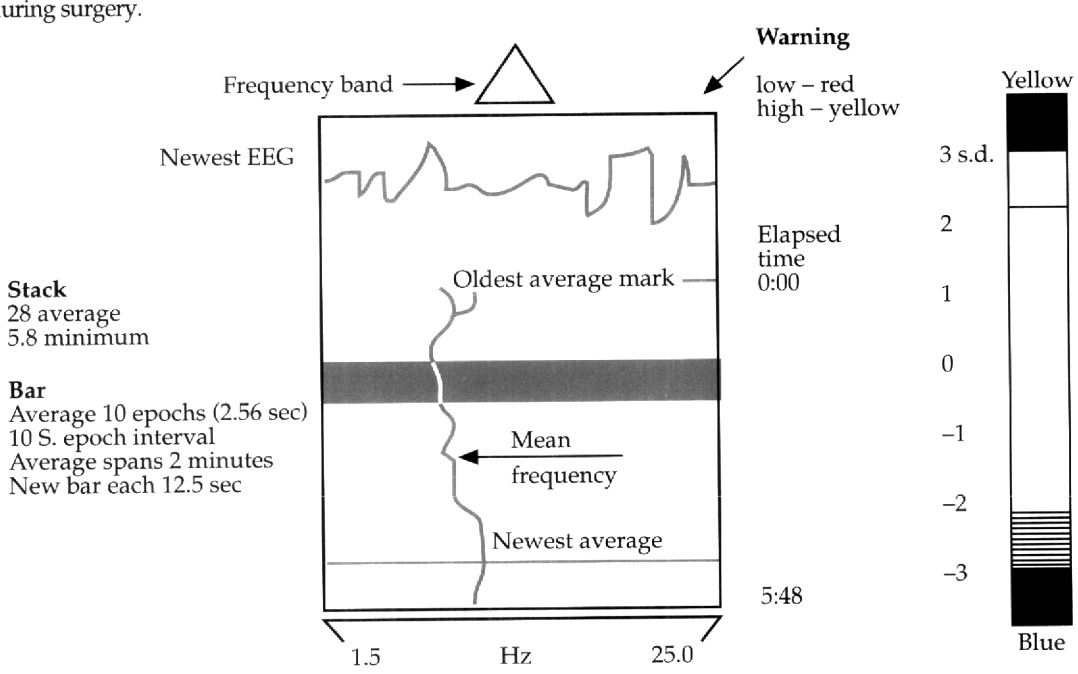

The criteria for intervention were:

- Any drop in power to 25% of baseline activity during the pump run.
- Any asymmetry or lateralized drop in power during the pump run.

The methods of intervention were:

- Increase cerebral perfusion (MAP minus CVP) to 60 to 65 mm Hg.
- Increase CPB pump flow.
- Increase MAP using Neo-Synephrine (Winthrop-Green Laboratories, New York, NY).
- Readjust the venous cannula.
- Increase blood CO_2.
- Readjust the arterial cannula for a lateralized deficit.

In summary, a drop in EEG spectral power was believed to be a significant EEG correlate of global neurological dysfunction postoperatively.

Another recent study also strongly supports the routine use of computer-processed EEG as a method to reduce the percentage of focal or global neurological deficits associated with cardiac surgery using cardiopulmonary bypass procedures.[78] Computerized quantitative electroencephalography was used to evaluate the intraoperative detection of

cerebral dysfunction. The quantitative EEG was recorded continuously during 96 myocardial revascularizations involving hypothermic cardiopulmonary bypass using Cerebrovascular Intraoperative Monitor (CIMON) software. This software relies on an adaptive statistical approach to detect subtle, but clinically relevant, changes in electroencephalographic activity indicative of cerebrocortical dysfunction (Figure 4.23). Relative (percent of total) low-frequency (1.5 to 3.5 Hz) power was chosen as the single quantitative electroencephalographic descriptor because it is an established hallmark of cortical dysfunction and is surprisingly insensitive to moderate changes in body temperature and level of opioid anesthesia. Reference values for this measure were established for each patient after anesthetic induction before sternotomy. The large sample variance often seen in low-frequency power was dramatically decreased by using log-transformed data and allowing each patient to serve as their own control. Quantitative electroencephalographic changes in standard deviation units, or z-scores, were determined from the individualized reference self-norm. Prolonged (greater than 5 minutes) and statistically significant (greater than 3 standard deviations) focal increases in relative low-frequency power were temperature-corrected to determine a standardized cerebrocortical dysfunction time at 37 degrees C (CDT37).

In phase I (n=48), this objective quantitative EEG-based numeric descriptor was used to predict neuropsychologic outcome. These CDT37 greater than 5-minute episodes occurred 38 times in 19 patients. The quantitative EEG-based descriptor predicted the occurrence of such disorientation (n = 14 or 29%) with a 68% false positive rate but only an 8% false negative rate. Since these intraoperative quantitative electroencephalographic episodes were often (19/38) associated with low (less than 50 mm Hg) pump pressures, phase II (n = 48) sought to correct the quantitative electroencephalographic abnormality and prevent postoperative disorientation by appropriate increases in cerebral perfusion. Although the number of episodes of quantitative electroencephalographic abnormality was similar (n = 31) in phase II, these ischemic events disappeared after prompt elevation of perfusion pressure. The phase II disorientation rate fell significantly to 4%. Thus, statistically significant increases in low-frequency electroencephalographic relative power, persisting for a temperature-corrected duration of 5 minutes or more, are a reliable means of alerting the surgical/anesthesia team to the presence of cerebrocortical dysfunction and provide a rational and objective basis for corrective intervention. This form of electroencephalographic monitoring appears to offer an opportunity for the timely correction of perfusion abnormalities or the administration of cerebroprotectant compounds.

4.6 *Intraoperative Transcranial Doppler*

The most recently developed brain monitor for the OR and ICU arenas is the transcranial Doppler (TCD).[79] TCD is a new application of ultrasonography that allows the noninvasive detection of blood flow velocity in the major intracranial arteries, particularly the circle of Willis (Figure 4.24). Current instrumentation records a continuous waveform of the pulsatile fluctuation in blood velocity (cm/sec^2) that occurs with the cardiac cycle. This flow is based on the Doppler shift caused by moving red blood cells and reflects cerebral blood flow. The application of TCD monitoring during CEA and cardiac surgeries involving cardiopulmonary bypass procedures is extremely valuable as an adjunct to EEG monitoring for the evaluation of adequate cerebral perfusion, particularly during cross-clamping procedures. The most significant drawbacks of this method of continuous monitoring is that in approximately 10% of the patients no signal can be obtained due to temporal hyperostosis, and the correlation between CBF is not absolute.

Figure 4.24 — (a) Normal circle of Willis; (b) vertebral and basilar arteries (A) and their major branches.

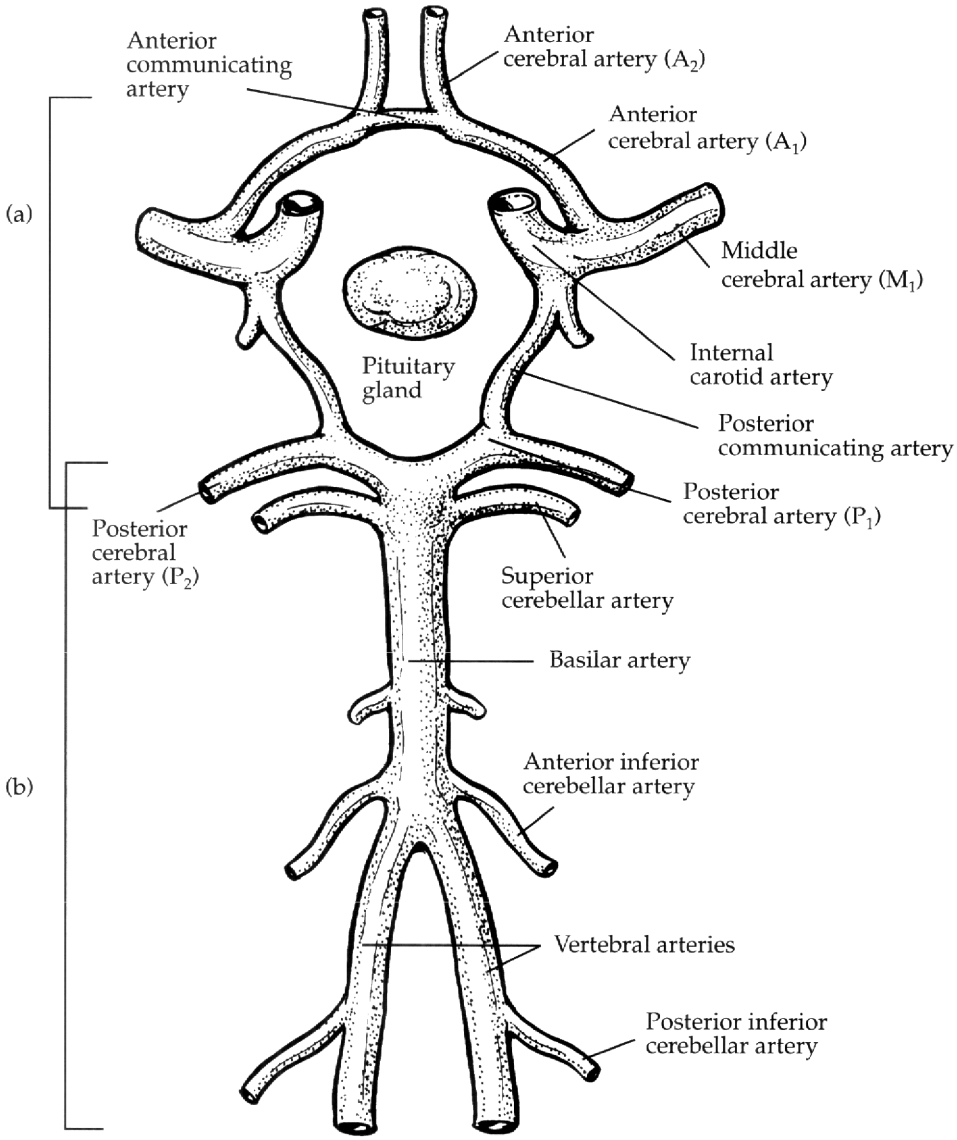

4.6.1 Methods

The devices currently available for intraoperative and ICU use are microcomputer-controlled directional Doppler units which utilize low frequency (2 MHz) pulsed probes. The TCD records the blood flow velocities of intracranial arteries through selected cranial "windows" such as thin regions of the skull and cranial foramina. Shown in Figure 4.25 and 4.26 is the hand-held Doppler placement over the temporal window above the zygomatic arch in order to measure blood flow in the horizontal (M1) segment of the middle cerebral artery (MCA), and other horizontally-oriented basal arterial branches of the circle of Willis such as the anterior cerebral artery (ACA).

The area of greatest risk for ischemic injury expected in the case of CEA surgery is the MCA. For intraoperative monitoring of the MCA during CEA, specially designed head-

Figure 4.25 — The transtemporal "acoustical window" is divided into four distinct areas: the posterior, middle, anterior, and frontal windows (left). Transducer angulations vary according to which transtemporal window is being utilized (right).

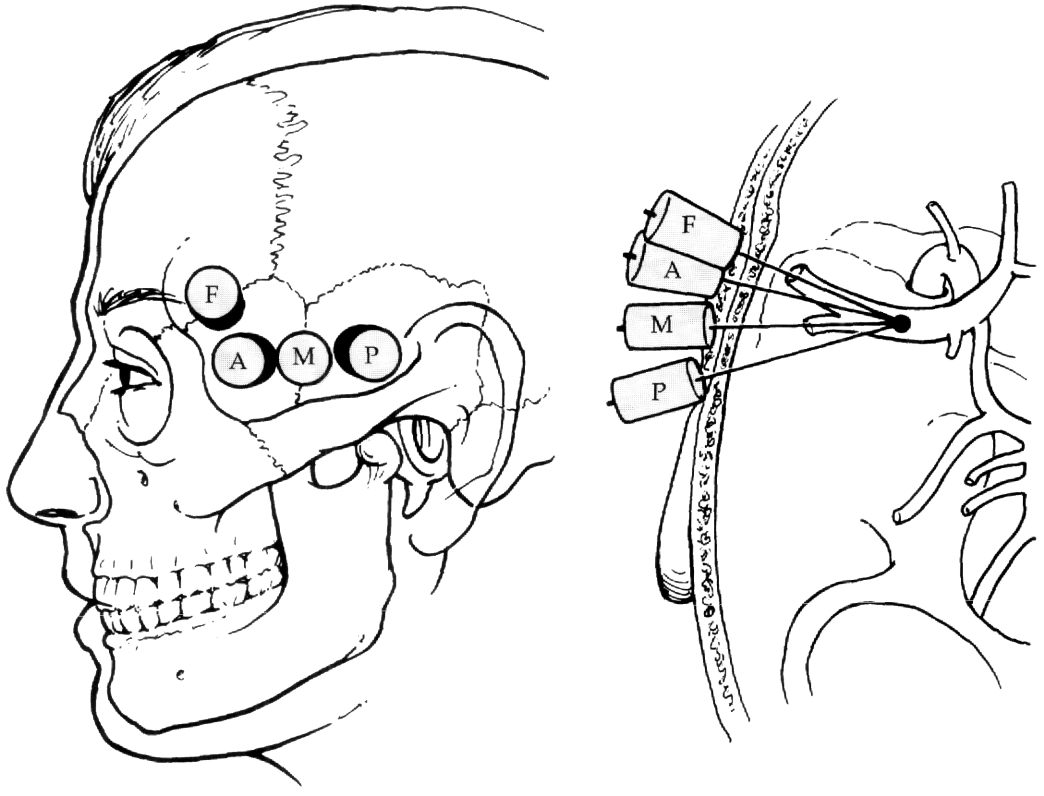

gear fixes the probe to the patient's head with the transducer probe placed over the temporal window. A coating of ultrasound gel is placed on the probe to ensure proper skin contact. The Doppler signal is gaited to focal depths between 3.0 cm to 6.0 cm in order to insonate the horizontal segment of the MCA ipsilateral to the operated carotid artery. With arterial identification of the MCA/ACA bifurcation, blood flow in the MCA is toward the transducer (above zero baseline), while the ACA normally demonstrates flow away from the transducer (below zero baseline). In addition, the MCA flow is generally greater than the ACA flow. Normal reference values are shown Figure 4.27.

In general, the continuous blood flow velocity is mathematically transformed using a FFT spectrum analyzer, which was described earlier for the analog EEG signal, and displayed as a real-time velocity spectrum as well as separate audio signals (Figure 4.27). The FFT spectrum analyzer automatically calculates time-mean velocity in cm/sec, peak systolic and diastolic values, and the pulsatility index [(systolic velocity-diastolic velocity)/mean velocity] using the maximum frequency envelope. These and other spectral features of interest to the evaluation of intracranial hemodynamics are illustrated in Figure 4.28.

4.6.2 Benefits of Continuous Monitoring

TCD offers several advantages for cerebral vascular monitoring during CEA. It is an effective, noninvasive test that can be applied continuously throughout anesthesia and sur-

Figure 4.26 — Placement of the sample volume or insonation by the TCD at the bifurcation of the terminal internal carotid artery into the anterior (ACA) and middle cerebral arteries (MCA). The MCA waveform is displayed above the zero baseline and the ACA waveform is displayed below the zero baseline.

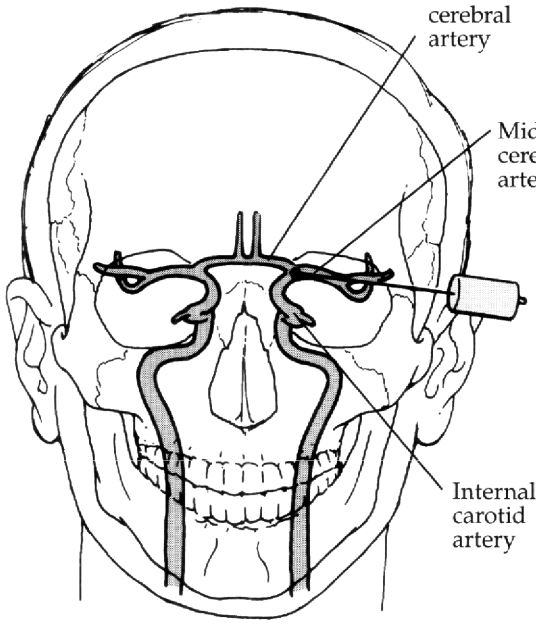

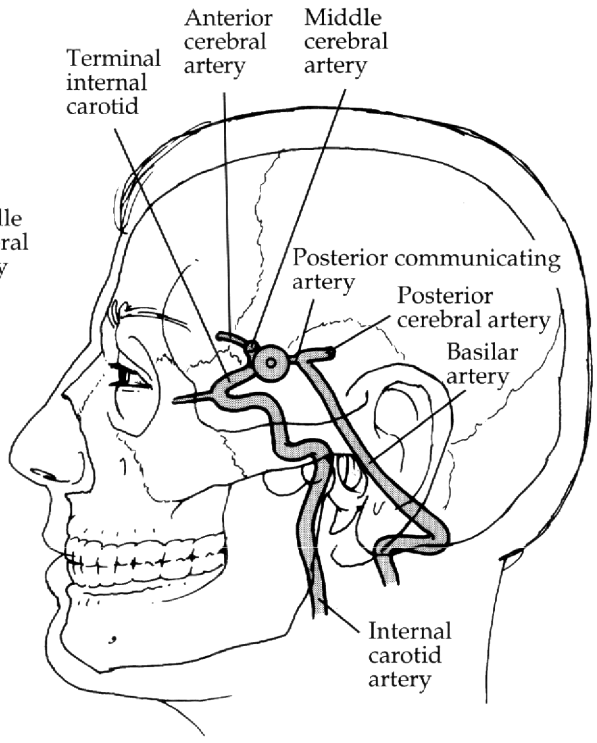

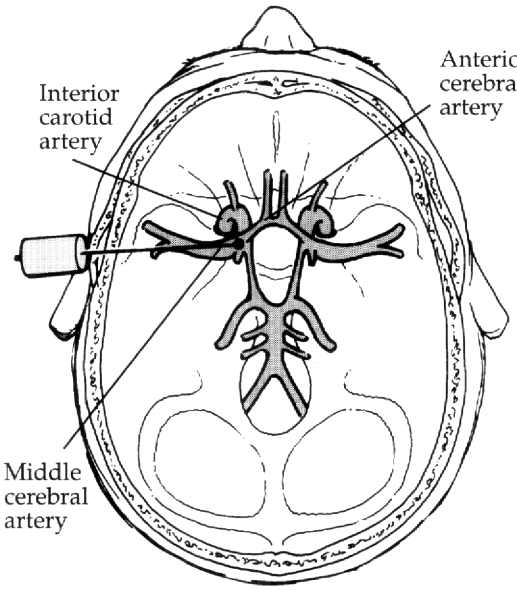

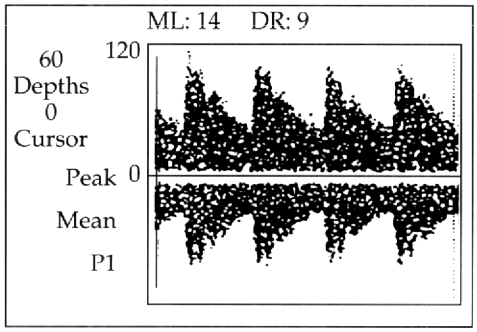

Depth:	55 mm – 65 mm
Direction of flow:	Biderectional
Spatial orientation	—
Velocity (mean):	—
Response to ipsilateral CCA compressions:	Identical to the ACA & MCA

Figure 4.27 — Typical spectral waveform generated by Medasonic's Transpect TCD of the MCA/ACA bifurcation during a premedication baseline prior to a carotid endarterectomy.

Left carotid endarterectomy
Male: 64 years
Unilateral TCD of MCA/ACA bifurcation

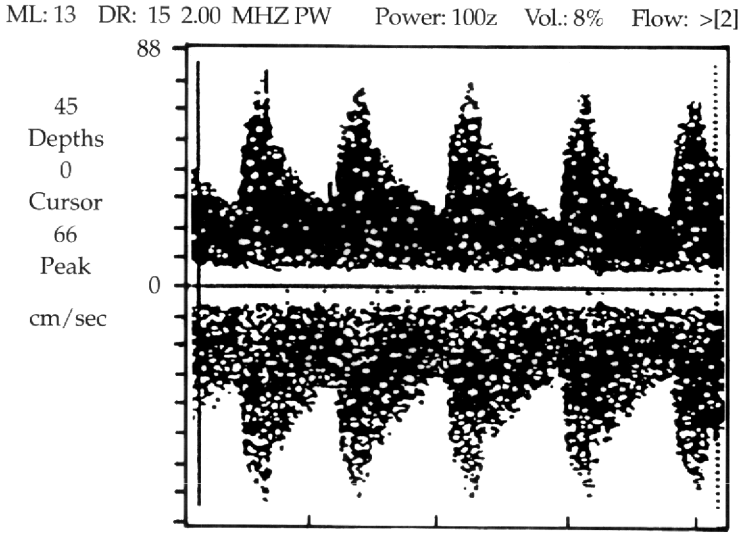

Premedication baseline
Peak velocity: 66cm/sec
HR: 72
ABP: 192/100, 125
Midazolam/fentanyl, nasal O_2

Artery	Transducer position	Depth of sample volume (mm)	Direction of flow	Spatial relationship ACA/MCA bifurcation	Mean velocity** (cm/sec)	Response ipsilateral carotid compressions
MCA[M1]	Transtemporal	30-60	Toward	Same	55 ± 12	Obliteration diminshment
ACA/MCA bifurcation	Transtemporal	55-65	Bidirectional	—	—	Identical to ACA/MCA
ACA[A1]	Transtemporal	60-80	Away	Anterior and superior	54 ± 11	Obliteration diminishment reversal

gery. One of the major advantages is evaluation of the patency of the shunt and detection of embolic phenomena during shunting procedures. TCD monitoring can also facilitate the rapid detection of hyperemia, emboli and the differentiation of emboli type, and any therapeutic method to minimize these potential complications. There is an approximately 12% incidence of post CEA reperfusion cerebral hyperemia. It has also been determined that these patients have a ten-fold increase in risk to develop significant neurologic sequelae. In addition, during or after CEA, 62% of patients sustain bubble emboli and 26% formed element emboli. Figure 4.29 shows examples of detecting air and particulate emboli from the MCA during CEA surgery.

Albin, and co-workers, evaluated the ability of the TCD to image micro-aggregates of air and particulate matter in the rhesus monkey.[80] The monkey's left internal carotids were sequentially injected with air volumes ranging from 0.8 ml to 100 ml in normal saline, or

Figure 4.28 — The spectral parameters calculated from the FFT transformation of the TCD blood flow velocity signals: a) velocity parameters such as peak systolic velocity (PSV, cm/sec), end diastolic velocity (EDV, cm/sec), and mean-time average (v, cm/sec); (b) systolic upstroke, which is defined as the initial slope of the peak velocity envelope during the acceleration phase of systole; (c) pulsatility, which describes the degree of variability in the maximal flow velocities during the different phases of the cardiac cycle (see diagram for calculation); and (d) spectral distribution, which refers to the content of the spectral waveform.

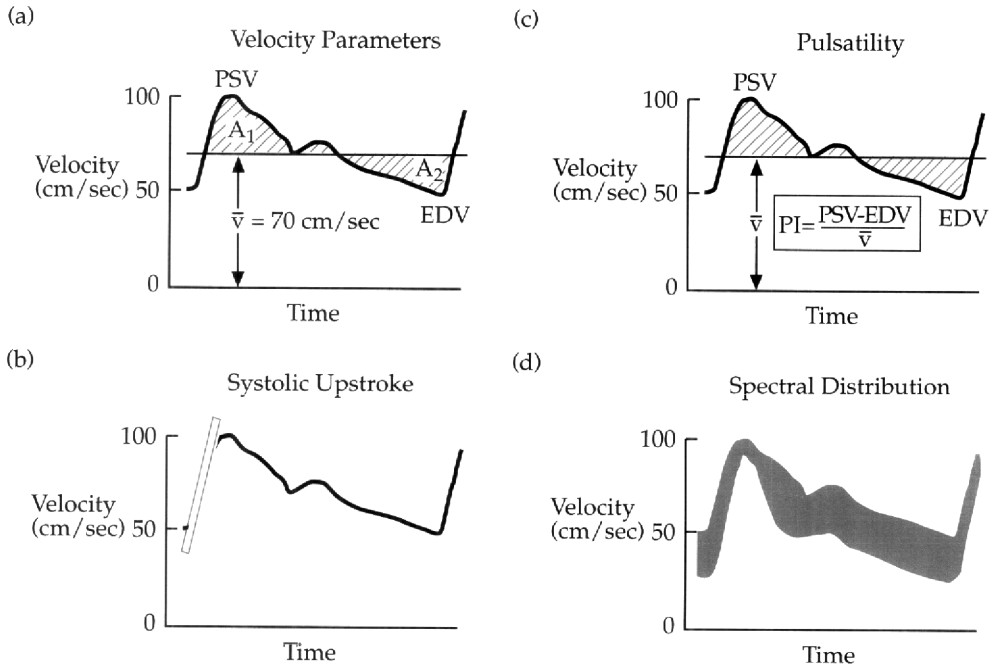

latex microspheres of 1.0 to 25.0 microns in diameter in 0.1 ml volumes of blood. The TCD sensitivity to air detection was at 0.8 ml and produced a characteristic high velocity peak of at least 120 cm/sec. Latex microspheres of 1.0 micron in diameter could be detected at concentrations of 5×10^7 aggregates in 0.1 ml of blood with multiple peaks not exceeding 90 cm/sec. Two distinct qualities differentiate these effects. First, air emboli characteristically are imaged above and below the baseline, while particulate emboli are primarily imaged above the baseline (i.e., 0 flow). Second, acoustically the auditory response of embolic air appears quite distinctly from particulate emboli, which sounds like birds chirping.

Unfortunately, bubble emboli during CEA are not always easy to count individually because of superimposition. However, one technique has involved the estimation by cumulative duration within the Doppler spectrum.[81] In this particular study, 38% of the patients displayed no bubble emboli signals; 15% displayed 0.5 to 1.0 seconds; 20% displayed 1 to 5 seconds; and 14% displayed 5 to 25 cumulative seconds of bubble emboli signals.

Various investigators have established a correlation between EEG activity and the adequacy of CBF.[66,67] The most important EEG charge is voltage attenuation, which correlated with regional CBF less than 10 ml/100 grams of brain per minute. Furthermore, shunting nearly always reversed occlusion-induced EEG changes. CBF greater than 24 ml/100g/min is most often associated with the absence of EEG changes. CBF threshold

Figure 4.29 — Typical examples of embolic signals passing through the MCA during cross-clamping and shunting procedures for carotid endarterectomy surgery recorded by the Transpect from Medasonics. The top panel illustrates the detection of multiple air emboli occurring during restoration of normal blood flow following shunt placement. The bottom panel illustrates the detection of particulate emboli during shunt insertion.

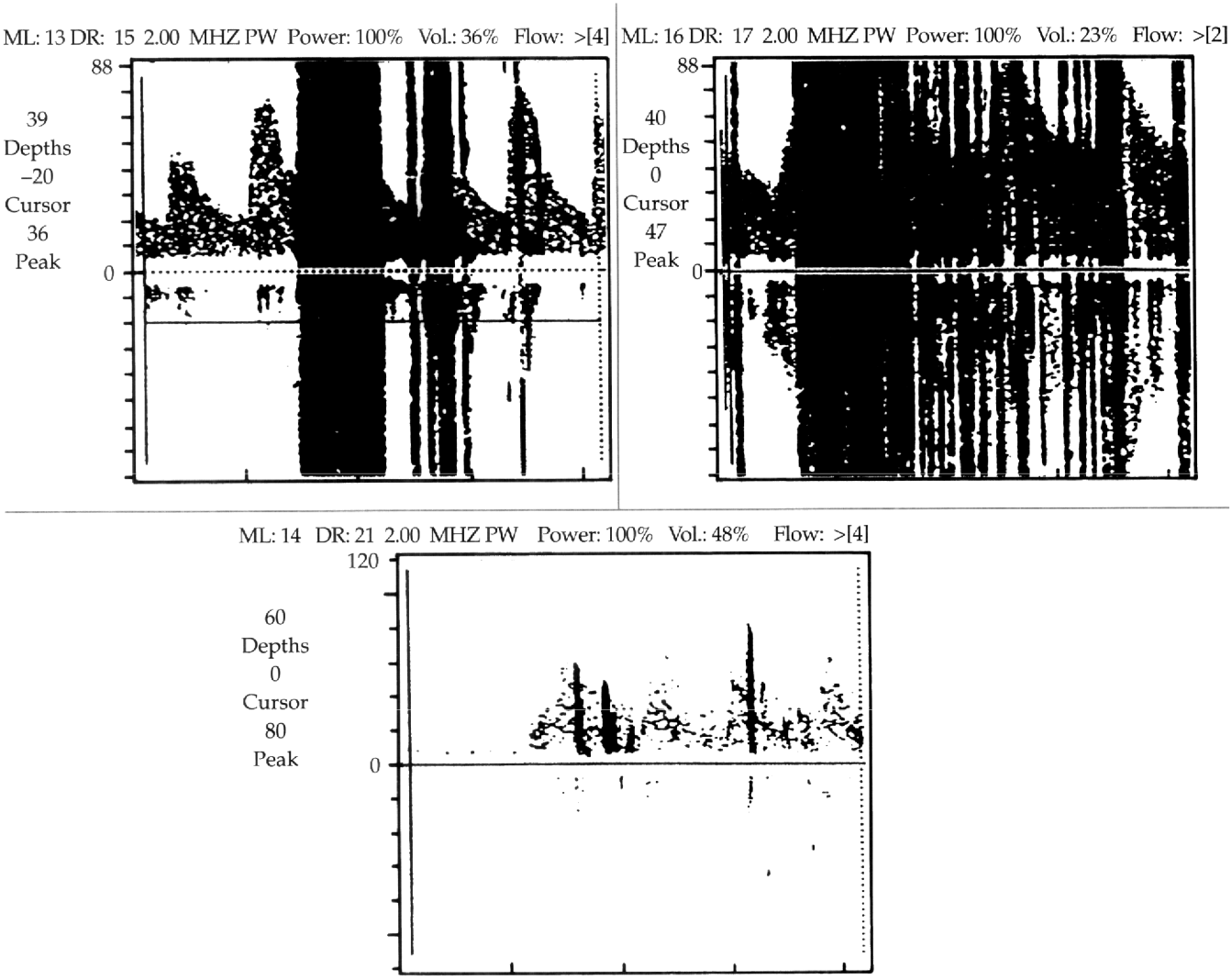

for EEG changes does vary with anesthetic agents. The critical CBF with isoflurane (10 ml/100g/min) is less than that for halothane (24 ml/100g/min), thus suggesting some protection provided by isoflurane over halothane for decreased CBF-induced ischemia. Halsey reported that after cross-clamping during CEA, patients with MCA velocities above 20 cm/sec as determined by TCD exhibited no EEG changes.[82] These patients (about 70% of the cases) were not shunted. Lastly, as an indirect cerebral blood monitor, TCD monitoring provides a clinically significant adjunct in determining the significance to EEG changes and, thus, supports the strategy that all such patients should have multimodality monitoring.

4.6.3 Summary

In 1989 the American Academy of Neurology released their position statement on TCD. TCD is of established value in:

- Detecting severe stenosis (>65%) in the major basal intracranial arteries.
- Assessing patterns and extent of collateral circulation in patients with known regions of severe stenosis or occlusion.
- Evaluating and following patients with vasoconstriction of any cause especially after SAH.
- Detecting AVMs and studying their supply arteries and flow patterns.
- Assessing patients with suspected brain death.

The following uses of TCD are under investigation but are not yet established:

- Assessing patients with migraine.
- Monitoring during CEA, cardiopulmonary bypass, and other cerebrovascular and cardiovascular interventions, and surgical procedures.
- Evaluating patients with dilated vasculopathies such as fusiform aneurysms.
- Assessing autoregulation, physiologic, and pharmacologic responses of cerebral arteries.
- Evaluating children with various vasculopathies such as sickle cell disease, moya moya, and neurofibromatosis.

4.7 *Conclusion*

The primary advantages of computer-processed EEG include: (1) the ability to determine preselected baselines in order to evaluate deviations during critical anesthetic/surgical manipulations; (2) enhanced visual graphics for easier on-line interpretation; and (3) the ability to quantify and statistically evaluate the integrated data. Furthermore, intraoperative brain monitors provide exceptional capabilities for the integration of major organ system data, including neural, cardiovascular, and respiratory; these can be recorded and processed on-line and permanently stored for off-line review and analysis.

One important outcome of the anesthetic drug studies was the discovery of a trend in anesthetic management: as experience and confidence grew with decisions based on brain monitoring, there resulted a clinically significant change in the protocol for anesthetic management. For the first time, the anesthesiologist can literally picture the global or focal physiological effects of anesthesia, as the induction effects and others described here dramatically illustrate, and thus, tailor drug administration to individual needs based on predefined neural end-points. Thus, anesthetic drugs can then be functionally classified according to neural as well as cardiovascular effects.

In addition, monitoring the EEG provides a sensitive and convenient measure of ischemic insults during anesthesia and surgery. The most important limitation to routine use of these monitoring techniques in many settings may be lack of experience and standardization of methods. The available clinical database on intraoperative neurophysiological monitoring has grown enormously over the past decade. Identifying patterns of clinical interest and determining meaningful alarm limits will certainly facilitate increasing acceptance and routine use.

5.0 ABBREVIATIONS

f	frequency of AC current
+3SD	plus 3 standard deviation
μ	micron
mΩ	megaohm
μA	microamp
μg	microgram
μV	microvolt
π	pi = 3.14
Ω	ohms
A	ampere
A^-	fixed intracellular ions
AAMI	Association for the Advancement of Medical Instrumentation
AC	alternating current
ACA	anterior cerebral artery
Ach	Acetylcholine
A – D	analog to digital
AH	abductor hallucis
AHC	anterior horn cell
AIS	anteriorly intermittent slow
ALS	amyotrophic lateral sclerosis (Lou Gehrig's Disease)
Amp/Turn μv	mean amplitude per turn, μv
AMP	amplitude
ANS	autonomic nervous system
ANSI	American National Standards Institute
APB	abductor pallicis brevis
ATP	adenosine triphosphate
ATPase	adenosine triphosphatase
AVM	arteriovenous malphamation
BAEP	brain stem auditory evoked potential
BAER	brain stem auditory evoked response
BEAM	brain electrical activity mapping
BETS	benign epileptiform sharp transients of sleep
C	capacitance or central
Ca^{++}	calcium ion
CABG	coronary artery bypass graft
CBF	cerebral blood flow
CDT37	cerebrocortical dysfunction time at 37∞C
CEA	carotid endarterectomy
CIMON	*cerebrovascular intraoperative monitor*
Cl^-	chloride ion
cm	centimeter
CMAP	compound muscle action potential
CMRR	common mode rejection ratio
CNS	central nervous system
CO_2	carbon dioxide
CPB	cardiopulmonary bypass
CPU	central processing unit
CSA	compressed spectral array
CSF	cerebrospinal fluid
CT	computer-aided tomography
CV	conduction velocity
CVP	central venous pressure
dB pe SPL	decibels peak equivalent sound pressure level
dB NHL	normal hearing level in decibels
dB	decibel
dB SL	sensation level in decibels
DC	direct current
DL	distal latency
dL	deciliter
DPSA	digital power spectral analysis
DSA	displayed spectral array
dV/dT	change in voltage over time
E	voltage
ECG	electrocardiograph/y/ic
EDB	extensor digitorum brevis
EDC	extensor digitorum communis
EDV	end diastolic velocity
EEG	electroencephalograph/y/ic
EMF	electromotive force
EMG	electromyogram or electromyographic
EMU	epilepsy monitoring units
EP	evoked potential (sometimes evoked response)
ERP	event-related potential
F	frontal or fast twitch muscle fiber or frequency
F(int)	subclassification of F
FF	subclassification of F
FFT	Fast Fourier Transform
FIRDA	frontal intermittent rhythmic delta activity
Fp	frontal-polar
FR	subclassification of F
gm/dl	gram per deciliter
H	Henry
HCO_3-	hydrogen carbonate or bicarbonate
HR	heart rate
Hz	hertz
I	current

IaEPSP	Ia excitatory post synaptic potential
ICA	internal carotid artery
ICU	intensive care unit
IP	interference pattern
IPI	immediately postinduction
K^+	potassium ion
K	kilo ohm
KHz	kilo hertz
L	inductance or liter or left
LES	Lambert-Eaton Syndrome
LO-MF	left occipital
LP	lumbar cord
m/sec	meters per second
m/h	meters per hour
m	meter
mA	milliamp
MAC	minimal alveolar concentration
MAP	mean arterial pressure
max	maximum
MCA	middle cerebral artery
MCD	mean consecutive difference
Megabytes	1 million bytes
mEq	milliequivalent
MF-A1	midfrontal
mg	milligram
Mg^{++}	magnesium ion
min	minute(s) or minimum
mm	millimeter
mm Hg	millimeters of mercury
MN	mean
MNAP	mixed nerve action potential
MND	motor neuron disease
MNSEP	median nerve SEP
mΩ	milliohm
MO	midoccipital
mph	miles per hour
MRI	magnetic resonance imaging
ms	milliseconds
MUAP	motor unit action potential
mV	millivolt
mx	mixed
n	number
N	negative peaks
N	number of points
N13	upper cervical spinal cord
NA	not applicable
Na^+	sodium ion
NCS	nerve conduction studies
NEE	needle electrode examination
neg	negative
N_2O	nitrous oxide
non-PNS	nonperipheral nervous system
NSS	number of small segments
O	occipital
O_2	oxygen
OR	operating room
P	parietal or power or positive peaks
PL	peak latency
P14	caudal brain stem medial lemniscus
P37	somatosensory parietal cortex
PDI	power drop index
pH	index of acidity/alkalinity
PIHA	preinduction holding area
PNS	peripheral nervous system
POSTS	positive occipital sharp transients of sleep
PSPs	postsynaptic potentials
PSV	peak systolic velocity
Q	charge
R	resistance or response or right
REM	rapid eye movement
RMS	root square mean
RO	right occipital
SD	standard deviation
sec	seconds
SEF	spectral edge frequency
SEF 90	spectral edge frequency, 90%
SEP	somatosensory evoked potential
SER	electrical skin stimulator
SFEMG	single fiber EMG
SNAP	sensory nerve action potential
SO_4-	sulfate
SpO_2	oxygen saturation
SR	sample rate
SAH	subarachnoid hemorrhage
t	time constant
T	time
TCD	transcranial Doppler
UCA	upper centile amplitude
V	voltage
VC	voltage capacitance
VEP	visual evoked potential
VER	visual evoked response
V_{in}	voltage in
V_{out}	voltage out
WAR	widespread anteriorly rhythmic
WPS	widespread persistent slow
Xc	capacitive reactance
X_L	inductive reactance
Z	midline or impedance

6.0 REFERENCES

1. Kandell ER, Schwartz JH, Jessell TM. *Principles of Neural Science.* Third Edition. New York, N.Y: Elsevier; 1991.
2. Creutzfeldt O, Watanabe S, Lux HD. Relations between EEG phenomena and potentials of single cortical cells. II. Spontaneous and convulsoid activity. *Electroencephalogr Clin Neurophysiol.* 1966;20: 19-37.
3. Cooper JR, Floyd EB, Roth RH. *The Biochemical Basis of Neuropharmacology.* Fifth Edition. New York, NY: Oxford University Press; 1986.
4. Litt B. Dipoles and the EEG. Am J EEG Technol. 1991;31: 119-121.
5. Niedermeyer E, da Silva FL. *Electroencephalography.* Third Edition. Baltimore, MD: Williams & Wilkins; 1993.
6. Cooper R, Osselton JW, Shaw JC. *EEG Technology.* London, UK: Butterworths; 1980.
7. Litt B, Fisher R. Daly DD, Pedley TA, Eds. In: *Current Practice of Clinical Electroencephalography.* Second Edition. New York, NY: Raven Press, Ltd.; 1990.
8. Silverman D. The anterior temporal electrode and the ten-twenty system. *Electroencephalogr Clin Neurophysiol.* 1960;12: 735-737.
9. Ojemann GA, Sutherlin WW. Engel J Jr, Ed. In: *Surgical Treatment of the Epilepsies.* Second Edition. New York, NY: Raven Press, Ltd.; 1993.
10. Engel J Jr, Ojemann GA. Engel J Jr Ed. In: *Surgical Treatment of the Epilepsies.* Second Edition. New York, NY: Raven Press, Ltd.; 1993.
11. Spencer SS, Spencer DD, Williamson PD, et al. The localizing value of depth electroencephalography in 32 patients with refractory epilepsy. *Ann Neurol.* 1982;12: 248-253.
12. Barlow JS, Kamp A, Morton HB, et al. EEG instrumentation standards: Report of the committee on EEG instrumentation standards of the International Societies for Electroencephalography and Clinical Neurophysiology. *Electroencephalogr Clin Neurophysiol.* 1974;37: 539-553.
13. Reilly EL. Niedermeyer E, Lopes da Silva F. In: *Electroencephalography.* Third Edition. Baltimore, MD: Williams & Wilkins; 1993.
14. Gotman J. Daly DD, Pedley TA, Eds. In: *Current Practice of Clinical Electroencephalography.* Second Edition. New York, NY: Raven Press, Ltd.; 1990.
15. Fisher RS, Arroyo SA, Lesser RP. Personal communication, publication in progress, Johns Hopkins Hospital Department of Neurology, Epilepsy Center; 1993.
16. Kellaway P. Daly DD, Pedley TA, Eds. In: *Current Practice of Clinical Electroencephalography.* Second Edition. New York, NY: Raven Press, Ltd.; 1990.
17. Duffy FH, Ed. *Topographic Mapping of Brain Electrical Activity.* London UK: Butterworths; 1986.
18. Nunez PL. *Electric Fields of the Brain.* New York, NY: Oxford University Press Inc.; 1981.
19. Chiappa KH, Hoch DB. Ropper AH Ed. In: *Neurological and Neurosurgical Intensive Care.* Third Edition. New York, NY: Raven Press, Ltd.; 1993.
20. Daube JR, Harper M. Daly DD, Pedley TA, Eds. In: *Current Practice of Clinical Electroencephalography.* Second Edition. New York, NY: Raven Press, Ltd.; 1990.
21. Luders HO, Engel J Jr., Munari C. In: *Surgical Treatment of the Epilepsies.* Second Edition. Engle J Jr (Ed). New York, NY: Raven Press, Ltd.; 1993.
22. Mckenna T, Davis J, Zornetzer SF. Eds. *Single Neuron Computation.* San Diego, CA: Academic Press, Inc.; 1992.
23. Vaughan HG, Arezzo JC. The nerual basis of event-related potentials. In: *Handbook of Electroencephalography and Clinical Neurophysiology: Human Event-related Potentials.* Volume 3. Picton TW (Ed). New York, NY: Elsevier Publishers.; 1988.
24. Chiappa KH. *Evoked Potentials in Clinical Medicine.* Second Edition. New York, NY: Raven Press Ltd.; 1990.
25. American Electroencephalographic Society Guidelines for Clinical Evoked Potential Studies. Bloomfield, CT; 1992.
26. Goldic WD, Chiappa KH, Young RR. Brain stem auditory evoked responses and short-latency somatosensory evoked responses in the evaluation of deeply comatose patients. *Neurology.* 1979; 29: 551.
27. Levy WJ, Shapiro HM, Maruchak G, et al. Automated EEG processing for intraoperative monitoring: A comparison of techniques. *Anesthesiology.* 1980; 53: 223-236.
28. Levy WJ. Power spectrum correlates of changes in consciousness during anesthetic induction with enflurane. *Anesthesiology.* 1986; 64: 688-693.
29. Niedermeyer E. The normal EEG of the waking adult. In: *Electroencephalography: Basic Principles, Clinical Applications, and Related Fields.* Niedermeyer E, da Silva FL (Eds). Baltimore, MD: Urban and Schwarzenberg; 1987.
30. Cooley JW, Tukey JW. An algorithm for the machine calculation of complex Fourier series. *Math Comp.* 1965; 19: 297-301.
31. Bickford RG, Fleming NI, Billinger TW. Compression of EEG data. *Transact Am Neurol Assoc.* 1971; 98: 118-122.
32. Bickford RG, Brunin J, Berger L, et al. Application of compressed spectral array in clinical EEG. In: *Automation of Clinical Electroencephalography.* Kellaway P, Peterson I (Eds). New York, NY: Raven Press Ltd.; 1973.
33. Fleming RA, Smith NT. An inexpensive device for analyzing and monitoring the electroencephalogram. *Anesthesiology.* 1979; 50: 456-460.
34. Duffy FH. *Topographic Mapping of Brain Electrical Activity.* Boston, MA: Butterworth Publishers; 1986.

35. Rampil IJ, Sasse FJ, Smith NT, et al. Spectral edge frequency: A new correlate of anesthetic depth. *Anesthesiology*. 1980; 53: S12.

36. Rampil IJ, Smith NT. Comparison of EEG indices during halothane anesthesia. *J Clin Monit*. 1985; 1: 89-90.

37. Scott JC, Poganis KV, Stanski DR. EEG quantification of narcotic effect: The comparative pharmacodynamics of fentanyl and alfentanil. *Anesthesiology*. 1985; 62: 234-241.

38. Scott JC, Stanski DR. Decreased fentanyl and alfentanil dose requirements with age: A simultaneous pharmacokinetic and pharmacodynamic evaluation. *J Pharmacol Exp Ther*. 1987; 240: 159-166.

39. Rampil IJ, Matteo RS. Changes in EEG spectral edge frequency correlate with the hemodynamic response to laryngoscopy and intubation. *Anesthesiology*. 1987; 67: 139-142.

40. Isley MR, Kafer ER, Zech BA, et al. High-dose fentanyl induction: The effect on spectral edge frequency and amplitude of the computer-processed EEG. *Anesth Analg*. 1988; 67: S101.

41. Isley MR, Lucas WJ, Zech BA, et al. Brain monitoring reduces fentanyl dosage during cardiac surgery. *Society of Cardiovascular Anesthesiologists*. 1989; 11: 228.

42. Isley MR, Kafer ER, Bloom MJ. Anesthesia monitoring during surgery: Intraoperative cerebral monitoring during cardiac surgery using computer-processed EEG. *Med Elec*. 1990; 122: 82-94.

43. Bowdle TA, Ward RJ. Induction of anesthesia with small doses of sufentanil or fentanyl: Dose versus EEG response, speed of onset, and thiopental requirement. *Anesthesiology*. 1989; 707: 26-30.

44. Kearse L, Saini V, deBros F, et al. Bispectral analysis may predict anesthetic depth during narcotic induction. *Anesthesiology*. 1991; 75: A175.

45. Sebel PS, Bowles S, Saini V, et al. Accuracy of EEG in predicting movement at incision during isoflurane anesthesia. *Anesthesiology*. 1991; 75: A446.

46. Vernon J, Bowles S, Sebel PS, et al. EEG bispectrum predicts movement at isoflurane or propofol anesthesia. *Anesthesiology*. 1992; 77: A502.

47. Mahla ME. Anesthetic effects on the electroencephalogram. *Neuro Sci Mon*. 1992; 3: 2-7.

48. Martin JT, Faulconer A Jr., Bickford RG. Electroencephalography and anesthesiology. *Anesthesiology*. 1959; 20: 359-376.

49. Guedel AE. Signs of inhalational anesthesia: A fundamental guide. In: *Inhalational Anesthesia*. Guedel AE (Ed). New York, NY: Macmillan; 1920.

50. Kugler J. Stages of anesthesia. In: *EEG Atlas for Anesthesiologists*. Pichlmayr I (Ed). New York, NY: Springer-Verlag, Inc.; 1987.

51. Nussmeier NA, Arlund C, Slogoff S. Neuropsychiatric complications after cardiopulmonary bypass: Cerebral protection by a barbiturate. *Anesthesiology*. 1986; 64: 165-170.

52. Nussmeier NA. Pro: Barbiturates should be used for brain protection during open heart surgery. *J Cardiothoracic Anesthesia*. 1988; 2: 385-389.

53. Blume WT, Sharbrough FW. EEG monitoring during carotid endarterectomy and open heart surgery. In: *Electroencephalography: Basic Principles, Clinical Applications, and Related Fields*. Niedermeyer E, da Silva FL (Eds). Baltimore, MD: Urban and Schwarzenberg; 1987.

54. Gravlee GP, Ramsey FM, Roy RC, et al. Rapid administration of a narcotic and neuromuscular blocker: A hemodynamic comparison of fentanyl, sufentanil, pancuronium, and vecuronium. *Anesth Analgl*. 1988; 67: 39-47.

55. Sebel PS, Bovill JG, Waquier A, et al. The effects of high-dose fentanyl anesthesia on the electroencephalogram. *Anesthesiology*. 1981; 55: 203-211.

56. Waquier A, Bovill JG, Sebel PS. Electroencephalographic effects on fentanyl-, sufentanil-, and alfentanil anesthesia in man. *Neuropsychobiology*. 1984; 11: 203-206.

57. Sidi A, Halimi P, Cotev S. Estimating anesthetic depth by electroencephalography during anesthetic induction and intubation in patients undergoing cardiac surgery. *J Clin Anesthesia*. 1990; 2: 101-107.

58. Smith NT, Dec-Silver H, Sanford TJ, et al. EEGs during high-dose fentanyl-, sufentanil-, or morphine-oxygen anesthesia. *Anesth Analg*. 1984; 63: 386-393.

59. Bovill JG, Sebel PS, Stanley TH. Opioid anesthesia with special reference to their use in cardiovascular anesthesia. *Anesthesiology*. 1984; 61: 731-755.

60. Veselis RA, Reinsel R, Alagesan R, et al. The EEG as a monitor of midazolam amnesia: Changes in power and topography as a function of amnesic state. *Anesthesiology*. 1991; 74: 866-874.

61. Mahla ME. Carotid artery surgery: Anesthesia and monitoring. Course review lecture, *Am Society Anesthesiologists*. 1990; 271: 1-7.

62. Chiappa KH, Burke SR, Young RR. Results of electroencephalographic monitoring during 367 carotid endarterectomies. *Stroke*. 1979; 10: 381-388.

63. Sundt TM Jr., Charbrow FJ, Piegas DG, et al. Correlation of cerebral blood flow and electroencephalographic changes during carotid endarterectomy. *Mayo Clin Proc*. 1981; 56: 533-543.

64. Chemtob G, Kearse LA. The use of electroencephalography in carotid endarterectomy. *International Anesthesiology Clinics*. 1990; 28: 143-146.

65. Blume WT, Ferguson GG, McNeal DK. Significance of EEG changes at carotid endarterectomy. *Stroke*. 1986; 17: 891-897.

66. Sundt TM Jr. The ischemic tolerance of neural tissue and the need for monitoring and selective shunting during carotid endarterectomy. *Stroke*. 1983; 14: 93-98.

67. Sharbrough FW, Messicks JM Jr., Sundt TM Jr. Correlation of continuous electroencephalograms with cerebral blood flow measurements during carotid endarterectomy. *Stroke*. 1973; 4: 674-683.

68. Blackshear WM Jr., DiCarol V, Zifert KB, et al. Advantages of continuous electroencephalographic monitoring during carotid artery surgery. *J Cardiovasc Surg.* 1986; 27: 146-153.

69. Crosby G. CNS dysfunction in the perioperative period: Causes and solutions. Course review lecture, *Am Society of Anesthesiologists.* 1990; 242: 1-7.

70. Hammeke TA, Hastings JE. Neuropsychologic alterations after cardiac surgery. *J Thorac Cardiovasc Surg.* 1988; 96: 326-331.

71. Shaw PJ, Bates D, Cartlidge NE, et al. Early neurological complications of coronary artery bypass surgery. *B Med J.* 1986; 293: 165-167.

72. Kubicki St. V, Trede M, Just O. Die bedeutung des EEG bei herzoperationen in hypothermie und bei extrakorporaler zirkulation. *Der Anaesthesist.* 1960; 9: 119-123.

73. Isley MR, Kafer ER, Zech BA, et al. Raw and computer-processed EEG during cardiac surgery using cardiopulmonary bypass. *Anesth Rev.* 1987; 14: 56-58.

74. Isley MR, Kafer ER, Zech BA, et al. Trends in raw and computer-processed EEG before, during, and after coronary artery bypass graft surgery. *Soc Cardiovasc Anesth.* 1988; 10: 60.

75. Isley MR, Kafer ER, Zech BA, et al. A brain monitoring program for the anesthesiologist. Scientific Exhibit, *Am Society of Anesthesiologists.* 1988.

76. Isley MR, Bloom MJ. Cerebral monitoring during cardiopulmonary bypass. Workshop, *Society of Cardiovascular Anesthesiologists;* 1989.

77. Arom KV, Cohen DE, Strobl FT. Effect of intraoperative intervention on neurological outcome based on electroencephalographic monitoring during cardiopulmonary bypass. *Ann Thorac Surg.* 1989; 48: 476-483.

78. Edmonds HL, Griffiths LK, van der Laken J, et al. Quantitative electroencephalographic monitoring during myocardial revascularization predicts postoperative disorientation and improves outcome. *J Thorac Cardiovasc Surg.* 1992; 103: 555-563.

79. Newell DW, Aaslid R (Eds). *Transcranial Doppler.* New York, NY: Raven Press Ltd.; 1992.

80. Albin MS, Bunegin L, Garcia C, et al. The transcranial Doppler can image microaggregates of intracranial air and particular matter. *Am Society of Anesthesiology.* 1990; 73: A466.

81. Spencer MP, Thomas GI, Nicholls SC, et al. Detection of middle cerebral artery emboli during carotid endarterectomy using transcranial Doppler ultrasonography. *Stroke.* 1990; 21: 514-523.

82. Halsey JH. Monitoring blood flow velocity in middle cerebral artery during carotid endarterectomy. Fall newsletter, *Society of Neurosurgical Anesthesia and Critical Care.* 1989; 3-6.

7.0 ILLUSTRATION CREDITS

Figure 1.2

Wilbourn A. How can electromyography help you? *Postgrad Med.* 1983; 6:188.

Figure 1.3

Downing JA, Darling RC. *A Physiological Basis of Rehabilitation.* Philadelphia, PA: WB Sanders; 1971.

Figures 1.6 and 1.7

Daube JR, Sandisk BA. *Medical Neurosciences.* Boston, MA: Little Brown; 1978.

Figure 1.9

Bloom W, Fawcett DW. *A Textbook of Histology.* Philadelphia, PA: WB Sander;. 1975.

Figures 1.10 and 1.13

Dudel J, Jänig W, Schmidt R, et. al. *Fundamentals of Neurophysiology.* New York, NY: Springer-Verlag, Inc.; 1985.

Figure 1.12

Guyton AC. *Textbook of Medical Physiology.* Eighth Edition. Philadelphia, PA: WB Sanders; 1991.

Figure 1.19

Ebashi S, Endo M, Ontsuki I. Control of Muscle Contraction. *Q Rev in Biophy.* 1969; 2:351-384.

Figure 1.28

Lenman JAR, Ritchie AE. *Clinical Electromyography.* Third Edition. London, United Kingdom: Pitman Books, Ltd.; 1983.

Figures 1.35 and 1.36

Hardy RW. *Seminars in Neurological Surgery: Lumbar Disk Disease.* New York, NY: Raven Press, Ltd.; 1982.

Figure 1.39

Hammer K. *Nerve Conduction Studies.* Springfield, IL: Charles C Thomas Publisher; 1982.

Figures 1.40, 1.42, and 1.47

Daube J. *AAEM Minimonograph #11: Needle Examination in Clinical Electromyography.* Rochester, MN: American Association of Electrodiagnostic Medicine; 1991.

Figures 1.41, 1.55, and 1.56

Stålberg E, Trontelj J. *Single Fibre Electromyography.* Surrey, United Kingdom: The Mirvalle Press Ltd.; 1979.

Figure 1.43

Ball RD. *Basics of Needle Electromyography: An AAEM Workshop.* Rochester, MN: American Association of Electrodiagnostic Medicine; 1985.

Figure 1.46

Burke RE. Patterns of gastrocnemius motor units in the decerebrate cat. *J Physiol.* 1968; 631-654.

Figures 1.57 and 1.58

Stålberg E. *AAEM Minimonograph #20: Macro EMG.* Rochester, MN: American Association of Electrodiagnostic Medicine; 1983.

Figure 1.59

Stålberg E. Macro EMG, a new recording technique. *J Neuro Neurosurg Psych.* 1980; 43:475-482.

Figures 1.60 and 1.70

Ludin HP. *Electromyography in Practice.* New York, NY: Thieme-Stratton; 1980.

Figure 1.61

Nandedkar SD, Saunders DB, Stålberg E. Automatic analysis of the electromyographic interference pattern. Part 1: Development of quantitative Features. *Muscle Nerve.* 1986; 9:431-439.

Figure 1.62

Fuglsang-Frederiksen A, Månsson. Analysis of electrical activity of normal muscle in man at different degrees of voluntary effort. *J Neuro Neurosurg Psych.* 1975; 38:685.

Figures 1.63 and 1.65

Stålberg E, Chu J, Bril V, et al. Automatic analysis of the EMG interference pattern. *Electroencephalography Clin Neurophysiology.* 1983; 56:672-681.

Figures 1.65 and 1.66

Nandedkar SD, Saunders DB, Stålberg E. Automatic analysis of the electromyographic interference pattern. Part 2: Findings in control subjects and in some neuromuscular diseases. *Muscle Nerve.* 1986; 9:491-500.

Figure 1.67

Clinical Examinations in Neurology. Sixth Edition. St. Louis, MO: CV Mosby; 1991.

Figure 1.68

Pickett JB. *Neuromuscular Transmission in Physiology of Peripheral Nerve Disease.* Philadelphia, PA: WB Sanders; 1980.

Figure 1.69

Kimura, J. *Electrodiagnosis in Disease of Nerve and Muscle.* Second Edition. Philadelphia, PA: FA Davis; 1989.

Figure 2.5

Litt B. Dipoles and the EEG. *Am J EEG Technol.* 31(2):120.

Figures 2.7, 2.8, 2.15(a), 2.19, 2.20, 2.21(a,b,e), 2.22, 2.23, 2.25, 2.32, and 2.35

Daly DD, Pedley TA. *Current Practice of Clinical Electroencephalography.* Second Edition. New York, NY: Raven Press, Ltd.; 1990.

Figures 2.3, 2.11, and 3.9

Kandell E, Schwartz J, Jessel T. *Principles of Neural Science.* Third Edition. New York, NY: Elsevier Science Publishing which has been assigned to Appleton and Lange, Norwalk, CT; 1991.

Figures 2.14, 2.16(a), 2.17, and 2.31

Grass Model 8 Instruction Manual. Quincy, MA: Grass Medical Instruments; 1974.

Figures 3.3, 3.5, 3.6, and 3.7

Handbook of Electroencephalography and Clinical Neurophysiology. Edited by Picton, ED. New York, NY: Elsevier Science Publishing Co; 1988.

Figure 3.11

Kandell E, Schwartz J, Jessel T. *Principles of Neural Science.* Third Edition. West Caldwell, NJ: CIBA-Geigy Corp.; 1991.

Figure 3.14

Chiappa KH. *Evoked Potentials in Clinical Medicine.* Second Edition. New York, NY: Raven Press, Ltd.; 1990.

Figure 4.1

Levy W, Shapiro H, Maruchak G, et al. Automated EEG processing for intraoperative monitoring: A comparison of techniques. *Anesthesiology.* 1980; 53:223-236.

Figures 4.3 and 4.9

Pichlmayr I, Lips U, Künkel H. *The Electroencephalogram in Anesthesiology: Fundamentals, Practical Applications, Examples.* New York, NY: Springer-Verlag, Inc.; 1984.

Figure 4.5

Neurotrac: A major advance in patient monitoring. Courtesy of Moberg Medical, Inc., Ambler, PA.

Figure 4.6

Rampil I, Smith N. Comparison of EEG indices during halothane anesthesia. *J of Clin Mon.* 1985; 1:89-90.

Figure 4.7

Scott JC, Poganis KV, Stanski DR. EEG quantification of narcotic effect: The comparative pharmacodynamics of fentanyl and alfentanil. *Anesthesiology.* 1985; 62:234-241.

Figure 4.8

Martin JT, Faulconer A Jr., Bickford RG. Electroencephalography and anesthesiology. *Anesthesiology,* 1959; 20:359-376.

Figures 4.10 and 4.15

American Society of EEG Technologists, Inc. *A Drug Reference for EEG Technologies.* Caroll, IA.; 1985.

Figures 4.12, 4.16, and 4.19

Blume WT, Sharbrough FW. *Electroencephalography: Basic Principles, Clinical Applications, and Related Fields.* Second Edition. Niedermeyer E, Lopes de Silva F (Eds). Baltimore, MD: Urban and Schwartzenberg; 1987.

Figure 4.13

Pichlmayr I. *EEG Atlas for Anesthesiologists.* New York, NY: Springer-Verlag, Inc.; 1987.

Figure 4.18

Chemtob G, Kearse LA. The use of EEG in carotid endarterectomy. *International Anesthesiology Clinics.* 1990; 28:143-146

Figure 4.22

Arom KV, Cohen DE, Strobl FT. EEG monitoring during cardiopulmonary bypass. *Ann Thorac Surg.* 1989; 48:476-83.

Figure 4.23

Edmonds H, Griffiths L, van der Laken J, et al. Quantitative electroencephalographic monitoring during myocardial revascularization predicts postoperative disorientation and improves outcome. *J Thorac Cardiovasc Surg.* 1992; 103:555-563.

Figures 4.24, 4.25, 4.26, 4.28

Newell D, Aaslid R. *Transcranial Doppler.* New York, NY: Raven Press, Ltd.; 1992.

8.0 BIBLIOGRAPHY

The following bibliography lists citations pertinent to electromyography/electroencephalography.

8.1 Electromyography

Wilbourn AJ. How can electromyography help you? *Postgraduate Medicine.* 1983; 73:189-195.

8.2 The EMG Examination

Kimura J. *Electrodiagnosis in Diseases of Nerve and Muscle.* Second Edition. Philadelphia, PA: FA Davis; 1989.

Wilbourn AJ. How can electromyography help you? *Postgraduate Medicine.* 1983; 73:189-195.

8.3 The Nerve

Brown WF. *The Physiological and Technical Basis of Electromyography.* Andover, MA: Butterworth-Heinemann; 1984.

Guyton AC. *Textbook of Medical Physiology.* Eighth Edition. Philadelphia, PA: WB Saunders Co.; 1991.

Wilbourn AJ. Nerve conduction studies in axonopathies and demyelinating neuropathies. In syllabus: AAEE Course A: Fundamentals of Electrodiagnosis. Rochester, MN: American Association of Electromyography and Electrodiagnosis. 1989; 7-20.

8.4 The Resting Membrane Potential

Brown WF. *The Physiological and Technical Basis of Electromyography.* Andover, MA: Butterworth-Heinemann; 1984.

Davison H. *A Textbook of General Physiology.* Third Edition. Boston, MA: Little Brown Co.; 1964.

Eyzaquirre C, Fidone SJ. *Physiology of the Nervous System.* Second Edition. Chicago, IL: Year Book Medical Pub.; 1975.

Guyton AC. *Textbook of Medical Physiology.* Eighth Edition. Philadelphia, PA: WB Saunders Co.; 1991.

8.5 The Action Potential

Brown WF. *The Physiological and Technical Basis of Electromyography.* Andover, MA: Butterworth-Heinemann; 1984.

Eyzaquirre C, Fidone SJ. *Physiology of the Nervous System.* Second Edition. Chicago, IL: Year Book Medical Pub.; 1975.

Guyton AC. *Textbook of Medical Physiology.* Eighth Edition. Philadelphia, PA: WB Saunders Co.; 1991.

8.6 Electricity and Electronics

Barry DT. Basic concepts of electricity and electronics in clinical electromyography. *Muscle and Nerve.* 1991; 14: 937-946.

Daly DD, Pedley TA. *Current Practice of Clinical Electroencephalopathy.* New York, NY: Raven Press Ltd.; 1990.

Kimura J. *Electrodiagnosis in Diseases of Nerve and Muscle.* Second Edition. Philadelphia, PA: F A Davis; 1989.

8.7 Equipment

Buchthal F. *An Introduction to Electromyography.* Copenhagen, Denmark: Scandinavian University Books; 1957.

Goodgold J, Eberstein A. *Electrodiagnosis of Neuromuscular Diseases.* Third Edition. Baltimore, MD: Williams & Wilkins; 1983.

Kimura J. *Electrodiagnosis in Diseases of Nerve and Muscle.* Second Edition. Philadelphia, PA: F A Davis; 1989.

8.8 Electrical Safety

Barry DT. Basic concepts of electricity and electronics in clinical electromyography. *Muscle and Nerve.* 1991; 14:937-946.

Daly DD, Pedley TA. *Current Practice of Clinical Electroencephalopathy.* New York, NY: Raven Press Ltd.; 1990.

8.9 Nerve Conduction Studies

Brown WF. *The Physiological and Technical Basis of Electromyography.* Andover, MA: Butterworth-Heinemann; 1984.

Hodes R, Larrabee MG, German W. The human electromyogram in response to nerve stimulation and the conduction velocity of motor axons. *Arch Neurol Psych.* 1984; 60:340-365.

Kimura J. *Electrodiagnosis in Diseases of Nerve and Muscle.* Second Edition. Philadelphia, PA: F A Davis; 1989.

8.10 Special Studies in the EMG Laboratory

Wilbourn AJ. How can electromyography help you? *Postgraduate Medicine.* 1983; 73:189-195.

8.11 H-Response

Goodgold J, Eberstein A. *Electrodiagnosis of Neuromuscular Diseases.* Third Edition. Baltimore, MD: William & Wilkins; 1983.

Hammer K. *Nerve Conduction Studies.* Springfield, IL: Charles C Thomas, Pub.; 1982.

Kimura J. *Electrodiagnosis in Diseases of Nerve and Muscle.* Second Edition. Philadelphia, PA: F A Davis; 1989.

8.12 F-Waves

Kimura J. *Electrodiagnosis in Diseases of Nerve and Muscle.* Second Edition. Philadelphia, PA: F A Davis.; 1989.

Wilbourn AJ. Electrodiagnosis: The electromyographic examination. Rothman RH, Simeone FA (Eds). In: *The Spine.* Third Edition. 1992.

8.13 Blink Response

Hammer K. *Nerve Conduction Studies.* Springfield, IL: Charles C Thomas, Pub.; 1982.

Kimura J. *Electrodiagnosis in Diseases of Nerve and Muscle.* Second Edition. Philadelphia, PA: F A Davis; 1989.

8.14 Pitfalls in Performance of NCS

Braddom RL, Schuchmann J. Motor conduction. E Johnson (Ed.): In: *Practical Electromyography*. Baltimore, MD: Williams & Wilkins; 1980.

Kimura J. *Electrodiagnosis in Diseases of Nerve and Muscle*. Second Edition. Philadelphia, PA: F A Davis; 1989.

Wilbourn AJ. How can electromyography help you? *Postgraduate Medicine*. 1983; 73:189-195.

8.15 Special EMG Methods

Buchthal F. *An Introduction to Electromyography*, Copenhagen, Denmark: Scandinavian University Books; 1957.

Buchthal F., Pinelli P, Rosenfalk P. Action potential perimeters in normal human muscle and their physiological determinants. *Acta Physiological Scandinavica*. 1954; 32:219-229.

Buchthal F, Kamiencka Z. The diagnostic yield of quantified electromyography and quantified muscle biopsy in neuromuscular disorders. *Muscle and Nerve*. 1982; 5:265-280.

Dorfman LJ, McGill KC. Automatic quantitative electromyography. *Muscle and Nerve*. 1988; 11:804-818.

Nandedkar SD, Sanders DB, Stålberg EV. Automatic analysis of the electromyographic interference pattern. Part I: Development of quantitative features. *Muscle and Nerve*. 1986; 9:431-439.

Nandedkar SD, Sanders DB, Stålberg EV. Automatic analysis of the electromyographic interference pattern. Part II: Findings in control subjects and in some neuromuscular diseases. *Muscle and Nerve*. 1986; 9:491-500.

Stålberg E, Trontelj J. *Single Fiber Electromyography*. Old Woking, Surrey, UK: The Mirvalle Press Limited; 1979.

Stålberg E. Macro EMG. *Muscle and Nerve*. 1983; 6: 619-630.

Stålberg EV, Chu J, Bril V, et al. Automatic analysis of the EMG interference pattern. *EEG Clin Neurophysiol*. 1983; 56:672-681.

8.16 Hysteria/Malingering/Upper Motor Neuron Disease

Wilbourn AJ. How can electromyography help you? *Postgraduate Medicine*. 1983; 73:189-195.

8.17 Neuropathies

Kimura J. *Electrodiagnosis in Diseases of Nerve and Muscle*. Second Edition. Philadelphia, PA: F A Davis; 1989.

Wilbourn AJ. How can electromyography help you? *Postgraduate Medicine*. 1983; 73:189-195.

Wilbourn AJ. Nerve conduction studies in axonopathies and demyelinating neuropathies. In syllabus: AAEE Course A: *Fundamentals of Electrodiagnosis*. Rochester, MN: American Association of Electromyography and Electrodiagnosis. 1989.

8.18 Myopathies

Burke JM. Electromyography in myopathies. Rochester, MN: American Association of Electromyography and Electrodiagnosis. Course, Fundamentals of Electrodiagnosis. September 1989.

Kimura J. *Electrodiagnosis in Diseases of Nerve and Muscle*. Second Edition. Philadelphia, PA: F A Davis; 1989.

8.19 Electroencephalography

Barlow, JS, Kamp A, Morton HB, et al. EEG Instrumentation Standards: Report of the committee on EEG instrumentation standards of the International Societies for Electroencephalography and Clinical Neurophysiology. *Electroenchephalogr Clin Neurophysiol*. 1974, 37:539-553.

Cooper R, Osselton JW, Shaw JC. *EEG Technology*. London, UK: Butterworths; 1980.

Creutzfeldt O, Watanabe S, Lux HD. Relations between EEG phenomena and potentials of single cortical cells. II. Spontaneous and convulsoid activity. *Electroencephalogr Clin Neurophysiol*. 1966; 20:19-37.

Daly DD, Pedley TA (Eds). *Current Practice of Clinical Electroencephalography*. Second Edition. New York, NY: Raven Press Ltd.; 1990.

Graf M, Niedermeyer E, Schiemann J, et al. Electrocorticography: Information derived from intraoperative recordings during seizure surgery. *Clin Electroencephalogr*. 1984; 15:83-91.

Grass Model 8 Instruction Manual. Quincy, MA: Grass Instrument Company; 1974.

Hjorth B. Multichannel EEG preprocessing: Analog matrix operations in the study of local effects. *Pharmakopsychiatr Neuro-psychopharmakol*. 1975; 12:111-118.

Kandell ER, Schwartz JH, Jessell TM. *Principles of Neural Science*. Third Edition. New York, NY: Elsevier Science Publishing Co.; 1991.

Lesser RP, Luders H, Dinner DS, et al. Extraoperative cortical functional localization in patients with epilepsy. *Clin Neurophysiol*. 1987; 4:27-53.

Lehmann D. Spatial analysis of EEG and evoked potential data. In: *Topographic Mapping of Brain Electrical Activity*. Duffy FH (Ed). Andover, MA: Butterworth-Heinemann; 1986.

Litt B. Dipoles and the EEG. *Am J EEG Technol*. 1991; 31:119-121.

Niedermeyer E, da Silva FL (Eds). *Electroencephalography: Basic Principles, Clinical Applications, and Related Fields*. Second Edition. Baltimore, MD: Urban and Schwarzenberg; 1987.

Silverman D. The anterior temporal electrode and the ten-twenty system. *Electroencephalogr. Clin Neurophysiol*. 1960; 12:735-737.

Spencer SS, Spencer DD, Williamson PD, et al. The localizing value of depth electroencephalography in 32 patients with refractory epilepsy. *Ann Neurol*. 1982; 12:248-253.

Throb RD, Miles R, Wong RKS. Large scale simulations of the hippocampus. *IEEE Eng Med Biol*. 1988; 7:31-38.

Weiser JG, Moser S. Improved multipolar foramen ovale electrode monitoring. *J Epilepsy*. 1988; 1:13-22.

Brazier MAB. *A History of the Electrical Activity of the Brain*. New York, NY: Macmillan Press; 1961.

Chiappa KH. *Evoked Potentials in Clinical Medicine.* Second Edition. New York, NY: Raven Press Ltd.; 1990.

Vaughan HG, Arezzo JC. The neural basis of event-related potentials. Picton TW (Ed). In: *Handbook of Electroencephalography and Clinical Neurophysiology: Human Event-related Potentials.* New York, NY: Elsevier Science Publishing Co.; 1988.

8.20 Evoked Potentials

Brazier MAB. *A History of the Electrical Activity of the Brain.* New York, NY: Macmillan Press; 1961.

Chiappa KH. *Evoked Potentials in Clinical Medicine.* Second Edition. New York, NY: Raven Press Ltd.; 1990.

Goldic WD, Chiappa KH, Young RR. Brain stem auditory evoked responses and short-latency somatosensory evoked responses in the evaluation of deeply comatose patients. *Neurology.* 1979; 29:551.

Guidelines for Clinical Evoked Potential Studies. Bloomfield, CT: American Electroencephalographic Society; 1992.

Kandel ER, Schwartz JH, Jessell TM (Eds.). *Principles of Neural Science.* Third Edition. New York, NY: Elsevier Science Publishing Co.; 1991.

Naatanen R. *Attention and Brain Function.* New Jersey: Erlbaum Pub.; 1992.

Vaughan HG, Arezzo JC. The neural basis of event-related potentials. Picton TW (Ed). In: *Handbook of Electroencephalography and Clinical Neurophysiology: Human Event-related Potentials.* New York, NY: Elsevier Science Publishing Co.; 1988.

8.21 Interoperative Brain Monitoring

A Drug Reference for EEG Technologies. Caroll, IA: American Society of EEG Technologists, Inc.; 1985.

Arom KV, Cohen DE, Strobl FT. EEG monitoring during cardiopulmonary bypass. *Ann Thorac Surg.* 1989; 48:476-83.

Blume WT, Sharbrough FW. *Electroencephalography: Basic Principles, Clinical Applications, and Related Fields.* Second Edition. Niedermeyer E, de Silva FL (Eds). Baltimore, MD: Urban and Schwarzenberg; 1987.

Chemtob G, Kearse LA. The use of EEG in carotid endarterectomy. *International Anesthesiology Clinics.* 1990; 28:143-146.

Edmonds H, Griffiths L, van der Laken J, et al. Quantitative electroencephalographic monitoring during myocardial revascularization predicts postoperative disorientation and improves outcome. *J Thorac Cardiovasc Surg.* 1992; 103:555-563.

Levy W, Shapiro H, Maruchak G, et al. Automated EEG processing for intraoperative monitoring: A comparison of techniques. *Anesthesiology.* 1980. 53:223-236.

Martin JT, Faulconer A Jr., Bickford RG. Electroencephalography and anesthesiology. *Anesthesiology.* 20:359-376, 1959.

Pichlmayr I, Lips U, Künkel H. *The Electroencephalogram in Anesthesiology: Fundamentals, Practical Applications, Examples.* New York, NY: Springer-Verlag; 1984.

Rampil I, Smith N. Comparison of EEG indices during halothane anesthesia. *J Clin Monit.* 1985; 1:89-90.

Scott JC, Poganis KV, Stanski DR. EEG quantification of narcotic effect: The comparative pharmacodynamics of fentanyl and alfentanil. *Anesthesiology.* 1985; 62:234-241.

9.0 GLOSSARY

acetylcholine — The chemical released at the ends of the nerve fibers in the somatic and parasympathetic nervous systems; it acts in the transmission of nervous impulses in the body.

action potential — A momentary change in the electrical potential or charge on the surface of a nerve or muscle cell that occurs when the cell is stimulated; an impulse transmitted along nerve and muscle membranes.

ampere — A unit of steady electric current, represented as meter-kilogram-second, that occurs when the current flows in straight parallel wires of infinite length and negligible cross section and separated by a distance of one meter in free space.

anode — A positively charged electrode, as seen in an electrolyte cell.

anterior cerebral artery — A horizontally-oriented basal arterial branch of the circle of Willis, a major intracranial artery.

anterior horn cell — A part of the motor unit of the nervous system located in the anterior, or ventral front, portion of the spinal cord.

anteriorly maximum, intermittent slow waves — An EEG pattern observed during increases in inhalation anesthetic concentrations.

averaging — The process whereby the recording segments synchronized to specific stimuli for somatosensory evoked potentials (EPs) are averaged to reduce the effects of unwanted noise on these signals; generally averaging reduces noise proportionate to the square root of the number of trials.

axon — The long process of a nerve fiber that usually conducts the impulses away from the nerve cell body.

band-pass filter — A filter that allows frequencies between two cut-offs to pass with minimal attenuation.

barbiturate — Agents used to induce and maintain anesthesia; have hypnotic properties but do not produce analgesia or relax muscles.

benzodiazepine — Agents commonly used for sedation and the production of amnesia as premedication or an adjunct to other anesthetic drugs; at low doses, these drugs increase the frontally dominant beta activity.

bispectral analysis — Measures the potential interactions between the waves on an EEG to determine whether dependent components are present; quantifies the phase coupling between every possible frequency pair combination and their sum.

brain stem auditory evoked response — Electrical responses elicited from the auditory system to evaluate the function of several levels of the peripheral and brain stem auditory system including the auditory nerves and the brain stem pons and midbrain; can distinguish signals recorded during right and left ear stimulation.

breach rhythm — Increased fast activity and amplitude of normal background seen on the surface EEG as a consequence of a disruption (or breech) in the skull. The skull, scalp, cerebrospinal fluid, dura and tissue on the head act as significant filters for the EEG signals, particularly in the high frequency range.

capacitance — The ratio of charge to potential on an electrically charged, isolated conductor; the property of a circuit element that allows it to store a charge.

capacitive resistance — The resistance to the current flow due to the capacitor; measured in ohms.

capacitor — An electric circuit element used to store charge temporarily, usually consisting of two metallic plates separated and insulated from each other by a dielectric; also known as a condenser.

capacity — The ability to receive, hold, or absorb; capacitance.

carotid endarterectomy — A surgical procedure used to reduce the incidence of stroke in patients with carotid occlusive disease (blockages of the carotid artery).

cathode — A negatively charged electrode; for example, an electrolytic cell, a storage battery, or an electron tube.

central nervous system — That part of the nervous system consisting of the brain and spinal cord.

cerebral blood flow — The blood circulation in the head.

charge — To cause the formation of a net electric charge on or in, such as in a conductor.

circuit — A closed path followed or capable of being followed by an electric current.

collateral circulation — The extra or additional circulatory pathways throughout the body and for various organs; not the major circulatory path in the body.

common mode rejection — Because electrical systems are not perfect, some failure occurs in the amplifier of the system so that it rejects the common voltage at both the recording and reference electrodes; the common mode rejection ratio for EMG equipment should be greater than 100,000.

common mode rejection ratio — A measure of differential amplifier amplification. It is defined as the amplitude of the amplifier output when a reference signal is put into one amplifier input and the other is connected to ground, divided by the output voltage when the same reference signal is directed into both amplifier inputs.

complex repetitive discharge — Abnormal spontaneous activity in a muscle seen in any chronic neuropathic or myopathic process or condition.

compound muscle action potential — The recorded electrical activity generated in one of the muscles supplied by a specific motor nerve.

compressed spectral array — A specially developed display format to visually enhance the computer-processed power spectrum.

concentric needle electrode — The most commonly used needle electrode for measuring the electrical properties of muscles; constructed with a thin, metallic wire about 0.1 mm in diameter, which is encased in an external canula of 0.3 mm diameter; it records from the thin wire filament at the tip with the canula serving as the reference electrode.

conductor — A substance of medium that conducts an electric charge.

constant voltage — A continuous, steady voltage source in an electrical circuit.

constant-current stimulator — A device used to directly stimulate peripheral nerves in nerve conduction studies; these stimulators provide a consistent stimulus current for such studies.

contralateral — On the opposite side (usually referring to the head when performing an electroencephalograph).

coulomb — The meter-kilogram-second unit of electrical charge equal to the quantity of charge transferred in one second by a steady current of one ampere.

current — A flow of electric charge; the amount of electric charge flowing past a specified circuit point per unit time.

cut-off frequency — An index of filtering, the limit for frequency set for a specific measurement.

decremental response —The classic response of a muscle fiber produced by repetitive stimulation of the muscle; correlates with the clinical observation of fatigue in exercised muscles.

depolarization — The process along a neuron and its axon in which a rapid change in action potential occurs, usually from -90 mV to +35 mV.

differential amplifier — A type of amplifier that amplifies the voltage difference between the recording and the reference electrodes based on the concept of common mode rejection.

digitize an artifact free signal — To separate the analog or continuous signal into discrete elements.

dot-density modulated spectral array — A specially developed display format to visually enhance the computer-processed power spectrum.

dynamic range — The range of signal amplitudes in which an amplifier will faithfully reproduce variation in the signal.

electrical hazard — The potential for injury from an electrical measurement or device; primarily due to unintended current traveling through the subject's body; can occur from improper grounding of the device systems.

electrical safety — Conducting human studies with equipment and formats that ensure electrical injury will not occur.

electricity — The physical phenomena based on the behavior of electrons and protons caused by the attraction of the particles with opposite charges and the repulsion of the particles with the same charge.

electrode — A solid electric conductor through which an electric current enters or leaves an electrolytic cell or other medium.

epilepsy — A disorder in which abnormal electrical activity in the brain gives rise to unpredictable epileptic seizures that come on without a clear cause.

epilepsy monitoring unit — An area of a hospital or clinic in which patients with intractable epilepsy are continuously followed with scalp or invasive electroencephalograms and by video cameras so that their behavior can be correlated with the outcomes of the electroencephalographs.

epileptic seizure — An event arising from abnormal electrical activity in the brain characterized by unpredictable movements, sensations, actions or other manifestations referable to the area of the brain generating the abnormal electrical activity. These events may be limited to a specific area of the brain (**focal or partial seizures**), may affect the entire brain (**generalized seizures**), may impair consciousness (**complex seizures**), or may leave consciousness intact (**simple seizures**). In their most severe form, seizures result in loss of consciousness and cause generalized stiffening followed by repetitive rhythmic movements (**generalized tonic-clonic seizures**).

epimysium — The external sheath of a connective tissue surrounding a muscle.

equal-potential ground bus — A device or arrangement that ensures all receptacles in a room have a common ground point; particularly necessary in intensive care units where multiple electrical devices are used simultaneously.

evoked potentials — The recorded neural signals coupled to an eliciting sensory stimulus or movement; clinically evaluate the integrity of the various segments of the sensory or motor-conducting pathways.

event-related potential — The long-latency evoked potential elicited by psychological responses to stimuli.

farad — The unit of capacitance in the meter-kilogram-second system equal to the capacitance of a capacitor having an equal and opposite charge of one coulomb on each plate and a potential difference of one volt between the plates.

fasciculation potential — The electrical potential occurring during a small local contraction of muscles, which can be visible through the skin; a spontaneous discharge of a number of fibers innervated by a single motor nerve filament.

fiber density — An index of the number of muscle fibers belonging to the motor unit.

fibrillation — The rapid, uncoordinated twitching movements that replace the normal rhythmic contraction of the heart and may cause a lack of circulation and pulse.

fibrillation potential — Abnormal spontaneous activities in muscle cells caused by degeneration of the muscle cell or necrosis in such conditions as muscular dystrophies and myositis; tend to occur in the axial and most proximal muscles first and later progress to the more proximal limb girdle muscles.

filter — Any various electric, electronic, or optical device that is used to reject signals or radiations of certain frequencies while passing other such signals.

fluothane — See halothane.

frequency spectrum data — Data representing or consisting of the power versus frequency parameters, or the decomposition of a signal into its component frequencies and the power contained in each frequency band.

frontal intermittent rhythmic delta activity — The EEG patterns produced during anesthesia induction with inhalation gases; usually observed as a burst of high amplitude, fast recordings.

ground electrode — The electrode used to establish an arbitrary zero of potential; a conducting electrode that is connected to such a position of zero potential; in electromyography, the ground electrode is applied to the skin with electrolyte cream or jelly.

halothane — Also known as fluothane, the first modern anesthetic gas that promotes progressive EEG frequency slowing and amplitude decreases proportional to the administered dose; associated with induced hepatitis, however.

henry — The unit of inductance in which an induced electromotive force of one volt is produced when the current is varied at the rate of one ampere per second.

high-frequency filter — A filter used to screen out radio frequencies in the range between 3 and 30 megahertz.

high-pass filter — Allow high frequencies to move through a circuit unattenuated and low frequencies to be filtered.

homologous — Corresponding in structure, position or design. In an EEG, homologous implies similar structural regions on different sides of the brain. Homologous regions need not be exactly the same.

human immunodeficiency virus (HIV) — The virus that causes acquired immune deficiency syndrome, or AIDS, a disease that breaks down a part of the body's immune system.

IgG (immunoglobulin G) — A specific member of the group of large glycoproteins secreted by plasma cells that function as antibodies in the immune response by binding to specific antigens.

immediately postinduction (IPI) — The measure for SEF and EEG amplitude taken promptly after intubation and anesthesia induction.

impedance — A measure of the total opposition to current flow in an alternating current circuit, composed of two components that include ohmic resistance and reactance; usually represented as **Z**.

inductance — The property of an electric circuit by which an electromotive force is induced in it or in a nearby circuit by a change of current in either circuit.

inductive reactance — The energy lost through inductance (inducing voltage in a conductor); written as X_L and measured in ohms.

insertional activity — Normal electrical activity produced by mechanically inducing the muscle fiber action potentials; usually lasts as long as the inserted needle moves.

insulator — A material that prevents the passage of heat, electricity or sound.

interference pattern — The pattern of inhibition or prevention of a clear reception of an electrical signal for a specific device.

interictal spikes — Discharges that occur between seizures in patients with epilepsy.

interpolation — A method in which a line connecting two discrete points is calculated. Points on this line are added to a data set to fill in the space between the points; the process of inserting or introducing materials or signals between parts.

intracranial — Occurring or situated within the head; e.g., inside the skull.

inverse problem — The problem in electrophysiology of trying to predict the location of a source of an electric field by mapping the field and calculating backward what produced the field. To date, no unique analytical solution exists to this problem.

ipsilateral — On the same side (usually refers to the head in an EEG).

jitter — A single-fiber EMG measurement performed when two or more muscle fibers belonging to the same motor unit are recorded simultaneously; the variability of the interpotential interval between two single fiber muscle action potentials during successive discharges.

Kirchoff's voltage and current laws — A unit of measurement and laws stating that all elements in parallel have the same voltage potential across them and that all elements in series have the same current passing through them; thus the effective overall resistance equals the sum of the individual resistors.

Lambert-Eaton syndrome — The classic clinical example of a presynaptic defect of neuromuscular junction transmission thought to be caused by the action of an as yet unidentified antibody that prevents the normal acetylcholine transmission.

leakage current — The electrical current unintentionally released.

low-frequency filter — Also called high-pass filters, measure the output taken across the resistor to attenuate about 30% of the signal amplitude for inputs at the cut-off frequency.

low-pass filter — Permits low frequencies to travel through the circuit unattenuated and higher frequencies to be filtered.

M-wave — A response wave obtained by stimulating the tibial nerve in the popliteal fossa while recording from the gastrocnemius/soleus group of muscles (calf muscles); the short latency response of about 10 msec that directly represents the muscle response due to the motor nerve activation.

macro-EMG — The single-fiber EMG technique that uses a specialized single-fiber EMG electrode with a typical single-fiber EMG recording surface but with a bare canula over the distal 15 mm; of the two channels, one records the single-fiber EMG potentials while the second channel records the macro-potential.

mean arterial pressure — The mean blood pressure in the artery near the site of EEG monitoring; measured along with the neural and other physiologic components during anesthesia induction.

miniature end-plate potential — The measurable electrical discharge produced after depolarization of the muscle membrane secondary to release of a single vesicle of acetylcholine; usually present at rest.

minimal alveolar concentration — The alveolar concentration at which 50% of the patients move in response to surgical incision or standard stimulation.

monopolar electrode — A commonly used needle electrode for electromyography, it is composed of a thin metal wire insulated by Teflon except at the recording surface at the very tip; requires a second monopolar needle or a surface electrode adjacent to the skin as a reference electrode.

montage — A pattern of linking electrodes together over the scalp in order to generate a display of EEG channels that present EEG data in a particular way. Montages can be bipolar or referential, or longitudinal, transverse, circular, etc.

motor unit — The peripheral motor system, including the anterior horn cell in the anterior spinal cord, the axon derived from it, branchings of the motor axon, the motor nerve terminals, their adjacent muscle endplates, and the muscle fibers innervated by all the terminal branches arising from the main axon.

motor unit action potential — The action potentials generated by the motor unit of the neuron; recorded by monopolar electrodes per needle electrodes.

myasthenia gravis — A disease characterized by progressive fatigue and generalized weakness of the skeletal muscles, especially those of the face, neck, arms and legs; the disease is thought to be caused by an impaired nervous impulse transmission resulting from an autoimmune attack on the acetylcholine receptors on the muscles.

myasthenic syndrome — The collection of signs and symptoms affecting patients, which usually include various weaknesses of the eyelids, eye movement, speech, swallowing, neck muscles and skeletal muscles; a general disorder disrupting the normal activity in the neuromuscular junction.

myelin — A white fatty material, composed chiefly of lipids and lipoproteins that enclose certain axons and nerve fibers.

myokymic discharge — An abnormal spontaneous muscle electrical activity prominently occurring in the myotonic disorders of myotonia congenita and myotonic muscular dystrophy; alters the morphology of the recorded MUAP on the electromyograph.

myopathy — A disease of the muscle or muscle tissue.

myotonic discharge — Abnormal insertional activity seen in inherited myopathies and chronic acquired neuropathic and myopathic disorders.

NEE — For needle electrode examination, an electrodiagnostic procedure used to assess patients with possible peripheral neuromuscular disorders; the oldest component of the electromyographic examination during which a recording needle electrode is inserted into various skeletal muscles.

needle electrode — Also called subdermal electrodes; fine metal needle electrodes made from stainless steel or platinum that are inserted under the skin after cleaning the region with a presurgical scrubbing compound; these electrodes record nervous or electrical responses that are recorded on the electromyograph.

neuromuscular junction — The synapse, or space, between the motor nerve terminal and the muscle endplate.

neurons — Nerve cells.

neurotransmitters — Chemical substances released by cells in the body that act on neurons to cause hyperpolarization or depolarization.

nitrous oxide — An inhalation anesthetic mixture of nitrous oxide and oxygen producing relatively weak effects on the EEG in the form of high-amplitude, slow-wave activity.

node of Ranvier — A constriction in the myelin sheath on the nerve fiber, usually occurring at intervals along the length of the axon.

nonbarbiturate induction agent — An ultra-short-acting drug that produces a sedative-hypnotic effect and causes dose-dependent central nervous system depression.

non-cephalic — Not on the head.

notch filter — A narrow band-pass filter designed to pass all frequencies except for a small band; for clinical EMGs, these filters filter the 50/60 Hz signals commonly generated from the power line interference.

Ohm's law — The electrical current (I, amp) is directly proportional to the voltage (E, volts) and inversely proportional to the resistance (R, ohms) in a conductor.

ohm — A unit of electrical resistance equal to that of a conductor in which a current of one ampere is produced by a potential of one volt across its terminals.

perimysium — The sheath of connective tissue enveloping bundles of muscle fibers.

peripheral nervous system — That part of the nervous system consisting of peripheral nerves, muscles and their interconnections.

phase — A particular stage in a periodic process or phenomenon; the fraction of a complete cycle as measured from a specified reference point, sometimes represented as an angle.

polymyositis — A highly infectious viral disease that affects children; in its acute phase, it causes inflammation of the motor neurons of the spinal cord and brain stem, leading to paralysis, muscular atrophy and, often, deformities. Polymyositis is preventable through vaccination.

polpharmacy — The use of a combination of anesthetic agents for premedication and balanced anesthesia.

positive wave — In electromyographic terminology, the discharges initiated by needle movement following axon loss that eventually disappear once the needle stops moving.

post-synaptic potentials — Summed electrical potentials resulting from all synapses acting on a particular neuron. Synaptic potentials are added together at the axon hillock region of the neuron.

power — The product of applied potential difference and current in a direct-current circuit; the product of the effective values of the voltage and current with the cosine of the phase angle between current and voltage in an alternating-current circuit.

power drop index — A numerical indicator of the severity and duration of the power decrease below the baseline power level across the patient's head during anesthesia.

power spectrum — The calculated measure of the EEG signals recording the spontaneous electrical potentials of the cortex of the brain across the scalp; calculated by squaring the amplitudes of the individual frequency components of the EEG signals.

preamplifier — An electronic circuit or device that strengthens weak signals, as in a radio receiver, for subsequent, more powerful amplification stages.

preinduction in the holding area — The measure for SEF and EEG amplitude taken before intubation and anesthesia induction.

pulsatility index — Calculated as [(systolic velocity-diastolic velocity)/mean velocity], it serves as a continuous measure of blood flow velocity.

quantitative EMG — The application of high-speed digital technology and analog-to-digital conversion of EMG data to permit quantitative manipulation of EEG signals.

recording electrode — The electrode placed in the subject that actually accepts the signal from the nerve or muscle and records it on a device; the recorded signal on an EMG represents the voltage difference between the recording and the reference electrodes.

recruitment — The progressive recruiting of more motor units to provide increased forceful contracting of the muscle.

reference electrode — The electrode used as a reference point for the measuring of the electrical signal from a nerve or muscle; the recorded signal on an EMG represents the voltage difference between the reference and the recording electrodes.

resistance — The opposition of a body or substance to current passing through it, resulting in a change of electrical energy into heat or another form of energy.

saltatory conduction — When the nerve action potential jumps from one node of Ranvier to the successive one.

sarcolemma — A thin membrane enclosing a striated muscle fiber.

Schwann cell — Any cells that cover the nerve fibers in the peripheral nervous system and form the myelin sheath.

sharp spike — In electromyographic terminology, the discharges initiate needle movement following axon loss that eventually disappear once the needle stops moving.

single-fiber EMG — The technique that measures the muscle action potential from individual muscle fibers belonging to the same motor unit; performed on most standard EMG units with special accessories.

somatosensory evoked potential — The evoked potentials recorded from the sensory portion of the median, tibial and other nerves eliciting responses from the proximal roots, spinal cord, brain stem/thalamus, and the parietal cortex.

spectral edge frequency — The highest visible frequency component of the EEG spectrum; it is calculated as the frequency below which 95% (SEF95) of the total brain power occurs.

spontaneous activity — The always abnormal electrical discharges in a muscle at rest without needle movement if one is inserted; usually occur after denervation.

stereotactically — Oriented in three dimensions using a three-dimension coordinate frame that is fixed to the patient's skull and aligned with the computed tomograph (CT) or magnetic resonance imaging (MRI) scanner-generated images.

stimulator — Devices on all EMG units that directly stimulate the peripheral nerves during nerve conduction studies.

stray capacitance — The situation in which currents leak from the central line or system allowing capacitive currents to run through the neutral and ground wires; can lead to improper grounding and patient injury.

stray inductance — The leakage of electrical current that induces magnetic fields that can produce current flow in other conducting structures and potentially injure patients.

temporal data — Data acquired in the time domain, for example, a measurement acquired as a function of time.

temperature — The degree of hotness or coldness of a body or an environment.

ten-twenty system — A standard adopted by the American EEG Society for placement of EEG electrodes. The head is divided into standard arcs, using anatomic landmarks on the head. Electrodes are placed in increments of 10% and 20% of the lengths of the arcs.

throughput — Refers to devices that process data, this is the total number of pieces of data that can be processed each second. For example, an A-D converter processing 32 channels of data per unit time.

time constant — The time for voltage across the resistor to fall approximately 37%, or the time for the capacitor to charge to 63%.

transcranial Doppler — An application of ultrasound methodology that measures the blood flow velocity in the major intracranial arteries.

turns analysis — A quantitative method for studying the interference pattern, usually with a computerized EMG unit outfitted with a special program to acquire the interference pattern and analyze the signal for amplitude and turns.

visual evoked response — One of the most frequently used evoked potentials used for clinical testing, this measure records the neural signals from the visual system and couples these signals to an elicited sensory stimulus (e.g., a checkerboard pattern) or movement (e.g., a strobe light) from the patient.

voltage — The electromotive force or potential difference, usually expressed in volts, in a body or electrical circuit.

volts — The International System unit of electric potential and electromotive force that equals the difference of the electric potential between two points on a conducting wire carrying a constant current of one ampere when the power dissipated between the two points is one watt.

Wada test — The clinical test to measure language dominance or codominance in patients having a seizure or stroke.

widespread anteriorly maximum rhythmic pattern — The EEG pattern observed at lighter levels of steady-state anesthesia; appears as a widespread anterior pattern.

widespread persistent slow waves — An EEG pattern observed during increases in inhalation of anesthetic concentrations.

INDEX

Spacelabs Medical, Inc.
15220 NE 40th Street, P.O. Box 97013
Redmond, WA 98073-9713
(425) 882-3700
ISBN 0-9627449-7-2